THE MECHANISM OF FREEZING RESISTANCE IN COLD-ACCLIMATED WINTER WHEAT AND RYE CROWNS

A Thesis Submitted to the College of
Graduate and Postdoctoral Studies
In Partial Fulfillment of the Requirements
For the Degree of Doctor of Philosophy
In the Department of Plant Sciences
University of Saskatchewan
Saskatoon

By

IAN ROBERT WILLICK

Permission to Use

In presenting this thesis/dissertation in partial fulfilment of the requirements for a Postgraduate degree from the University of Saskatchewan, I agree that the Libraries of this University may make it freely available for inspection. I further agree that permission for copying of this thesis/dissertation in any manner, in whole or in part, for scholarly purposes may be granted by the professor or professors who supervised my thesis/dissertation work or, in their absence, by the Head of the Department or the Dean of the College in which my thesis work was done. It is understood that any copying or publication or use of this thesis/dissertation or parts thereof for financial gain shall not be allowed without my written permission. It is also understood that due recognition shall be given to me and to the University of Saskatchewan in any scholarly use which may be made of any material in my thesis/dissertation.

Requests for permission to copy or to make other use of material in this thesis in whole or part should be addressed to:

Head of the Department of Plant Sciences
College of Agriculture and Bioresources
University of Saskatchewan
51 Campus Drive
Saskatoon, Saskatchewan S7N 5A8, Canada

OR

Dean
College of Graduate and Postdoctoral Studies
University of Saskatchewan
116 Thorvaldson Building, 110 Science Place
Saskatoon, Saskatchewan S7N 5C9, Canada
Canada

Abstract

The ability of cold-acclimated crowns to survive freezing is an important environmental factor limiting winter wheat (*Triticum aestivum* L.) expansion in Western Canada. Cold-acclimation refers to the physiological and biochemical processes by which plants acquire freezing resistance. Cold-acclimation establishes an ice segregation freezing survival mechanism. The shoot apical meristem (SAM) cold-acclimates through the accumulation of dehydrins, vernalization-responsive and cold shock proteins. Modifications to the vascular transition zone (VTZ), are centered on increases in pathogenesis-related, antifreeze proteins, sugar hydrolyzing enzymes and increased cell wall glucuronoarabinoxylans. In cold-acclimated winter wheat and rye (*Seacale cereale* L.), magnetic resonance microimaging revealed a desiccative intermediate zone between the SAM and VTZ with reduced water mobility. Slow cooling rates ($\leq 2°C\ h^{-1}$) are required to establish freezing injury in the VTZ prior to injury in the SAM. Infrared thermography was used to observe in the absence of an extrinsic ice nucleator that freezing initiated from the base of the crown. The first freezing event (-3°C to -5°C) corresponded with warm ice nucleation temperatures (-3.5°C) and ice formation in the leaf sheath. Removal of the leaf sheath prior to cooling reduced cold hardiness and resulted in injury to the SAM prior to the VTZ. The second freezing event (-8°C to -12°C) corresponded with non-lethal injury to the VTZ. The third freezing event (-21°C in Norstar, -27°C in Hazlet and -30°C in Puma rye) corresponded with injury to the SAM and the plant's killing temperature based on whole plant survival tests. It is hypothesized that cold-acclimated crowns survive sub-zero temperatures through the following mechanism. The leaf sheath is established as an ice sink relative to the SAM. An intermediate zone acts as a barrier to ice propagation, allowing the SAM to supercool and avoid freezing. The VTZ acts as an ice sink within the crown. Possible differences in SAM freezing survival between rye and wheat could explain their contrasting cold hardiness.

Co-Authorship Statement

This thesis includes four manuscripts and a section of one book chapter. I designed and conducted the experiments, collected and analyzed the data and wrote the manuscripts. I am or will be, the first author of all four publications and second author of one book chapter.

Sections pertaining to plant antifreeze proteins in the literature review (Chapter 2) were modified and included in the recently submitted book chapter 'Plant antifreeze proteins' *In* Antifreeze proteins: ice, environment biology, systematics and evolution Vol I. Book Chapter co-authors Michael Wisniewski, John G Duman, David Livingston and Samuel Newton did not contribute to the literature review.

The first manuscript entitled 'Tissue-specific changes in apoplastic proteins and cell wall structure during cold-acclimation of winter wheat crowns' (Chapter 3) was accepted by the Journal of Experimental Botany. This manuscript was co-authored with Daisuke Takahashi, Matsuo Uemura, D. Brian Fowler and Karen K. Tanino. D Takahashi provided in lab guidance for the purification and analysis of the apoplast proteins. DB Fowler provided financial support and guidance in the manuscript design. M Uemura guidance for the proteomics component including financial and laboratory support. KK Tanino provided financial and laboratory support, guidance in experimental design and manuscript preparation.

The second manuscript entitled 'Effect of cooling rate and durational stress on freezing behaviours in cold-acclimated and winter wheat and rye crowns' (Chapter 4) is in preparation for publication. This manuscript was co-authored with Andrew Lewis, D. Brian Fowler and Karen K. Tanino. A. Lewis provided in lab guidance and advice for the experimental design of the magnetic resonance microimaging experiment. DB Fowler provided financial support and laboratory support. KK Tanino provided financial and laboratory support, guidance in experimental design and manuscript preparation.

The third manuscript entitled 'Effect of cold-acclimation on crown tissue ice nucleation temperatures' (Chapter 5) is in preparation for publication. This manuscript was co-authored with D. Brian Fowler and Karen K. Tanino. DB Fowler provided financial and laboratory support. KK Tanino provided financial and laboratory support, guidance in experimental design and manuscript preparation.

The fourth manuscript entitled 'Water behavior during freezing in the crown of cold-acclimated winter cereals: evidence of an ice segregation survival mechanism' (Chapter 6) will be

submitted to Plant Physiology. This manuscript was co-authored with Lawrence V. Gusta, D. Brian Fowler and Karen K. Tanino. LV Gusta provided guidance for the freezing component including experimental design. DB Fowler provided financial support and guidance during manuscript preparation. KK Tanino provided financial and laboratory support, guidance in experimental design and manuscript preparation.

Acknowledgements

I would like to express my sincere thanks to my supervisor, Karen Tanino, for her unwavering encouragement and support. Many foolish thoughts were tolerated, which was appreciated when it seemed like nothing was ever going to work. Appreciation is extended to my advisory committee members - Brian Fowler, Gordon Gray, Yangdou Wei and Pierre Hucl for their sobering advice, criticisms and suggestions. Appreciation is also extended to my external examiner, Masaya Ishikawa, for his thoughtful criticisms and comments which undoubtedly improved the quality of this thesis.

I would like to acknowledge the financial support provided by various scholarships including the National Science and Engineering Research Council of Canada Post Graduate Scholarship (2015-2017), the Robert P Knowles Postgraduate Scholarship (2015-2018), the Devolved Postgraduate Scholarship (2014-2015), the Rene Vandeveld Postgraduate Scholarship (2015), the JD MacFarlane Postgraduate Bursary (2014), the Norman and Kathleen Lean Postgraduate Scholarship (2014) and the Purdy Postgraduate Scholarship (2014).

During this thesis, I have found direction from people with skills, experience, enthusiasm, and insight. Particularly, Matsuo Uemura, Daisuke Takahashi, Keita Endoh, Andrew Lewis, Marco Gruwel, Rod Wasylishen, Rosalind Bueckert, Eiko Kawamura, Michael Wisniewski, Rachid Lahlali, Chithra Karunakaran, Perumal Vijayan, Prakash Venglat, Raju Soolanayakanahally, Krista Thompson, Yeonkyeong Lee, David Livingston, Phyllis Shand and Jackie Bantle. My heartfelt appreciation is extended to Larry Gusta for reminding me the importance of scientific debate. Our discussions were instrumental in the development of this thesis.

I cannot thank all my friends and lab mates individually for their friendship over the last four years. There were a few who went above and beyond. To Dustin Maclean and Tony Wang for encouraging me to maintain sanity by lifting ‘heavy things’. To Kaila Hamilton for participating in the Japan acclimation study and to Kirby Nilsen for insightful discussions over coffee and at our bi-monthly safety meetings.

Finally, to my parents for supporting me no matter the situation. Even if that meant marathon phone conversations and spending the last four years halfway across the country.

Table of Contents

List of Tables

List of Figures

List of Abbreviations

ABA	Abscisic acid
ADC	Apparent diffusion coefficient
AFP	Antifreeze protein
ANOVA	Analysis of variance
COR	Cold-regulated (protein)
CSP	Cold-shock protein
CWMP	Cell wall modifying protein
DTA	Differential thermal analysis
EL_{50}	Temperature at which half the population did not survive freezing as measured by electrolyte leakage
FPA	Focal plane array
FT	Flowering locus T
FTIR	Fourier transform infrared spectroscopy
GPI	Glycosylphosphatidylinositol
INA	Ice nucleating activity
INA^+	Ice nucleating active bacteria/substance
IRVT	Infrared video thermography
LSD	Fisher's least significant difference
LD_{50}	Number of days half the population did not survive a specific freezing temperature
LT_{50}	Temperature at which half the population did not survive freezing as measured by recovery
MRMI	Magnetic resonance microimaging
NMR	Nuclear magnetic resonance
PPFD	Photosynthetic photon flux density
SAM	Shoot apical meristem
SEM	Scanning electron microscopy
TTC	2,3,5-triphenyl-2H-tetrazolium chloride
VRN	Vernalization gene
VTZ	Vascular transition zone

Chapter 1

1 Introduction

1.1 Background

Early Fall establishment and acclimation provide winter cereals with a competitive advantage over conventional spring habit cereals in years with an ideal winter. Winterkill from exposure to lethal sub-zero temperatures is an important environmental factor limiting Western Canadian winter wheat (*Triticum aestivum* L.) expansion into more Northern latitudes (Fowler, 2012a). Improved cold-hardiness in winter wheat requires a whole plant physiological, biochemical and molecular response to environmental cues (Fowler et al., 1976; Gusta et al., 1982; Brule-Babel and Fowler, 1989; Hurry and Hüner, 1991; Limin and Fowler, 2002; Fowler, 2012a; Trischuk et al., 2014; Hüner et al., 2016; Li et al., 2017). These cues could be in the form of an environmental stress, such as a reduction in photoperiod, light quality, cooler temperatures or a combination thereof to induce a cold-acclimation response. The goal of improving winter wheat cold hardiness is to develop a model that describes how the plant acclimates to these environmental cues and then identify the induced mechanism to tolerate and or avoid freezing injury. Once the mechanism of survival has been identified, breeders can then select for this trait.

The vegetative crown organ is divided into two major constituents. (I) The shoot apical meristem (SAM) comprises the apical meristem tissues as well as newly formed leaves. (II) The vascular transition zone (VTZ) comprises root meristem cells, pith and xylem responsible for the translocation of water from the roots to the above ground organs. The leaf sheath which encapsulates the crown is associated with fully developed mature leaves (organ). Due to the complex nature of the vegetative crown, the critical organ for survival, not all these constituents achieve the same level of hardiness (Pauli, 1960; Beard and Olien, 1963; Olien, 1964; Olien and Marchetti, 1976; Chen et al., 1983; Tanino and McKersie, 1985; Livingston et al., 2005b; Livingston et al., 2013; Livingston and Tuong, 2014).

When cold-acclimated plants are slowly cooled (1 to 5°C h^{-1}), on a cellular level water freezes first in the extracellular space and ice nucleation forms a water vapor pressure difference between the ice (low) and unfrozen cells (high) (Levitt, 1980). Water migrates towards the growing ice crystal. In the crown, ice crystalizes in the VTZ located between the SAM and the nodal plate (Olien, 1964; Olien and Marchetti, 1976; Livingston and Tuong, 2014). The VTZ was postulated as the preferred site of ice crystallization due to its proportionally high volume of free water (Gusta et al., 1975). In spite of the physiological (Beard and Olien, 1963; Olien, 1964; Olien and Marchetti, 1976; Chen et al., 1983; Tanino and McKersie, 1985; Livingston et al., 2005b; Livingston et al., 2013) and biochemical (Livingston et al., 2005a; Livingston et al., 2006; Willick et al., 2018a) evidence reporting that the VTZ and SAM have contrasting responses to sub-zero temperatures, recent cold-acclimation studies tend to quantify biochemical and molecular responses in the whole crown (Kosová et al., 2012; Vítámvás et al., 2012; Trischuk et al., 2014) or leaves (Takahashi et al., 2013a). It is possible that tissue-level phenotypes are masked in bulk analysis.

Differential patterns of freezing injury have long been reported in other complex structures such as the overwintering tree bud organ (Wiegand, 1906b; Dorsey, 1934; George et al., 1974; Graham and Mullin, 1976; Dereuddre, 1978; Sakai, 1979; Ishikawa and Sakai, 1982; Ishikawa et al., 1997; Endoh et al., 2014; Ishikawa et al., 2016). Freezing injury to the primordia or floret tissues was prevented by the segregation of ice in the bud scale organ or subtending bud vascular tissue (Ishikawa and Sakai, 1981; Ishikawa and Sakai, 1982; Ishikawa et al., 2015). The primordia desiccate during the fall and winter, establishing a tissue level water vapor gradient between the primordia and the ice sinks (Sakai, 1982; Sakai, 1983). Ice propagation from the ice sink to the primordia is avoided due to a tissue-level barrier (George et al., 1974; Ashworth, 1984; Kuprian et al., 2017; Lee et al., 2017). Water translocation from supercooling tissues to ice sinks in adjacent tissues (extra-tissue freezing) and/or outside of the organ (extra-organ freezing) are two of the mechanisms of freezing survival used in higher plants (reviewed by Sakai and Larcher, 1987). Despite similarities in the general pattern of freezing injury reported in winter cereal crowns and tree buds, no published literature has proposed that cold-acclimated crowns segregate ice into freezing tolerant tissues and organs to avoid lethal injury.

1.2 Objectives and hypotheses

The goal of this research was to evaluate the effects of cold-acclimation and sub-zero temperatures on the establishment of freezing tolerance and avoidance mechanisms in Norstar winter wheat (Grant, 1980) and contrast these behaviours in the winter rye (*Secale cereale* L.) cultivars Hazlet (McLeod and Gan, 2008) and Puma (Shebeski et al., 1973). The effect of cold-acclimating, sub-lethal and lethal low temperatures on tissue-specific freezing tolerance and avoidance mechanisms were evaluated from a physiological, biophysical, biochemical and proteomic perspective. Little is known regarding the tissue and organ level water mobility and sequestration in crowns exposed to cold-acclimating and sub-zero temperatures. A better understanding of the physiological processes can identify new traits associated with greater cold hardiness in winter rye and where improved tolerance and or avoidance is required in winter wheat.

Winter wheat crowns have a greater cold hardiness than winter oat (*Avena sativa* L.) and barley (*Hordeum vulgare* L.). Unlike the comparatively more cold hardy winter rye, winter wheat cannot overwinter in Saskatchewan without adequate snow cover. It is for these reasons that winter wheat and winter rye were selected to study the cold-acclimation and freezing behaviour responses in the crown. Norstar winter wheat was selected as a model organism due to its importance in North American breeding programs since the 1970s and continued use as a freezing survival check cultivar (Fowler, 2012a). Hazlet winter rye was selected because it had the highest number of insured commercial acres of all rye cultivars in Saskatchewan and Manitoba and the second highest in Alberta since 2015 (Statistics Canada). Puma rye was selected for its predominant use in the literature since the 1980s and its greater cold-hardiness than Hazlet rye.

The following hypotheses are proposed. (I) Cold acclimated Norstar SAM and VTZ have two distinct apoplast proteomes that are optimized for tissue-specific freezing survival strategies. (II) In cold-acclimated winter wheat and rye, slow cooling reduced the initial injury to the VTZ. (III) In cold-acclimated winter wheat and rye, high leaf sheath ice nucleation temperatures increase crown cold hardiness by acting as an ice sink relative to the SAM and VTZ. (IV) Cold-acclimated winter wheat and rye crowns survive freezing using an ice segregation freezing strategy and rye is better able to survive due to higher SAM freezing avoidance. To test the above hypotheses, experiments with the following objectives were conducted.

Experiment I. Cold-acclimation responses in the SAM and VTZ (Chapter 3)

The objectives of this study were to determine if exposure to 0, 21, or 42 d at 4°C induced a differential accumulation of apoplast proteins and cell wall modifications in the SAM or VTZ.

Experiment II. Effect of cooling rate on the pattern of injury (Chapter 4)

The objectives of this study were to test the effects of cooling rate (2°C h^{-1}, 5°C h^{-1} or 10°C h^{-1}) on the pattern of freezing injury at the whole plant, tiller, crown and organ level. The secondary objective of this experiment was to observe if the initial site of injury in the crown corresponded to injury to the VTZ using infrared thermography and magnetic resonance micro-imaging (MRMI).

Experiment III. Tissue-specific ice nucleation study (Chapter 5)

The objectives of this study were to investigate the effect of cold-acclimation on the temperature at which individual crown organs or cellular extracts initiate ice nucleation. The secondary objective of this chapter was to determine if the leaf sheath serves as an ice sink for the crown.

Experiment IV. Confirmation of ice segregation in the crown (Chapter 6)

The objectives of this study were to determine if crowns avoid and or tolerate freezing using an ice segregation mechanism, such as extra-organ or extra-tissue freezing. The secondary objective of this study was to map changes in water mobility during cold-acclimation using MRMI to determine if a desiccative barrier was established between the SAM and VTZ prior to freezing.

Chapter 2

2 Literature review

2.1 Freezing injury

The formation of ice can lead to immediate injury in freezing-sensitive plants while other plants have adapted over evolutionary time to be able to resist freezing, either through tolerance or avoidance mechanisms, before injury or death occurs (Scarth and Levitt, 1937; Vasilyev, 1961; Levitt, 1980). Duhmel and Buffton (1741) were two of the first to theorize that the expansion of ice within plants causes death from cell wall rupture (reviewed by (Vasilyev, 1961). Goppert in the mid 1800s using basic microscopy observed that ice formed in the extracellular spaces of cold-hardy plants (Vasilyev, 1961). Formation of ice as a factor in causing injury and death in plant cells is an accepted theory today (Wiegand, 1906a; Luyet and Gehenio, 1937; Scarth and Levitt, 1937; Siminovitch and Scarth, 1938; Scarth, 1941; Aoki et al., 1953; Weiser, 1970; Burke et al., 1976; Levitt, 1980; Thomashow, 1999; Pearce, 2001; Gusta et al., 2009; Gusta and Wisniewski, 2013; Duman and Wisniewski, 2014). The species-specific mechanism of tolerance and avoidance of freezing is still an active topic of debate.

Luyet and Gehenio (1937) were proponents of the two stages of freezing theory in plants first mentioned in the literature in the early 1900s (reviewed by Levitt 1980). Luyet and Gehenio hypothesized the initial rise in temperature at the beginning of ice formation corresponded to the first freezing plateau visualized using thermocouples. The second plateau was much longer and occurred at a lower temperature. Aoki et al. (1953) reported the shape of the freezing curve reflected the temperature of freezing survival. Both Aoki and Luyet hypothesized in frost susceptible plants, the initial intracellular freezing event would release a large enough quantity of heat to temporarily prevent further freezing and caused a depression in the freezing curve. Levitt criticized this point and hypothesized the double freezing curve could be explained by cell turgor and the initial exotherm attributed to the crystallization of extracellular water (Levitt, 1980). Ice formation resulted in reduced vapour pressure in the extracellular space, and reduction in turgor pressure in the protoplasts as well as an increase in cell sap concentration.

Levitt argued this led to a depression of the freezing point and a separation of the two stages of ice crystallization. Siminovitch and Scarth (1938) argued that the difference in the second plateau was due to an increase in low molecular weight cell sap sugars. Siminovitch and Scarth (1938) suggested in woody perennials, ice crystal formation along the cell walls in hardy plants was related to the accumulation of sugars. Higher concentrations of sugars would result in higher osmotic pressure, less freezable water and a smaller release of latent heat. After the first phase of freezing the increase in solute concentration in the remaining liquid water results from a melting of extracellular ice. Re-crystallization transpires during the second phase of freezing and the protoplasts separate from the cell walls by a thin layer of ice in a process known as frost plasmolysis (Burke et al., 1976). Intracellular liquid water is extracted along the vapor pressure gradient resulting in a loss of cell turgor. Additional freezing events associated with tissue or organ-specific freezing events were identified in cold-acclimated tissues using differential thermal analysis (Quamme, 1978; Ishikawa and Sakai, 1981; Endoh et al., 2014; Ishikawa et al., 2015), acoustic emissions (Charrier et al., 2014; Kasuga et al., 2015) and visualized using traditional microscopy (Ishikawa and Sakai, 1981; Ishikawa and Sakai, 1982; Endoh et al., 2014) and infrared video thermography (Hacker and Neuner, 2007, 2008; Kuprian et al., 2014).

The current theory on freezing injury of cold-acclimated cells hypothesizes the porosity of the cell wall can promote intracellular supercooling while the plasma membrane is essential for supercooling to occur at lower temperatures (Scarth and Levitt, 1937; Siminovitch and Levitt, 1941; Asahina, 1956; Vasilyev, 1961; Towill and Mazur, 1976; Olien and Smith, 1977; Levitt, 1980; Tanino et al., 1991; Rajashekar and Burke, 1996; Rajashekar and Lafta, 1996; Fujikawa et al., 1997; Uemura and Steponkus, 1997a; Fujikawa et al., 1999; Uemura et al., 2006; Gusta et al., 2009). As water is slowly lost from the intracellular space, cell solutes concentrate, which lowers the ice nucleation temperature. As freezing progresses, the plasma membrane remains attached to the cell wall, causing the cell wall to collapse. Injury or death of the cell can occur if (I) the extracellular space is too small to accommodate the growing ice crystal; (II) cells are crushed by ice growth; (III) the cells are separated by splitting the cell wall along the middle lamella; (IV) the protoplasm is pushed against the cell wall resulting in cell rupture; (V) the plasma membrane ruptures and loses its ability to concentrate solutes; (IV) or the cell wall cannot expand to its original shape after freeze-thaw due to loss of turgor.

2.2 Types of freezing

2.2.1 Chilling and intracellular freezing

Any form of stress may interfere with the plant's ability to survive and acclimatize to its environment, resulting in a less hardy plant and reduction in yield. In extreme conditions, this can result in injury and death of the plant (Levitt, 1980; Gusta et al., 2009). Tropical or sub-tropical plants exposed to temperatures below 15°C suffer from chilling injury, which results in reduced germination rates, inhibited growth, wilting, and tissue, organ or whole plant death (Gusta et al., 2009). Chilling (> 0°C) and natural freezing (< 0°C) in plants are slow and gradual processes, which are dependent upon tissue, seasonal changes, and geographic location. In tender or non-acclimated cereals, ice nucleation within the cell's intracellular space disrupts cell integrity leading to its immediate death (Siminovitch and Scarth, 1938). This process is irreversible and therefore mechanisms of freezing stress resistance are required for cell survival. In the case of freezing-sensitive crops, such as winter and spring wheat following booting, the plant avoids freezing by supercooling in the head (Fuller et al., 2007; Livingston et al., 2016). Freezing-sensitive field grown plants, such as spring wheat, during the summer months tend to be more freezing tolerant as opposed to the same plant grown in controlled environment conditions due an acclimation response to environmental stress such as wind, herbivory, ultra-violet, light or water (Gusta and Wisniewski, 2013; Duman and Wisniewski, 2014).

Intracellular freezing can occur in cold-acclimated plants. When protoplasts supercool in the presence of an ice nucleator, the intracellular space will freeze (Asahina, 1956; Steponkus, 1984). If ice nucleation and freezing occur within the extracellular space in cold-acclimated cells (Siminovitch and Levitt, 1941; Siminovitch and Briggs, 1953; Vasilyev, 1961; Rajashekar and Burke, 1996), intracellular freezing is still possible under non-equilibrium freezing conditions (Olien, 1964; Olien, 1973; Knight et al., 1995; Olien and Livingston, 2006). Non-equilibrium freezing occurs when tissues have a high-water content or are cooled quickly (> 2°C h^{-1}), which does not allow water to diffuse before supercooling and the formation of intracellular ice (Olien, 1964; Olien, 1973).

2.2.2 Dehydration

Cold-acclimated winter cereals undergo extracellular freeze dehydration stress in which ice propagation initiates in the apoplast. Since ice has a lower water potential than water,

intracellular water will diffuse into the apoplast resulting in cellular osmotic shrinkage and cellular dehydration (Scarth, 1941; Towill and Mazur, 1976). Further decreases in temperature result in a subsequent drop in ice water potential (George et al., 1974; Gusta et al., 1975). The severity of injury caused by freezing induced dehydration is affected by the temperature and duration (Gusta et al., 1997; Waalen et al., 2011; Min et al., 2014), regulation of ice nucleation sites (Verslues et al., 2006), the rate of ice propagation throughout the plant organ (Wisniewski et al., 1997; Gusta et al., 2004; Hacker and Neuner, 2007), relative humidity, soil temperature and wind speed (Gusta and Wisniewski, 2013).

During thawing, an influx of water into the intracellular space results in cell expansion. Damage caused during the freeze thaw cycle was later postulated by Ilijin (1933) to be a result of the rapid movement of the cell wall during the thawing process (reviewed by Levitt 1980). Subsequent freezing events require less energy to produce additional injury (Olien 1967). This can lead to the formation of large masses of ice upon the next freezing event in cold-acclimated winter wheat, rye (Gusta and Fowler, 1977) and spinach leaves (*Spinacia oleracea* L.) (Min et al., 2014). In the field, crowns would not be exposed to mid-winter thaws. The soil would not undergo the same temperature fluxuations as the air.

While it can be difficult to account for most environmental factors in laboratory research freezing duration, a critical factor in cellular ice propagation can be controlled for in laboratory stress tests. Temperatures classified as sub-lethal based on traditional LT_{50} tests can become lethal depending on how long winter wheat is exposed to that temperature (Gusta et al., 1982; Gusta et al., 1997). Field acclimated Norstar winter wheat and Tosca canola survive to -23°C and -20°C respectively when cooled at a rate of 2°C per hour. However, Norstar winter wheat was killed after exposure to -15°C for 13 d (Gusta et al., 1997) and Tosca after 20 d at -8°C (Waalen et al., 2011).

Olien and Smith (1977) proposedas temperature decreases, the quantity of liquid water in the plant decreases. The cell membranes and growing ice crystals would then compete for the remaining liquid water. Ice crystals are generally angular and by forcing the membrane and cell wall to adhere to this shape may result in injury (Olien and Smith, 1977). Adhesive freezing stress is predicted thermodynamically in the temperature range near -10°C in winter oat (*Avena sativa* L.) (Olien and Smith, 1977), corresponding to injury to the VTZ in winter wheat (Willick et al., 2018a).

2.2.3 Vitrification

Vitrification occurs at sub-zero temperatures when water freezes into a glass-like solid with no recognizable crystalline structure (Hirsh, 1987). During dehydration, sugars and cellular components increase in concentration relative to the remaining cellular water. This results in increased cytoplasmic viscosity and a reduction in the rate of dehydration (Goff and Sahagian 1996). Vitrification was first noted using single cell layer sections frozen in liquid nitrogen and then thawed at ultra-fast rates (10,000°C s^{-1}) (Luyet and Hodapp, 1938). If samples were thawed at a slow rate, large ice crystals form resulting in membrane rupture and cell death. Sakai and Yoshida (1968) hypothesized the increase in cytoplasmic free sugar due to cold-acclimation and sub-zero hardening was the primary reason for cytoplasmic glass formation (Sakai and Yoshida, 1968). This was supported by research demonstrating that low molecular weight sugars stabilized glass structure (Crowe et al., 1984). In contrast, Siminovitch and colleagues argued the increase in soluble proteins due was the primary reason for cytoplasmic glass formation (Siminovitch et al., 1968).

2.2.4 Bifringence, supercooling and deep supercooling

Differential thermal analysis (DTA) of woody plants produced two exotherms associated with plant freezing. The first high temperature exotherm corresponded with bulk water freezing in xylem vessels and extracellular spaces (Quamme et al., 1972; Ishikawa and Sakai, 1981; Ishikawa et al., 2015). A second low temperature exotherm corresponded with the freezing of a fraction of supercooled water (Ishikawa and Sakai, 1981). Plants can avoid freezing in critical tissues by undergoing supercooling in which cells remain unfrozen below their freezing point. The term bifringence was first used by Tumanov and colleagues to describe this mechanism of freezing avoidance by freezing-sensitive organs (Tumanov and Krasasvtsev, 1959) and identified in tree buds that could supercool to -26.5 ºC (Wiegand, 1906b). According to Levitt (1980) there are five requirements for bifringence: (I) small cell size; (II) little or no extracellular space to facilitate nucleation; (III) low moisture content; (IV) absence of internal nucleators; (V) and barriers against external nucleators as well as substances which oppose the formation of nucleators.

DTA has been used to study supercooling in Norstar and Frederick winter wheat (Pukacki and McKersie, 1990). However, most of the research on supercooling and deep supercooling has been conducted in hardwood perennials. Hardwood tree stem DTAs produce high (-5°C) exotherms correlated with apoplastic water and a low (-20°C) exotherm following intracellular

freezing (Quamme et al., 1972; Burke et al., 1976). Xylem ray parenchyma cells exhibit extracellular freezing with no detectable low temperature exotherm. This was believed to be due to intracellular water migrating to extracellular ice crystals. When the remaining water in the intracellular space freezes, the exotherm produced is too small to detect. Xylem ray parenchyma cells with thick lignified cell walls were capable of supercooling (Fujikawa et al., 1999). Increased wall rigidity and reduced porosity minimize cytorrhysis (the collapse of cell walls and protoplasts) during extracellular freezing (Scarth, 1941). The temperature limit of supercooling varies on evolutionary adaptations to geographical latitudes (Kuroda et al., 2003), seasonal (Quamme et al., 1982; Gusta et al., 1983; Fujikawa et al., 1997) and artificial (Takata et al., 2007) cold-acclimation and de-acclimation.

Deep supercooling occurs when cells avoid intracellular freezing without dehydration by supercooling. This has been noted in xylem parenchyma cells that can maintain a supercooled state for multiple days when exposed to below freezing temperatures (Quamme et al., 1982) and maintain their pre-freezing morphology due to the absence of cellular dehydration (Fujikawa et al., 1994; Fujikawa et al., 1997). Deep supercooling xylem ray parenchyma cells have thick rigid cell walls, lignified secondary cell walls (Fujikawa et al., 1997) and greater total sugar concentrations than cortex parenchyma cells (Kasuga et al., 2007). Intracellular substances are believed be the limiting factor in increased freezing tolerance in boreal hardwood species (Kasuga et al., 2007; Kasuga et al., 2008) and beech (*Fagus crenata*) (Kasuga et al., 2006). Deep supercooling has never been reported in cold-acclimated winter cereals.

2.2.5 Flooding and ice encasement

In humid regions, where there is considerable winter precipitation, heaving or smothering by ice will injure crops rather than sub-zero temperatures (Wright, 1890; Andrews and Pomeroy, 1975; Andrews and Pomeroy, 1979; Andrews and Pomeroy, 1981; Tanino and McKersie, 1985). Flooding in Eastern Canada occurs in the Fall and Spring, whereas ice-encasement occurs during mid-winter thaws or after late Fall or Winter precipitation. Ice encasement, shown in the literature since the 1890s (Wright, 1890), increases anaerobic respiration, resulting in increased carbon dioxide and the accumulation of anaerobic respiration end products resulting in increased winterkill (Andrews and Pomeroy, 1979). In contrast, flooding results in decreased gas exchange between the soil and air. Soil can become anoxic and/or hypoxic within hours resulting in a decreased uptake of nutrients, reduction in root growth and loss of beneficial microorganisms. In

Eastern Canada the effects of standing water (from excessive precipitation) and early season frosts (resulting in ice encasement) on crown cold hardiness and yield could not be separated (reviewed by Pomeroy and Andrews, 1983). However, strong correlations have been shown between cold hardiness and crown water content (Gusta et al., 1975; Gusta et al., 1979; Brule-Babel and Fowler, 1989; Yoshida et al., 1997), flooding (Andrews and Pomeroy, 1981) as well as soil water content during freezing (Andrews and Pomeroy, 1975). In traditionally drier regions, such as the continental climate of the Canadian Prairies and Scandinavia, these indirect effects have a minor impact on crop overwintering survival. However, with the onset of climate change, increasingly erratic rainfall patterns, the occurrence of snow melt and humidity over winter could change the kinds of stress that play a role in winterkill in Western Canada.

2.2.6 Secondary stresses during recovery

Damage can either occur immediately following a freezing event or once the plant begins active regrowth. The latter suggests damage could occur via a metabolic breakdown or from a secondary external stressor such as pathogens. Thawing of ice in extracellular spaces results in a change in water balance and can lead to a rapid influx of water into the cell. Since cell membrane expansion is slower than water balance adjustment, this influx of water can result in cell swelling, rupture or death (Steponkus et al., 1983). Cold-acclimated protoplasts can produce exocytotic extrusions that are responsive to osmosis and can avoid cell lysis. Sparse cell death or even the death of non-essential organs such as leaves and roots in winter wheat is not fatal to the plant (Chen et al., 1983). Freezing disrupts the cells between the SAM and VTZ but the undifferentiated pro-meristem near the SAM is uninjured (Olien, 1964). Crowns that have been injured by ice propagation within the VTZ, can be further stressed by the pathogenic attack in abscesses left by melted ice crystals (Olien and Marchetti, 1976; Livingston et al., 2005b). Mechanical damage can result in necrotic lesions bordered by healthy tissue. Lesions expand until both the crown and plant are killed. Olien (1964) hypothesized autotoxicity ensues in tissues adjacent to the necrotic lesions, resulting in protein degradation by lysosome membrane bound hydrolytic enzymes.

2.2.7 Agronomic practices to reduce winterkill

Winter cereals such as winter wheat (*Triticum aestivum* L.) have yield potentials of up to 30 % greater than modern spring cultivated varieties under ideal field conditions, but any potential yield gains are mitigated by reduced overwintering survival, known as winterkill (Fowler, 2012a).

Expansion of winter habit crops into more northern latitudes that experience increased probability of exposure to lethal sub-zero temperatures over winter present challenges in crop management. To guarantee overwintering survival, winter wheat can regenerate from uninjured crowns capable to producing new roots (Chen et al., 1983). Soil temperature is important in determining this degree of injury. Snow cover was identified as an important insulator by agronomists in South Dakota as far back as 1918 (Evans and Janssen, 1922). In the absence of snow cover, heat stored in the soil is lost resulting in a reduced capacity to resist cool temperature fluctuations. It is critical in Saskatchewan during long periods of cold from December to February, that winter wheat fields are covered by 8 to 10 cm of unpacked snow (Fowler et al., 1976; Fowler, 2012a). The difference in soil temperature between bare summer-fallow and zero-till stubble with 10 cm of snow can have a ten-degree difference in soil temperature. This difference in soil temperature can mean the complete winterkill or near-complete recovery. Packed snow or snow deeper than 10 cm can result in poor insulation from cold air temperatures, anaerobic stress or the proliferation of snow molds. Including proper snow management resulted in the expansion of winter wheat production into the black and grey soil zones in Saskatchewan and Manitoba in the 1970s (Fowler et al., 1976; Fowler, 2012a).

The most efficient way to trap snow is by seeding directly into the stubble of the previous crop, known as zero-till cropping. To achieve maximum freezing survival using the zero-till cropping method, the winter wheat crowns must be fully developed and have a minimum of two to three leaves (Martin and Parker, 1926; Janssen, 1929). The stubble crop must be harvested early enough to facilitate winter wheat planting. Flax, rapeseed, barley, and oat are all ideal candidates with strong enough stems to trap snow and can be harvested in early August before the recommended winter wheat seeding dates (Fowler et al., 1976; Fowler, 2012a). Late planting, which varies by region (latitude) in Saskatchewan, can result in underdeveloped crowns. The seed also requires sufficient moisture for germination. This can be achieved by seeding shallow, around 2.5 cm (Freyman, 1978). Saskatchewan soils deficient in phosphorus can reduce spring recovery. Application of phosphorus during seeding (Fowler and Gusta, 1982) and nitrogen in the spring (Tyler et al., 1981) increases winter wheat spring recovery and maximum yield.

2.3 Cold sensing in winter habit plants

In many plant species, the ability to initiate floral development requires exposure to low temperatures for a quantifiable duration, a process referred to as vernalization (Gott, 1957; Fowler

et al., 1996; Limin and Fowler, 2002; Fowler, 2008). The temperature at which the winter cereal senses cold and begins to cold-acclimate is proportional to its maximum attainable cold-hardiness (Fowler, 2008). Winter rye initiates cold-acclimation at a warmer temperature than winter wheat, which initiates cold-acclimation at a warmer temperature than winter barley. Winter cereals that perceive a low temperature signal at warmer temperatures have a longer period to cold-acclimate are less sensitive to mixed temperature signals during the period of cold-acclimation. Such plants can acclimate faster at warmer temperatures, assimilate higher concentrations of sugars and are more capable of overcoming photoinhibition.

The requirement for the prolonged cold to initiate a switch from vegetative to reproductive growth has been studied extensively in winter-habit Arabidopsis (Bäurle and Dean, 2006; Liu et al., 2010; Crevillen and Dean, 2011). In winter-habit Arabidopsis, vernalization represents a quantitative reduction in the expression of a floral repressor known as flowering locus C (*FLC*) (Bäurle and Dean, 2006; Crevillen and Dean, 2011). This 'switching-off' mechanism is a quantitative epigenetic event (Bäurle and Dean, 2006; Liu et al., 2010; Crevillen and Dean, 2011) established by (I) the modification of DNA through transmittable DNA methylation; (II) chromatin modification; or (III) non-coding RNA-based mechanisms (King, 2015).

In winter wheat the vernalization gene (*VRN*), *VRN2* represses flowering locus T (*FT*) (Yan et al., 2004). The FT protein, also known as a 'florigen', is produced in the crown's vascular tissues and is transported to the SAM. The FT protein forms a floral activator complex that triggers the SAM to form floral structures. *VRN1* encodes for a MADS domain protein that is induced by cold (Yan et al., 2003) resulting in the removal of H3K27me3 repressive marks and the deposition of H3K4me3 activating markers at the *VRN1* chromatin (Oliver et al., 2009). *VRN1* binds to the FT promoter, resulting in a positive feedback loop. This ensures the transition from the vegetative to reproductive stage. The roles of *VRN3* (an ortholog for *FT*), VRN4 (a duplicate of *VRN1*) and the overall mechanism of epigenetics in winter cereal vernalization are still active areas of research (reviewed by Bouché et al., 2017).

2.4 Cold-acclimation

Plants are capable of surviving freezing by pre-exposure to low but non-freezing temperatures which result in acclimation (increasing plant cold hardiness). While non-acclimated winter cereal seedlings are no more cold-tolerant than non-acclimated spring cereals, cold-acclimated winter rye can survive temperatures as low as -34ºC. In decreasing order of freezing

resistance, rye is followed by winter wheat, winter triticale, durum winter wheat, winter barley and then winter oat (Fowler et al., 1977; Gusta et al., 2009). Variation in freezing hardiness is also present among cultivars. When acclimated at 6ºC with 16 h of light per day for 42 days, Norstar winter wheat had an LT_{50} (lethal temperature at which half of the population survives) of -22ºC while freezing susceptible 'Winter Manitou' had an LT_{50} of -11.6ºC (Fowler and Limin, 2004).

Cold-acclimation in winter habit plants can be triggered by changes in photoperiod (Weiser, 1970), light intensity, spectral distribution (Gray et al., 1997; Öquist and Hüner, 2003) as well as exposure to a threshold (< 14°C) cold temperature in winter cereals (Fowler, 2008) and *Lollium perenne* L. (Fuller and Eagles, 1980). This acquisition of cold hardiness is not a static entity, in that a return to warmer temperatures due to the early onset of spring or temperature fluctuations in the fall can stop, reverse and restart the acclimation process (Trischuk et al., 2014). However, following de- and re-acclimation, winter cereals cannot re-obtain the maximum level observed in mid-winter plants (Gusta and Fowler, 1977; Gusta et al., 1982), due to an inability to synthesize additional cryo-protective sugars (Trischuk et al., 2014). To gain a competitive advantage over spring habit crops, winter cereals can respond to temperatures favourable for growth and reproduction or temperatures that signal long term environmental change (Fowler, 2008). This becomes more significant if the growing season extends into the early spring and late fall due to changing climate patterns. Prolonged low temperature acclimation of winter wheat at temperatures of 8, 6 and 4ºC increases winter hardiness and reduces winterkill in field-based experiments (Fowler and Limin, 2004).

Plants exhibit a wide range of the maximum cold hardiness attained. This ability is dependent upon the species, cultivar, variety and whether the plant maintains active photosynthesis as a cold-tolerant species or reduces photosynthesis as a cold-sensitive species (Öquist and Hüner, 2003). Winter wheat, rye, and winter barley exhibit greater carbon assimilation at cold-acclimation conditions (< 10°C) than cold-sensitive spring wheat (Hurry and Hüner, 1991) and spring rape (*Brassica napus* L.) (Hurry et al., 1995). Greater carbon assimilation at low, cold-acclimating temperatures are associated with increased sink capacity (Hurry et al., 1995; Gray et al., 1996; Strand et al., 1999). Enhanced carbon assimilation at low, cold-acclimating temperatures is a multi-component process requiring photosynthesis for the accumulation of sugars such as sucrose and fructans. Sugars act not only as a source of energy but as a cryo-protectant, and a signalling molecule to trigger the induction of specific genes, proteins and metabolites, all of which

contribute to increased cold hardiness (Stitt and Hurry, 2002).

Winter cereal cultivars enhance sink capacity and concomitant carbon export during cold-acclimation by storing photosynthates as sucrose and fructans in the crown and leaf vacuoles (Wagner et al., 1983; Strand et al., 1999; Livingston et al., 2005a; Livingston et al., 2006). Storage of fructans and a concomitant increase in sugars in the apoplast (Livingston and Henson, 1998) has been linked to Weiser's second and third stages of acclimation (Weiser, 1970). Weiser postulated that during the second stage of acclimation there is a shift in the metabolic processes resulting in the accumulation of both short and long branching sugars when plants are exposed to cold-acclimation (4°C to 16°C). Additional tolerance can be gained during when plants are exposed to frost hardening temperatures below 0ºC but just above a plant's freezing point, providing anywhere from 3ºC to 5ºC of additional freeze tolerance (third stage) (Scarth and Levitt, 1937; Tumanov and Krasasvtsev, 1959; Weiser, 1970; Livingston et al., 2005a). In cereals, frost hardening has been linked to a decrease in fructan concentrations in the VTZ (described by Livingston and colleagues as the lower crown) as well as carbohydrate partitioning within the crown itself, with an increase in the SAM (Livingston et al., 2005a; Livingston et al., 2006). In oat and rye crowns, the SAM were had 10 % more non-structural carbohydrates than the VTZ.

2.4.1 Cold-induced modifications to the plasma membrane

Cold-acclimated cells tend to be smaller than non-acclimated cells, lower water content, and high concentrations of solutes (reviewed by Levitt 1980). Acclimated cells also maintain a different membrane lipid phase transition temperature by increasing the ratio of glyceroglycolipids, monogalactosyldiglyceride to digalactosyldiglycerides (Uemura and Steponkus, 1997b). Modifications to lipid raft composition (Minami et al., 2008), membrane-associated dehydrins (Danyluk et al., 1998) and increased concentrations of glycosylphosphatidylinositol (GPI) anchor proteins (Takahashi et al., 2013a; Takahashi et al., 2014; Takahashi et al., 2016) have been linked to cold-acclimation. Dehydrin localization to the plasma membrane (Danyluk et al., 1998) may be due to its primary role in desiccation tolerance. Modifications to the plasma membrane limit the development of hexagonal phase II complexes, improving membrane ability to bind water molecules to reduce dehydration (Steponkus, 1984; Uemura et al., 1995). Freezing-induced dehydration can destabilize the plasma membrane through phase separation of membrane lipids, resulting in physical tearing of the membrane from the cell wall during the freeze-thaw process (Steponkus et al., 1983; Uemura et al., 2006).

2.4.2 Cold-induced modifications to the cell wall

The primary cell wall in *Poaceae* is comprised of cellulose microfibrils embedded in a matrix of pectin, cross-linking glycan and protein. Unlike other angiosperms, members of Poaceae such as wheat have Type II primary cell walls which contain lower concentrations of pectin polysaccharides (2 to 10 % overall) but greater concentrations of cross-linking glycans (β-1,3/1,4-glucans) and hemicellulose. In *Poaceae* cell walls approximately 30 % are 1,3 linked and 70 % are 1,4 linked glucans and the proportion can vary 4 to 15 % during rapid cell growth to 75 % in barley endosperm walls (Albersheim et al., 2011). Type I cell walls have a greater proportion of xyloglucan but a low concentration of gluconoarabinoxylan whereas Type II cell walls contain a greater concentration of gluconoarabinoxylan than xyloglucan.

Pectin polysaccharides such as homogalacturonan, xylogalacturonan, rhamnogalacturonan I and II are anchored to the plasma membrane by proteins. All members of the homogalacturonan class; homogalacturonan, xylogalacturonan, and Rhamnogalacturonan II, have backbones comprised of α-1,4-linked galacturonic acid residues. Rhamnogalacturonan I backbone is comprised of interchanging 1,4-linked galacturonic acid and rhamnose residues. The middle lamella in primary cell walls is comprised of homogalacturonans linked by Ca^{2+} cross-linkages (Jarvis, 1984). In plant cells with secondary cell walls, lignification initiates from the middle lamella (Westermark, 1985). Rhamnogalacturonan II can be cross-linked via borate diester bonds *in vivo* (Matoh and Kobayashi, 1998; Kobayashi et al., 1999). When experimentally supplied with an adequate amount of B, greater than 90 % of the rhamnogalacturonan II polymers are cross-linked (O'Neill et al., 1996). When *Chenopodium album* L. cells were grown in the absence of B^+, they had pore sizes that were 60 % larger than if they were grown with a B^+ source (Fleischer et al., 1999), indicating a potential role for B^+ linked rhamnogalacturonan II in regulating wall permeability.

During cold-acclimation, there is also a biochemical remodelling of the cell wall matrix within the apoplastic or extracellular space (Weiser et al., 1990; Rajashekar and Burke, 1996; Kubacka-Zębalska and Kacperska, 1999; Solecka et al., 1999; Stefanowska et al., 2002; Solecka et al., 2008; Domon et al., 2013; Tanino et al., 2013). These modifications result in the formation of calcium pectin cross-linkages in Type I angiosperms/dicots cell walls (Solecka et al., 2008), accumulation of phenolic secondary compounds (Domon et al., 2013) and cell wall modifying proteins (Weiser et al., 1990; Takahashi et al., 2013a; Takahashi et al., 2013b; Takahashi et al.,

2016). In Type II cell walls, found in *Poaceae*, cell wall rigidity is increased through the cross-linking of glucuronoarabinoxylan and lignin. Glucuronoarabinoxylans are cross-linked by ferulates or p-coumarates to form diferulates and p-coumaric cyclodimers (Fry, 1986). Ferulates act as nucleation sites for lignin formation (Grabber et al., 1998), and form covalent bonds with lignin via free-radical mediated cross-linking (Grabber et al., 2000). Radicals are generated in the cell wall by increased concentrations of peroxidases (Passardi et al., 2004). This cross-linking reaction couples glucuronoarabinoxylan to lignin, which increases wall rigidity and decreases the ability to degrade the cell wall (Grabber et al., 1998).

Cell wall modifications result in enhanced rigidity and reduced porosity of the cell wall matrix serving as a barrier to ice propagation (Wisniewski et al., 1991a; Wisniewski et al., 1991b; Rajashekar and Burke, 1996; Rajashekar and Lafta, 1996). Cells wall expansion is dependent upon water (turgor) pressure within the cell. Cells synthesize, and deposit new material required for cell wall growth and to maintain wall thickness (Hüner et al., 1981; Solecka et al., 2008). A decrease in wall thickness results in the inability to hold turgor pressure and therefore most plants maintain a wall thickness within a factor of two (Bret-Harte et al., 1991). Rigid cell walls reduce the chances of cell collapse during extracellular freezing through improved wall strength and a decrease in pore size (Wisniewski et al., 1991a; Rajashekar and Burke, 1996; Rajashekar and Lafta, 1996). Water diffusivity, carbohydrate, lipid, and protein accumulation are all connected to freezing resistance. Water flows through the cell wall via aquaporins and the plasmodesmata. When plants are subjected to low temperatures, aquaporin genes are down-regulated (Sakurai et al., 2005; Yooyongwech et al., 2008).

2.4.3 Cold-induced modifications to the apoplast

Water potential and turgor pressure gradients are required to move water and solutes from various points within the plant (Boyer and Silk, 2004) and enlarging cells can produce their own growth-induced gradients to facilitate the movement of solutes required for expansion (Boyer, 2001). During cell wall biosynthesis, endoplasmic reticulum can become trapped in the cell plate during vesicle fusion, resulting in the formation of plasmodesmata (reviewed in Albersheim et al., 2011). Plasmodesmata are lined with a single connected plasma membrane, and this space (and the movement of solutes among cells) is called the symplast. Water, ions, signaling molecules, as well as sugars, amino acids, and other organic molecules, can move from cell to cell via symplastic transport. The apoplast comprises the extracellular space (middle lamella and the cell wall).

Apoplastic transport is used to move larger concentrations of water, ions and signaling molecules within the plant. The physiological and biochemical relationship between these two transport systems is important in understanding how plants modify their cell walls in preparation for low temperature stress.

Xylem vessels also play a major role in water transport. Vessels undergo short-term changes in xylem resistance and an increase in ion concentration can cause rapidly reversible decreases in hydraulic resistance (Zwieniecki and Holbrook, 1998; Zwieniecki and Holbrook, 2000; Zwieniecki et al., 2001). Zwieniecki et al. (2000) localized this activity to xylem pit membranes which are comprised of cellulose fibers and pectin. When minerals are taken up by the plant, pectin either swell or shrink. Swelling causes pores in the membranes to expand, which results in slower lateral water flow (Wisniewski et al., 1991b; Zwieniecki and Holbrook, 2000; Zwieniecki et al., 2001). Low concentrations of these ions cause the pectin matrix to contract to result in expanded pores and both Ca^{2+} and B^{+} have been implicated in cell wall integrity (reviewed by (Albersheim et al., 2011).

The apoplast itself undergoes a series of additional modifications during cold-acclimation resulting in the accumulation of soluble sugars, fructans (Livingston and Henson, 1998; Livingston et al., 2005a; Livingston et al., 2006), and AFPs (Antikainen et al., 1996; Pihakaski-Maunsbach et al., 1996; Pihakaski-Maunsbach et al., 2003; Griffith and Yaish, 2004; Griffith et al., 2005). Exposure to temperatures below 0°C, but above lethal sub-zero injurious temperatures enhance freezing tolerance by an additional 3°C to 4°C beyond cold-acclimation (Tumanov and Krasasvtsev, 1959) in part through increased accumulation of cryo-protectant fructans (Livingston et al., 2005a), arabinoxylans (Kindel et al., 1989) and antifreeze proteins (AFPs) (Herman et al., 2006) within the apoplast as well as a reduction in crown free water (Gusta et al., 1975; Gusta et al., 1979; Yoshida et al., 1997).

2.5 Antifreeze proteins

Substances like AFPs, sucrose or arabinoxylans depress the hysteresis freezing point of a solution but have a small effect on their melting point. This difference is known as thermal hysteresis (DeVries and Wohlschlag, 1969). During freezing, AFPs bind to the growing ice crystal surface. The surface of ice between AFPs curves, resulting in a hexagonal or bipyramidal shape and increased ice surface free energy (Griffith and Yaish, 2004). According to the Kelvin effect, ice crystal growth is delayed until temperatures decrease sufficiently to match and surpass the

hysteresis freezing point. Binding interactions between ice and AFPs are thought to be a combination of hydrogen bonding, hydrophobic interactions, and Van der Waals forces (Jia and Davies, 2002). However, the mechanism of ice and plant AFP interactions is still an active area of research.

Since their discovery, AFPs can be considered ice-active if they meet one of the following criteria: (I) proteins that modify ice crystal morphology; (II) inhibit ice re-crystallization with either (III) high or (IV) low thermohysteresis activity. Plant AFPs meet criteria I, II, and IV are found in species that can tolerate freezing tolerance, such as cold-acclimated plants (Griffith et al., 1992; Urrutia et al., 1992; Griffith et al., 2005). The initial definition of AFPs (more specifically antifreeze glycoproteins) reflected their role as 'proteins that prevented freezing' (DeVries, 1971). Advancements in our understanding of plant freezing tolerance, ice restructuring, and ice adhesion, however, have led some to argue that the original AFP definition does fully encompass our current understanding of AFP function in plants (reviewed by Davies, 2014). For this reason, plant AFPs are often referred to in the literature with the more general term, ice-binding proteins. For consistency, these proteins will be referred to as AFPs in this thesis.

2.5.1 Identification and localization of native plant AFPs

Most of the historical research on AFPs in plants has been conducted in winter cereals. Using size exclusion chromatography and gel electrophoresis Griffith and colleagues identified six major and several minor polypeptides with ice crystal modification properties and thermal hysteresis of up to 0.3°C in acclimated winter rye (Griffith et al., 1992). Several plants have been investigated for proteins with antifreeze activity (**Table 2.1**). Ice crystal growth was inhibited with less than 10 μg mL^{-1} of AFPs isolated from perennial ryegrass (*Lollium perenne*), making it 300 x more effective at inhibiting ice re-crystallization than sugars or other antifreeze substances (Sidebottom et al., 2000).

Table 2.1 Selected native plant AFPs.

Plant	Molecular mass (kDa)	Homology	Exposure[a]	Accession No.	Reference
Antarctic hair grass (*Deschampsia antarctica*)	21.9 - 29.2	ice re-crystallization inhibition	C	ACN38302	(John et al., 2009)
Bittersweet nightshade (*Solanum dulcamara*)	29	chitinase-like	C	AAP32201	unpublished, NCBI
Bittersweet nightshade	25	Osmotin-like	C	AAG16625	(Newton and Duman, 2000)
Brachypodium distachyon	16	ice re-crystallization inhibition	C	Unknown	(Bredow et al., 2017)
Perrenial ryegrass (*Lollium perenne*)	29	ice re-crystallization inhibition	C	AJ277399	(Sidebottom et al., 2000)
Wild carrot (*Daucus carotta*)	36	Polygalacturonase inhibitor	C	AAC62932	(Worrall et al., 1998; Meyer et al., 1999)
Winter rye (*Secale cereale*)	32	endo β-1,3-endoglucanase	C, E	AAB35914	(Hon et al., 1995)
Winter rye	Unknown	Lipid transfer protein 1	C	ABG27011	(Doxey et al., 2006)
Winter rye	Unknown	Lipid transfer protein 2	C	ABG27012	(Doxey et al., 2006)
Winter rye	16	Thaumatin-like	C	AAB35912	(Hon et al., 1995)
Winter wheat	26.8	ice re-crystallization inhibition	C, JA, E	AY968588	(Tremblay et al., 2005)
Winter wheat	40.7	ice re-crystallization inhibition	C, JA, E	AY968589	(Tremblay et al., 2005)

[a] Environmental condition required to induce antifreeze response includes exposure to cold temperatures (C), ethylene (E), or jasmonic acid (JA).

Proteins with antifreeze qualities have been isolated from apoplast extracts of cold-acclimated rye crowns (Antikainen et al., 1996) and leaves from rye (Pihakaski-Maunsbach et al., 1996; Hiilovaara-Teijo et al., 1999; Griffith et al., 2005) as well as winter wheat (Tremblay et al., 2005) and other cold-acclimating plants (**Table 2.1**). Using an immunolocalization-tissue printing method, Antikainen et al. (1996) reported AFPs were localized to the apoplast and epidermal cells of cold-acclimated rye leaves. Immunogold localization studies identified antifreeze active glucanases accumulated in xylem vessels, the middle lamellae, as well as cell wall junctions between the mestome sheath cells (Pihakaski-Maunsbach et al., 1996). Endochitinases with thermal hysteresis activity were identified in the growth media of acclimated winter rye callus that lacked an apoplastic region (Pihakaski-Maunsbach et al., 2003). In contrast, the overexpression of a cold-responsive chitinase (*BiCHT1*) in bromegrass (*Bromus inermis* Leyss.) cell suspension cultures resulted in proteins with chitinase activity that lacked the ability to modify ice (Nakamura et al., 2008). More recent shotgun proteomic studies on cold-acclimated Arabidopsis (Takahashi et al., 2016), winter oat and rye leaves (Takahashi et al., 2013a) and winter wheat crowns (Willick et al., 2018a) identified multiple AFPs from apoplast fluids associated with the plant secretome. Together this supports the theory of plant's secreting AFPs into the apoplastic space.

2.5.2 Dual role of AFPs as pathogenesis-related proteins

Hon and colleagues identified five major apoplast proteins with 38, 36, 32, 29 and 26 kDa molecular weights exhibiting high ice re-crystallization inhibition activity and three minor proteins; 15, 13, and 10 KDa, with low ice re-crystallization inhibition activity (Hon et al., 1994). Interestingly, no common epitopes with known fish or insect AFPs could be identified. Hon and colleagues determined these AFPs had a 75 to 88 % sequence similarity with pathogenesis-related proteins; endo-β-1,3-glucanases (38 and 32 kDa), endochitinases (36 and 29 kDa), osmotin/thaumatin-like proteins (26 and 15 kDa) and a lipid transfer protein (13 kDa) (Hon et al., 1995). It should be noted that Nakamura et al. (2008) reported that not all endochitinases synthesized under cold-acclimating conditions modify ice crystals morphology.

Antikainen and Griffith conducted a study of 12 sensitive or tolerant varieties of monocots and dicots exposed to either 20 or 5°C. Antifreeze activity was identified in pathogenesis-related proteins expressed in grasses grown under 5°C (Antikainen and Griffith, 1997). Treatment of nightshade (*Solanum ducalmara* L.) with citrate enhanced antifreeze activity three-fold in samples collected in November and December (Huang and Duman, 2002). However, the only samples that

contained antifreeze activity were those collected during those two cold months. Similarly, cold-acclimated winter cereals had improved tolerance to pathogenic infection as opposed to non-acclimated infected plants (Hiilovaara-Teijo et al., 1999). Similar responses were also noted in Douglas fir (*Pseudotsuga menziesii* var. menziesii) bark infected by pathogens during fall and winter months with greater endochitinase activity and enhanced inhibition of ice re-crystallization (Zamani et al., 2003). Together, these studies intimate that plants require low temperatures to induce the accumulation of antifreeze active pathogenesis-related proteins.

Subsequent experiments involving pathogenesis-related proteins identified applications of abscisic or salicylic acid to winter rye resulted in increased abundance of pathogenesis-related proteins with undetectable antifreeze activity (Yu and Griffith, 2001). Yu and colleagues found only the exposure to cold, drought, ethylene induced antifreeze activity in winter rye (Yu et al., 2001; Yu and Griffith, 2001). In winter wheat, ice re-crystallization inhibition proteins encoded by TaIRI-1 and 2 were identified to have antifreeze activity when exposed to jasmonic acid, ethylene, or cold (Tremblay et al., 2005). Interestingly, winter rye chitinases with antifreeze activity induced by cold-acclimation had the same molecular mass as predicted by the cDNA sequence as the same chitinases induced by ABA treatment (Yu and Griffith, 2001). This demonstrations rye chitinase did not undergo post-translational modification to either gain or lose its antifreeze ability.

2.5.3 Modifications of AFPs and complexing with carbohydrates

Using native gels, acclimated winter rye pathogenesis-related proteins with AFP activity were identified to assemble to form oligomeric complexes. These oligomers were comprised of glucanases, chitinases, thaumatin-like, and lipid transfer proteins (Yu and Griffith, 1999). Formation of these complexes facilitated ice surface binding. Stressmann and colleagues reported calcium ions (Ca^{2+}) interacted with antifreeze active oligomers that had been extracted from cold-acclimated rye leaves (Stressmann et al., 2004). Exposure of oligomers isolated from acclimated rye to Ca^{2+} resulted in their partial dissociation, which revealed ice binding domains. Interestingly, this addition of Ca^{2+} only enhanced chitinase activity but not antifreeze activity. Gupta and Deswal reported the application of Ca^{2+} increased activity as well as β-strand confirmation in two class I chitinases purified from common sea buckthorn (*Hippophae rhamnoides* L.) leaves (Gupta and Deswal, 2014).

Biochemical modifications of AFPs suggest these oligomeric complexes are also associated with oligosaccharides. Two chitinase-like proteins isolated from the rubber tree (*Hevea brasiliensis* Müll.Arg.) were analyzed using crystal structure analysis and docking experiments with oligosaccharides $(GlcNAc)_6$ and provided preliminary evidence for pathogenesis-related protein oligomers complexing with long branching sugars (Martínez-Caballero et al., 2014). In bittersweet nightshade (*Solanum dulcamara* L.) a 67 kDa AFP when exposed to β-galactosidase or lectins resulted in a loss of thermohysteresis properties (Duman, 1994). Collectively, this raises some interesting questions in the field of low temperature plant stress research. First, is the accumulation of arabinoxylans and fructans first reported by Olien and colleagues associated with the formation of pockets of water within ice masses (Olien, 1965; Kindel et al., 1989) due to an association of AFPs complexing with long branching sugars. Second, if these putative AFP-oligosaccharides complexes are present within the apoplast, do they only form under cold conditions, be it acclimating or sub-zero acclimation conditions.

2.5.4 Accumulation of other cryoprotectants and anti-ice nucleating compounds

Exposure to low temperatures results in a myriad of structural, biochemical and physiological changes in plants. The observed changes include a reduction in tissue water content; and increased levels of reactive oxygen species, antioxidants, proline, chlorophyll metabolism, late-embryogenesis- abundant proteins (including dehydrins) and growth-inhibiting compounds such as ABA (Thomashow, 1999). Aquaporins, chaperonins, water binding proteins, lipid transfer proteins, energy production, regulators of cell vesicular traffic, proteins required for PSII functionality and thylakoid integrity, and universal stress proteins can all be induced and regulated by low temperature (Thomashow, 1999; Griffith and Yaish, 2004; Gusta et al., 2009; Hüner et al., 2016).

2.6 Water and ice nucleation

Phase changes of liquid water occur by lowering temperatures or by changes in pressure (Olien, 1973; Olien and Livingston, 2006). However, the importance of changes in pressure near water's melting point is miniscule when compared to the role of cooling. Therefore, liquid water cooled below 0°C if referred to as supercooled. Water has three major states; liquid, vapour and solid. For water to transition from one state to another (liquid to solid), a nucleator must be present. As the phase change occurs, the nucleator initiates growth of the new phase (solid) until (I) all the

mass is converted or (II) the temperature stabilizes at a new equilibrium point. The growth of the new phase is controlled by the rate at which the latent heat is released.

Pure water can remain un-frozen, referred to as the homogenous nucleation temperature, to temperatures as low as -40°C (Gusta et al., 2009). In nature, supercooling of free water in plants is limited by the presence of a mineral or organic substance occurring at temperatures above -10°C. Heterogenous ice nucleation is most often initiated extrinsically, on the surface of the plant tissue (Maki et al., 1974; Lindow et al., 1978a; Lindow et al., 1982; Hill et al., 2014). Conversely, the presence of ice nucleators within the plant, such as within an ice sink or the extracellular space can initiate intrinsic ice nucleation (Brush et al., 1994; Kishimoto et al., 2014a; Kishimoto et al., 2014b). The temperature at which a heterogenous nucleator induces ice formation is dependent upon the ice-nucleating properties of the specific compound (Maki et al., 1974; Lindow et al., 1978a; Lindow et al., 1982; Brush et al., 1994; Wisniewski et al., 1997; Kishimoto et al., 2014a; Kishimoto et al., 2014b; Ishikawa et al., 2015; Bredow et al., 2017).

In the last century, multiple organic and biological extrinsic nucleators have been identified (**Table 2.2**). While published research on the role of extrinsic nucleators decreased in the 1990s, interest in the subject specifically the use of nucleators to visualize pattern of ice nucleation with infrared video thermography (Wisniewski et al., 1997; Gusta et al., 2004; Griffith et al., 2005; Fuller et al., 2007; Wisniewski et al., 2008; Kuprian et al., 2014; Livingston et al., 2016), identification of plant tissues or organs acting as ice sinks (Kishimoto et al., 2014a; Kishimoto et al., 2014b; Ishikawa et al., 2015) has gained attention in the last ten years.

Water can also be bound in a plant system, through weak hydrophobic or strong (H-bond) interactions with intrinsic structures or substances within the plant. In both micro-organisms (Mazur, 1969) and cold-acclimated wheat crowns (Gusta et al., 1975) approximately 10 % of water remains unfrozen beyond -20°C. A fraction of unfrozen water is bound to extra and intracellular colloids of varying strength (Towill and Mazur, 1976; Gusta et al., 1979; Rajashekar and Burke, 1996). Nuclear magnetic resonance (NMR) (Gusta et al., 1975; Gusta et al., 1979) and magnetic resonance microimaging (MRMI) (Millard et al., 1995; Ishikawa et al., 1997; Fennell and Line, 2001; Yooyongwech et al., 2008; Kalcsits et al., 2009; Pielot et al., 2015) can be used to differentiate between bound and liquid water based upon water mobility and diffusivity in the plant tissue (Tanner, 1983; Gruwel et al., 2007; Kalcsits et al., 2009).

Table 2.2 List of select heterogeneous ice nucleators.

Nucleator	Source	Temperature (°C)	Reference
AgI	Mineral	-5	(Vonnegut, 1947)
PbI_2	Mineral	-6	(Vali, 1995)
CuI	Mineral	-6	(Vali, 1995)
HgI_2	Mineral	-6	(Vali, 1995)
Covellite (CuS)	Mineral	-4 to -5	(Vali, 1995)
Vaterite ($CaCO_3$)	Mineral	-4 to -5	(Vali, 1995)
Miersite (CuI & AgI)	Mineral	-1.4	(Passarelli Jr et al., 1974)
Metalaldehyde	Organic	-0.4	(Fukuta, 1963)
Aliphatic alcohols ($C_nH_{2n+1}OH$)	Organic	Around 0	(Gavish et al., 1990)
Pseudomonas syringae (and spp.)	Leave, root xylem, soil	-2 to -4	(Maki et al., 1974; Lindow et al., 1978a; Lindow et al., 1982)
Erwinia spp.	Leaves, aerial organs	-2 to -4	(Lindow et al., 1978b)
Xanthomonas spp.	Leaves, aerial organs	-2 to -4	(Kim et al., 1987)

Olien argued that cell wall carbohydrates interact with the ice liquid interface which resulted in less perfectly structured ice (Olien, 1965). Similar arguments have been made by Griffith and colleagues, suggesting that plant AFPs interface with the ice crystal lattice to modify future direction and growth (Griffith and Antikainen, 1996; Griffith and Yaish, 2004; Griffith et al., 2005). Sugars can retain and substitute water via hydrogen bonds in proteins sensitive to dehydration (Heber and Santarius, 1964). Sugars are also thought to interact with proteins and water associated with plant membranes. If the ice lattice draws water away from lipid-protein complexes within the membrane, this could result in membrane disruption (Steponkus, 1984).

2.6.1 Barriers to ice nucleation and propagation

Throughout the literature three types of barriers have been identified to isolate freezing-sensitive tissues from ice nucleation; structural, thermal, and nucleation barriers (Ishikawa and Sakai, 1981; Wisniewski et al., 1991a; Ishikawa et al., 1997; Wisniewski et al., 1997; Kuprian et al., 2014; Ishikawa et al., 2016; Kuprian et al., 2016). Wisniewski and Fuller (1999) hypothesized that ice nucleation induces the physical growth of an ice crystal into the leaf through a stomate, wound, broken epidermal hair or a surface lesion. Visualization of freezing in leaves using IRVT has shown the mid-rib, base of leaf petioles, vascular bundles and phloem can all act as preferential sites for freezing (Wisniewski and Fuller, 1999; Taschler et al., 2004; Hacker and Neuner, 2007, 2008). In both rhododendron (*Rhododendron ferrugineum* L.) (Wisniewski and Fuller, 1999) and cranberry (*Vaccinium macrocarpon* Ait. Stevens) (Workmaster et al., 1999) leaves, ice propagation occurred through cracks in the cuticle layer, stroma and epidermal trichomes. Internally, the initial formation of an ice crystal acts as the nucleus to induce the freezing of extracellular water. Remaining intracellular water will equilibrate with the vapour pressure of the ice in a temperature-dependent manner (Olien, 1973; Olien and Livingston, 2006). In the field, the temperature at which leaves would freeze individually was based on their age, location within the canopy (Legge et al., 1983) and whether they were wet or dry (Levitt, 1980; Antikainen et al., 1996; Gusta et al., 2004). In reproductive cereals exposed to freezing, nodes within the stem (Single, 1964; Single and Olien, 1967) and rachis within the head developing head (Fuller et al., 2007; Livingston et al., 2016) inhibit the propagation of ice. A barrier was postulated between the leaves, stem and overwintering crown (Pearce and Fuller, 2001).

Epicuticular waxes (Wisniewski and Fuller, 1999; Aryal and Neuner, 2010; Hacker et al., 2011; Neuner, 2014) or synthetic substances endogenously applied to the leaf surface (Fuller et

al., 2003; Wisniewski et al., 2008) act as a hydrophobic barrier and prevent the initiation of an ice-nucleating event. Wisniewski and colleagues reported foliar application of a synthetic hydrophobic kaolin film to tomato (*Lycopersicon esculentum* L.) (Fuller et al., 2003), potato (*Solanum tuberosum* L.), citrus (*Citrus limon* L.) and grape (*Vitis vinifera* L.) (Wisniewski et al., 2008) induced supercooling to around -6°C, regardless of the presence of an INA^+. Whereas un-coated plants sprayed with an INA^+ were killed at around -2°C. Neuner and colleagues reported in high altitude plants with low night-time temperatures and dew formation is frequent that the presence of thick waxy cuticles is essential for alpine plants to avoid freezing of sensitive reproductive tissues (Hacker and Neuner, 2007, 2008; Aryal and Neuner, 2010; Hacker et al., 2011; Kuprian et al., 2014; Neuner, 2014; Kuprian et al., 2016).

Thermal ice barriers modified during dormancy induction in tree buds or cold-acclimation in herbaceous and woody plants result in the accumulation of cryoprotectants (i.e. sucrose, arabinoxylans, fructans) to increase differences between melting and freezing point of cellular fluids (Kuprian et al., 2017). Structural barriers are associated with chemical modifications to the cell wall (Griffith and Brown, 1982; Griffith et al., 1985; Tanino et al., 1990; Wisniewski et al., 1991b; Rajashekar and Lafta, 1996; Zabotin et al., 1998; Kubacka-Zębalska and Kacperska, 1999; Boudart et al., 2005; Solecka et al., 2008; Domon et al., 2013; Kasuga et al., 2013; Carvajal et al., 2015) or plasma membrane (Steponkus, 1984; Uemura et al., 1995; Danyluk et al., 1998; Yamada et al., 2002; Uemura et al., 2006; Minami et al., 2008; Takahashi et al., 2013a; Takahashi et al., 2013b; Takahashi et al., 2014) that act as a physical barrier to ice propagation into freezing sensitive tissues. Intrinsic nucleators can also act as a barrier and manage the location of initial ice formation by initiating intracellular or extracellular freezing in freezing tolerant due to increased concentrations of polysaccharide ice nucleators (Griffith and Antikainen, 1996) or structures such as the scales of tree buds (Wiegand, 1906b; George et al., 1974; Ishikawa and Sakai, 1981; Rajashekar, 1989; Ishikawa et al., 2015).

2.7 Freezing in crowns and plant organs

2.7.1 Crown anatomy

The vegetative crown is classified as a plant organ. The crown can be further subdivided into two major groups of tissues, the SAM and VTZ, that initiate the growth of new leaf and root organs (**Figure 2.1**). The SAM is located above the first internode. The apical meristem in the

SAM is comprised of small non-vacuolated cells that have a tunica-corpus organization (Purvis and Gregory, 1937). The tunica consists of peripheral cell layers that divide perpendicular to the apical meristem surface (anticlinal). Whereas the corpus cells are less organized and undergo cell division in various planes. The number of tunica layers varies in angiosperms, but on average, festucoid grasses contain two tunica layers while cereals contain only one (Brown et al., 1957).

Leaves are initiated by periclinal divisions in a small group of cells at the side of the apical meristem. As leaves develop, peripheral corpus cells form a hypodermal layer that resembles a second tunica layer (Sharman and Hitch, 1967). Tiller buds develop in the axils of the first leaf. Axillary buds are flattened by developing leaf bases and form vascular connections with the adjacent nodes and bundles descending from higher leaves connecting to the VTZ (Williams et al., 1975). Procambial strands provide vascular connections for individual leaves. In wheat, strands associated with the apical meristem terminate in a layer of cells at the base of the meristem tissue (Sharman and Hitch, 1967). Sharman and Hitch (1967) did not visually observe any strands within this intermediate region of cells. Similar observations regarding the strands led to the hypothesis that the strands were not directly connected to the vascularized tissue in the VTZ. This intermediate zone, between the VTZ and SAM, is comprised of smaller vacuolated cells (reviewed by Gusta et al., 2009).

Winter wheat crown VTZ has large, highly vacuolated cells (reviewed by Gusta et al., 2009). The VTZ and the primary root stele are joined at the nodal plate (Avery, 1930; Boyd and Avery, 1936). A wheat seedling produces on average six seminal roots originating from parenchyma cells near the pericycle of the primary root, whereas adventitious roots develop from the mature root axis, intercalary and lateral crown meristems (Bonner and Devirian, 1939; Evert, 2006). Chen et al. (1983) reported the limiting factor to recovery in Norstar wheat and Puma rye was adventitious roots regeneration. The rate of injury was correlated to the degree of vascular segmentation at the base of the crown (Aloni and Griffith, 1991).

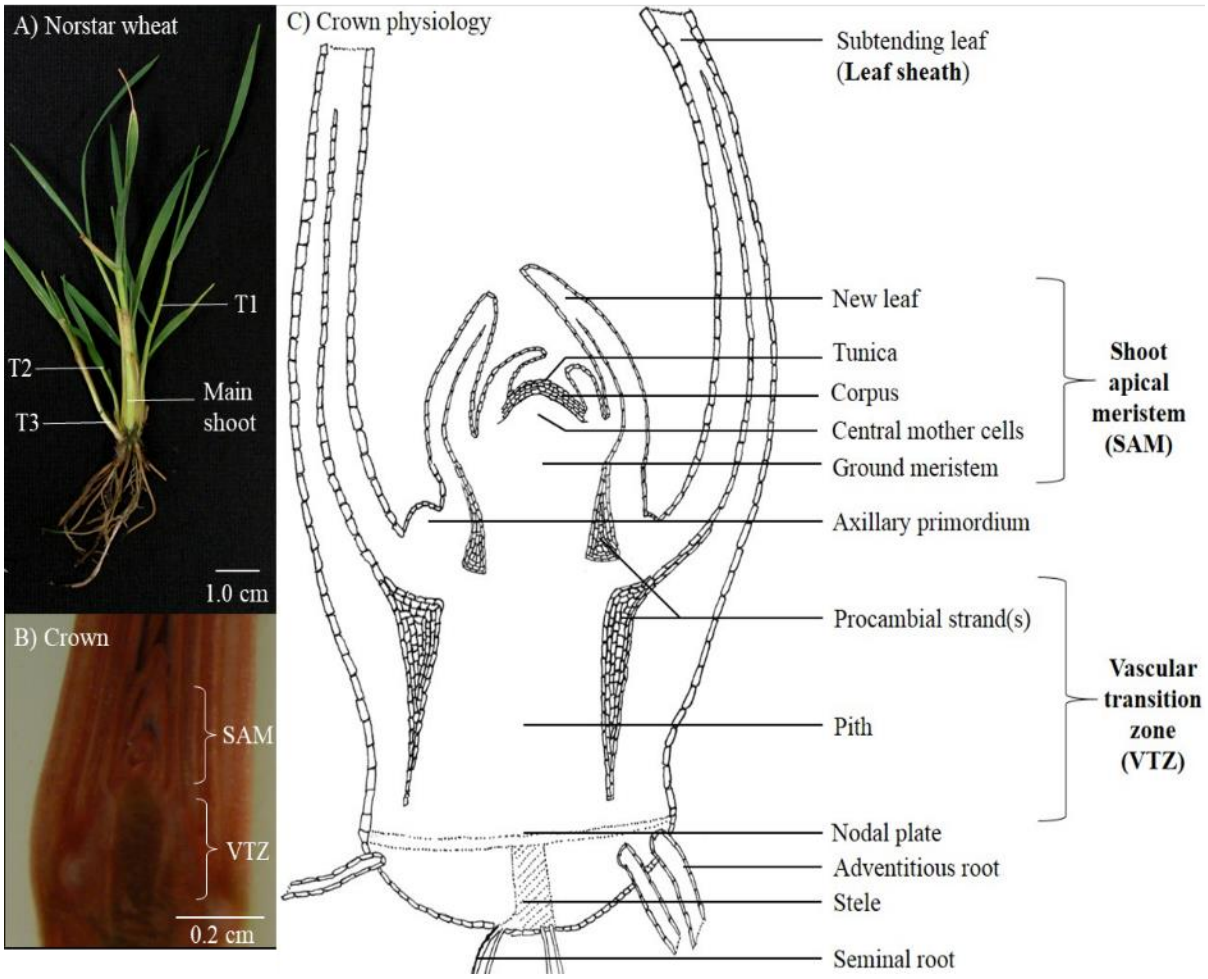

Figure 2.1 Anatomy of the winter wheat crown.

A) Cold-acclimated Norstar wheat grown hydroponically with labelled main shoot and first three tillers (T1 to T3). B) Cold-acclimated Norstar wheat crown, sectioned longitudinally and stained with a tetrazolium chloride viability stain to provide contrast. C) Schematic drawing from visual observations of a median longitudinal section through the winter wheat crown. Anatomical notes are provided as described by Boyd and Avery (1936) and Sharman and Hitch (1967).

2.7.2 Freezing strategies in plants and parallels with crowns

Extra-organ freezing in overwintering tree buds was independently re-discovered by French (Dereuddre, 1978), Japanese (Sakai, 1979), Canadian (Quamme, 1978) and American (Graham and Mullin, 1976) researchers in the 1970's, following its previous identification earlier in the 20th century (Wiegand, 1906a; Wiegand, 1906b; Dorsey and Strausbaugh, 1923; Dorsey, 1934). Sakai (1979) and Dereuddre (1978) independently postulated the theory of 'extra-organ freezing'. Extra-organ freezing was initially defined in complex plant organs as the segregation of ice into sinks, outside of freezing sensitive tissues (Dereuddre, 1978; Sakai, 1979). Sakai and Larcher (1987) would clarify that extra-organ freezing requires the ice sink to be located outside of the freezing sensitive organ. In the case of trees, the bud scale is classified as a separate plant organ from the tree bud.

Sakai postulated that for extra-organ freezing two criteria must be met. (I) The primordia (freezing sensitive tissue) must survive freezing-induced dehydration and (II) ice cannot penetrate the freezing sensitive tissue (Sakai, 1979; 1982; 1983). These findings were independently confirmed in hard-wood and alpine plants (Quamme, 1978; Quamme et al., 1982; Ashworth, 1984; Quamme et al., 1995; Kuprian et al., 2014; Kuprian et al., 2016). Ishikawa and colleagues would expand upon this definition. (III) Freezing-sensitive tissue must be slowly cooled (2°C h^{-1}). (IV) Tissue between the freezing-sensitive tissue and the ice sink may act as a barrier to freezing. (V) Ice sinks have higher ice nucleation temperatures than the remainder of the plant organ (Ishikawa and Sakai, 1981; Ishikawa et al., 1997; Ishikawa et al., 2015; Ishikawa et al., 2016).

In overwintering flower buds, scales act as an ice sink for nucleation while water is withdrawn from freezing-sensitive primordium and/or florets (Dorsey, 1934; Graham and Mullin, 1976; Dereuddre, 1978; Quamme, 1978; Ishikawa and Sakai, 1981; Ishikawa and Sakai, 1982; Quamme et al., 1995; Ishikawa et al., 1997; Ishikawa et al., 2015; Ishikawa et al., 2016). Similarly, bark can act as an ice sink to draw water away from freezing sensitive cells in blueberry stems (Kishimoto et al., 2014a; Kishimoto et al., 2014b). Both winter wheat and rye have a visually analogous bud scale structure, known as the leaf sheath, that surrounds the SAM (**Figure 2.1; Figure 2.2**). No research on the potential role of the leaf sheath in the mechanism of cold-acclimated crown freezing survival has been postulated in the literature.

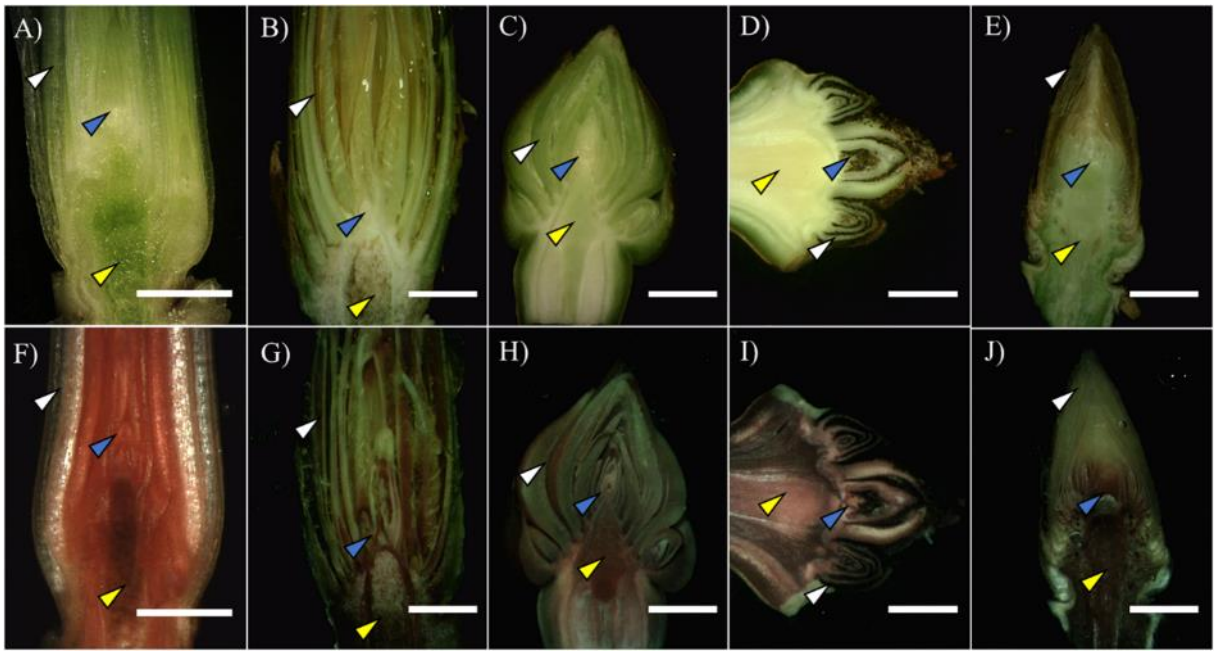

Figure 2.2 Comparison of winter wheat Norstar crown and terminal tree bud anatomy.

Crowns (A, F) were collected from cold-acclimated wheat (*Triticum aestivum* L.) grown hydroponically in the phytotron (Section 3.2.1). Canadian poplar (*Populus* x *canadensis* Moench) (B, G), lilac (*Syringa vulgaris* L.) (C, H), green ash (*Fraxinus pennsylvanica* Marshall) (D, I) and Norway spruce (*Picea Abies* L. [H. Karst]) (E, J) were sampled on October 17, 2017 near the University of Saskatchewan campus. All samples were sectioned longitudinally, mounted in distilled water and imaged with a dissecting microscope (A-E). Sections were stained overnight with tetrazolium chloride to provide contrast (F-J). White arrows indicate the leaf sheath in wheat and the scale in tree buds. Blue arrows indicate the shoot apical meristem in wheat and the shoot primordia in buds. The yellow arrow indicates the vascular tissue. Scale bar = 0.4 cm.

The term extra-organ freezing is often confused with extra-tissue freezing, which is defined as the translocation of water from supercooling tissues to ice sinks in adjacent tissues. In dormant peach (*Prunus* spp) (Dorsey, 1934; Quamme, 1978; Ashworth, 1984; Ashworth et al., 1989), larch (*Larix kaempferi*) (Endoh et al., 2014), and different North American and Asian conifer buds (Sakai, 1979, 1982; Sakai, 1983), an additional ice sink forms in the stem tissues subtending the bud. In winter cereal crowns, the VTZ acts as an ice sink and is freeze injured before the SAM (Olien, 1964; Olien and Marchetti, 1976; Chen et al., 1983; Tanino and McKersie, 1985; Livingston et al., 2005b; Livingston et al., 2013).

The alpine shrub, *Calluna vulgaris*, lacks a bud scale and instead has a barrier region between the floral and vegetative tissues located at the base of the pedicel (Kuprian et al., 2014; Kuprian et al., 2016). This 250 μm thick region lacks pith and intercellular spaces. The cell walls were thicker and had higher concentrations of lignin, suberin, cutin and cellulose than the surrounding floral or vegetative tissues (Kuprian et al., 2016). Livingston and colleagues reported suberized xylem plugging occurred in the vascular tissue in cold-acclimated winter oat, barley, wheat and rye seven days after freezing injury (Livingston et al., 2005b; Livingston et al., 2013). However, this was hypothesized to reduce the spread of necrotic post-secondary injury and not ice propagation. In reproductive wheat, ice propagation was halted at stem and rachis nodes (Single, 1964). These nodes contain higher concentrations of lignin, cellulose and alkyl esters in cultivars more resistant to Fusarium Head Blight (Lahlali et al., 2015; Lahlali et al., 2016). Lahlali and colleagues suggested reduced permeability of the cell wall to water movement.

Kuprian et al. (2016) reported an increase in vascular segmentation and smaller pit apertures at the base of the pedicel. Aloni and Griffith (1991) reported differences in cereal vascular segmentation that was hypothesized to protect roots from embolism formation. Winter rye wheat and barley were highly segmented and contained a greater abundance of tracheid's than maize (*Zea mays* L.), oat and sorghum (*Sorghum bicolor* L.) which has a continuous vascular system from the roots up into the crown (Aloni and Griffith, 1991). In field grown winter wheat, triticale (× *Triticosecale*), and rye, a high degree of vascular segmentation reduces the rate of ice propagation into the crown from the roots (Zámećník et al., 1994).

Single and Olien (1967) postulated the re-distribution of water prior to freezing resulted in 'dry barrier regions' that slowed the spread of ice crystallization. Vascular tissue connecting the scales to the primordium or floret can act as a barrier to ice propagation into the freezing-sensitive

tissue. These vascular traces, also known as the crown cell plate, act as a barrier to water translocation (Yooyongwech et al., 2008; Kalcsits et al., 2009) due to a decrease in aquaporin activity (Yooyongwech et al., 2008). Following cold-acclimation, the crown cell plate developed thickened cell walls (Owens and Molder, 1976; MacDonald and Owens, 1993).

The barrier region between the freezing sensitive tissues may have a different chemical composition. In cold-acclimated Norway Spruce (*Picea abies* L. Karst) terminal buds, di-, tri- and tetra- oligosaccharins and pectin increases in the crown plate below the primordia (Kuprian et al., 2017). Lee and colleagues reported an increase in de-methylesterified pectin and callose in the crown plate of cold-acclimated terminal Norway spruce buds (Lee et al., 2017). This region may slow or mitigate the spread of ice into the primordia. An intermediate region between the SAM and VTZ has been postulated in the literature (Gusta et al., 2009). Post-freezing histological analysis of cold-acclimated oat identified a suberized region between the VTZ and SAM (Livingston et al., 2005b; Livingston et al., 2013). Vital staining of freeze-injured winter wheat (Tanino and McKersie, 1985) and oat (Livingston et al., 2013) revealed the intermediate region beneath the SAM was the farthest limit of injury in recovering crowns. The intermediate region's role in mitigating ice propagation into the SAM has not been elaborated on outside of observational studies. It is possible that the crown survives freezing by using the leaf sheath (extra-organ freezing) and VTZ (extra-tissue freezing) as ice sinks, in a similar fashion to the bud scale and vascular bud trace region to allow the SAM to supercool during cold-acclimation and freezing.

2.8 Fourier transform infrared spectroscopy

Use of gas-chromatography mass-spectrometry is the classical method for obtaining precise chemical information but can destroy critical complementary information such as the spatial localization of compounds at the tissue and cellular (McCann et al., 1992; McCann et al., 1997). FTIR was developed with conventional light sources to study chemical constituents within plant cell walls (McCann et al., 1997) and whole plant tissues (Lahlali et al., 2015; Willick et al., 2018b). Recent synchrotron FTIR spectroscopic studies on cell wall and plant tissues using Japanese bunching onion (*Allium fistulosum* L.) mapped changes in the ratios of carbohydrate/ester and alpha helical/beta sheet protein secondary structures during cold-acclimation (Tanino et al., 2013). Whole cell and tissue level changes in apoplastic and plasma membrane regions may be a mechanism directly involved in cold-acclimation and tolerance to potential low temperature stress.

Mapping with FPA has also been used to quantify amide I and II protein damage caused by frost (Xin et al., 2013) or fungal (Singh et al., 2011) damage in spring wheat kernels.

Yu et al. (2003) used FTIR-FPA to localize total lignin, protein, cellulose, carbohydrates, and lipid distributions in the pericarp, seed coat, aleurone and endosperm of barley seed cross sections. Research on malting and feed barley varieties revealed relative differences in the proportion and ratio of protein α-helices, β-sheets, β-turns, and random coils (Yu 2006). Focal plane array mapping with FTIR spectroscopy allowed for both the localization of relatively pure protein areas within tissues as well as reveal protein secondary structure explaining the biological differences noted among varieties. While FTIR can semi-quantify protein secondary structures, the identification of individual proteins requires proteomic analysis (Boudart et al., 2005).

2.9 Wheat

Wheat (*Triticum aestivum* L.) accounts for over 20 % of the worlds food source, rivaled only by rice (*Orzya sativa* L.) and corn (*Zea mays* L.) in terms of overall caloric consumption (Shiferaw et al., 2013). Most cultivated wheat is allohexaploid (2m = 6x = 42) composed of three genomes (BBAADD). The genomes originate from a cross of *Triticum urartu* Thum. Ex Gandil (AA) and an ancestor of *Aegilops speltoides* (Tausch) Gren. (BB) with *Aegilops tauschii* (DD). Winter wheat is postulated to be of Mediterranean origin as inferred from SSR markers (Dvorak et al., 2012) and nuclear rDNA sequence (Hsiao et al., 1995) studies. Historically, winter and spring growth habits were identified by Linnaeus in his 'Species Plantarum' (Linnaeus 1753, reviewed by (Hayes and Aamodt, 1927). Takahashi (1925) would later divide the growth habit into four groups: (I) a winter growing habit; (II) a spring growing habit; (III) an intermediate habit that is winter hardy and ripens if sown in the spring; and (IV) a pseudo-habit that has a winter habit but is not winter hardy (Takahashi 1925, reviewed by Hayes and Aamodt, 1927). Spring and winter growth habits are determined by the *VRN* genes; *VRN1, VRN2*, and *VRN3* (Galiba et al., 2009) and *VRN4* (Kato et al., 2003). The *VRN4* is only responsive when plants are exposed to a short vernalization period (Yoshida et al., 2010). The *Vrn-A1* is the strongest inducer of the spring growth habit (Yan et al., 2003).

In 2014 of the 23.8 million acres of wheat were grown in Canada, winter wheat accounted for only 9.6 % (www.statcan.gc.ca). Winter wheat has a long history in Western Canada. Buller (1919) reported that in Southern Alberta, 24,300 ha of winter wheat, comprised predominantly of

Turkey Red and Kharkov, was seeded in comparison to over 6 Mha of spring wheat (reviewed by McCallum and DePauw, 2008). Kharkov MC22 was selected for in 1912 at Macdonald College (Quebec, Canada) had a high level of winter hardiness, and remained the predominant winter wheat seeded in Western Canada until the 1970s (Klinck and Grant, 1964; McCallum and DePauw, 2008). Kharkov MC22 would be replaced by Winalta, due to its shorter height, earlier maturity and higher yields. Winalta was then replaced by Norstar (registered in 1977) which had superior freezing survival compared to Winalta and Kharkov as well as 11 % higher yield than Winalta (Grant, 1980). Norstar was the major winter wheat in Western Canada from 1985 to 1992 but was replaced by semi-dwarf cultivars less prone to lodging, with higher resistance to leaf (*Puccinia triticina* Eriks.) and stem (*Puccinia graminis* Eriks. and E. Henn.) rust (McCallum and DePauw, 2008). Norstar was the starting point for most North American breeding programs studying cold hardiness in the 1980's to the present day. As of 2016, the three most prominent winter wheat cultivars (insured commercial acres) seeded in Alberta (Radiant), Saskatchewan (CDC Buteo, Emerson and Moats) and Manitoba (Emerson) (www.grainscanada.gc.ca, accessed Oct 16, 2017) were selected from the progeny of a cross with Norstar (Fowler, 2010; Thomas et al., 2012) or a cultivar whose parent was selected from a cross with Norstar (Fowler, 2012b; Graf et al., 2013). Norstar continues to be used in field and laboratory freezing tests as a check (Fowler, 2012a).

2.10 Rye

Winter rye is the most cold hardy cultivated cereal grown in Canada (LT_{50} -34°C) and can be grown under poor environmental conditions and soil types. Cultivated rye grown in Canada is predominantly diploid and believed to originate from the regions surrounding the Black and Caspian seas (Bushuk, 2001). In Canada, rye production is relatively small in comparison to wheat. In 2014, only 206,000 acres were planted in Canada (www.statcan.gc.ca). Hazlet rye was first developed at the Semiarid Prairie Research Centre of Agriculture and Agrifood Canada, Swift Current, Saskatchewan, and was registered with the Canadian Food Inspection Agency in April 2006 (McLeod and Gan, 2008). From 2014 to 2016, Hazlet was the dominant rye seeded in Saskatchewan and Manitoba (www.grainscanada.gc.ca, accessed Oct 16, 2017). Preliminary artificial freezing tests reported Hazlet was not as cold-hardy as its predecessor, Puma. Puma (Shebeski et al., 1973) has been widely used for cold-acclimation and freezing studies in the last thirty years. This thesis uses a combination of Norstar and/or Hazlet and Puma as model systems to study the cold-acclimated mechanism of crown freezing.

Chapter 3

3 Tissue-specific changes in apoplastic proteins and cell wall structure during cold-acclimation of winter wheat crowns.

3.1 Abstract

The wheat (*Triticum aestivum* L.) crown is the critical organ of low temperature stress survival over winter. In cold-acclimated crowns, ice formation in the apoplast causes severe tissue disruption as it grows at the expense of intracellular water. While previous crown studies have shown the vascular transition zone (VTZ) to have a higher freezing sensitivity than the shoot apical meristem (SAM), the mechanism behind the differential freezing response is not fully understood. Cooling cold-acclimated crowns to -10°C resulted in an absence of VTZ tetrazolium chloride staining. Whereas the temperature at which 50 % of SAM stained positive and 50 % of plants recovered (LT_{50}) were similar after cold-acclimation for 21 (-16°C) and 42 d (-20°C) at 4°C. Proteomic analysis of the apoplastic fluids identified dehydrins, vernalization-responsive, and cold shock proteins preferentially accumulated in the SAM. In contrast, modifications to the VTZ centred on increases in pathogenesis-related proteins, antifreeze proteins and sugar hydrolyzing enzymes. Fourier transform infrared spectroscopy focal plane array analysis identified the biochemical modification of the cell wall to enhance methyl-esterified cross-linking of glucuronoarabinoxylans in the VTZ. These findings indicate the SAM and VTZ express two distinct tissue-specific apoplastic responses during cold-acclimation.

3.2 Introduction

Overwintering success is contingent on the degree of tolerance and/or avoidance within the crown to freezing – a combination of cold, mechanical, drought, and osmotic stresses (Levitt, 1980). Within the crown, mechanical damage from ice crystallization occurs first in the vascular transition zone (VTZ) located between the shoot apical meristem (SAM) and the nodal plate (Olien and Marchetti, 1976; Tanino and McKersie, 1985; Livingston et al., 2013). Severe VTZ freezing injury impedes the regeneration of new roots resulting in plant starvation and a delayed death response (Chen et al., 1983). However, the interplay between the initial damage to the VTZ and a perceived lack of damage to the SAM is not fully understood.

Winter cereals pre-exposed to cold temperatures undergo a series of biochemical, biophysical and molecular modifications, known as cold-acclimation (Olien, 1964; Griffith et al., 1985; Griffith et al., 2005; Livingston et al., 2006; Takahashi et al., 2013a). In cold-acclimated plants, ice propagates in the apoplast and must remain in this space for the plant to avoid lethal intracellular freezing (Siminovitch and Scarth, 1938). Despite evidence supporting different physiological (Chen et al., 1983; Tanino and McKersie, 1985; Livingston et al., 2013) and biochemical (Livingston et al., 2006) tissue-specific responses to freezing, most winter cereal cold-acclimation studies treat the crown as a single unit (see review by Gusta et al., 2009). Identification of differences in cold-acclimated SAM and VTZ apoplastic space could explain differences in tissue-specific freezing injury but has largely been unexplored.

The apoplast encompasses the primary cell wall, middle lamella and intercellular air spaces. Type I cell walls contain equal amounts of cellulose and xyloglucans embedded in a pectin matrix (Carpita and Gibeaut, 1993; Hatfield et al., 2016). Winter wheat and other members of *Poales* have Type II cell walls composed of cellulose interlocked with glucuronoarabinoxylans, mixed linked β-glucans and small quantities of pectin and xyloglucans (Carpita and Gibeaut, 1993; Carpita et al., 2001; Hatfield et al., 2016). As plant cold hardiness is acquired, in both ABA-acclimated cell suspension cultures (Reaney et al., 1989; Tanino et al., 1990; Tanino et al., 1991) and cold-acclimated plants (Hüner et al., 1981; Griffith et al., 1985; Weiser et al., 1990; Rajashekar and Burke, 1996; Rajashekar and Lafta, 1996; Kubacka-Zębalska and Kacperska, 1999; Yamada et al., 2002; Solecka et al., 2008; Domon et al., 2013; Kasuga et al., 2013; Baldwin et al., 2014; Tenhaken, 2015) cell walls increase in thickness and rigidity. Cell walls can be modified during the natural turnover of components (Carpita and Gibeaut, 1993; Hatfield et al., 2016) or

reconfigured by modifying proteins (CWMPs) during cold-acclimation (Weiser et al., 1990; Takahashi et al., 2013a; Takahashi et al., 2013b; Takahashi et al., 2016). In cold-acclimated winter oilseed rape (*Brassica napus* subsp. *oleifera* L.), pectin methylesterase cleaves methyl ester groups to promote calcium cross-linking and subsequent increases cell wall strength and rigidity (Stefanowska et al., 2002; Solecka et al., 2008). In Type II cell walls, peroxidases oxidize phenolic compounds to synthesize radicals needed to dimerize of cell wall covalent esterified linkages (Fry, 1986; Hatfield et al., 2016). Glucuronoarabinoxylans are cross-linked with lignin to enhance wall rigidity by phenylpropanoid hydroxycinnamates such as ferulic acid (Fry, 1986; Carpita and Gibeaut, 1993; Domon et al., 2013; Baldwin et al., 2014). In cold-acclimated cereals, the apoplastic space contains a range of solutes including arabinoxylans (Olien, 1965; Kindel et al., 1989), fructans, and sucrose (Livingston and Henson, 1998; Livingston et al., 2005a; Livingston et al., 2006) that modify ice crystal growth (Olien and Smith, 1977). Proteomic studies on apoplastic fluids collected from cold-acclimated winter cereals have also identified transport, oxidative response, pathogenesis-related, and antifreeze proteins (AFPs) (Herman et al., 2006; Takahashi et al., 2013a; Takahashi et al., 2013b) associated with enhanced freezing tolerance and ice re-crystallization inhibition (Knight et al., 1995; Griffith and Yaish, 2004).

The use of gas chromatography-mass spectrometry has provided valuable information on cell wall composition (Carpita and Gibeaut, 1993; Carpita et al., 2001; Hatfield et al., 2016). However, bulk sampling can unintentionally mask modifications to the cell wall. Fourier transform infrared spectroscopy (FTIR) coupled with a spectro-microscope address this problem by selecting a point of interest within the cell wall. Individual bonds associated with specific chemical functional groups have unique vibrational frequencies (see reviews by McCann et al., 1997; Vijayan et al., 2015). Infrared spectra specific peak width and absorbance intensity can then be used to explain the relative difference in cell wall composition when exposed to environmental stress. In spring wheat kernels, FTIR coupled with a focal plane array (FPA) detector was used to identify frost injury to the cell wall (Xin et al., 2013).

Tanino et al. (2013) identified differences in pectin methyl-esterification and protein secondary structure differences within the apoplastic space of cold-acclimated onion (*Allium fistulosum* L.) epidermal cells. By overlaying optical images of crown sections with chemical information from infrared spectra, relative changes in cell wall composition can be characterized following cold-acclimation.

3.2.1 Hypothesis

Cold acclimated Norstar SAM and VTZ have two distinct apoplast proteomes that are optimized for tissue-specific freezing survival strategies.

3.2.2 Objectives

Due to the vast number of potential factors involved in freezing tolerance and/or avoidance, a systematic approach is needed to identify important tissue-specific proteomic and biochemical changes localized with the apoplast. The following objectives were proposed for the study: (I) identify differences in the cold-acclimated SAM and VTZ apoplast using shotgun proteomics and (II) contrast these proteomic changes with FTIR-FPA tissue level mapping in the crowns of winter wheat Norstar (Grant, 1980).

3.3 Materials and methods

3.3.1 Plant growth conditions

Imbibed Norstar seeds were held at 4°C for 48 h. Seeds were transferred onto 14 x 24 cm polyethylene trays and then incubated in the dark at 21°C for 48 h. Once roots were 1 to 2 cm in length, plants were transferred to hydroponic tanks and grown in aerated half strength modified Hoagland's solution as described by Chen et al. (1983). Tanks were transferred into a constant 20°C growth chamber, with a 16 h day and photosynthetic photon flux density (PPFD) of 400 µmol m^{-2} s^{-1} until seedlings reached the third to fourth leaf stage. For cold-acclimation, plants were transferred to a constant 4°C growth chamber with a 16 h photoperiod and PPFD of 350 µmol m^{-2} s^{-1}. Tanks were arranged in a completely randomized design, re-supplied with half-strength Hoagland's solution every week and re-filled with reverse osmosis water as required.

3.3.2 Determination of freezing survival

Crowns acclimated for 0, 21 or 42 d were covered in moist sand in aluminum weighing cans and placed in a programmable freezer held at -4°C for 12 h and cooled at 2°C h^{-1} to -28°C as described by Chen et al. (1983) with the following modifications. Fifteen crowns were removed from the freezer at five pre-determined test temperatures at two-degree intervals over a temperature range expected to bracket the LT_{50}. Crowns were thawed overnight at 4°C, transplanted into pots

containing Sunshine Mix #3 (Terralink Horticulture Inc., Abbotsford, British Columbia, Canada) in a growth chamber maintained at 20°C with a 16 h photoperiod and a PPFD of 400 μmol m^{-2} s^{-1}. Plants were rated for survival after 21 d. The LT_{50}, or the temperature at which 50 % of the plants recover was predicted from a survival versus temperature sigmoid curve. Determinations were repeated four times for each temperature treatment.

3.3.3 Tetrazolium chloride

The TTC_{50}, or the temperature at which 50 % of the VTZ or SAM positively stained red, was determined for each acclimation interval (0, 21, and 42 d). Crowns were frozen as outlined above, but plants were removed at three sub-zero temperatures (at 2°C intervals) around the estimated LT_{50} value. Twenty crowns were removed from the freezer (five per replicate) for each treatment temperature. After 7 d of recovery, crowns were washed in reverse osmosis water and then sectioned longitudinally. Sectioned crowns were stained with TTC and viewed under a dissecting microscope as described by Tanino and McKersie (1985) and Livingston et al. (2013). Tissues were rated as viable if the entire SAM or VTZ stained positive for TTC. The experiment was repeated four times. Twenty fully acclimated crowns were removed following exposure to -12°C for imaging during the first seven days of recovery.

3.3.4 Isolation of apoplastic fluids

The SAM and VTZ apoplastic fluids were extracted using a modified protocol as described by Boudart et al. (2005). For each of four replicates, excised SAM and VTZ was collected from 20 plants and vacuum infiltrated in a syringe with 0.3 M sorbitol solution for 5 min. Crown tissues were blotted with an absorbent tissue, transferred into a 15 mL syringe packed with glass wool and placed in a conical centrifuge tube. The syringe-in-tube apparatus was centrifuged in a swinging bucket at 6000 x g at 4°C for 2 h and the apoplastic fluids were collected as described by Gusta et al. (2004). The process was repeated three times and for the final infiltration step, sorbitol was substituted with 0.2 M calcium chloride. Apoplastic fluid osmolarity was determined using a psychrometer (PsyPro, Wescor Inc, Utah, USA) according to the manufacturer's instructions.

For total protein extraction, 0.5 g of tissue was ground in a chilled mortar with extraction buffer [100 mM HEPES-KOH pH 8.0, 10 mM EDTA, 2 mM EGTA, 0.2 % (v/v) Triton X-100, 1 % (w/v) PVPP, 2 mM DTT] in a 1:2 ratio (Gregory et al., 2009). Samples were transferred to

sterile microfuge tubes, centrifuged (15 min, 6,000 x g at 4°C) and the supernatant was collected. Total and apoplast extracts were filtered using Amicon Ultra 0.5 filters (molecular weight cut-off = 3,000, Millipore, Bedford, Massachusetts, USA) and assayed for protein concentration using the Bio-Rad (Bio-Rad, Berkley, California, USA) protein assay kit according to the manufacturer's instructions. To evaluate the degree of symplastic contamination in the apoplastic fluids, malate dehydrogenase (EC 1.1.1.37) activity was determined as described by Boudart et al. (2005). Duplicates were run, and four replicates were included for each experimental group.

3.3.5 Sample preparation and data acquisition for nano-LC-MS/MS analysis

Prior to proteomic analysis, apoplastic fluids were fractionated using SDS-PAGE and visualized by silver staining (Kawamura and Uemura, 2003) to test for sample integrity. Samples were subjected to in-gel tryptic digestion for nano-LC-MS/MS analysis as described by Takahashi et al. (2013a). Peptide solutions were subjected to nano-LC-MS/MS analysis as described by Takahashi et al. (2013a) with the following modifications; spray voltage of 2.0 kV and collision-induced fragmentation was applied to the ten most intense ions for identification of proteins at a threshold above 500. The raw mass spectrometry proteomics files have been deposited to the ProteomeXchange Consortium via the PRIDE partner repository (Vizcaíno et al., 2015) with the dataset identifier PXD007796 and 10.6019/PXD007796.

3.3.6 Fourier transform infrared microscopy (FTIR)

Crowns were freeze-fixed in water and longitudinally sectioned using a cryo-microtome (Leica CM3050 S, Concord, Ontario). Sections (12 μm) were mounted on BaF_2 polished circular discs (25 mm diameter, 1 mm thick; Crystran Ltd. Poole, United Kingdom) and placed in a desiccator for 48 h. Sections were imaged using a modified protocol as described by Tanino et al. (2013). Samples were maintained under a dry nitrogen purge to remove CO_2 and H_2O interference. Spectral maps were acquired using the following parameters: transmission mode, 4 cm^{-1} resolutions with 128 co-additions, 64 x 64-pixel mid-infrared FPA detector (Bruker Optics Inc., Milton, Ontario, Canada) connected to a Hyperion 3000 microscope using a 15 x objective. Spectral maps were collected using Bruker Optics Opus software over the mid-infrared range (4000 – 900 cm^{-1}). The most representative of the three separate maps were included in this study.

Principal component analysis on the fingerprint region (1800 – 900 cm^{-1}) was performed

using Minitab (version 16, State College, Pennsylvania, United States). Score plots for the first two principal components were examined for spectra clustering. The percentage of variability in the dataset was calculated for the two largest principal components. Protein secondary structure analysis of averaged spectra was carried out on fifteen spectra from three separate biological samples in the Amide I protein region (1700 – 1600 cm^{-1}) using OPUS 7.2 as described by Lahlali et al. (2014).

3.3.7 Statistical analysis

Analyses of freezing injury tests, osmoles and protein concentrations were performed using SigmaPlot 12.5 (Systat Software Inc., Chicago, Illinois, United States) two-way analysis of variance procedure with Fisher's LSD test. Where applicable, the effects of acclimation time (0, 21, and 42 d) and tissue (SAM and VTZ) were considered as fixed effects, while repeated experiments, blocks and replications within each block were considered as random effects.

For semi-quantitative analysis of apoplastic proteins, experimental raw MS/MS data were analyzed with Progenesis LC-MS software (version 4.0, Nonlinear Dynamics, Newcastle, United Kingdom). From the generated list of peptides, a reference run was selected and based upon this run, retention times for each subsequent run were aligned. Each feature was normalized based on the quantitative abundance ratio. Peptide abundances were compared using analysis of variance ($P < 0.05$) and a two-fold threshold was used to determine increasing and decreasing proteins. Protein identification was conducted using the full peptide list with the MASCOT search engine (Matrix Science, London, United Kingdom) and the NCBInr Green Plants database utilizing the procedure outlined by Takahashi et al. (2013a). Protein information was exported from the Mascot xml format to Progenesis software which then associated protein information with the peptide results. Only proteins identified in all four biological replicates in each treatment group were considered in this analysis. Proteins identified were cross-referenced against NCBI protein blast (https://blast.ncbi.nlm.nih.gov/Blast.cgi?PAGE=Proteins) [accessed January 4, 2017], UniProtKB (http://www.uniprot.org/) [accessed January 4, 2017], TargetP 1.1 (http://www.cbs.dtu.dk/services/TargetP/index.php?infile=../prjanalysis/tmp/lotus49212.fsa) [accessed December 23, 2016], SOSUI/G (http://harrier.nagahama-i-bio.ac.jp/sosui/sosuiG/sosuigsubmit.html) [accessed December 23, 2016] and Pred-GPI (http://gpcr.biocomp.unibo.it/predgpi/pred.htm) [accessed December 4, 2016], to determine

protein function, subcellular localization, secretome association, as well as predictions on whether the protein is soluble or membrane-bound and putative identification of GPI-anchored proteins. The annotated protein list is available at the Dryad Digital Repository (**Table S3.1** at http://dx.doi.org/10.5061/dryad.p65dp).

To estimate carbohydrate and methyl esterification contents, spectra were normalized using the protein peak (1700 – 1650 cm^{-1}) whereas amide I and II peaks were normalized using the esterification peak (1740 cm^{-1}). Estimation of individual components was determined by integrating the area under specific bands. Integrated peak areas were determined using the OPUS integration method C (Lahlali et al., 2016). Significance in integrated peak areas was determined from fifteen spectra collected from three biological samples. In instances where analysis of variance detected significant differences, Fisher's LSD was used to determine significant differences among cold-acclimation treatments ($P < 0.05$).

3.4 Results

3.4.1 Tissue-specific differences in freezing survival resulting from the length of cold-acclimation treatment

Norstar crowns acclimated for 0, 21 and 42 d were subjected to a controlled freeze test were evaluated by regrowth and TTC staining (**Figure 3.1**; **Table 3.1**). One day after freezing, an absence of TTC staining (off-white) was visualized in the VTZ (**Figure 3.1A**). Following three days of recovery, a clear demarcation between live and damaged tissues was visible (**Figure 3.1B**) and the damaged region expanded to incorporate a greater proportion of the VTZ. By seven days, recovering plants maintained the degree of damage to only the VTZ (**Figure 3.1C**). Plants unable to recover lost their capacity to reduce TTC in the SAM and surrounding leaf sheath (**Figure 3.1D**). Damage to the SAM and VTZ, as revealed by TTC staining, varied depending on the duration of cold-acclimation. After 21 or 42 d of cold-acclimation, Norstar TTC_{50} for VTZ was around -10°C (**Table 3.1**). At 21 or 42 d, the SAM TTC_{50} was significantly lower than the VTZ TTC_{50} ($P < 0.05$). Furthermore, SAM TTC_{50} values at 21 or 42 d were more comparable to whole plant recovery LT_{50} values at 21 or 42 d than VTZ TTC_{50} (**Table 3.1**). The tissue-specific osmotic potential of the apoplastic fluids varied significantly based upon tissue and acclimation time ($P < 0.05$; **Table 3.2**). Irrespective of the length of cold-acclimation, osmotic potential decreased significantly in both the SAM and VTZ as compared to fluids collected at 0 d of acclimation ($P < 0.05$). While there was

no significant difference in osmotic potential between fluids collected in the SAM and VTZ after 21 d ($P > 0.05$), there was significantly greater osmotic potential in apoplastic fluids collected from the SAM as opposed to the VTZ after 42 d of cold-acclimation ($P < 0.05$). The use of sorbitol in the apoplastic fluid extraction protocol would have affected the osmotic potential. However, the same volume of sorbitol solution was used in each extraction and would therefore not account for differences among the treatment groups.

Table 3.1 Whole plant recovery and tetrazolium staining of the shoot apical meristem (SAM) and vascular transition zone (SAM) of Norstar winter wheat after freezing.

Determination of the temperature at which 50 % of the population was unable to recover from freezing (LT_{50}) and the temperature at which 50 % of the Norstar crown shoot apical meristem or vascular transition zone tissues stained positive for tetrazolium chloride vital staining (TTC_{50}). Plants were acclimated for 0, 21, or 42 d at 4°C. The data was presented as a means of four experiments (N = 4; 20 crowns per temperature per treatment, 4 replicates in time and space). Means within a row (TTC_{50}) were determined to be significantly different using the two-tailed t-test (ns $P > 0.05$, * $P < 0.05$). Means followed by the same letter within each column are not significantly different based on Fisher's LSD test ($P < 0.05$).

Acclimation (d)	LT_{50}	TTC_{50}		
		SAM	VTZ	P
0	-4.8 c	-3.6 c	-3.5 c	ns
21	-15.6 b	-15.7 b	-9.5 b	*
42	-19.8 a	-19.9 a	-10.9 a	*
$LSD_{0.05}$	2.1	1.6	0.5	

Table 3.2 The osmotic potential of apoplastic fluids collected from Norstar crown tissues

Following 0, 21, or 42 d of cold-acclimation, apoplast fluids were collected from the shoot apical meristem (SAM) and vascular transition zone (VTZ). Means followed by the same letter within each column are not significantly different based on Fisher's LSD test ($P < 0.05$).

Tissue	Time (d)	Osmotic potential (MPa)
SAM	0	-1.91 c
	21	-2.13 b
	42	-2.19 a
VTZ	0	-1.97 c
	21	-2.11 b
	42	-2.11 b
$LSD_{0.05}$		0.05

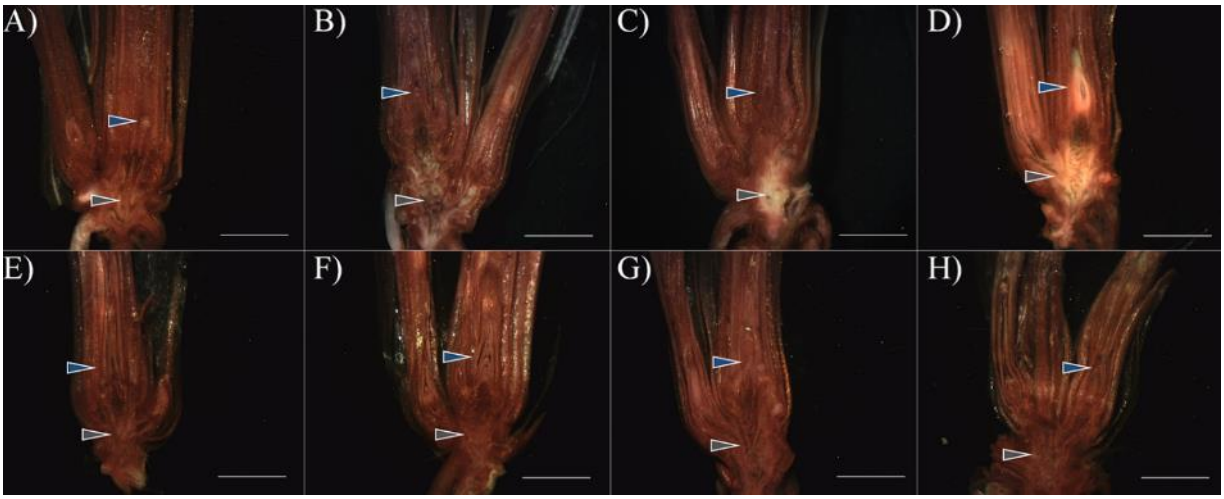

Figure 3.1 Tetrazolium chloride vital staining of hand sectioned cold-acclimated Norstar winter wheat crowns observed after freezing to -12°C.

Plants were placed in aluminum weighing cans filled with moist sand, (A-D) held at -4° C for ice nucleation, then cooled to -12°C at a rate of -2°C h^{-1}. (E-H) A subsection of plants were not exposed to freezing temperatures to act as unfrozen controls. Frozen plants were thawed overnight and then both freeze exposed and unfrozen controls were planted in potting mix and allowed to recover at 20°C. Crowns were sampled after (A & E) 1 d, (B & F) 3 d, (C, D, G, H) or 7 d of recovery and stained with tetrazolium chloride. A red colour identified live cells/tissue that reduced tetrazolium while the off-white and yellow tissue was injured or dead as a result of freezing. After 7 d post-freezing, two patterns emerge, with either (C) a loss of red colouration in the vascular transition zone (VTZ) or (D) a loss of colouration within the VTZ and the shoot apical meristem (SAM). Blue arrows indicate the SAM and grey arrows indicate the VTZ. Scale bar = 0.6 cm.

3.4.2 Subcellular localization and functional classification of proteins

Malate dehydrogenase activity, an indicator of symplastic contamination, was less than 0.5 % in all apoplast samples (**Table S3.2**). To investigate proteome alterations during cold-acclimation (21 or 42 d) in the SAM and VTZ, changes in the presence and abundance of apoplastic proteins were quantified using the shotgun proteomic technique. A total of 545 proteins were identified in all tissues and treatments. Of the proteins with a putative subcellular localization (422 in total), 72 % (305 proteins) were identified to be extracellular or plasma membrane proteins and 29 were identified as putative GPI-anchored proteins. Of the classified proteins (343 in total), 75 % were determined to have the putative secretory capacity (**Table S3.1**). Proteins were classified into 12 functional categories (**Figure 3.2**). The majority were classified as defense (120 proteins, 22.0 %), oxidative stress response (79 proteins, 14.5 %), CWMPs (77 proteins, 14.1 %) and transport (43 proteins, 7.9 %) proteins.

3.4.3 The relationship between SAM and VTZ cold-acclimated proteins

When considering apoplast proteins displaying responses in the SAM or VTZ irrespective of the duration (21 and 42 d) and direction (increased or decreased), about 20 % of proteins only responded in the SAM while 11 % were identified to change in response to cold only in the VTZ (**Figure S3.1**). The proportions of proteins in the SAM or VTZ increased along with the duration of cold-acclimation (**Figure S3.1**; **Figure 3.3**). The percentage of tissue-specific apoplast proteins from 42 d and 21 d fractions induced in the SAM (47 %) and VTZ (58 %) was higher than the 0 d acclimation in the SAM (23 or 35 %) and VTZ (28 or 38 %; **Figure 3.3B**; **Figure S3.1**). Similar trends were observed with proteins of decreasing abundance (**Figure 3.3C**; **Figure 3.1**).

3.4.4 Functional categorization of SAM and/or VTZ cold responsive proteins

In general, the proportion of cold-responsive proteins within each functional category at 21 or 42 d compared to 0 d of acclimation at 4°C, were similar in the SAM and VTZ (**Figure S3.1**). This was consistent with the results of whole apoplast proteins. As was the case with the whole apoplast proteome, defense, CWMP, oxidative stress, protein modification and storage were the predominant categories in SAM and VTZ (**Figure S3.1**).

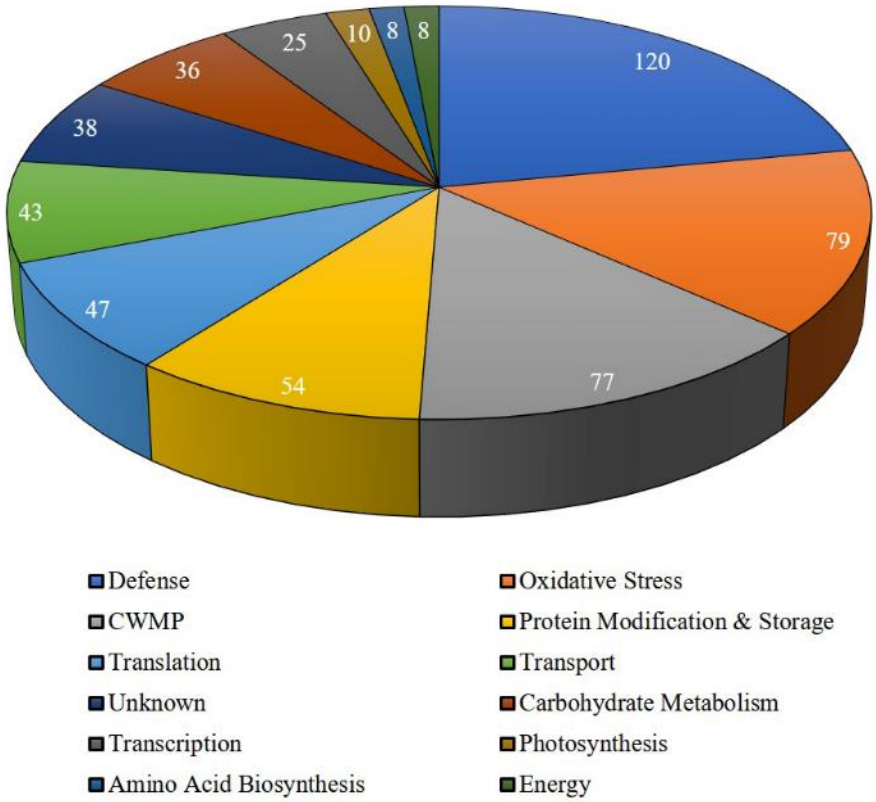

Figure 3.2 Functional categorization of all 545 apoplast proteins identified in the SAM and VTZ .

Apoplastic proteins were classified into 12 functional categories based on a modified definition proposed by Boudart et al. (2005).

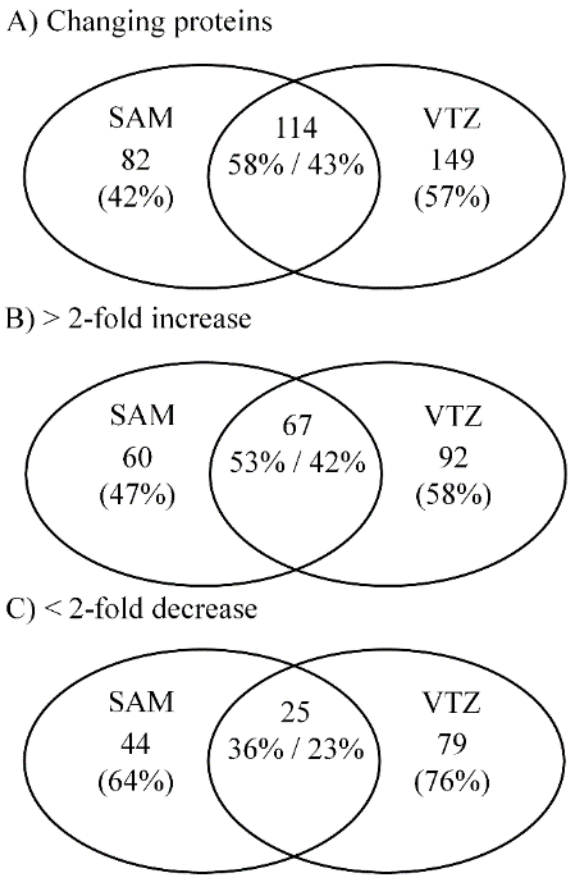

Figure 3.3 Venn diagrams of increasing and decreasing apoplast proteins from cold-acclimated tissues

Venn diagrams of (A) changed, (B) increasing (C) or decreasing apoplast proteins when contrasting abundance in the shoot apical meristem (SAM) and vascular transition zone (VTZ) at 42 and 21 d of cold acclimation. Venn diagrams were generated using http://bioinfogp.cnb.csic.es/tools/venny/.

Differences in SAM and VTZ proteins from the four functional categories (defense, oxidative response, CWMP, and transport) were identified when contrasting 42 and 21 d acclimation apoplastic fluid fractions. Of CWMP proteins, a greater proportion increased instead of decreased in the SAM (23 increased, 8 decreased) as opposed to the VTZ (19 increased, 17 decreased). The ratio of increased to decreased proteins was greater in the VTZ when focusing on defense (51 increased, 19 decreased) or transport (22 increased, 4 decreased) as opposed to SAM defense (33 increased, 22 decreased) or transport (11 increased, 2 decreased) apoplast proteins (**Table S3.1**). When comparing 42 and 21 d apoplast fluid fractions, there was no difference in the ratio of increased to decreased oxidative response proteins in the SAM (32 increased, 6 decreased) and the VTZ (36 increased, 7 decreased). Studying these proteins only as functional groups can mask certain trends within the cold-acclimated SAM and VTZ apoplast. Among CWMPs, invertases and fructan exohydrolases preferentially accumulated overall within the VTZ. Cold-responsive proteins of interest associated with transport and CWMP (**Table 3.3**) as well as defense and oxidative stress response proteins (**Table 3.4**) were identified in the SAM and VTZ.

3.4.5 Identification of bands of interest in the FTIR spectra

Bands associated with different functional groups within the fingerprint region (1800 to 900 cm^{-1}) such as carbonyl esterification (C=O stretching at 1740 cm^{-1}), amide I (C=O stretching and N-H bending of protein peptide bonds between 1700 and 1600 cm^{-1}) and glucuronoarabinoxylan (C-O-C stretching of glycosidic bonds at 1050 cm^{-1} and C-C ring vibration at 995 cm^{-1}) were identified (**Figure 3.4A, C**) and assigned as described previously (McCann et al., 1997; Vijayan et al., 2015). Spectra were deconstructed into individual data points and variability in the fingerprint region was analyzed using principal component analysis. 79 % of the total variation amongst all spectra were explained by the first and second principal components.

Table 3.3. Selected cell wall modifying proteins (C) and transport (T) apoplast proteins that are significantly increasing or decreasing in response to cold in the shoot apical meristem (SAM) or vascular transition zone (VTZ).

Accession	Description	Mean normalized abundance [a]			
		SAM 21 d	SAM 42 d	VTZ 21 d	VTZ 42 d
BAG72143.1	Alpha-glucosidase[C]	14734 (2.6)	13227 (2.3)	6616 (4.1)	7773 (4.8)
EMS58120.1	Alpha-xylosidase[C]	15037 (1.9)	15702 (2.0)	6755 (2.3)	10518 (3.6)
CAD58960.1	Apoplastic invertase 1[C]	9670 (48.2)	7328 (36.4)	2707 (99.9)	734 (27.1)
AAM13694.1	Beta-D-glucan exohydrolase[C]	55931 (3.4)	86623 (5.3)	20123 (4.3)	16124 (3.5)
AJA71651.1	Beta-expansin 1a[C]	31 (nd)	95 (nd)	293 (nd)	320 (nd)
XP_003579704.1	Beta-fructofuranosidase 2-like[C]	12084 (134.8)	9069 (101.2)	1654 (86.5)	404 (21.1)
AAS97960.1	Cell wall beta-glucosidase[C]	16611 (2.7)	29388 (4.7)	5655 (8.1)	5143 (7.3)
BAM74038.1	Cell wall invertase[C]	159 (0.1)	1099 (0.7)	1832 (34.5)	4554 (85.6)
BAM74037.1	Cell wall invertase[C]	9240 (62.9)	7658 (52.1)	2485 (78.4)	602 (19.0)
AAS48872.1	Expansin EXPA3[C]	1848 (0.7)	4211 (1.7)	4922 (2.6)	11042 (5.9)
ABI95405.1	Fasciclin-like protein FLA15[C]	19037 (2.0)	29350 (3.1)	8173 (3.7)	8054 (3.6)
BAE44509.1	Fructan exohydrolase[C]	3327 (6.9)	5865 (12.2)	2161 (5.9)	4170 (11.5)
EMT31770.1	Glucan endo-1,3-beta-glucosidase 13[C]	141 (1.1)	612 (4.8)	613 (0.9)	138 (0.2)
ABB90546.1	Lipid transfer protein[C]	1896 (nd)	2727 (nd)	608 (30.2)	4022 (200.1)
EAY95514.1	Lipid transfer protein OsI_17360[C]	16511 (4.0)	55580 (13.6)	10708 (4.4)	12388 (5.1)
AAG27707.1	Lipid transfer protein precursor[C]	30867 (1.5)	59259 (2.8)	36639 (1.3)	219881 (7.9)
AAK20395.1	Lipid transfer protein precursor[T]	33750 (1.3)	63712 (2.5)	40958 (0.9)	199771 (4.4)
BAJ96826.1	Lipid transport predicted protein[T]	2615 (9.6)	10157 (37.3)	6133 (3.6)	53984 (31.9)
EMT05022.1	Pectinesterase 3[C]	3454 (1.6)	5378 (2.4)	2362 (7.1)	3691 (11.1)
BAJ98765.1	Pectinesterase inhibitor[C]	7570 (76.6)	8092 (81.9)	751 (0.5)	2508 (1.8)
EMT00190.1	Putative polygalacturonase[C]	17648 (0.6)	34941 (1.1)	24208 (1.9)	85193 (6.6)
CAH69206.1	Type 1 non-specific lipid transfer protein[T]	5200 (8.3)	14520 (23.1)	3281 (2.5)	12196 (9.2)
AAC49404.1	WCOR719[C]	30160 (63.0)	17909 (37.4)	10625 (9.3)	5237 (4.6)
ABU55395.1	Xylanase inhibitor 602OS[C]	217779 (2.1)	328160 (3.1)	215744 3.0)	543555 (7.7)

[a] Values in parentheses are the fold change difference from 0 d. Instances where proteins were not identified were indicated in parentheses as not detected (nd).

Table 3.4 Selected defense (D) and antioxidant response (R) apoplast proteins that are significantly increasing or decreasing in response to cold in the shoot apical meristem (SAM) or vascular transition zone (VTZ).

Accession	Description	Mean normalized abundance [a]			
		SAM 21 d	SAM 42 d	VTZ 21 d	VTZ 42 d
ACT65562.1	70 kDa heat shock protein^{D}	5097 (21.3)	3514 (14.7)	21 (0.9)	69 (3.0)
AAD09343.1	ABA-responsive protein^{D}	3327 (4.1)	5164 (6.4)	5404 (2.0)	14134 (5.3)
EMS52349.1	Cationic peroxidase SPC4^{R}	16333 (2.8)	28670 (5.0)	25309 (1.0)	132178 (5.4)
XP_003580049.1	Chitinase 5-like^{D}	0 (nd)	0 (nd)	1093 (0.6)	5969 (3.2)
BAD06324.1	Cold shock domain protein 2^{D}	0 (nd)	1225 (nd)	0 (nd)	750 (24.6)
EMS48364.1	Cold shock protein CS66^{D}	4747 (nd)	2332 (nd)	0 (nd)	0 (nd)
CAC12881.1	Cold-regulated protein^{D}	1718 (17.2)	1731 (17.4)	5756 (87.3)	14340 (217.5)
XP_015631567.1	Cucumisin-like serine protease^{D}	2900 (4.9)	8564 (14.4)	225 (0.3)	1646 (1.9)
BAB18766.1	Cysteine proteinase inhibitor^{D}	98673 (46.7)	51758 (24.5)	64001 (32.1)	77628 (39.0)
BAJ89304.1	Defensin^{D}	8221 (6.7)	7463 (6.1)	15743 (34.9)	23273 (51.5)
BAC10287.1	Defensin^{D}	41633 (9.4)	38121 (8.6)	52798 (52.2)	50127 (49.6)
CAI65403.1	Dehydrin^{D}	18956 (80.0)	5764 (24.3)	27338 (45.9)	2177 (3.7)
AAY16796.1	Early salt stress/cold acclimation-induced protein 2-3^{D}	651 (0.8)	5826 (7.5)	3432 (1.3)	11224 (4.2)
XP_014753148.1	GDSL esterase/lipase^{D}	13303 (2.2)	9482 (1.5)	10075 (66.9)	5666 (37.6)
AAG00426.1	Germin B^{D}	87348 (0.9)	230880 (2.3)	120156 (2.0)	313249 (5.2)
BAD10332.1	Glutaredoxin^{R}	21740 (58.4)	19880 (53.4)	16047 (65.5)	25233 (103.0)
Q43472.1	Glycine rich RNA-binding protein^{D}	195887 (19.8)	102286 (10.3)	92000 (16.7)	62158 (11.3)
EMT06661.1	Monothiol glutaredoxin-S10^{R}	5768 (36.1)	4481 (28.0)	3196 (85.6)	6118 (163.8)
EMT19353.1	Peroxidase 70^{R}	4520 (31.0)	13652 (93.7)	19792 (13.6)	112959 (77.6)
EMS57180.1	Subtilisin-like protease^{D}	1084 (184.3)	1146 (194.8)	2 (0.0)	20 (0.2)
EMT30759.1	Subtilisin-like protease^{D}	637 (0.5)	1869 (1.6)	3204 (5.7)	9040 (16.2)
BAJ85823.1	Thaumatin^{D}	80492 (15.1)	65217 (12.2)	52439 (10.9)	17965 (3.7)
EMT27591.1	Thaumatin^{D}	210 (0.6)	459 (1.3)	3637 (2.2)	21071 (12.6)
ACV20868.1	Thioredoxin-dependent peroxidase^{R}	25110 (10.9)	11478 (5.0)	4904 (253.0)	8987 (463.6)
AAB18208.1	WCOR 615^{D}	8289 (568.5)	7040 (482.8)	259 (nd)	14 (nd)
BAK07537.1	Wheat cold induced 16-like^{D}	5922 (6280.0)	3405 (3610.5)	65 (2.6)	280 (11.3)

[a] Values in parentheses are the fold change difference from 0 d. Instances where proteins were not identified were indicated in parentheses as not detected (nd).

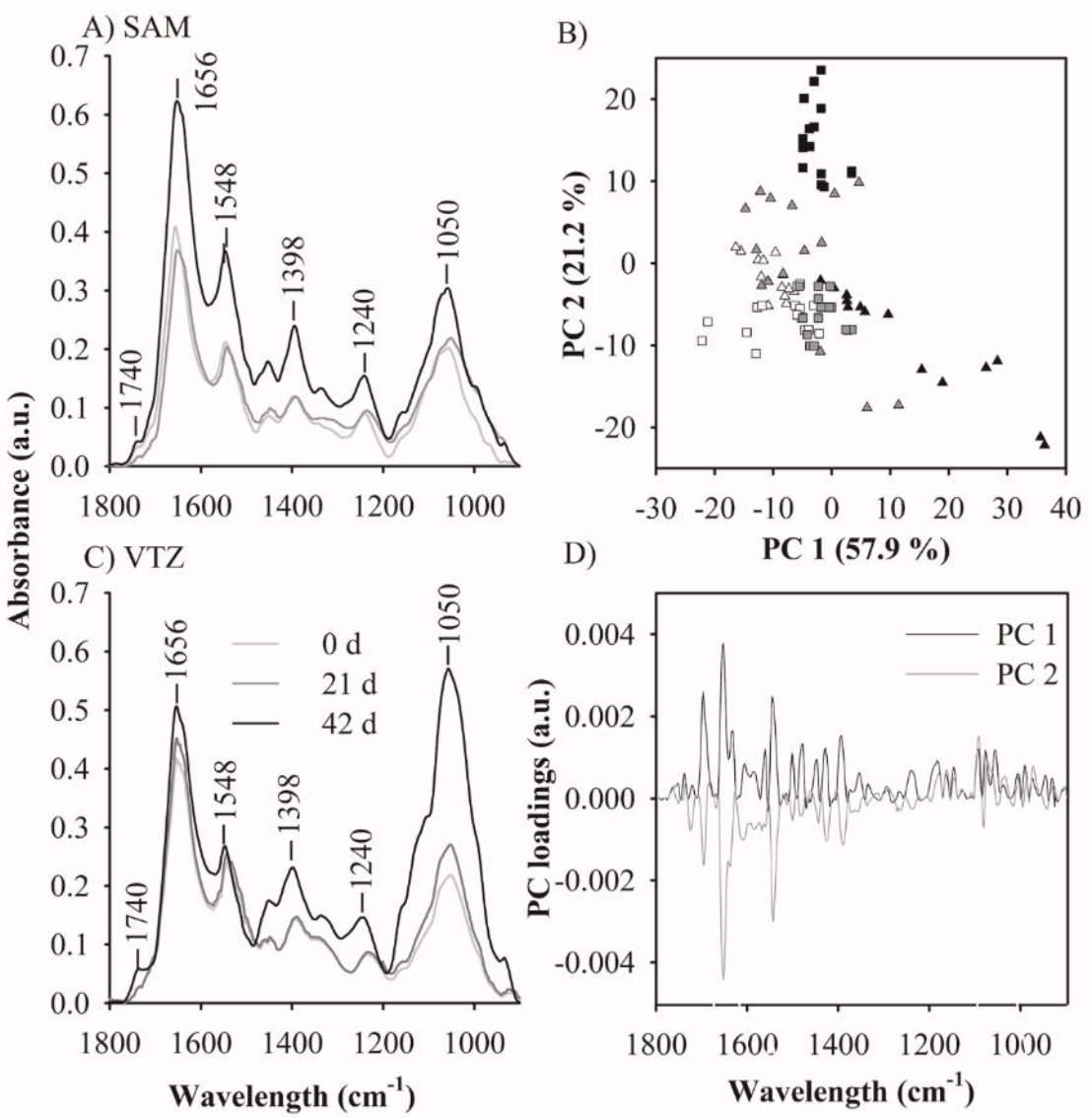

Figure 3.4 Analysis of the Fourier-transformed infrared (FTIR) spectra fingerprint region (1800 – 900 cm^{-1}) collected from the apoplast of cold-acclimated Norstar crown tissues.

Plants cold-acclimated for 0, 21, or 42 d at 4°C were freeze-sectioned for focal plane array-FTIR imaging. Averaged infrared spectra were collected from two regions of interest; (A) the shoot apical meristem (SAM) and (B) the vascular transition zone (VTZ). (C) Within the score plot, 15 individual co-added spectra correspond to samples taken from the SAM (triangle) and VTZ (square) of 0 (white), 21 (grey) or 42 d (black) acclimated crowns. (D) An enrichment in the PC1 and PC2 loading values around 1650 cm^{-1} indicates higher amounts of protein by characteristic peaks of wave numbers in the fingerprint region. The positive PC1 and negative PC2 value at 1650 cm^{-1} within the loading plot corresponds with spectra from 42 d SAM in the score plot. Whereas the highest positive PC2 peak corresponds to a loading value around 1050 cm^{-1} which corresponds to the carbohydrates and spectra from the 42 d VTZ score plot.

3.4.6 Protein and secondary structures

The positive influence of principal component one loadings and negative influence of principal component two corresponded to peak values around amide I (1656 cm^{-1}) when the score plot (**Figure 3.4B**) was compared with the loading plot (**Figure 3.4D**). In the score plot, 42 d SAM spectra coalesce as an individual group due to amide I peak intensity (**Figure 3.4B**). Amide I integrated absorption peak areas were significantly different based on temperature treatment ($P < 0.05$; **Table 3.5**; **Figure 3.5**). At 42 d of cold acclimation Amide I absorption peak areas were significantly higher ($P < 0.05$) in the SAM as opposed to the VTZ.

Absorbance peaks observed at 1656 and 1638 cm^{-1} (**Figure 3.4**) within the amide I region were previously identified in plant tissue as protein secondary structures (Lahlali et al., 2014). Smaller individual peaks were visible in the second derivative of the absorbance spectra (**Figure S3.2**). Peaks associated with secondary structures were assigned to loops or β-turns (1662 – 1678 cm^{-1}), α-helices (1648 – 1660 cm^{-1}), β-sheets (1630 – 1640 cm^{-1}), or random side chains (1610 – 1620 cm^{-1}) as described by Lahlali et al. (2014). These band positions were used in curve fitting analysis as a resolution enhancement technique to separate overlapping bands. Differences in α-helical β-sheet were noted due to acclimation treatment in the SAM and VTZ. The β-sheet peak area significantly increased ($P < 0.05$) in the VTZ in comparison to the SAM after 42 d of cold-acclimation. The α-helical peak area significantly increased ($P < 0.05$), irrespective of tissue, due to cold-acclimation (**Table 3.6**). The ratio of α-helical to β-sheet significantly increased ($P < 0.05$) in the 21 and 42 d spectra, irrespective of tissue, compared to 0 d.

3.4.7 Carbohydrate and methyl-esterification

Visible increases in FTIR spectral peaks associated with enhanced methyl-esterification and glucuronoarabinoxylans were noted in the VTZ of cold-acclimated crowns but not the SAM. The integrated carbohydrate peak was the most significant at 42 d of acclimation in the VTZ (**Figure 3.4B, C**; **Table 3.5**). When contrasting the principal component score plots (**Figure 3.4B**) with the loading plot (**Figure 3.4D**), the most intense peak in principal component two had a positive influence on the score plot around 1050 cm^{-1} and was associated to the greatest degree with spectra collected from 42 d VTZ. Integration at 1050 cm^{-1} indicates a significant increase in peak area as a result of cold-acclimation, with significantly greater peaks associated with spectra collected from the VTZ as opposed to the SAM. Visible increases in the C=O vibration of the

esterification peak at 1740 cm^{-1} and a peak of medium intensity at 1240 cm^{-1} were noted in VTZ spectra and in false colour FTIR-FPA chemical maps after 42 d of cold-acclimation (**Figure 3.5**). Integration of the SAM and VTZ spectra indicate significant increases in esterification peak area as a result of 42 or 21 d of cold-acclimation in the VTZ as opposed to the SAM (**Table 3.5**).

Table 3.5 Integrated absorption spectra for methyl esterification (carbonyl ester, 1740 cm^{-1}), protein (amide I, 1650 cm^{-1}) and carbohydrates (glycosidic bond, 1050 cm^{-1}) regions collected from cold-acclimated (0, 21, or 42 d at 4°C) shoot apical meristem (SAM) and vascular transition zone (VTZ) crown tissues of Norstar winter wheat.

Areas beneath each peak were quantified using OPUS software. Each treatment group represents the mean value of 15 spectra. Means followed by the same letter within each column are not significantly different based on Fisher's LSD test ($P < 0.05$).

Tissue	Time (d)	Peak area (a.u.)		
		Methyl esterification	Protein	Carbohydrates
SAM	0	0.2 c	13.9 d	13.0 e
	21	0.4 c	24.1 c	17.7 b
	42	0.4 c	39.8 a	23.4 d
VTZ	0	0.3 c	14.8 d	22.1 c
	21	2.6 b	22.7 c	24.7 b
	42	4.1 a	35.6 b	49.1 a
$LSD_{0.05}$		0.2	3.4	2.9

Table 3.6 Protein secondary structure absorbance peak areas (a.u.) identified from cold-acclimated (0, 21, or 42 d at 4°C) shoot apical meristem (SAM) and vascular transition zone (VTZ) crown tissues of Norstar winter wheat.

Smaller peaks were identified within the amide I band when observing the spectra's second derivative (see **Figure S3.2**). Curve fitting analysis was conducted using OPUS software to identify and quantify each individual peak area. Bands associated with each peak were assigned as described by Lahlali et al. (2014). Each treatment group represents the mean value of 15 spectra. Means followed by the same letter within each column are not significantly different based on Fisher's LSD test ($P < 0.05$).

Tissue	Time (d)	Peak area (a.u.)				
		α-helix	β-sheet	β-turn	R-coil	α: β ratio[a]
SAM	0	0.14 c	0.14 d	0.15 c	0.08 c	1.00 b
	21	0.22 b	0.16 c	0.11 d	0.13 b	1.26 a
	42	0.29 a	0.19 b	0.11 d	0.16 a	1.63 a
VTZ	0	0.15 c	0.16 c	0.27 a	0.11 bc	1.00 b
	21	0.23 b	0.16 c	0.26 a	0.09 c	1.50 a
	42	0.31 a	0.23 a	0.19 b	0.14 ab	1.43 a
$LSD_{0.05}$		0.03	0.02	0.02	0.03	0.25

[a]α-helix to β-sheet ratio

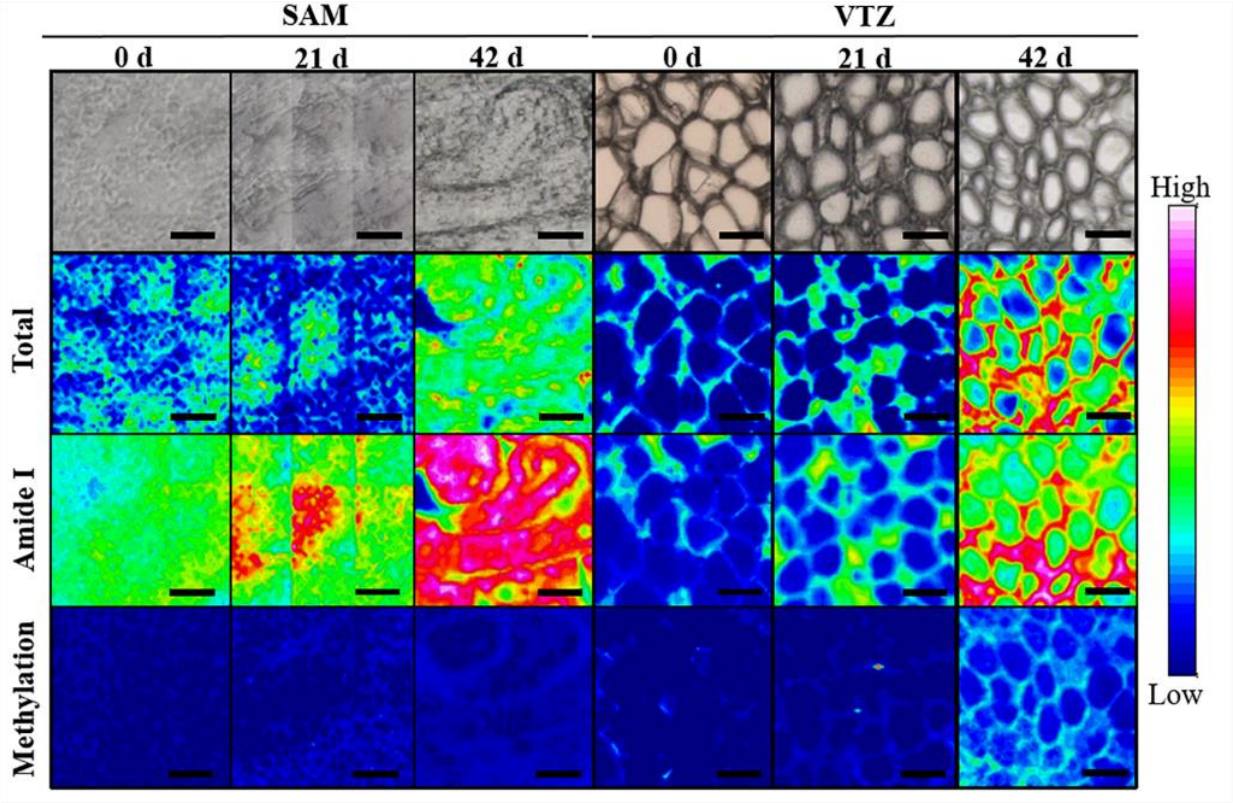

Figure 3.5 Comparisons between chemical maps of a Norstar crown transverse sections using Fourier transform infrared (FTIR) microscope.

Sections were taken from plants exposed to 0, 21 and 42 d of cold acclimation. Images are representative of sections taken from one of three biological crown replicates. Each individual micrograph is comprised of nine separate images captured sequentially using a motorized stage and OPUS software. The first row of images shows a light micrograph of the mapped section. The second row of images shows the micrograph overlaid with a false colour map created with infrared spectroscopy using the integrated absorbance of the spectral region between 4000 and 900 cm^{-1}. The third row of images shows the micrograph overlaid with infrared spectroscopy using the integrated absorbance of the spectral region between 1700 and 1580 cm^{-1} (amide I), attributed to protein. The third row of images shows the micrograph overlaid with infrared spectroscopy using the integrated absorbance of the spectral region between 1760 and 1700 cm^{-1}, attributed to the degree of methyl esterification. A rainbow scheme has been used to denote absorbance, with the warmest colours (red) indicate the highest absorbance while cool colours (blue) represent a low spectral intensity. Scale bar = 50 μm.

3.5 Discussion

3.5.1 Differential freezing damage in the SAM and VTZ

In the present study, TTC vital staining showed the TTC_{50} for the VTZ was near -10°C in both 21 and 42 d acclimated crowns while the SAM TTC_{50} was comparable to the LT_{50} at -16°C and -20°C (**Figure 3.1**; **Table 3.1**). This supports the theory that the VTZ in winter wheat is more susceptible to freezing damage at a slow cooling rate (2°C h^{-1}) (Chen et al., 1983; Tanino and McKersie, 1985; Livingston et al., 2013) and could act as a putative ice sink. In overwintering tree buds, scales act as ice sinks allowing for the slow desiccation and survival of critical floret tissues (Ishikawa and Sakai, 1981). Damage to the VTZ was not lethal if the expansion of ice crystals did not completely sever the vasculature linking the SAM with the VTZ in winter oat (Olien and Marchetti, 1976) or if cells responsible for root regrowth associated with the VTZ remained intact in winter wheat (Chen et al., 1983).

3.5.2 Pathogenesis-related and antifreeze protein accumulation

Fifty-five putative AFP or pathogen-related proteins were identified in this study, with 31 responding in the VTZ (26 increased, 5 decreased) while 23 changed in the SAM (17 increased, 6 decreased) when comparing protein abundance at 42 and 21 d (**Table S3.1**). Increases in β-sheet secondary structures, as noted in the cold-acclimated VTZ (**Table 3.6**), have been associated with AFP ice-binding sites purified from perennial ryegrass (*Lolium perenne* L.) (Middleton et al., 2009) and carrot (*Daucus carota* L.) (Worrall et al., 1998). Pathogenesis-related β-1,3-glucanases, endochitinases and thaumatins synthesized during cold-acclimation have cold-acclimation capacity to control and inhibit ice crystal growth (Hon et al., 1995; Chun et al., 1998; Griffith and Yaish, 2004; Griffith et al., 2005), degrade pathogen cell walls and inhibit fungal enzymes (Hiilovaara-Teijo et al., 1999; Griffith and Yaish, 2004). In cold-acclimated crowns, the formation of large ice crystals disrupts tissue structure in the VTZ (Livingston et al., 2005b; Livingston et al., 2013; Livingston and Tuong, 2014). Since the VTZ is the largest source of free water in winter wheat crowns (Gusta et al., 1975), and is more sensitive to freezing than the SAM, a higher abundance VTZ AFPs would be necessary to buffer against ice re-crystallization over winter.

Maintenance of a constant near freezing temperature and increased humidity under snow cover increases the propagation of psychrophilic snow molds (Hiilovaara-Teijo et al., 1999; Griffith and Yaish, 2004). The VTZ is further stressed by the pathogenic attack in cavities left by

melted ice crystals (Olien and Marchetti, 1976). This can result in the browning phenomena within the crown associated with cellular degeneration. Mechanical damage caused by ice propagation and the degeneration of VTZ cells during recovery also results in the formation of abscesses targeted by psychrophilic plant pathogens (Olien and Marchetti, 1976). Accumulation of antifungal proteins during cold-acclimation within the VTZ (**Table 3.4**) could account for the acquisition of a systemic but non-specific defense against pathogenic stress (Hiilovaara-Teijo et al., 1999; Griffith and Yaish, 2004).

3.5.3 Vernalization-associated proteins

In the present study, a cold-regulated protein (CAC12881.1) was identified to have a 93.9 % homology with WCOR18 and increased in abundance to a greater degree in the SAM after 42 d of cold-acclimation. WCOR18 was previously reported to be expressed under prolonged cold stress conditions, tied to floral development, and a marker for vernalization (Rinalducci et al., 2011). A wheat cold shock protein 2 (WCSP2; BAD06324.1), associated with apical meristem floral development (Sasaki et al., 2013), was present after 42 d of cold-acclimation and in a higher abundance in the SAM as opposed to the VTZ (Supplementary Table S1 at Dryad). As was the case with the present study, Sasaki et al. (2013) observed the level of WCSP2 was below detectable limits in non-acclimated plants, but gradually increased during cold-acclimation and reduced freezing tolerance in Arabidopsis (*Arabidopsis thaliana*) mutants when overexpressed. How WCOR18 or WCSP2 are tied to the developmental control of vernalization is currently unknown.

3.5.4 Membrane and lipid transfer proteins

Alterations to plasma membrane proteins during cold-acclimation have been characterized using proteomic approaches (Kawamura and Uemura, 2003; Boudart et al., 2005; Takahashi et al., 2013a; Takahashi et al., 2013b; Takahashi et al., 2016) and the maintenance of membrane integrity has been recognized as a critical mechanism to freezing survival (Steponkus, 1984; Uemura et al., 2006). Previous reports using the calcium and sorbitol infiltration technique have identified extraction of apoplast and membrane-associated proteins (Boudart et al., 2005). Four late embryogenesis abundant family proteins; dehydrin (CAI65403.1), WCS66 (EMS48364.1), WCOR 615 (AAB18208.1) and wheat cold-induced 16 (BAK07537.1) were found to preferentially increase in the SAM in response to cold (**Table 3.4**). Proteins with dehydrin-like

properties have been identified in association with the plasma membrane (Danyluk et al., 1996). If the VTZ acts as an ice sink relative to the SAM, then increased the abundance of SAM dehydrins could be one mechanism to reduce interaction between membrane bilayers during dehydration (Steponkus, 1984; Uemura et al., 2006) and maintain membrane stability throughout thawing (Chen et al., 2013).

The majority of the 19 cold-increased lipid transfer proteins were found in the VTZ (**Table 3.3**; **Table S3.1**). Lipid transfer proteins have numerous roles in response to cold-acclimation including increased soluble sugar content (Guo et al., 2013), psychrophilic pathogen inhibition (Hon et al., 1995), higher thermal hysteresis and ice re-crystallization inhibition (Doxey et al., 2006). Lipid transfer proteins are also involved in the deposition of suberin (Edstam et al., 2013), which has been identified as a putative component of a post-freeze barrier surrounding the VTZ (Livingston and Tuong, 2014).

3.5.5 Modification of sugar side chains by apoplastic invertases

Increased abundance of apoplastic and extracellular glucosidases, invertases and fructan exohydrolases were observed to a greater degree in cold-acclimated VTZ as opposed to SAM apoplastic fluids (**Table 3.3**). Sugar hydrolyzing enzymes are responsible for cleaving cell wall bound arabinoxylans as well as sucrose and fructan side chains, increasing unbound extracellular sugar concentrations (Livingston and Henson, 1998; Zabotin et al., 1998). High concentrations of sugar hydrolyzing enzymes result in oligosaccharin accumulation during hemicellulose turnover, the acquisition of cold hardiness in winter wheat and account for the presence of free arabinoxylans in the extracellular space as well as the postulated increase in cell ABA (Zabotin et al., 1998). Application of ABA significantly increased [U-^{14}C]-sucrose uptake into the cell, with the largest fraction in the the cell wall (Tanino et al., 1990). Higher concentrations of soluble carbohydrates such as arabinoxylans or sucrose in the VTZ prevent ice adhesions and provide additional forms of protection to the cell walls (Olien and Smith, 1977) and the plasma membrane (Uemura et al., 2006).

3.5.6 Modifications to the cell wall matrix

In the present study, FTIR peaks associated with glucuronoarabinoxylans in VTZ more than doubled after 42 d of cold-acclimation and was 1.5 times greater in comparison with 42 d SAM (**Table 3.3**; **Figure 3.4**). This may indicate a preferential substitution of arabinosyl sugars,

as was the case with cold-acclimated *Miscanthus* cultivars (Domon et al., 2013). A ten-fold increase in the esterification peak of 42 d VTZ as opposed to 42 d SAM also indicates enhanced cross-linkage with ferulic and p-coumaric hydroxycinnamic acids and a stiffening of the matrix (Hatfield et al., 2016) linked to enhanced freezing tolerance (Rajashekar and Lafta, 1996).

Interestingly, there was an increase in pectin esterase (BAJ96804.1), polygalacturonase (EMT00190.1) and a GDSL esterase (EMT02121.1) in the SAM and VTZ cold-acclimated apoplast (**Table 3.3**). The low, SAM methyl-esterified peak area in comparison to control conditions (**Table 3.5**) could be due to the increase in pectin esterase inhibitor (BAJ98765.1) abundance (**Table 3.4**). Traditional analysis of Type II cell walls indicates pectins comprise a relatively small fraction (< 5 %) of the cell wall in comparison to glucuronoarabinoxylans, however, these measurements are traditionally based on leaf or stem tissue (Carpita, 1983, 1984; Carpita and Gibeaut, 1993; McCann et al., 1997; Carpita et al., 2001). Recent experiments with spring wheat 'Recital' identified high tissue-specific homogalacturonan deposition in the seed coat (Chateigner-Boutin et al., 2014) and rhamnogalacturonan I was identified to be important in maintaining cell wall integrity during rapid cell expansion in spring wheat 'Cadensa' endosperm during germination (Palmer et al., 2015). Baldwin et al. (2014) concluded that frost tolerance in pea (*Pisium sativum* L.) was associated with increased pectin and a higher methyl-esterification ratio. Since there has not yet been a definitive cell wall compositional study of winter wheat crown tissues, it is possible methyl-esterified pectins, in conjunction with other cell wall matrix components such as increased concentrations of neutral sugars enhance cell wall strength.

The observation that: I) apoplastic fluids containing peroxidases and germin-like proteins with oxalate oxidase activity preferentially accumulated in the 42 d VTZ, II) enhanced VTZ methyl esterification in comparison to the 42 d SAM, III) as well as evidence of low temperature-induced diferulic acid (Wakabayashi et al., 2011) collectively suggest cold-acclimation may result in preferential formation of diferulic wall linkages in the VTZ. If so, this would increase cell wall mechanical resistance to ice propagation (Rajashekar and Lafta, 1996). During wall re-organization, glucuronoarabinoxylans exposed by sugar hydrolysis are cross-linked via an ester linkage to ferulic or p-coumaric acid (Scalbert et al., 1985; Grabber et al., 1995; Grabber et al., 2000; Palmer et al., 2015; Hatfield et al., 2016). Germin-like proteins with an oxalate oxidase activity (AAG00426.1) as well as peroxidases (EMS52349.1 and EMT19353.1) capable of oxidizing hydrogen peroxide during this cross-linking reaction increased in abundance in the SAM

and VTZ (**Table S3.1**; **Table 3.4**). Parallels between cross-linkages and subsequent increases in wall rigidity and enhanced freezing tolerance can be drawn with cold response wall rigidity in studies conducted on plants with Type I cell walls (Solecka et al., 2008; Tanino et al., 2013).

Cell wall-related expansins, xyloglucan transglucosylases and endo-glucanases play a central role in modulating wall extensibility (Cosgrove, 2000). Unlike the decrease in protein abundance of xyloglucan transglucosylases and endo-glucanases (**Table S3.1**), β-expansins (AJA71651.1 and AAS48872.1) have been identified to preferentially increase in the VTZ during cold-acclimation (**Table 3.3**). This may seem counterintuitive since expansins weaken non-covalent bonds between wall polysaccharides facilitating wall extensibility (Cosgrove, 2000). However, β-expansins genes have been identified to be positively cold-regulated in Arabidopsis (Lee et al., 2005), improving chilling stress resistance in postharvest zucchini (*Cucurbita pepo* L. morphotype *Zucchini*) flowers (Carvajal et al., 2015) and postulated as a counterbalance against cold-induced growth depressing effects in Petunia (*Petunia hybrida)* (Bauerfeind et al., 2015). Conceivably, expansins in the VTZ may play a role in increasing the flexibility of the cell wall during ice accumulation or post-freezing to reduce injury during water influx into the intracellular space.

3.5.7 Conclusions

After exposure to 4°C for 42 d acclimation responses within the SAM and VTZ apoplast diverged. Within the SAM, dehydrin-like proteins act as an anti-desiccant to minimize damage to the membrane during extracellular freeze dehydration (Danyluk et al., 1998). Similarly, SAM proteins with putative vernalization regulatory roles (WCSP2 and WCOR18) were present to assist in the apical meristem transition from vegetative to floral development through an unknown mechanism (Sasaki et al., 2013). The SAM and VTZ accumulated tissue-specific peroxidases in response to cold-acclimation. In the VTZ, the increase in methyl-esterification could be associated with increased abundance of peroxidase and Germin B proteins that play a role in peroxide-mediated diferulic crosslinking of glucuronoarabinoxylans. These peroxidases act as a defensive response to the pathogenic attack in the VTZ post-thawing. As suggested by Levitt (1980) when cells such as those found in the SAM, are exposed to freezing-induced desiccation, tissue-specific peroxidases are expected to play a greater role in the oxidation of reactive oxygen species to minimize damage to the plasma membrane or other apoplast proteins.

While specific AFPs and pathogenesis-related proteins accumulated in the SAM and VTZ, they were found in greater abundance in the VTZ at 42 d of cold acclimation, which would result in significantly reduced rates of ice migration. Cell wall invertases, fructan exohydrolases and certain lipid transfer proteins associated with increased accumulation of apoplast sugars, preferentially increased in the VTZ. Accumulation of VTZ proteins that directly or indirectly reduce ice propagation and re-crystallization rates are required since the region has the greatest amount of free water (Gusta et al., 1975) and is the initial site of frost injury (Tanino and McKersie, 1985) within the crown. This differential freezing response, in which the VTZ mitigates and controls the region of damage while the SAM avoids freezing and desiccation injury relative to the VTZ, supports the theory of a ice segregation as a method of freezing survival within Norstar winter wheat crowns.

In Chapter 3, the combination of FTIR-FPA and shotgun proteomics was a useful method to analyze and localize cold-acclimation induced tissue-specific accumulation of cell wall modifying and defense proteins. The SAM and VTZ have separate cold-acclimation responses. Future advancements in the understanding of tissue-specific cold-acclimation mechanisms in winter cereals will be particularly useful to plant breeder's intent on improving winter hardiness in these crops. Based on these results, Chapter 4 was designed to determine if the tissue-specific cold-acclimation influenced individual tissue freezing survival. This was accomplished by investigating the influence of cooling rate and freezing duration on the pattern of injury in cold-acclimated Norstar wheat and compare these responses to Hazlet and Puma rye crowns.

Supplementary information

Table S3.1 List of identified and quantified proteins.

This table is an excel file containing the analysis of all proteins identified in this chapter. Due to its size, it could not be included in the body of the thesis. It can be found online at the Dryad Digital Repository (http://dx.doi.org/10.5061/dryad.p65dp).

Table S3.2 Apoplastic fluid malate dehydrogenase (MDH) specific activity in Norstar shoot apical meristem (SAM) and vascular transition zone (VTZ) following exposure to 0, 21, or 42 d of cold acclimation.

Means followed by the same letter in each column are not significantly different based on Fisher's LSD (Two-way ANOVA, $P < 0.05$).

Tissue	Time	Apoplastic protein ($\mu g\ mg^{-1}$)	MDH Specific Activity ($\mu g\ mg^{-1}$)		Apoplast contamination (%)
			Apoplast	Whole Tissue	
SAM	0	32.98 b	0.05 ab	13.26 b	0.34 a
	21	34.05 ab	0.05 ab	13.45 b	0.34 a
	42	39.20 a	0.04 b	14.27 b	0.29 a
VTZ	0	31.26 b	0.07 a	14.59 ab	0.46 a
	21	33.97 b	0.06 ab	16.24 a	0.36 a
	42	39.95 b	0.05 ab	16.21 a	0.34 a
$LSD_{0.05}$		5.99	0.02	1.93	0.14

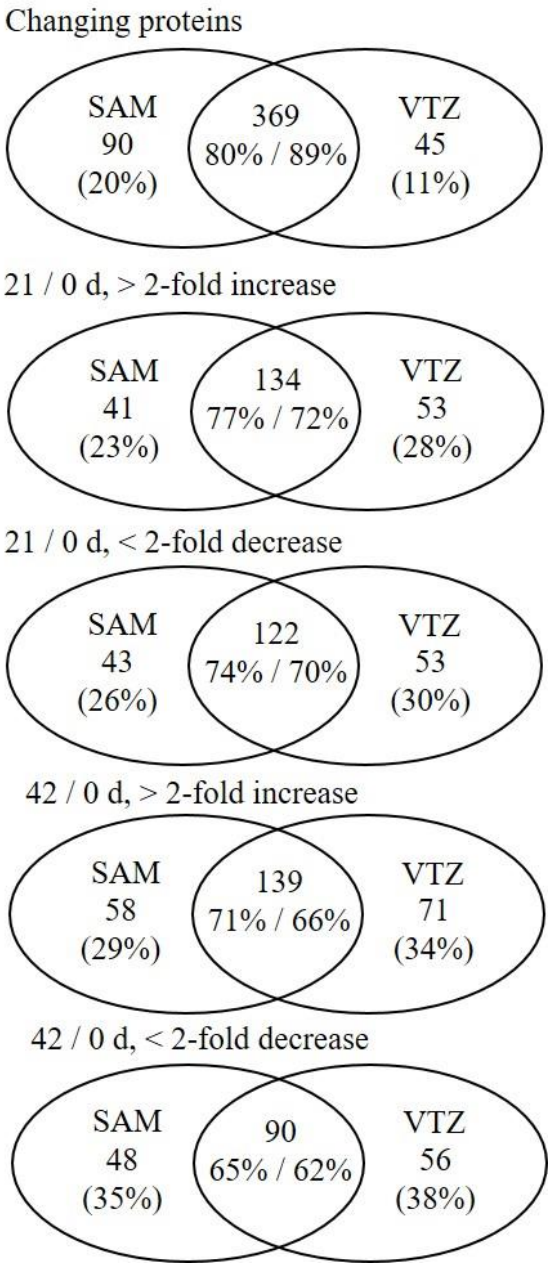

Figure S3.1 Venn diagrams of 42/0 and 21/0 d cold responsive proteins in the SAM and VTZ.

Venn diagrams were generated using http://bioinfogp.cnb.csic.es/tools/venny/.

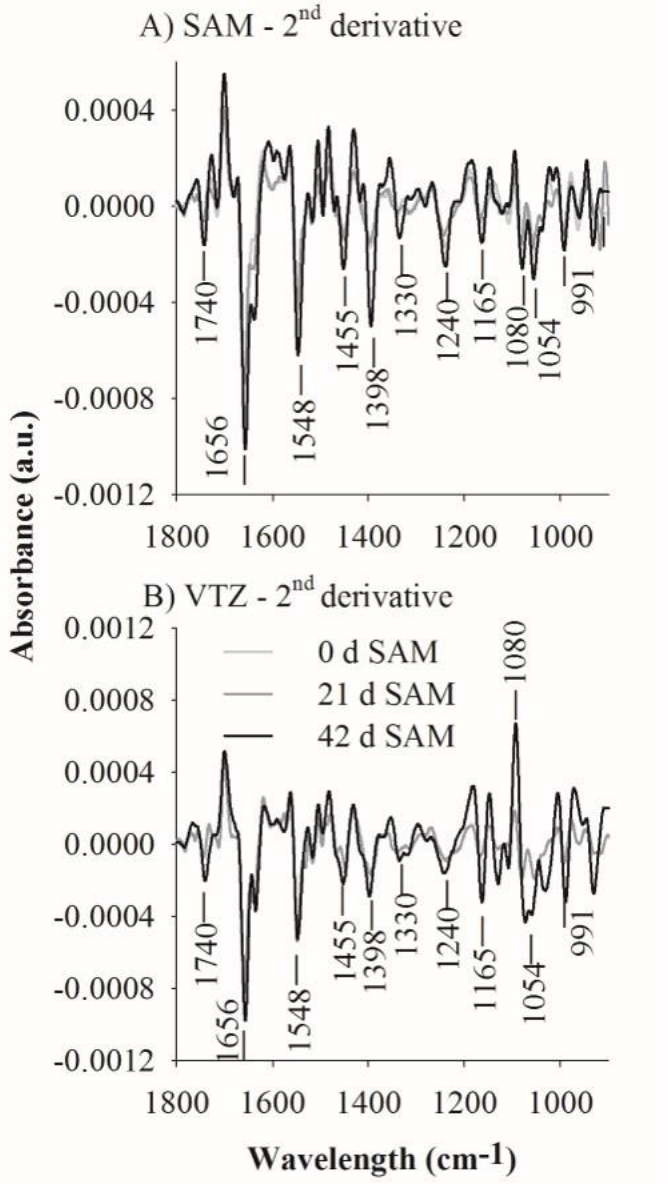

Figure S3.2 Second derivative of absorbance spectra collected from the shoot apical meristem (SAM) and vascular transition zone (VTZ).

Spectra fingerprint region (1800 – 900 cm^{-1}) were collected from crowns exposed to 0, 21, and 42 d of cold acclimation.

Chapter 4

4 Effect of cooling rate on freezing injury of cold-acclimated crowns

4.1 Abstract

In cold-acclimated winter wheat and rye crowns, slow cooling rates (< 2°C h^{-1}), found under field conditions, are required to develop maximum cold hardiness. Fast cooling rates (≥ 5°C h^{-1}) were employed to reveal structure-function mechanisms due to the increased physical force of ice propagation. No published reports have studied the influence of cooling rates on the tissue-specific crown injury. When cold-acclimated Norstar winter wheat, Hazlet and Puma winter rye plants were cooled at 2°C h^{-1}, the youngest tiller (tiller 3) and the main shoot were observed to have a more negative LT_{50} than the two oldest tillers (tillers 1 and 2). Cold-acclimated Puma rye was reported to have a lower LT_{50} than Hazlet, which had a lower LT_{50} than Norstar. This order of cold hardiness corresponded to crown shearing strength. In cold-acclimated crowns, injury was observed using aniline blue and TTC staining in the VTZ prior to injury in the SAM. Cold-acclimated crowns recovered after injury to the VTZ but injury to the SAM was lethal. This pattern of injury did not differ in crowns cooled slowly in an LT_{50} test or cooled slowly and then held at -10°C, -12°C or -14°C for 30 d in a duration test (LD_{50}) the latter which simulates overwintering field conditions. By contrast, in cold-acclimated crowns cooled at 5°C h^{-1} (Norstar) or 10°C h^{-1} (Norstar and Puma), injury was first observed in the SAM and not in the VTZ.

In cold-acclimated plants, intrinsic nucleation was visually observed with IRVT in the lower crown. Exotherms induced by an extrinsic nucleator at the roots initiated freezing in the crown. Extrinsic nucleation of leaves resulted in independent freezing events. After -5°C, proton signal was only visually observed in the VTZ using MRMI. The loss of proton signal in the rest of the crown corresponded with the high temperature exotherm using DTA. The VTZ proton signal was lost in MRMI collected at -10°C, which corresponded with the mid temperature exotherm (DTA). This research indicated the crown tissues froze independently and the order of tissue freezing was important to survival.

4.2 Introduction

The accurate assessment of crown freezing injury, the critical tissue for survival, is an essential feature of artificial freezing tests. Freezing injury in cereals has been evaluated in individual leaves, the crop canopy (Chen et al., 1983; Eagles et al., 1993; Rizza et al., 2001), whole plants (Olien, 1964; Olien and Marchetti, 1976; Fowler, 1979), or individual tillers (Fowler et al., 1981; Legge et al., 1983; Eagles et al., 1993; Rizza et al., 2001). Although these approaches assess whole plant and crop recovery, they do not identify the mechanisms of freezing tolerance and avoidance in the critical crown tissue. Numerous cold-acclimation studies have reported tissue-specific physiological (Pauli, 1960; Olien and Marchetti, 1976; Chen et al., 1983; Tanino and McKersie, 1985; Livingston et al., 2005b; Livingston et al., 2013; Livingston and Tuong, 2014) and biochemical (Livingston et al., 2005a; Livingston et al., 2006; Willick et al., 2018a) crown responses. Despite this evidence, recent studies have largely focused on freezing and cold-acclimation responses in the whole crown (Kosová et al., 2012; Vítámvás et al., 2012; Trischuk et al., 2014; Skinner and Bellinger, 2016; Kalapos et al., 2017; Sun et al., 2017). Analysis of homogenized crown tissues could mask tissue level responses in the SAM or VTZ. A clearer understanding of tissue level freezing behaviour is needed to identify the mechanism of crown freezing survival.

Freezing injury is not uniform in the crown. Mechanical ice damage in the crown's VTZ disrupts water conduction to the SAM and leaves (Pauli, 1960; Olien and Marchetti, 1976). Visual observations with TTC staining (Tanino and McKersie, 1985; Livingston et al., 2013; Chapter 3), discolouration of degenerated tissue from oxidation (Olien and Marchetti, 1976) and root regrowth freezing studies (Chen et al., 1983) reported the VTZ was more freezing sensitive than the SAM. Freezing injury was first observed at the base of oat (*Avena sativa* L.) crowns (Livingston and Tuong, 2014). The nodal plate in winter cereals was composed of discontinuous xylem (Aloni and Griffith, 1991) that reduced the rate of ice propagation into the VTZ (Zámećník et al., 1994). Since these measurements were made with thermocouples affixed at either side of the nodal plate, Zámećník et al. (1994) could not confirm if freezing was a result of directional freezing from the roots or from independent nucleation events in the crown and roots.

The initial ice nucleation temperature and rate of cooling are critical to crown recovery. Cold-acclimated winter wheat crowns held at -3°C for 72 h then cooled at 10°C h^{-1} or 15°C h^{-1} had

a significantly higher LT_{50} than crowns cooled at 2°C h^{-1} or 5°C h^{-1} (Gusta et al., 1982). In cold-acclimated plants with a low water content that tolerate equilibrium freezing, injury was observed at temperatures cooler than the temperature of initial ice formation. Non-equilibrium freezing in supercooled tissues results in the rapid formation of large ice masses which shears tissue and crushes cells (Olien, 1964). Non-equilibrium freezing has been observed in tissues with a high-water content or supercooled more than 5°C (Olien, 1961, 1967). Cyclic freezing and thawing (Mazur, 1966; Gusta and Fowler, 1977; Min et al., 2014) and the length of time the tissue is frozen (Pomeroy et al., 1975; Gusta et al., 1982; Gusta et al., 1997; Waalen et al., 2011) influences the degree of ice growth and injury.

In cold-acclimated crowns, 60 % of water is frozen by -5°C and 90 % by -10°C (Gusta et al., 1975). Small changes in crown free water at temperatures cooler than -10°C become the limiting factor for freezing tolerant tissues. Magnetic resonance micro-imaging (MRMI) was used to visually observe the decline in proton signal associated with free water exposed to sub-zero temperatures in tree buds (Ishikawa et al., 1997; Ishikawa et al., 2016). Use of MRMI provides a high level of resolution of free water in a non-destructive manner. The drawbacks of MRMI are that the technique cannot discern between water tightly bound to chemical constituents and frozen water as well as determine the site and direction of freezing. Freezing of supercooled water is an exothermic reaction. The release of heat can be detected with thermocouples (Quamme et al., 1972) or visually with IRVT (Wisniewski et al., 1997; Livingston et al., 2017). The use of IRVT has facilitated the observation of the initial site of ice nucleation and helped advance the study of nucleators and structural barriers (Hacker and Neuner, 2007).

4.2.1 Hypothesis

In cold-acclimated winter wheat and rye, slow cooling reduced the initial injury to the VTZ.

4.2.2 Objectives

A clear understanding of the mode of injury in cold-acclimated winter wheat crowns is essential to understanding how crowns, and through extrapolation, the plant, survives freezing. In Chapter 3, SAM and VTZ in Norstar winter wheat had a differential response to cold-acclimation. The SAM and VTZ could also have two separate freezing behaviours. Altering cooling rate will alter the rate of ice propagation throughout the crown and can provide insight into structure-

function relationships and separate mechanisms of resistance between tissues. As such, the objective of this chapter was to (I) contrast the effect of cooling rate and freezing duration on tissue-specific patterns of injury in the crown. (II) Under natural cooling rates (2°C h^{-1}), determine how ice propagates into the crown using IRVT. (III) Determine whether a barrier reduces the rate of ice propagation into the crown tissues.

4.3 Materials and methods

4.3.1 Plant material and growth conditions

Norstar winter wheat, Hazlet rye and Puma rye were germinated and grown hydroponically as described in section 3.3.1. To induce frost hardening, plants (in either the test tube or sand in can freezing apparatus) were held for 1 h at 0°C, cooled at 2°C h^{-1} to -4°C and then ice nucleated. Plants were held at -4°C for 72 h.

4.3.2 Collection and storage of ice nucleation active substance (INA^+)

Grass (*Poa pratensis* L. and *Elmyrus repens* L.) leaves were collected in the Fall (2015 and 2016) from the University of Saskatchewan Horticulture Field (Saskatoon, Saskatchewan, Canada) after air temperatures dropped below 10°C for a minimum of two weeks. Samples were placed in a 2 L Nalgene beaker with distilled water and stored in the dark at 4°C for 24 h on a rocking shaker set at 80 rpm (VWR International, Randor, Pennsylvania, USA). The beaker's contents were passed through a filter under vacuum and then tested for its ice nucleating temperature. The ice nucleating substance (INA^+) had a warmer ice nucleating temperature (-3°C) than silver iodide (-4.5°C) when tested using the tube-in-bath system (see section 4.3.4 for a detailed outline). Prior to every experiment, an ice nucleation test was conducted to confirm the INA^+ ice nucleation temperature. The INA^+ collected from November 2015 maintained an average ice nucleating temperature of -3°C for up to seven months if stored at 4°C. When flash frozen with LN_2, stored at -80°C, and thawed in warm water (40°C for 3 min), the INA^+ collected on November 2015 maintained an ice nucleating temperature of -3°C as of the last testing date (March 1st, 2017).

4.3.3 Whole plant freezing survival

Whole plant freezing survival (LT_{50}) after 21 d of recovery was determined as described in section 3.3.2. A separate LT_{50} experiment scored the survival of the main shoot and tillers after

21 d of recovery. There were five plants per pot with four pots per treatment group. This experiment was repeated three times for monitoring tiller and main shoot survival. Tillers and main shoot were scored as 'recovered' when able to produce new adventitious roots and live shoot tissue. For the freezing duration test (LD_{50}), three sub-lethal temperatures (-10°C, -12°C and -14°C) were selected based on results from the 2°C h^{-1} LT_{50}. Crowns were cooled slowly, then held at -10°C, -12°C or -14°C and sampled at 2 d intervals over 30 d, thawed overnight at 4°C, planted in potting mix under non-acclimating conditions for 21 d and plant were scored for survival as described in section 3.3.2.

4.3.4 Crown shearing strength

Shearing strength was used to simulate the crown's resistance to shearing by the propagation of ice. Allo-Kramer shear force was determined by shearing four crowns using a 10-blade Allo-Kramer shearing compression cell attached to a TMS-Pro Texture Press (Food Technology Corp., Sterling, Virginia, USA). The full-scale load was set at 1000 N with the crosshead speed of 500 mm min^{-1}. Peak shear force was recorded and divided by sample weight to calculate the shear force in N force per g sample (N g^{-1}). Data were reported as the average of four replicates per treatment group. The experiment was repeated four independent times.

4.3.5 Aniline blue and tetrazolium chloride (TTC)

Recovering crowns were incubated in TTC as described in section 3.2.3. To determine the ability of conducting vessels to transport water, plants were cooled to -14°C using the aluminum can freeze test (section 3.2.2), thawed at 4°C overnight, recovered at 20°C for 3 d and then placed in a test tube with 2 mL aniline blue solution (1 % aniline blue, 0.1 M phosphate buffered saline, pH 4.0). Aniline blue solution was only in contact with the roots. After 24 h, crowns were sectioned longitudinally and observed under a dissecting microscope for aniline blue uptake. A minimum of 30 crowns was tested per treatment group.

4.3.6 Effect of cooling rate on the pattern of freezing injury

The DTA was conducted as described by George and Burke (1977) with the following modifications. Plants were trimmed to 1 cm of roots and 6 cm from the base of the crown. Prior to testing, one plant was desiccated at 70°C for 72 h to be used as a control. Thermocouples were

placed against the main stem at the point closest to the crown base. Crowns were wrapped in parafilm to hold the thermocouple in place. To initiate either freezing, 200 µL of INA^+ was pipetted into 10 X 75 mm test tubes. Crowns were placed with roots in direct contact with the INA^+ to initiate freezing. Thermocouples were held against the base of the crown with parafilm. Tubes were placed in a rate-controlled ethylene glycol low-temperature bath (Haake G50, Thermo Scientific, Newington, New Hampshire, USA) held at 0°C for 20 min. Samples were cooled at a rate of 2°C h^{-1}, 5°C h^{-1} or 10°C h^{-1} from 0°C to -30°C. Thermocouples recorded temperatures every 1 s for the duration of the experiment (Octotemp datalogger, Fisher Scientific, New Hampshire, USA). In each treatment group, seven plants were tested with a dried control.

To determine which exotherm was associated with the killing temperature, the LT_{50} was determined using the 21 d recovery method (section 3.3.2). Plants were removed at three sub-zero temperatures (at 2°C intervals) around the mean exotherm value. A separate experiment using the tube-in-bath system was conducted to score the tissue-specific region of injury using TTC viability stain (TTC_{50}, section 3.3.2). A total of 12 plants were tested per temperature and the experiment was independently repeated four times.

4.3.7 Pressurized root test

Xylem continuity at the nodal plate was tested by the pressurized air method as described by Aloni and Griffith (1991). Plants were rinsed in reverse osmosis water and roots were trimmed to within 3 cm of the base of the crown. Stems were sectioned 2 mm above the nodal plate. Individual roots, cut 3 mm from the base of the crown, were inserted into a plastic pipette (0.5 mm in diameter) and manually held in place. Crowns were placed under water in a glass petri dish and observed with a dissecting microscope. Pressurized air (approximately 50 kPa) was applied to individual roots. The cut surface was observed for the presence of air bubbles. If air bubbles were observed, then the root vessels were categorized as continuous (through the root-shoot junction) and labeled as ‘unsafe’. If no air bubbles emerged, then the root vessels were categorized as discontinuous and the root was categorized as ‘safe’. The experiment was repeated with cold-acclimated and frost hardened crowns cooled at 2°C h^{-1} to -10°C and -14°C.

4.3.8 Infrared video thermography (IRVT)

Freezing of non- and cold-acclimated plants were observed by IRVT using a modified protocol described by Wisniewski et al. (1997). Whole plants were positioned so that their adaxial leaf surface was within the camera's (FLIR T650 SC, Wilsonville, Oregon, USA) field of view. Plants were equilibrated at 0°C for 30 min. Chamber temperature was ramped down to -4°C or -8°C at a rate of -2°C h^{-1}. A 50 µL droplet of INA^{+} was used as an ice nucleator either on the roots, leaves, or both. Images were captured using the following camera settings; false color monochromatic image, camera temperature gradient of 4°C, image recorded every 5 s. To observe supercooling, the experiment was repeated with plants blotted dry with absorbent tissue prior to cooling. Freezing events and the time required for tissue to attain temperature equilibrium with chamber temperatures following a freezing event were recorded by IRVT. A minimum of 20 plants was observed for each treatment group.

4.3.9 Magnetic resonance microimaging (MRMI)

The MRMI experiments were conducted using a Bruker Avance 400 NMR spectrometer (Bruker, Rheinstetten, Germany) with a vertical 9.4 T magnet. Twelve-stacked axial plane two dimensional MRMI were obtained with a 0.0039 cm per pixel resolution and a 0.6 mm slice thickness. Intact main stems were trimmed and placed inside a glass capillary along with a 0.5 mm glass capillary tube containing a standard solution (0.5 g L^{-1} copper sulfate in 50 % D_4-Methanol, 40 % D_2O 10 % H_2O; **Figure 4.1A**). The capillary tube was capped and secured in the NMR probe (**Figure 4.1B**) and positioned inside the superconducting magnet (**Figure 4.1C, D**). The crown region of interest was identified by first conducting a 3 min longitudinal scan. The region of interest was re-calibrated and twelve stacked transverse slices were imaged from above the SAM to the roots. The temperature surrounding the capillary tube was monitored with a thermocouple. Chamber temperature was cooled stepwise (2.5°C h^{-1}), from 0°C, to -5°C and -10°C held at each temperature of interest for 1 h and then imaged. Images were captured with Bruker Micro 2.5 microimaging hardware setup employing echo times of 14 ms and recycle delays of 1400 ms. The total acquisition time was 24 min per set of twelve axial images. False-color axial images were processed with ImageJ using the Bruker MRI imaging plugin. A minimum of three plants were tested per treatment group.

4.3.10 Statistical analysis

Data from three or four independent tests were combined because the effects of the experimental treatments were consistent. An ANOVA with Fisher's LSD test ($P < 0.05$) was used to analyze effects of cultivar, tissue acclimation or treatment on freezing survival (LT_{50}), crown fresh weight or shearing strength, exotherm temperature, percentage of safe roots or time to equilibrium using Sigma Plot statistical software (version 12.5, Systat Software Inc., San Jose, California, USA).

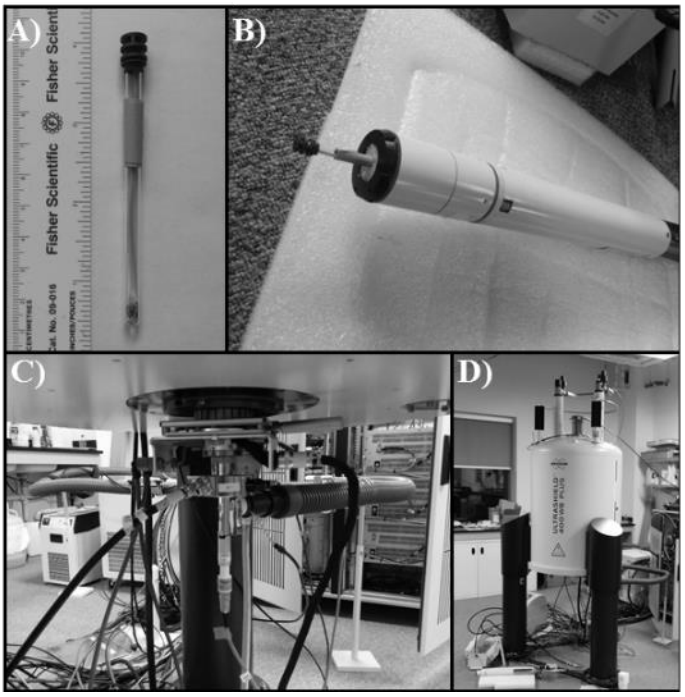

Figure 4.1 Experimental setup for MRMI at Simon Fraser University.

Main shoot was excised and placed in a glass capillary tube with a methanol standard (A). The capillary tube was placed in the magnet aligned so that the crown was positioned near the center of the magnet (white arrow; B). The magnet was fixed in the NMR along with a thermocouple, cooling, heater and image collector (C). Image of NMR Bruker AVANCE 400 MHz (D).

4.4 Results

4.4.1 Freezing survival of Norstar, Hazlet and Puma

Cold-acclimated or frost hardened Puma rye had a more negative LT_{50} than Hazlet, which had a more negative LT_{50} than Norstar ($P < 0.05$; **Table 4.1**). Puma and Hazlet had significantly greater survival rates than Norstar when held for various lengths of time at -10, -12 or -14°C ($P < 0.05$; **Table 4.1**) in an LD_{50} duration freezing test. Crown strength was defined as the amount of force required to shear tissues. There were no significant differences in the amount of force required to shear non-acclimated crowns ($P > 0.05$; **Table 4.2**). However, cold-acclimated Puma rye had a significantly higher ($P < 0.05$) crown shearing strength compared to cold-acclimated Hazlet, which had a significantly higher ($P < 0.05$) crown shearing strength compared to cold-acclimated Norstar. Injured non-acclimated plants wilted following thawing and were unable to recover in Norstar and Hazlet phenotypes. In cold-acclimated Norstar, the two oldest tillers (tillers 1 and 2) were the least cold hardy organs (**Table 4.3**). Survival of the main shoot and/or the youngest tiller (tiller 3) determined if the plant recovered. Regeneration of new leaves from the main shoot in some of the recovering seedlings were attributable to the growth of tiller 3 (**Figure 4.2D**).

4.4.2 Visualization of injury with tetrazolium chloride (TTC) and aniline blue

Frozen non-acclimated plants could not be sectioned due to compromised tissue integrity (data not shown). In unfrozen cold-acclimated plants, TTC was reduced in all tissues (**Figure 4.3A**). In cold-acclimated crowns exposed to -14°C and allowed to recover for 3 d, the VTZ no longer reduced TTC (**Figure 4.3B**). By 7 d of recovery, injured SAM no longer reduced TTC (**Figure 4.2C**). There was also a positively stained region between the SAM and VTZ (**Figure 4.2C**). After 21 d of recovery, surviving SAM reduced TTC (**Figure 4.3D**). There was no difference in the initial pattern injury visualized by TTC staining between plants slowly cooled (2°C h^{-1}; **Figure 4.3**) and plants slowly cooled and then held at -10°C, -12°C or -14°C for multiple days in the duration test (**Figure 4.4**).

Table 4.1 Recovery (LT_{50}) of winter cereals following exposure to short and prolonged duration freezing (LD_{50}) using the 21 d recovery test

For prolonged freezing tests, cold-acclimated plants were cooled at 2°C h^{-1} to -4°C and held for 72 h. Plants were then cooled at 2°C h^{-1} and then held at -10, -12 or -14°C over a 30 d period and removed at 2 d intervals. Plants were thawed overnight and recovered at 20°C for 21 d. Data was presented as a means of four replicates in time and space (N = 4; 20 crowns per temperature per treatment in each LT_{50} experiment). Means followed by the same letter within each column were not significantly different based on Fisher's LSD test (One-way ANOVA, $P < 0.05$).

Cultivar	LT_{50} (°C)			LD_{50} (d)		
	Non-acclimated	Cold-acclimated	Frost-hardened	-10°C	-12°C	-14°C
Norstar	-5 a	-20 a	-22 a	8 c	5 c	4 c
Hazlet	-6 a	-25 b	-26 b	14 b	11 b	8 b
Puma	-6 a	-30 c	-31 c	25 a	21 a	14 a
$LSD_{0.05}$	1	2	1	3	1	1

Table 4.2 Crown shearing strength of non- and cold-acclimated Norstar, Hazlet and Puma.

Data was presented as a means of the total number of individuals (N = 16; 4 replicates and 4 replicates in time and space). Means followed by the same letter within each column were not significantly different based on Fisher's LSD test (One-way ANOVA, $P < 0.05$). Means within a row (crown fresh weight or shearing strength) were determined to be significantly different using the two-tailed t-test (ns $P > 0.05$, * $P < 0.05$).

Cultivar	Crown fresh weight (g)			Shearing strength (N g^{-1})		
	Non-acclimated	Cold-acclimated	P	Non-acclimated	Cold-acclimated	P
Norstar	0.35 b	0.45 b	*	474.0 a	635.7 c	*
Hazlet	0.42 a	0.48 b	*	498.8 a	735.6 b	*
Puma	0.42 a	0.52 a	*	451.9 a	847.8 a	*
$LSD_{0.05}$	0.03	0.04		47.2	56.3	

Table 4.3 Twenty-one-day recovery (LT_{50}) of cold-acclimated Norstar, Hazlet and Puma main shoot and tillers after test tube freezing in a controlled low temperature bath.

Data are presented as a means of three independent experiments (N = 3; 20 replicates per temperature per treatment in each LT_{50} experiment and 3 replicates in time and space). Values within a column followed by a different lowercase letter are significantly different (One-way ANOVA, Fisher's LSD, $P < 0.05$). Values within a row followed by a different uppercase letter are significantly different (One-way ANOVA, Fisher's LSD, $P < 0.05$).

Cultivar	LT_{50} (°C)					
	Whole plant	Main shoot	Tiller 1	Tiller 2	Tiller 3	$LSD_{0.05}$
Norstar	-20 a B	-19 a AB	-16 a A	-16 a A	-20 a B	3
Hazlet	-25 b B	-20 a A	-17 a A	-16 a A	-23 b AB	4
Puma	-30 c C	-25 b B	-21 b A	-19 b A	-27 c BC	3
$LSD_{0.05}$	3	1	1	1	2	

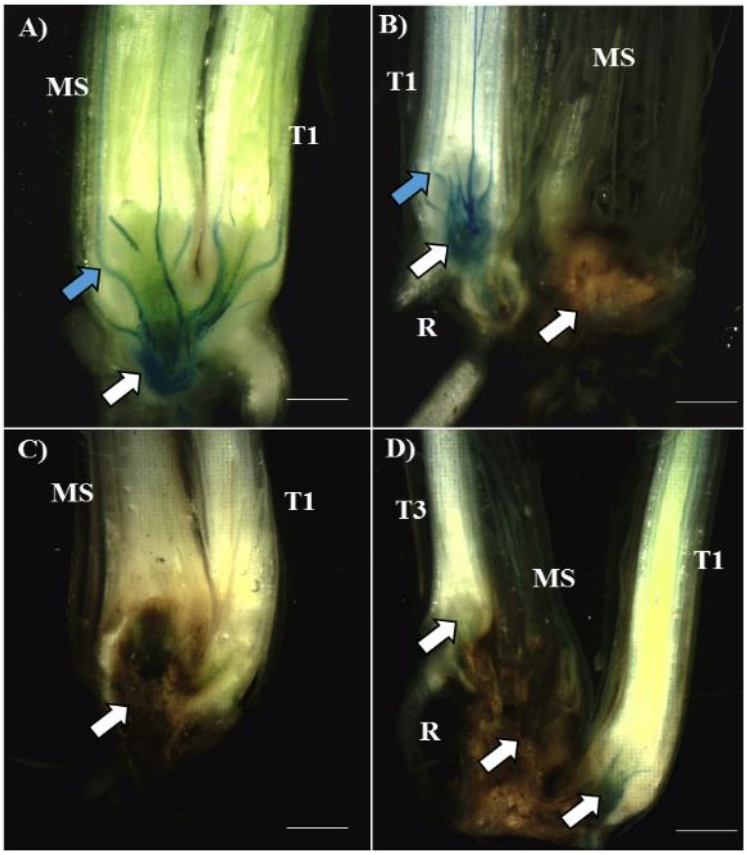

Figure 4.2 Aniline blue uptake by cold-acclimated Norstar prior to and during recovery from exposure to -14°C.

Samples include (A) a non-frozen seedling with aniline blue uptake, (B) 21 d of recovery with aniline blue uptake, (C) 21 d of recovery without staining with survival of the main shoot, (D) 21 d recovery with growth of a tertiary tiller from a dead main shoot. New roots associated with T3 were not exposed to aniline blue, but roots associated with T1 were. White arrows indicate the vascular transition zone in the main shoot or tillers. Blue arrows indicate staining of the procambial strands. Abbreviations include: main shoot (MS), first tiller (T1) tertiary tiller (T3) and the new root (R). Scale bar = 0.4 cm.

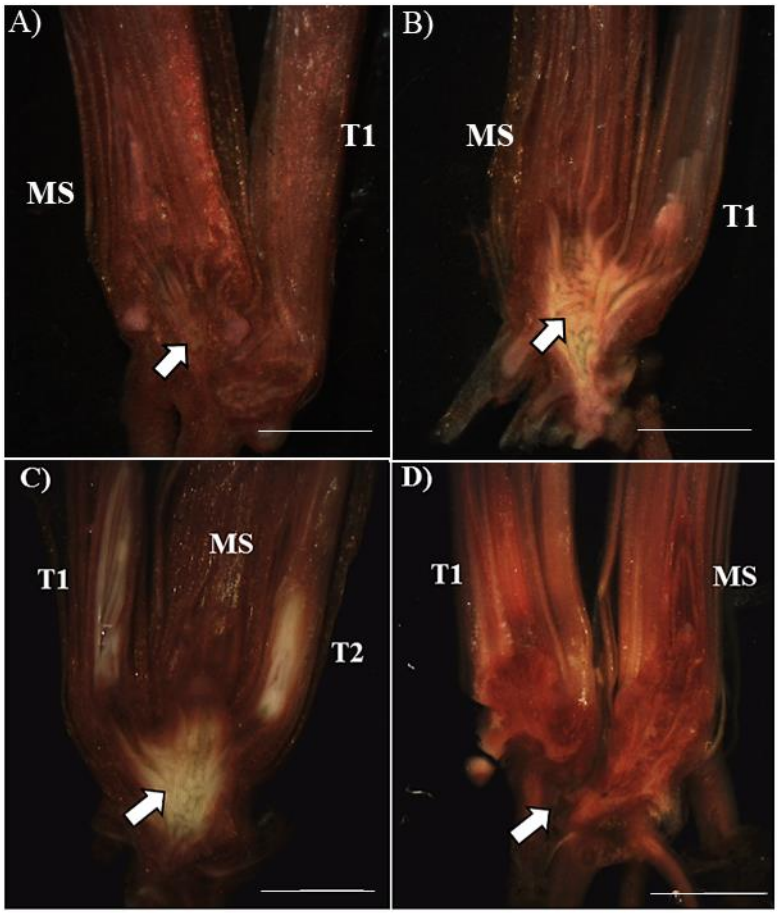

Figure 4.3 Tetrazolium chloride staining of cold-acclimated Norstar winter wheat crowns prior to and during recovery from exposure to -14°C.

(A) Crowns 5 d of recovery after exposure to 4°C, (B) 7 d of recovery after exposure to -14°C with injured VTZ, (C) 7 d after exposure to -14°C with injured VTZ, T1, and T2, (D) 21 d of recovery after exposure to -14°C in crowns with browning of the VTZ. White arrows indicate the region of damage within the vascular transition zone. Similar staining patterns were observed in cold-acclimated Norstar, Hazlet and Puma. Abbreviations include: main shoot (MS), first tiller (T1) and second tiller (T2). Scale bar = 0.8 cm.

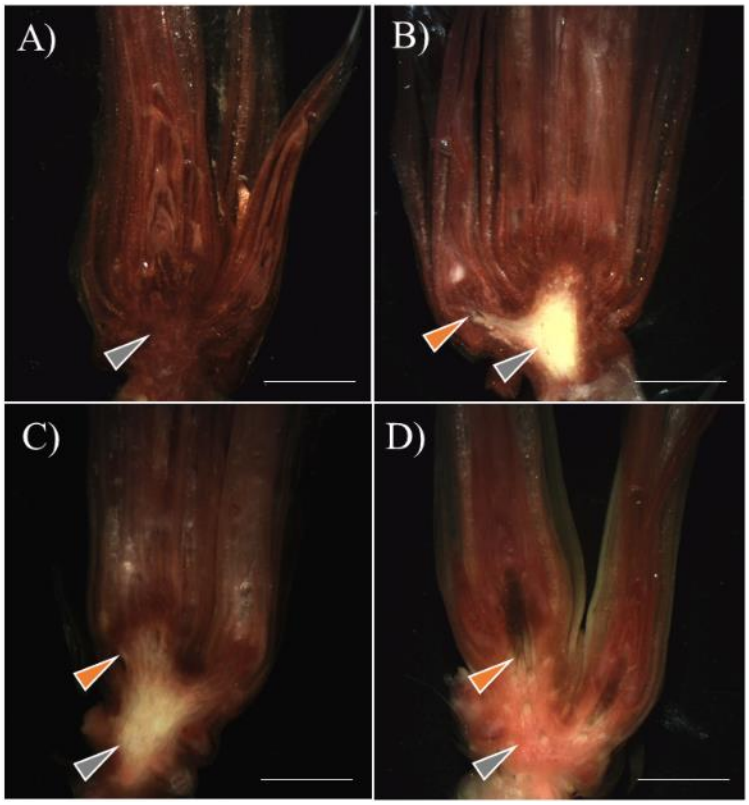

Figure 4.4 Tetrazolium chloride (TTC) staining of cold-acclimated Norstar winter wheat crowns slowly cooled to -10°C, 12°C or -14°C and held at each temperature for 5 d.

Crowns were thawed overnight, recovered at 20°C for 3d and then stained with TTC. (A) Unfrozen stained crown. Cold-acclimated crowns were cooled at 2°C h^{-1} and to and held at (B) -10°C, (C) -12°C or (D) -14°C for 5 d. Grey arrows indicate the vascular transition zone. Orange arrows indicate the farthest region of injury as indicated by an absence of TTC reduction. Similar staining patterns were observed in cold-acclimated Hazlet and Puma. Scale bar = 0.6 cm.

Vasculature associated with the nodal plate was the first site of injury in the crown. Uninjured cells adjacent to freeze injured tissue degenerated after 10 to 14 d of recovery. Two predominant patterns of tissue degeneration were observed in freeze injured main shoots (**Figure 4.2; Figure 4.3**). Degenerated tissue in the main shoot was contained to the VTZ or expanded to encompass the SAM. Tiller 3 regenerated from main shoot meristem tissues. Browning from tissue degeneration in the VTZ (**Figure 4.2B, C, D**) gave a false visual appearance of TTC stained tissue (**Figure 4.3D**). Crown survival was not reliant on the presence or absence of a viable first or second tiller.

4.4.3 Effect of cooling rate on the pattern of injury

Increased cooling from 2°C h^{-1} to 5°C h^{-1} or 10°C h^{-1} resulted in a significantly less negative LT_{50} ($P < 0.05$) (**Table 4.4**; **Figure 4.5**; **Figure 4.6**). When cold-acclimated plants were cooled at 2°C h^{-1}, they produced an intense high temperature exotherm around -4°C, a mid temperature exotherm between -6°C and -9°C and a low temperature exotherm (**Figure 4.7A**). The mid temperature exotherm corresponded with injury to the VTZ (TTC_{50}) while the low temperature exotherm corresponded with the injury to the SAM (TTC_{50}) and the LT_{50}. The high and mid temperature exotherms were observed in cold-acclimated plants cooled at 5°C h^{-1}. Under fast cooling rates (5°C h^{-1}), the mid temperature exotherm corresponded with injury to the SAM (**Figure 4.7B**). When cold-acclimated plants were cooled at 10°C h^{-1}, the mid and low temperature exotherms could not be distinguished from the high temperature exotherm (**Figure 4.7C**). Similar trends were observed in Puma rye (**Table 4.4; Figure 4.6**).

4.4.4 Differences in VTZ connectivity

All roots and crown tissues were injured in non-acclimated crowns cooled to -10°C or -14°C (**Table 4.5**). In cold-acclimated crowns, exposure to -10°C or -14°C significantly increased damage to the nodal plate and the VTZ, as measured by the root air pressure technique. Frost and cold hardening of cold-acclimated crowns prior to -10°C or -14°C treatments significantly decreased ($P < 0.05$) damage to the nodal plate and in the case of Norstar, induced a significantly higher ($P < 0.05$) percentage of safe seminal and adventitious roots. Hazlet cold-acclimated and frost hardened crowns exposed to -14°C have significantly less ($P < 0.05$) injury to the nodal plate and VTZ than Norstar as measured with the seminal and adventitious root air pressure technique.

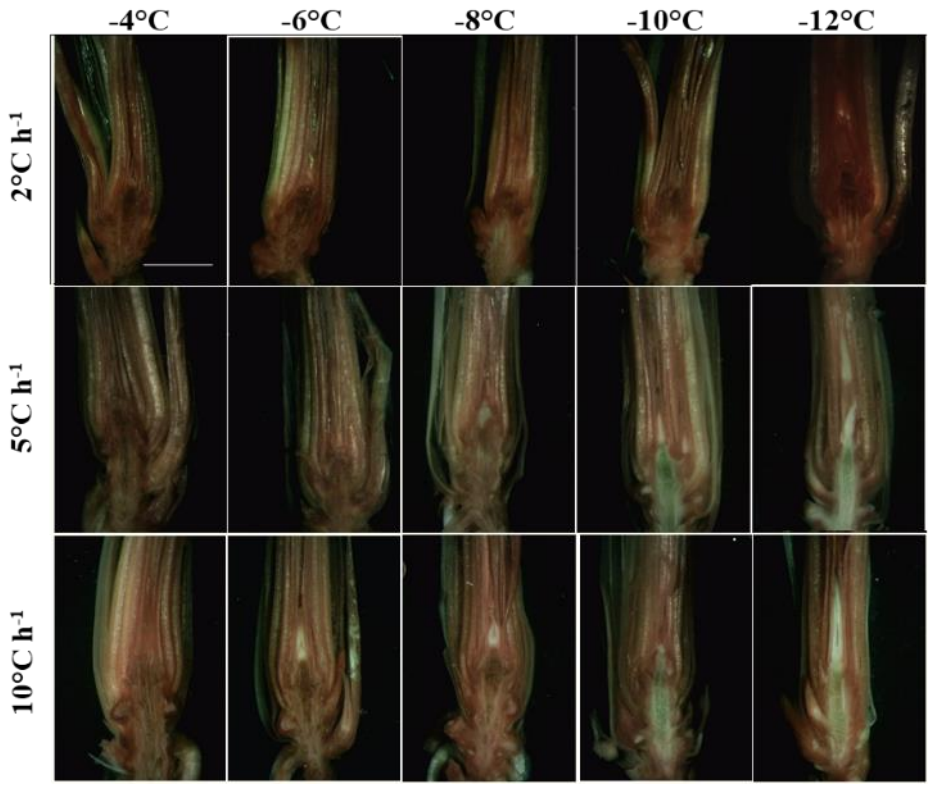

Figure 4.5 Effect of cooling rate on the region of injury in cold-acclimated Norstar crowns

Crowns were cooled using the tube-in-bath system at a rate of either 2, 5 or 10°C h^{-1}. Crowns were sampled at each temperature, recovered at 20°C for 3 d and then stained with tetrazolium chloride. The most representative images were displayed. Scale bar = 0.8 cm

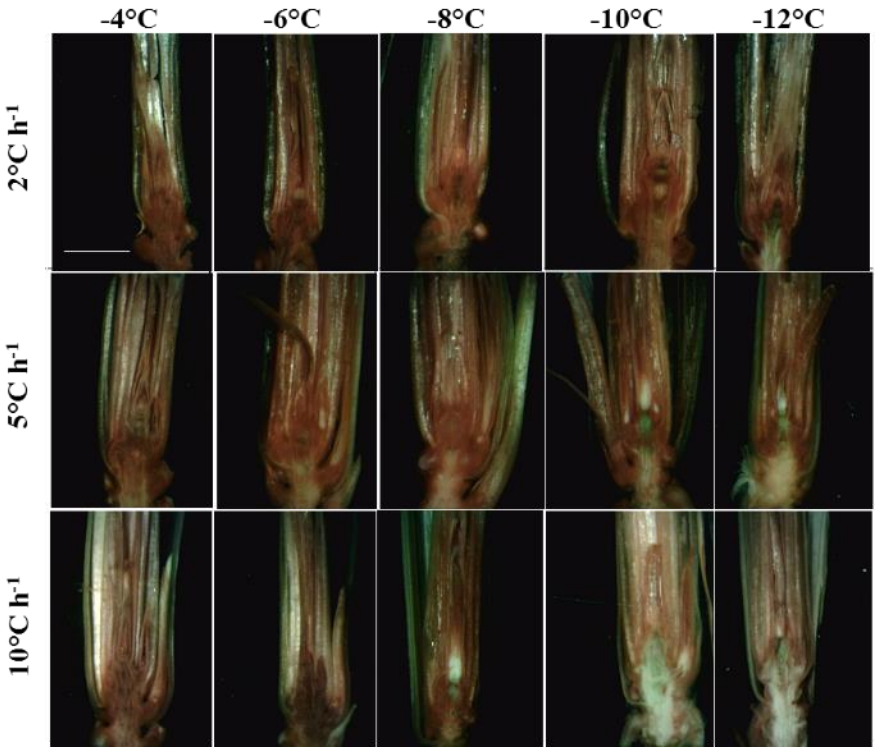

Figure 4.6 Effect of cooling rate on the region of injury in cold-acclimated Puma crowns

Crowns were cooled using the tube-in-bath system at a rate of either 2°C, 5°C or 10°C h^{-1}. Crowns were sampled at each temperature, recovered at 20°C for 3 d and then stained with tetrazolium chloride. The most representative images were displayed. Scale bar = 0.8 cm

Table 4.4 Freezing in the moist sand of cold-acclimated Norstar and Puma at a cooling rate of 2, 5 or 10°C h^{-1}.

Whole plant freezing recovery (LT_{50}) and tissue-specific injury (TTC_{50}) were presented as a means of three independent experiments (N = 3; 20 crowns per temperature per treatment in each LT_{50} or TTC_{50} experiment with 3 replicates in time and space). The exotherms were presented as a means of the total number of plants (N = 21; 7 crowns and 3 replicates in time and space). Means with different letters in a column were significantly different according to Fisher's LSD (Two-way ANOVA, $P < 0.05$). Means within a row (TTC_{50}) were determined to be significantly different using the two-tailed t-test (ns $P > 0.05$, * $P < 0.05$).

Cultivar	Cooling rate (°C h^{-1})	LT_{50} (°C)	TTC_{50} (°C)			High temperature exotherm (°C)	Mid temperature exotherm (°C)	Low temperature exotherm (°C)
			SAM	VTZ	P			
Norstar	2	-18 c	-19 c	-12 a	*	-3.9 a	-8.1 b	-17.0 a
	5	-8 ab	-8 ab	-12 a	*	-3.8 a	-6.1 a	bdl
	10	-6 a	-6 a	-11 a	*	-3.7 a	bdl	bdl
Puma	2	-28 d	-30 d	-13 a	*	-3.8 a	-8.9 c	-25.8 b
	5	-10 b	-10 b	-13 a	ns	-3.7 a	-7.5 b	bdl
	10	-8 ab	-8 ab	-11 a	ns	-3.8 a	bdl	bdl
$LSD_{0.05}$		2	3	2		0.2	0.5	1.6

Abbreviations include: below detectable limits (bdl), shoot apical meristem (SAM) and vascular transition zone (VTZ).

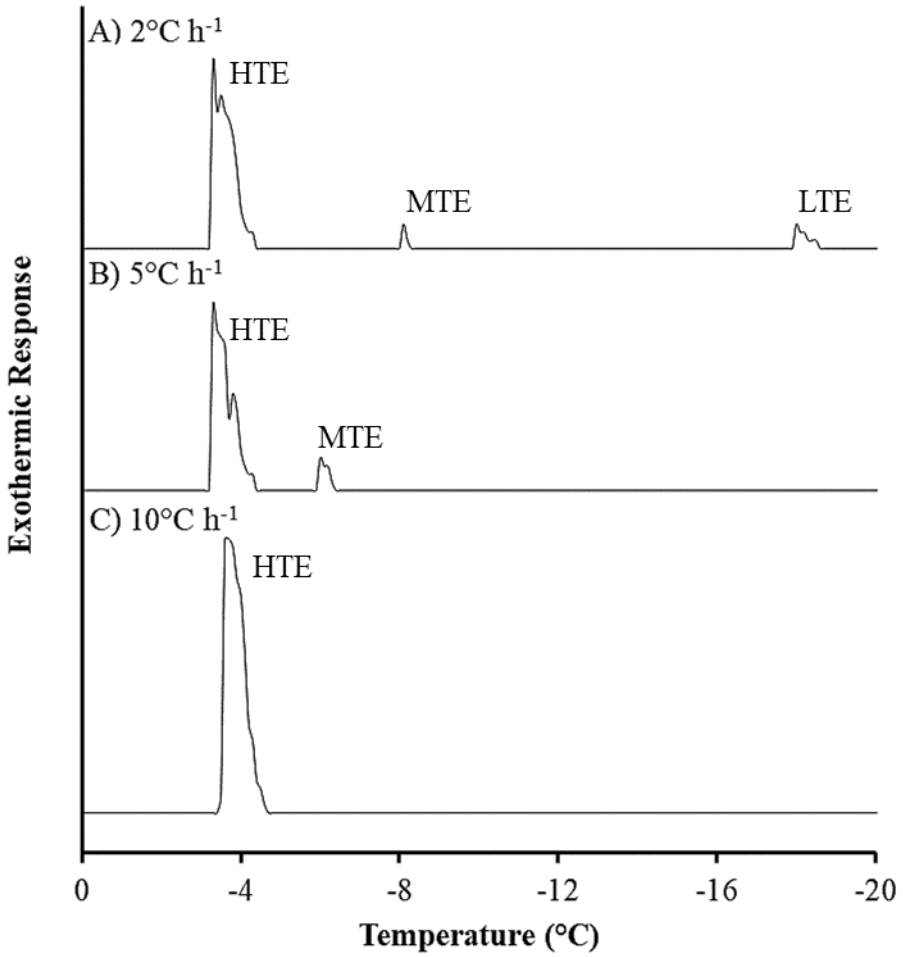

Figure 4.7 Differential thermal analysis (DTA) of cold-acclimated Norstar wheat cooled at 2°C h^{-1}, 5°C h^{-1} or 10°C h^{-1}.

Representative DTA profiles of A) 2°C h^{-1} depicting a high (HTE), mid (MTE) and low (LTE) temperature exotherm, B) 5°C h^{-1} with a HTE and MTE and C) 10°C h^{-1} with a HTE. Thermocouples were placed near the VTZ at the base of the crown and held in place with parafilm. Plants were placed in a test tube with INA^{+} suspension. Similar DTA profiles were generated for cold-acclimated Puma rye (data not shown).

Table 4.5 Percentage of seminal (S) and adventitious (A) safe roots in non (NA), cold (ACC) and frost hardened (FH) winter wheat and following slow cooling to -10°C or -14°C.

Data are presented as a mean of the total number of plants (N = 30; 10 replicates and 3 replicates in time and space). Means with different letters in a column were significantly different according to Fisher's LSD (Two-way ANOVA, $P < 0.05$). Mean values greater than 95 % were deemed safe. Non-acclimated crown roots were damaged (DMG) after sub-zero temperature treatments and could not be rated.

Cultivar	Acclimation	Percentage of safe roots (%)					
		Non-treated		-10°C		-14°C	
		S	A	S	A	S	A
Norstar	NA	69 b	75 a	DMG	DMG	DMG	DMG
	ACC	76 a	79 a	62 b	72 a	49 c	67 c
	FH	80 a	78 a	70 a	74 a	66 b	75 b
Hazlet	NA	> 95	> 95	DMG	DMG	DMG	DMG
	ACC	> 95	> 95	> 95	> 95	76 a	89 a
	FH	> 95	> 95	> 95	> 95	85 a	93 a
Puma	NA	> 95	> 95	DMG	DMG	DMG	DMG
	ACC	> 95	> 95	> 95	> 95	92	> 95
	FH	> 95	> 95	> 95	> 95	> 95	> 95
$LSD_{0.05}$		6	6	7	7	5	4

Furthermore, frost hardened Puma cooled to -14°C had significantly less injury to the nodal plate and VTZ than Hazlet. There was no significant difference ($P > 0.05$) in the percentage of safe or unsafe root systems amongst Puma rye crowns after cold acclimation or sub-zero temperature treatments.

4.4.5 Visual observations of exotherms with infrared video thermography (IRVT)

In non-acclimated plants, freezing initiated near the base of the crown, independently of the INA^+ droplet (**Figure 4.8**). The initial site of ice nucleation at the base of the crown could not be localized to either the nodal plate, VTZ or base of the leaf sheath surrounding the crown. Cold-acclimated Norstar, Hazlet and Puma exhibited an initial exotherm from the INA^+ droplet at the roots, which radiated up the roots and through the base of the crown. Exotherms observed in aerial leaves were independent of crown freezing events and never penetrated the crown. No specific pattern of freezing amongst aerial leaves was observed. There was no difference in the pattern of the exothermic events among the three cultivars. In the absence of an extrinsic nucleator, the high temperature exotherm in cold-acclimated plants originated from the base of the crown. This initial exotherm radiated up the lower 8 cm of the main shoot and adjoining tillers and down the root tissue.

Regardless of the presence or absence of an extrinsic nucleator, there was no difference in the amount of time required for non-acclimated plants to obtain a complete dissipation of all exothermic events after exposure to -4°C (**Table 4.6**). In cold-acclimated plants, crowns became isothermal after 34 min in Norstar and between 41 to 44 min in Hazlet or Puma rye. In cold-acclimated plants, the addition of INA^+ at the roots resulted in a significant increase in the length of time for complete dissipation of crown exothermic events following exposure to -4°C (two-tailed t-test, $P < 0.001$). In plants held at -4°C for 12 h, there were no observed exothermic events recorded after the first hour. All plants held at -4°C for 12 h with exposed roots were capable of recovery and root re-generation (data not shown). No additional exothermic events were observed in non-acclimated plants cooled at 2°C h^{-1} from -4°C to -8°C. The non-acclimated plants remained isothermal with the chamber temperature. In Norstar, Hazlet and Puma, a second exothermic event initiated from the center of the lower crown was observed in cold-acclimated plants around -8°C. This second exothermic event lasted approximately 30 min.

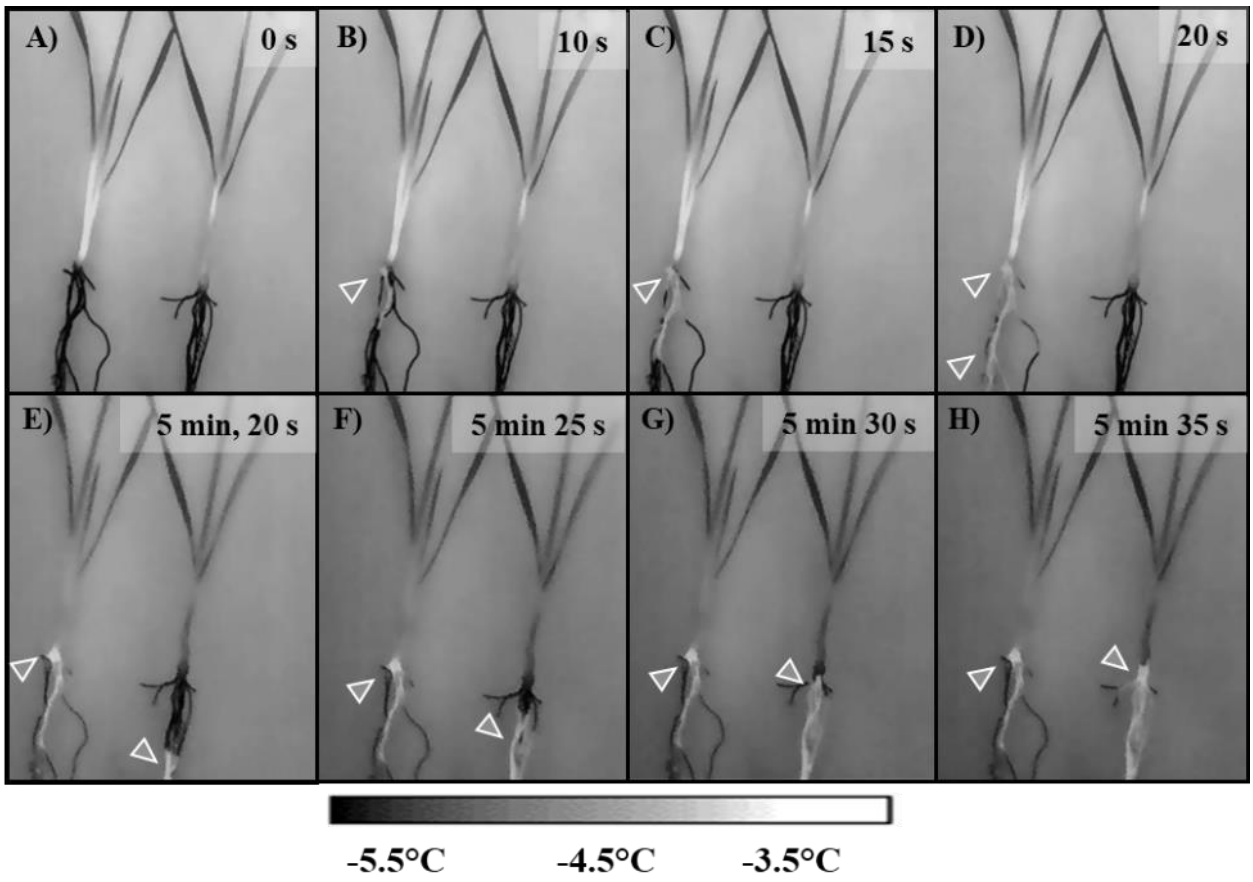

Figure 4.8 Visualization of exotherms with infrared imaging in non-acclimated (left plant) and cold-acclimated (right plant) Norstar winter wheat cooled to -4°C.

Freezing was induced by INA+ at the leaf tip and the root base. When water undergoes a phase transition, from a liquid to a solid, stored energy is released in form of exothermic heat. Exotherms are visualized using a HgCdTe long-wave (7.5 – 13.0 µm) detector. Time course (A – H) of the initial freezing in a non-acclimated and cold-acclimated Norstar. Plants were nucleated with INA^+ at the leaf tip and the root base. (A-D) In non-acclimated plants, exotherms (arrow) were visually observed at the base of the crown prior to freezing at either INA^+ droplet. (E-H) In cold-acclimated Norstar, exotherms were visually observed to initiate from the root INA^+ droplet, through the base of the crown.

Table 4.6 Length of time required to attain a complete dissipation of crown exothermic events at -4°C for non-acclimated (NA) and cold-acclimated (ACC) Norstar, Hazlet and Puma

INA^+ was applied to the leaf tip and root base to initiate freezing. Data was presented as a means of the total number of plants (N = 15; 5 plants and 3 replicates in time and space). Means with different letters in a column were significantly different according to Fisher's LSD (One-way ANOVA, $P < 0.05$). Means within a row (NA or ACC) were determined to be significantly different using the two-tailed t-test (ns $P > 0.05$, * $P < 0.05$).

Cultivar	Time (min)					
	NA	NA + INA^+	P	ACC	ACC + INA^+	P
Norstar	17 a	26 a	*	21 b	34 b	*
Hazlet	18 a	24 a	*	25 a	41 a	*
Puma	18 a	25 a	*	26 a	43 a	*
$LSD_{0.05}$	2	2		3	3	

4.4.6 Exposure of crowns to sub-zero temperatures visualized by magnetic resonance microimaging (MRMI)

Axial MRMI images of non- and cold-acclimated Norstar (**Figure 4.9**), Hazlet (**Figure 4.10**) and Puma (data not shown) were observed after cooling (2.5°C h^{-1}) to a final temperature of 0°C, -5°C and -10°C. No visual differences in terms of the proton signal intensity were noted between Hazlet and Puma. As such, only one set of images for the rye cultivars was presented. The regions of SAM, an intermediate zone between the SAM and VTZ, and the VTZ were imaged in the three consecutive images 0.6 mm apart. In cold-acclimated plants held at 0°C, there was a visible decline in VTZ core and the intermediate zone proton signal intensity when compared to non-acclimated plants. At 0°C, proton signal intensity in rye was visibly higher compared to Norstar wheat. After 1 h at -5°C, proton signal was lost in non-acclimated SAM and intermediate zone sections. In non-acclimated and cold-acclimated plants, the core of the VTZ retained a proton signal after 1 h at -5°C. In cold-acclimated plants, the vascular tissue associated with the leaf sheath encapsulating the SAM and intermediate zone tissues maintained a visible proton signal. After 1 h at -10°C, there was a visible decrease in cold-acclimated crown proton signal in the leaf sheath and VTZ. Overall, signal intensity decreased in the crown by greater than 80 % between 0°C and -10°C in all twelve axial slices of cold-acclimated Norstar and Hazlet.

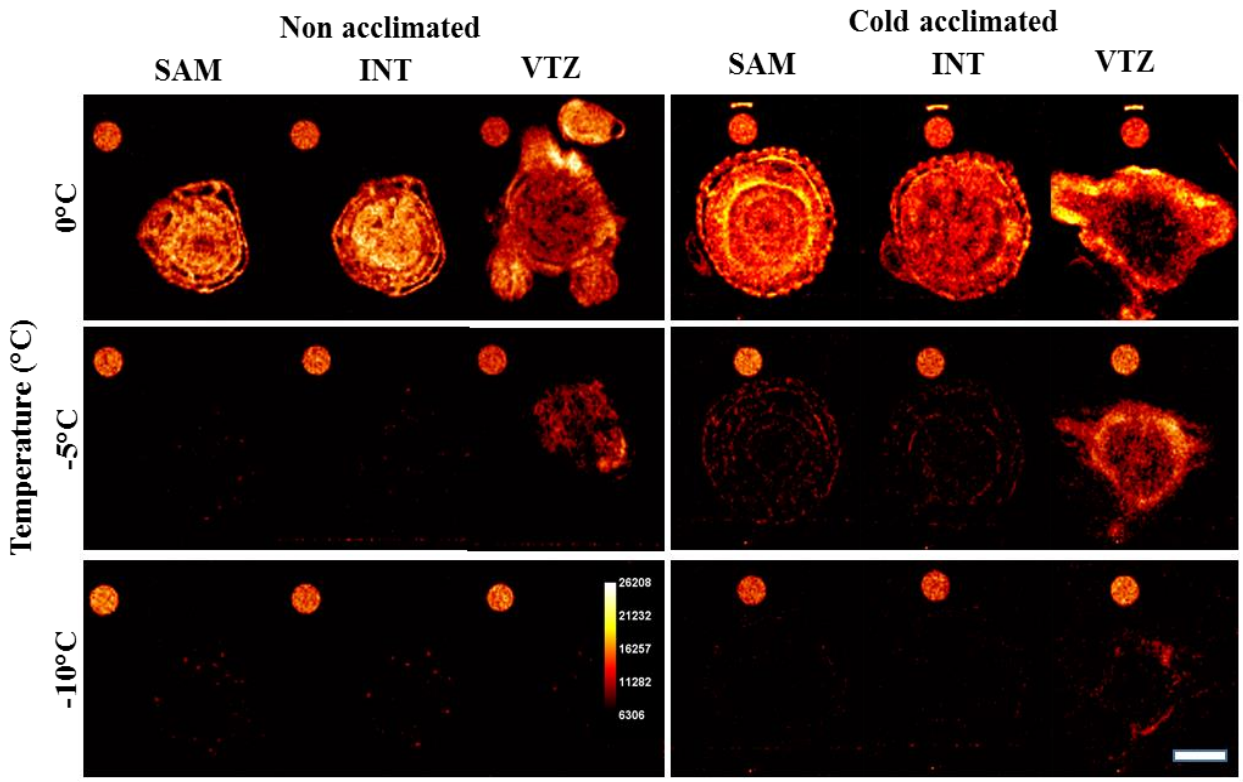

Figure 4.9 Morphological images in axial sections of non- and cold-acclimated Norstar exposed to 0°C, -5°C and -10°C for 1 h prior to MRMI.

Each temperature and treatment group were imaged a minimum of three times and a representative image was included. Signal intensity is greater (off white and yellow) in regions with higher water mobility. Standards of deuterated methanol (top row of 3 circles within each panel) were included as a non-freezing control. Scale bar = 0.5 cm.

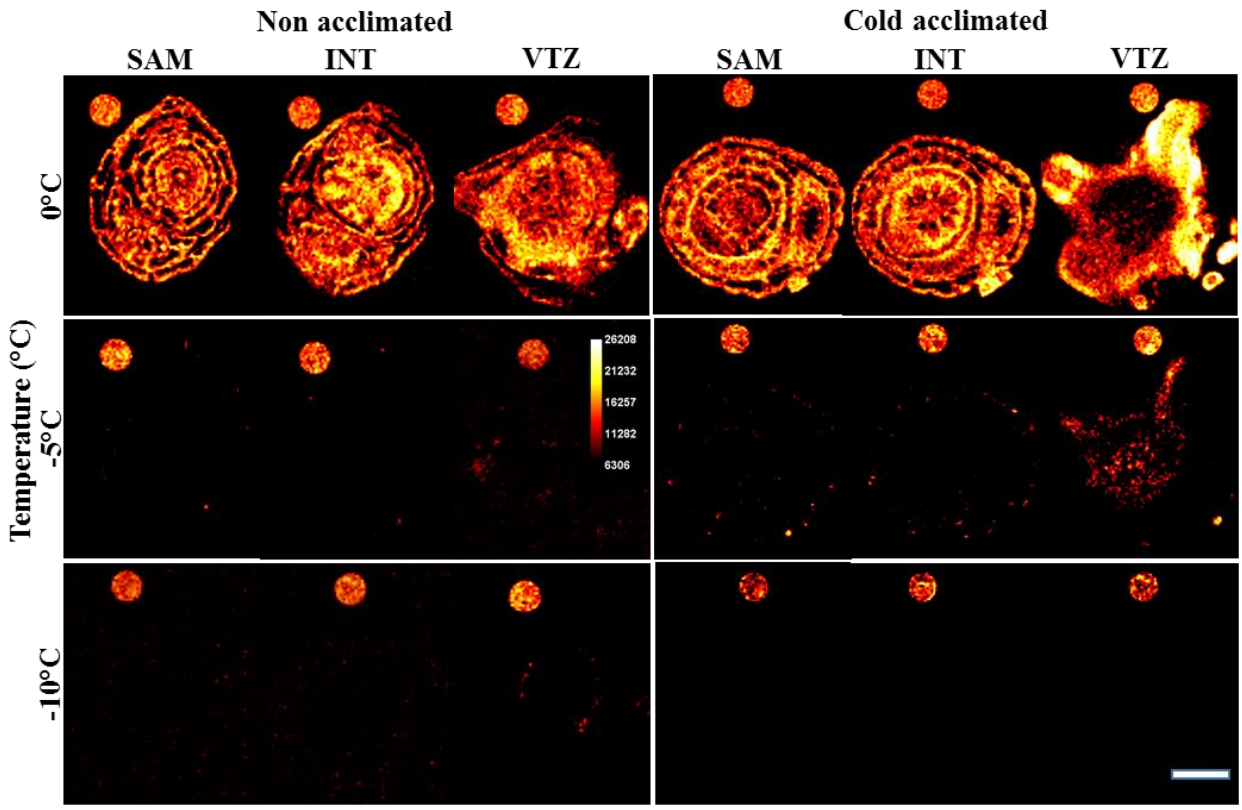

Figure 4.10 Morphological images in axial sections of non- and cold-acclimated Hazlet exposed to 0, -5 and -10°C for 1 h prior to MRMI.

Each temperature and treatment group were tested a minimum of three times and a representative image was included. Signal intensity is greater (off white and yellow) in regions with higher water mobility. Standards of deuterated methanol (top row of 3 circles within each panel) were included to act as a non-freezing control. Scale bar = 0.5 cm.

4.5 Discussion

4.5.1 The pattern of injury in crowns slowly cooled (2°C h^{-1})

Cold-acclimated Puma winter rye had a significantly more negative LT_{50} compared to Hazlet winter rye or Norstar winter wheat (**Table 4.1**). Development of cold hardiness in Norstar, Hazlet and Puma corresponded with a higher crown shearing strength (**Table 4.2**). In Chapter 3, development of cold hardiness in Norstar corresponded with increased VTZ lignification and glucuronoarabinoxylan accumulation. Increased glucuronoarabinoxylan and lignin in *Miscanthus* ecotypes corresponded with increased freezing survival (Domon et al., 2013). In winter rape (*Brassica napus L.*) leaves, cold-acclimation increased leaf tensile strength, cell wall thickness and freezing tolerance (Solecka et al., 2008). Xylem ray parenchyma cells use rigid cell walls and increased tensile strength to inhibit ice propagation and avoid freezing (Fujikawa et al., 1999). Increased cold-induced crown shearing strength in the rye cultivars, as opposed to Norstar wheat, may reflect the presence of a mechanism to protect cells against collapse, cytorrhysis (Yamada et al., 2002) and/or cell wall deformation (Fujikawa et al., 1999).

Tiller recovery was not uniform in cold-acclimated plants (**Table 4.3**). In Norstar, Hazlet and Puma, the main shoot and youngest third tiller had a more negative LT_{50} than the first and second tillers. Aniline blue staining and visual observation of lesion formation (brown tissue) revealed the plant recovered if the main shoot resisted injury or a third tiller developed from the main shoot (**Figure 4.2**). Whether the third tiller had developed prior to freezing or during the 21 d recovery phase was not established in this study. Age-dependent injury and freezing of tillers, stems or leaves were previously reported in the literature (Legge et al., 1983; Pearce and Fuller, 2001; Hacker and Neuner, 2007; Livingston et al., 2017). Crescini and Tettamanzi (1929) provided anecdotal evidence that young tillers had a higher winter survival rate than older tillers (reviewed by Legge et al., 1983). Legge et al. (1983) argued tiller freezing survival was associated with the accumulation of cryoprotectant sugars at the time of fall acclimation

The main shoot and the youngest fully developed tiller (tiller 3) had a more negative LT_{50} than the two oldest tillers (tillers 1 and 2). Livingston et al. (2017) reported an age dependent leaf and tiller freezing pattern in four field-acclimated wheat genotypes. Field-acclimated older leaves had a higher water content and froze before the younger leaves (Livingston et al., 2017). After the initial exothermic events originating from the roots, cold-acclimated barley leaves froze in an age-dependent pattern (Pearce and Fuller, 2001). Older leaves and shoots froze before younger leaves

in the alpine shrub *Buxus sempervirens* (Hacker and Neuner, 2007). Similar observations of age-dependent freezing were reported in the needles of *Taxus baccata* and stems of *Fagus sylvatica* (Hacker and Neuner, 2007).

4.5.2 Effect of cooling rate on the pattern of freezing injury

When cold acclimated Norstar, Hazlet and Puma were cooled at < 2°C h^{-1} to -40°C, the VTZ was injured prior to the SAM (**Table 4.4**; **Figure 4.3**). This pattern of injury was consistent with the previous visual observations of degenerated tissue (Beard and Olien, 1963; Olien and Marchetti, 1976), staining with TTC (Tanino and McKersie, 1985; Livingston et al., 2013), root regeneration (Chen et al., 1983) and histological analysis (Livingston et al., 2005b; Livingston et al., 2013; Livingston and Tuong, 2014). Fast cooling (5°C h^{-1} or 10°C h^{-1}) does not represent natural cooling rates in the field. However, supercooling of plant tissues is dependent on slow cooling rates (George et al., 1974; Ishikawa and Sakai, 1981; 1985). Fast cooling rates can then be used to reveal structure-function mechanisms due to the increased physical force of ice propagation in supercooling tissues. Cooling of Norstar (5°C h^{-1} or 10°C h^{-1}) and Puma (10°C h^{-1}) resulted in SAM injury prior to the VTZ (**Table 4.4**; **Figure 4.5**; **Figure 4.6**). Injury to the SAM, as identified by TTC staining, was lethal in cold-acclimated Norstar cooled at 2°C h^{-1} (Chapter 3) and in Norstar and Puma cooled at > 5°C h^{-1}. This was the first report of visual tissue-specific injury observations in cold-acclimated crowns exposed to rapid cooling. Faster cooling rates induced a warmer LT_{50} and floret injury in *Cornus offieinalis* Sieb, et Zucc overwintering tree buds (Ishikawa and Sakai, 1985). When buds were cooled at 9°C h^{-1}, the scales and florets froze around -7°C. When *C. offieinalis* buds were cooled at 5°C h^{-1}, the scales froze around -5°C and the florets froze independently between -8°C and -18°C. Holding *C. offieinalis* buds at -9°C for 48 h, then cooled at 5°C h^{-1} resulted in a shift of the low temperature exotherms to between -15°C and -25°C.

The SAM in cold-acclimated Puma rye may avoid freezing injury to a more negative sub-zero temperature when cooled at 5°C h^{-1} due to a lower tissue-specific water content or higher total sugar concentration compared to SAM in Norstar. Olien (1964) using an electrophoretic method, reported non-equilibrium freezing was induced in young leaves and the SAM of Hudson barley crowns with a high-water content (> 3.2 g H_2O g dry weight). Ishikawa and colleagues hypothesized an increase in cooling rate resulted in a warmer low temperature exotherm due to a break in floret supercooling (Ishikawa and Sakai, 1982, 1985; Ishikawa et al., 2015; Ishikawa et

al., 2016). A slower cooling rate was required to establish the scales as an ice sink and re-distribute water from freezing sensitive floret tissues. The volume of crown water and the cooling rate determines if the winter cereal undergoes equilibrium or non-equilibrium freezing at a tissue or whole crown level (Olien, 1964; Olien and Livingston, 2006). A similar freezing tolerance and avoidance mechanism as observed in overwintering tree buds could occur in crowns.

4.5.3 Mode of freezing in crowns cooled at a rate of 2°C h^{-1} or exposed to durational freezing

Livingston and colleagues recently reported in field and chamber experiments using IRVT, that exotherms were first observed at the base of the crown (Livingston et al., 2016; Livingston et al., 2017). This corroborated our chamber-based ice nucleation and supercooling study (**Figure 4.8**; **Table 4.6**) and Pearce and Fuller (2001) who reported exotherms associated with the roots were observed before freezing events associated with aerial leaves. If bare roots are held at the same temperature as aerial leaves and if both roots and aerial leaves are extrinsically nucleated, roots will freeze first with exotherms propagating up through the nodal plate and initiates crown freezing (**Figure 4.8**). In the absence of an extrinsic nucleator, the initial nucleation was observed in the lower crown. Livingston et al. (2017) reported high intensity exotherms developed from the soil in the field prior to the plant's 'bottom-up' freezing event. The high intensity exotherms were hypothesized to be from a thin layer of water within the soil matrix that served as an ice nucleator and initiated crown nucleation.

If ice nucleation was not initiated extrinsically, it is possible that intrinsic nucleators present in the lower crown were responsible for ice nucleation. Gusta et al. (1975) reported cold-acclimated winter wheat crown tissues had a high concentration of water. The probability of ice nucleation increases with the volume of available water (Ashworth et al., 1985) and the amount of time and temperature at which plant tissues were supercooled (Vali, 1995). Ice nucleation was reported in the vascular tissue of winter rye leaves (Griffith et al., 2005) and non-grass species (Wisniewski et al., 1997; Ball et al., 2002; Gusta et al., 2004; Hacker and Neuner, 2007, 2008; Hacker et al., 2011; Neuner and Hacker, 2012) due to a high concentration of free water. Given the vascular tissue near the base of the crown (VTZ) was the initial site of injury in *Poaceae* (Beard and Olien, 1963; Olien, 1964; Olien and Marchetti, 1976; Chen et al., 1983; Tanino and McKersie, 1985; Livingston et al., 2013; Chapter 3), it is plausible that tissue associated with or part of the

VTZ contains intrinsic nucleators. Brush et al. (1994) reported on intrinsic plant nucleators in the aerial leaves of cold-acclimated rye.

Additional frost hardening of cold-acclimated crowns reduced freezing injury to the VTZ to a greater degree in rye as opposed to Norstar as measured by the root pressure test (**Table 4.5**). If ice nucleation was extrinsically initiated at the roots (**Figure 4.8**) or intrinsically at the base of the crown, a reduced VTZ water content inhibits the rate of ice propagation through crown tissues. Prolonged exposure to non-lethal sub-zero temperatures re-distributes water amongst tissues and cellular constituents (Tumanov and Krasasvtsev, 1959; Ishikawa and Sakai, 1985; Livingston and Henson, 1998; Livingston et al., 2005a; Herman et al., 2006; Olien and Livingston, 2006; Ishikawa et al., 2016). The remaining fraction of liquid water was bound to intracellular constituents, the plasma membrane or the cell wall (Towill and Mazur, 1976; Levitt, 1980; Olien and Livingston, 2006). Olien (1964) reported that freezing injury in crown vascular elements was dependent on crown water content. Equilibrium freezing, and the accumulation of small ice crystals were observed in the VTZ of cold-acclimated Hudson barley crowns with a low water content (< 1.9 g H_2O g dry weight) (Olien, 1964). Hudson crowns with more than 2.5 g H_2O g dry weight resulted in non-equilibrium freezing in the VTZ, large ice crystal formation and the shearing of plant tissues.

Injury to the VTZ prior to the SAM was visually observed in plants cooled at 2°C h^{-1} and then held at -10°C, -12°C or -14°C for up to 30 d (**Table 4.4**; **Figure 4.4**). This was the first report of tissue-specific injury observations in cold-acclimated crowns exposed to a durational freezing. In the VTZ vascular elements, slow cooling coupled with durational freezing would promote VTZ dehydration and equilibrium freezing. Additional experimentation is required to determine if freezing duration at a temperature warmer than the VTZ TTC_{50} (**Table 4.4**) induces injury to the VTZ prior to the SAM.

4.5.4 Conclusions

The initial injury to the VTZ was dependent on slow cooling and that rye was better able to reduce SAM freezing injury compared to Norstar. In cold-acclimated wheat and rye crowns, cooling rates of less than 2°C h^{-1} are required to develop maximum cold hardiness. This is consistent with reports that slow cooling is required for the desiccation of the primordia or florets to avoid freezing, and the reduction of water in the vascular tissue below the crown plate to tolerate

freezing injury (George et al., 1974; Graham and Mullin, 1976; Quamme, 1978; Sakai, 1979; Ishikawa and Sakai, 1981; Ishikawa and Sakai, 1985; Quamme et al., 1995; Endoh et al., 2009; Endoh et al., 2014; Ishikawa et al., 2015; Ishikawa et al., 2016). Cold-acclimated crowns cooled at 2°C h^{-1} have a high, mid and low temperature exotherm. The high temperature exotherm corresponds with the freezing of free water as visually observed with MRMI and IRVT. The mid temperature exotherm corresponds with injury to the VTZ as reported by the VTZ TTC_{50} and a loss in proton signal in the VTZ. The low temperature exotherm corresponds to the SAM TTC_{50} and death of the plant (LT_{50}). This corroborates the previous SAM and VTZ TTC_{50} for partially and fully cold-acclimated Norstar reported in Chapter 3.

Cold-acclimated crowns exposed to a -10°C, -12°C or -14°C for up to 30 d were first injured in the VTZ. Frost hardening of cold-acclimated crowns for 72 h at -4°C prior to cooling, reduced the degree of injury to the nodal plate and VTZ. Cooling rates faster than 5°C h^{-1} reveal the SAM in Puma were more resistant than Norstar and that slow cooling rates are required for cold-acclimated SAM and VTZ to avoid non-equilibrium freezing. Extrinsic nucleation of exposed roots resulted in ice propagation up into the crown. In the absence of an extrinsic nucleator, ice nucleation was initiated in the lower crown. The location and source of this nucleator could not be determined with MRMI or IRVT. This question was the focus of the following chapter to I) determine if freezing in the lower crown was a result of an intrinsic nucleator. II) If a nucleator is present, determine if it was associated with the VTZ or the leaf sheath encapsulating the crown. III) Does the site of nucleation act as an ice sink for the crown.

Chapter 5

5 Localization of ice nucleating activity to the leaf sheath and its role in freezing survival

5.1 Abstract

The crown is the critical organ for winter cereal survival. Remarkably, little work has investigated the tissue-specific mechanism of resistance within the crown. Specifically, the role of the leaf sheath surrounding these crowns and how its freezing affects overall crown resistance has not been explored. High ice nucleation temperatures (-3.5°C) in the leaf sheath and intermediate ice nucleation temperatures (-5°C to -6°C) in the VTZ were determined using the test tube assay. Leaf sheath ice nucleation temperature decreased after this tissue was washed. Exogenous fluids washed from the leaf sheath had a high ice nucleating activity (-3.8°C) and significantly decreased (-8°C) if autoclaved (121°C for 20 min). Cell wall extracts from the leaf sheath and VTZ had an intermediate ice nucleation temperature (-6°C) and were unaffected by the autoclave treatment. Cold-acclimated SAM had a low ice nucleation temperature (-10°C to -13°C) regardless of treatment groups. Apoplast fluids from the SAM and VTZ had low ice nucleation temperatures. Infiltrating non-acclimated crowns with cold-acclimated fluids lowered the ice nucleation temperature and infiltrated crowns were killed upon freezing. Ice was visually observed between the leaf sheaths of cold-acclimated Norstar and Puma. Norstar SAM was more sensitive to the loss of the leaf sheath than Puma. Early injury to the SAM in main shoots lacking a leaf sheath was confirmed by differential thermal analysis and tetrazolium chloride staining. The high leaf sheath ice nucleation temperatures appear to contribute to the sequential order of freezing among crown tissues and in turn, to freezing resistance of the winter cereal crown.

5.2 Introduction

Cold-acclimated crowns display diverse but controlled freezing behaviours when exposed to sub-zero temperatures. In cold-acclimated cereals, leaf and root freezing injury were reported around -8°C (Olien, 1964; Gusta and Fowler, 1977; Chen et al., 1983). Whereas crowns have a wide range in freezing survival temperatures, from -8°C in cold-acclimated spring cereals (Fowler et al., 1977; Limin and Fowler, 2002) to -34°C in Puma rye (*Secale cereale* L.) (Gusta et al., 1997). The degree of freezing survival depends on the length of cold-acclimation, the cooling rate (Chapter 4), the temperature and length of time exposed to sub-zero temperatures as well as field or chamber growth conditions and/or exposure to additional environmental stressors (Olien, 1964; Metcalf et al., 1970; Gusta and Fowler, 1977; Chen et al., 1983; Tanino and McKersie, 1985; Livingston et al., 2013; Chapter 3). Cold-acclimated crown tissues do not have a uniform pattern of freezing injury. Tanino and McKersie (1985) reported the VTZ was injured at a warmer sub-zero temperature than the SAM. This corroborated visual observations of VTZ 'browning' post recovery in freeze-injured barley (*Hordeum vulgare* L.) (Olien, 1964; Olien and Marchetti, 1976), Norstar wheat (*Triticum aestivum* L.) and Puma rye (Chapter 4). Chen et al. (1983) reported freezing impeded VTZ root meristem cells re-growth prior to SAM injury. In Chapter 3 the VTZ was injured in partially and fully cold-acclimated Norstar wheat around -10°C, whereas the SAM was injured near the actual whole plant LT_{50} survival. These types of freezing injury were specific to tissues in the plant and important determinants of their degree of cold-acclimation and survival. This corresponded to two significantly different patterns of cold-acclimation revealed in the SAM and VTZ apoplast proteome.

Mechanisms controlling tissue-specific freezing behaviours remain unanswered. These include controlled management of ice nucleation and propagation, water flow, stabilization of supercooling and inhibition of ice growth. Among these, the initial location of ice nucleation establishes freezing behaviours on a cellular (extracellular freezing) or tissue (extra-organ freezing) scale. Initiation of ice formation outside the cell, in the apoplast, generates the driving force for withdrawing cellular water from the intracellular space (Siminovitch and Scarth, 1938; Levitt, 1980). Ice can form in specific tissues known as ice sinks (Wiegand, 1906a; Wiegand, 1906b; Dorsey, 1934; Dereuddre, 1978; Sakai, 1979; Ishikawa and Sakai, 1981; Ishikawa and Sakai, 1985; Ashworth et al., 1989; Endoh et al., 2014; Kishimoto et al., 2014b; Ishikawa et al., 2015), establishing tissue chemical potential differences. Ice formation in the scales of

overwintering rhododendron (*Rhododendron japonicum* A. Gray) buds, facilitated water migration from the florets (Ishikawa and Sakai, 1981; Ishikawa et al., 2015). A reduction in floret water increased the degree of supercooling and freezing survival. In chapter 4, exotherms were visually observed with IRVT to initiate at the base of cold-acclimated crowns in the absence of an extrinsic nucleator. The location and source of the nucleation event could not be identified with IRVT or MRMI. In cold-acclimated winter barley (*Hordeum vulgare* L.) crowns, the leaf sheath was disrupted by ice crystal formation prior to VTZ freezing injury (Livingston and Tuong, 2014). However, the leaf sheath's role as an ice sink has not been proposed in the literature.

Efforts to identify plant ice nucleators have been most prominent during late spring or early frost injury in annual crops (Lindow et al., 1978b; Lindow et al., 1982; Brush et al., 1994) and fruit-bearing woody perennials (Dorsey, 1934; Quamme, 1978; Ashworth et al., 1989; Kishimoto et al., 2014a; Kishimoto et al., 2014b). Most freezing sensitive crops lack intrinsic ice nuclei active at temperatures warmer than -6°C (Lindow et al., 1982). Bacterial nuclei responsible for lethal freezing injury in annual crops have a higher ice nucleation temperature than intrinsic plant ice nucleators (Lindow et al., 1978a, b; Lindow et al., 1982), are proteinaceous and heat sensitive (Lindow, 1983; Wolber et al., 1986). Identification of intrinsic plant nucleators was less common in the literature (reviewed by Wisniewski et al., 2009).

Intrinsic plant ice nucleators from *Lobelia telekii* retained high ice nucleation temperatures (-4°C) after boiling and were identified as carbohydrates (Krog et al., 1979). Rhododendron flower bud scale ice nucleation temperatures (-5°C to -6°C) were unaffected by temperatures as high as 121°C (Ishikawa et al., 2015). Peach (*Prunus persica* L.*)* wood ice nucleation temperatures (-2°C to -6°C) had a higher resistance to protein denaturing and heating treatments than bacterial ice nucleators (Ashworth and Davis, 1984). Intrinsic winter rye leaf ice nucleators (-6°C to -8°C) were composed of protein, phospholipids and carbohydrates (Brush et al., 1994). Dreischmeier and colleagues reported polysaccharides in European alder (*Alnus glutinosa* L. Gaertn), birch (*Betula pendula* L.) and Scots pine (*Pinus sylvestris* L.) pollen were responsible for heterogenous ice nucleation (Dreischmeier et al., 2017). Kishimoto and colleagues reported high ice nucleation temperatures (-1°C to -4°C) in blueberry (*Vaccinium corymbosum* L.; *Vaccinium ashei* Reade) stem bark (Kishimoto et al., 2014a; Kishimoto et al., 2014b). Stem bark ice nucleators isolated from the apoplast and cell wall extracts were resistant to anti-microbial treatments (Kishimoto et al., 2014b).

5.2.1 Hypothesis

In cold-acclimated winter wheat and rye, high leaf sheath ice nucleation temperatures increase crown cold hardiness by acting as an ice sink relative to the SAM and VTZ.

5.2.2 Objectives

The overall mechanism of controlled initiation of freezing in cold-acclimated crown tissues remains obscure. Determination of ice nucleating activity (INA) in tissues, the capacity to cause heterogeneous ice nucleation and the identification of ice nucleators will address this long unanswered question in cold-acclimated crowns. The objective of this chapter was to characterize the ice nucleation temperatures of cold-acclimated winter wheat and rye crowns and spatially localize nucleators in organ, tissue and crude extracts, evaluate the effect of heat and vacuum infiltration treatments.

5.3 Materials and methods

5.3.1 Plant material and growth conditions

Norstar winter wheat, Hazlet rye and Puma rye were germinated and grown hydroponically as described in section 3.3.1.

5.3.2 Whole plant freezing survival (LT_{50})

Whole plant freezing survival (LT_{50}) after 21 d of recovery was determined as described previously in section 3.3.2.

5.3.3 Preparation of crown tissue and crude extractions

Crowns were excised from Norstar, Hazlet or Puma as described in section 3.3.2. Individual tissues were excised under aseptic conditions using sterilized forceps and razor blades. The apoplast extract was collected using the swinging bucket method described in section 3.3.4. Approximately 0.5 g of tissue was placed in a test tube with 2 mL of MilliQ water, moved to a rotary shaker at 80 rpm for 30 min at 4°C. Washing fluid was decanted, frozen in liquid nitrogen, and stored at -80°C until needed. Tissue was blotted dry with absorbent paper and homogenized with a chilled mortar and pestle with 2 mL chilled phosphate buffered saline (137 mM NaCl, 2.7 mM KCl, 10 mM Na_2HPO_4, 1.8 mM KH_2PO_4, pH 6.5) as described by Gusta et al. (2004). The

homogenate was vacuum-filtrated through filter paper, pipetted into sterile microcentrifuge tubes, frozen in liquid nitrogen, and stored at -80°C until needed (crude extract). Sample on the filter paper was rinsed twice with 10 mL phosphate buffered saline and twice with 10 mL MilliQ water. Washed sample was collected in sterile microcentrifuge tubes, freeze-dried, frozen in liquid nitrogen, and stored at -80°C until needed (cell wall extract) as described by Solecka et al. (2008).

5.3.4 Test tube assay for heterogeneous ice nucleation temperatures

Tissue was placed into 2 mL autoclaved MilliQ water in sterilized 12 cm X 3 cm coring test tubes with a transparent polyester film lid. For each crude extract, 200 µL of apoplast fluids, 50 µL of homogenate suspended in 150 µL of phosphate buffered saline or 20 mg of cell wall suspended in 180 µL phosphate buffered saline were dispensed into 10 mm X 75 mm test tubes. The tubes were cooled in a stepwise manner in an ethylene glycol bath from 0°C to -20°C at a rate of 0.5°C every 15 min. At the end of every 15 min, the number of frozen tubes were counted. To determine the heat stability of the ice nucleation active substances within the samples, tubes containing crown tissues were autoclaved for 20 min at 121°C. After cooling to room temperature, autoclaved tubes were cooled in an ethylene glycol bath from 0°C to -20°C at a rate of 0.5°C every 15 min. To determine the effects of the leachate, crown tissues were rinsed with MilliQ water and then aseptically transferred to a fresh tube. In each experiment, ten tubes per treatment group were tested and the experiment was independently repeated three times.

5.3.5 Crown infiltration with apoplast fluids

Apoplastic fluids from crowns cold-acclimated for 42 d at 4°C then hardened at -4°C for 72 h were collected using the swinging bucket method. Apoplast fluids were diluted (1:10, 1:100 or 1:1000) in phosphate buffered saline. Non-acclimated Puma and Norstar crowns were vacuum infiltrated at -50 kPa for 10 min in 3 cm x 5 cm flat-bottomed glass vials filled with 5 mL diluted extract. Infiltrated crowns and/or diluted fluids were frozen using the test tube assay to determine the ice nucleation temperature. A subsection of infiltrated crowns was frozen and tested for freezing survival to determine the effect of apoplast fluids on the crowns ability to recover from freezing as per section 3.3.2. In each experiment, ten crowns per treatment group were tested and the experiment was independently repeated three times.

5.3.6 Sugar analysis of apoplast fluids using RP-HPLC

Norstar and Puma SAM and VTZ from non-acclimated, cold-acclimated and frost hardened (acclimated and then exposed to -4°C for 72 h) were excised using sterile forceps and a razor blade, rinsed in MilliQ water and then placed in a 15 mL syringe pre-packed with glass wool. The syringe was placed in a larger test tube. The syringe in tube system was placed in a swinging bucket and centrifuged at 6000 rpm for 2 h. Fluids collected in the test tube were filtered (0.45 µm) into a clean, sterile microfuge tube and stored at -80°C. For reverse phase HPLC analysis 80 µL of sample was diluted 1:1 with solvent (95 % acetonitrile, 5 % water, 0.1 % triethanolamine) in a 1.5 mL glass vial with a 100 µL insert. Analysis of sugars by reverse phase high performance liquid chromatography (RP-HPLC) was performed according to Agriculture and Agrifood Canada (Saskatoon) guidelines (Krista Thompson, Personal Communication) using a Waters Acquity UPLC (Mississauga, ON, Canada) with a Waters UPLC ELS detector (Mississauga, ON, Canada). A 2 µL sample was injected onto an Acquity UPLC BEH Amide 1.7 µm packing column (2.1 X 100 mm, Milford, MA, USA) with a mobile phase (95 % acetonitrile, 5 % water) at a flow rate of 0.12 mL min^{-1}. Sugars were detected at 500 nm with a UV detector. Standards for each sugar were made in HPLC grade reverse osmosis water and calibration curves were generated for each. To verify running conditions, a mixture of standards (and a duplicate) was run before each batch of samples. Sample duplicates were included every fifteen samples to confirm column integrity and repeatability of the separation and quantification of the chromatographic peaks.

5.3.7 Visual observation of crowns at sub-zero temperatures

Cold-acclimated Norstar and Puma plants were enclosed in sealed polyethylene bags, cooled at 2°C h^{-1} from 0°C to -20°C in a programmable freezer (Cincinnati Sub-Zero, Cincinnati, Ohio, USA), then transferred to a cold room (-5°C) without thawing. Crowns were dissected longitudinally and observed under a dissecting microscope. A minimum of twelve crowns was sectioned for each temperature treatment.

5.3.8 Scanning electron microscopy (SEM)

Crowns washed with distilled water, sectioned longitudinally and placed in fixative (45 % ethanol, 40 % water, 10 % formaldehyde, 5 % glacial acetic acid) for 3 d at 4ºC. Samples were then washed twice with phosphate buffered saline and dehydrated with ethanol step-wise at room

temperature; 1 h (30 % ethanol, 70 % phosphate buffered saline), 1 h (50 % ethanol, 50 % phosphate buffered saline), 1 h (70 % ethanol, 30 % phosphate buffered saline), 1 h (80 % ethanol, 20 % phosphate buffered saline), 1 h (90 % ethanol, 10 % phosphate buffered saline), 1 h (95 % ethanol, 5 % phosphate buffered saline) and 1 h (100 % ethanol). Samples were held in 100 % ethanol overnight at 4ºC. Samples were then substituted with amyl acetate step-wise at room temperature; 20 min (25 % amyl acetate, 75% ethanol), 20 min (50 % amyl acetate: 50 % ethanol), 20 min (75 % amyl acetate, 25 % ethanol), 20 min (100 % amyl acetate), 20 min (100 % amyl acetate). Samples were critically point dried (Polaron E3000, East Sussex, UK), mounted on 15 mm discs and sputter coated with gold. Images were recorded using a scanning electron microscope (Hitachi FE-SEM SU8010, Tokyo, Japan). Images presented are the most representative of four biological replicates.

5.3.9 Crown manipulation – leaf sheath removal

Two treatment groups (intact and removed), and cultivars (Norstar and Puma) were used to determine the effect of the leaf sheath on crown freezing survival. The differential thermal analysis was conducted as described by George and Burke (1977) with the following modifications. Plants were trimmed to 1 cm of roots and 6 cm from the base of the crown. Prior to testing, one plant was desiccated at 70°C for 72 h to be used as a control. Thermocouples were placed against the main stem at the point closest to the crown base. Crowns were wrapped in parafilm to hold the thermocouple in place. To initiate either freezing, 200 µL of the INA^+ suspension was pipetted into 10 X 75 mm test tubes. Crowns were placed with roots in direct contact with the chilled water to initiate freezing. Crown tissues were not in direct contact with the solution. Thermocouples were held against the base of the crown with parafilm. Tubes were placed in a rate-controlled ethylene glycol low-temperature bath (Haake G50, Thermo Scientific, Newington, NH, USA) held at 0°C for 20 min. Samples were cooled at a rate of 2°C h^{-1} from 0°C to -30°C. Thermocouples recorded temperatures every 1 s for the duration of the experiment (Octotemp datalogger, Fisher Scientific, New Hampshire, USA). In each treatment group, seven plants were tested with a dried control. The experiment was repeated four times.

A separate experiment using the tube-in-bath system was conducted concurrently to score the survival of the main shoot where the outer sheath was removed or left intact. Plants were frozen using a test tube system, to identify the LT_{50} and the tissue-specific region of injury using the TTC

staining method (TTC_{50}, section 3.3.3). A total of 12 plants were tested per temperature and the experiment was independently repeated four times.

5.3.10 Statistical analysis

Data from three or four independent tests were combined because the effects of the experimental treatments were consistent. The students t-test or Analysis of Variance (ANOVA) with Fishers Least Significance Difference (LSD) test ($P < 0.05$) was used to analyze effects of cultivar, tissue acclimation or treatment on ice nucleation temperatures freezing/tissue survival (LT_{50}, TTC_{50}), sugar concentration or exotherm temperature using Sigma Plot statistical software (version 12.5, Systat Software Inc., San Jose, California, USA).

5.4 Results

5.4.1 Freezing survival (LT_{50}) of Norstar, Hazlet and Puma

Non-acclimated Norstar winter wheat, Hazlet rye and Puma rye had an LT_{50} around -6°C (**Table 5.1**). Cold-acclimation treatments at 4°C for 42 d increased freezing survival. Cold-acclimated Puma had a significantly higher freezing survival than Norstar or Hazlet ($P < 0.05$; **Table 5.1**). Cold-acclimated Hazlet had a significantly higher freezing survival than Norstar ($P < 0.05$; **Table 5.1**). A cold-acclimation pre-treatment increased the LT_{50} by 14.7°C in Norstar, 19.7°C in Hazlet and 24.2°C in Puma. Additional exposure of the cold-acclimated plant to -4°C for 72 h prior to freezing increased the LT_{50} in each cultivar by a minimum of 2°C.

5.4.2 Crown tissue ice nucleation temperatures

There was no difference in ice nucleation temperatures among non-acclimated tissues (**Table 5.2**). Autoclaving (121°C for 20 min) pre-treatment significantly decreased ($P < 0.05$) the ice nucleation temperature of non-acclimated VTZ. In the cold-acclimated leaf sheath, autoclaving and autoclaving with a water change significantly decreased the ice nucleation temperature ($P < 0.05$; **Table 5.3**). Cold-acclimated Norstar SAM had a significantly higher ice nucleation temperature than cold-acclimated Puma SAM when comparing the intact and autoclaved treatment groups. Autoclaved Norstar VTZ had a significantly higher ice nucleation temperature than Puma VTZ ($P < 0.05$; **Table 5.3**).

Table 5.1 Determination of freezing survival (LT_{50}) of non- and cold-acclimated Norstar, Hazlet and Puma using the 21 d recovery method.

Data are presented as a means of three independent experiments (N = 3; 20 crowns per temperature per treatment in each LT_{50} experiment, 3 replicates in time and space). Means followed by the same letter within each column are not significantly different based on Fisher's LSD test (One-way ANOVA, $P < 0.05$). Means within a row were determined to be significantly different using the two-tailed t-test (ns $P > 0.05$, * $P < 0.05$).

Cultivar	LT_{50} (°C)		
	Non-acclimated	Cold-acclimated	P
Norstar	-5.8 a	-20.5 a	*
Hazlet	-6.1 a	-25.8 b	*
Puma	-5.9 a	-30.1 c	*
$LSD_{0.05}$	0.4	2.8	

Table 5.2 Mean ice nucleation temperatures of non-acclimated leaf sheath, SAM and VTZ collected from Norstar, Hazlet and Puma crowns.

Samples were washed, then either left intact (INT), autoclaved (AC) or autoclaved, rinsed and then placed in a new sterile tube (AC/WC). Samples were cooled at a rate of 2°C h^{-1}. Data was presented as a means of the total number of individuals (N = 30; 10 replicates and 3 replicates in time and space). Means followed by the same letter within each column (lowercase) and row (uppercase) are not significantly different based on Fisher's LSD test (Two-way ANOVA, $P < 0.05$).

Cultivar	Treatment	Ice nucleation temperature (°C)			
		Leaf sheath	SAM	VTZ	$LSD_{0.05}$
Norstar	INT	-5.9 a B	-5.9 a B	-5.1 a A	0.6
	AC	-5.9 a A	-6.0 a A	-5.7 b A	0.5
	AC/WC	-5.7 a A	-6.0 a A	-5.9 b A	0.7
Hazlet	INT	-5.6 a A	-5.6 a A	-5.1 a A	0.6
	AC	-5.8 a A	-5.8 a A	-5.7 b A	0.6
	AC/WC	-5.5 a A	-5.5 a A	-6.2 b A	0.7
Puma	INT	-5.7 a A	-5.9 a A	-4.9 a A	0.5
	AC	-5.9 a A	-6.0 a A	-5.8 b A	0.6
	AC/WC	-5.7 a A	-5.5 a A	-6.1 b A	0.6
$LSD_{0.05}$		0.5	0.5	0.6	

Table 5.3 Mean ice nucleation temperatures of cold-acclimated leaf sheath, SAM and VTZ collected from Norstar, Hazlet and Puma crowns.

Samples were washed, then either left intact (INT), autoclaved (AC) or autoclaved, rinsed and then placed in a new sterile tube (AC/WC). Data was presented as a means of the total number of individuals (N = 30; 10 replicates and 3 replicates in time and space). Means followed by the same letter within each column (lowercase) and row (uppercase) are not significantly different based on Fisher's LSD test (Two-way ANOVA, $P < 0.05$).

Cultivar	Treatment	Ice nucleation temperature (°C)			
		Leaf sheath	SAM	VTZ	$LSD_{0.05}$
Norstar	INT	-6.5 a A	-7.4 a B	-6.8 a A	0.7
	AC	-10.4 c A	-11.3 d A	-10.7 b A	0.8
	AC/WC	-8.6 b B	-8.8 c B	-7.3 a A	0.7
Hazlet	INT	-6.1 a A	-7.9 ab B	-6.7 a A	0.8
	AC	-10.3 c A	-12.7 e C	-11.7 c B	0.7
	AC/WC	-8.1 b B	-9.3 c C	-6.8 a A	0.8
Puma	INT	-6.8 a A	-8.5 bc B	-6.7 a A	0.7
	AC	-10.4 c A	-12.4 e C	-11.8 c B	0.6
	AC/WC	-8.7 b B	-9.0 c B	-7.1 a A	0.6
$LSD_{0.05}$		0.9	0.8	0.8	

To test for the association of ice nuclei, crown tissues were either washed or unwashed prior to cooling. Puma was selected instead of Hazlet for the remaining experiments due to its significantly greater freezing survival. In cold-acclimated crowns, the leaf sheath had a 2°C higher ice nucleation temperature when not washed prior to cooling ($P < 0.05$; **Table 5.4**). Cold-acclimated Puma SAM had a 0.5 to 1°C lower ice nucleation temperature than Norstar SAM. Cold-acclimated VTZ had a significantly higher ice nucleation temperature when not washed prior to cooling ($P < 0.05$; **Table 5.4**). To investigate the localization of ice nuclei, crown tissues were washed, homogenized and separated into cell wall extracts. Individual extracts were analyzed using the test tube assay. The washing fluid from cold-acclimated leaf sheaths had the highest ice nucleation temperature (**Table 5.5**). Autoclaving treatment of the leaf sheath washing fluid significantly decreased the ice nucleation temperature ($P < 0.05$; **Table 5.5**). Cell wall extracts from both the leaf sheath and VTZ had an intermediate ice nucleation temperature (~ -8°C) not affected by autoclaving pre-treatment ($P > 0.05$; **Table 5.5**). Regardless of tissue or cultivar, autoclaving treatment significantly decreased the ice nucleation temperature of the homogenized extract ($P < 0.05$; **Table 5.5**).

5.4.3 Effect of cold-acclimated apoplast fluids on freezing survival

Irrespective of cultivar, there was no significant difference in the ice nucleation temperature of non-acclimated apoplast fluids ($P > 0.05$; **Table 5.6**). Cold-acclimation resulted in a significantly higher ice nucleation temperature in apoplast fluid VTZ than the SAM ($P < 0.05$; **Table 5.6**). Cold-acclimated Puma apoplast fluids had a significantly lower ice nucleation temperature ($P < 0.05$) than both Norstar and Hazlet. Frost hardened Puma rye had the lowest ice nucleation temperatures. The ice nucleation temperature Norstar and Puma crown apoplast fluids were confirmed to be significantly different ($P < 0.05$) and decreased when serially diluted (**Table 5.7**). Infiltrated crowns with apoplast fluids had a lower INA ($P < 0.05$) than those infiltrated with phosphate buffered saline or non-infiltrated crowns. Infiltration with frost hardened apoplast fluids (1:10 dilution) had a 4°C increase in freezing survival (LT_{50}). Fructose, glucose raffinose and stachyose concentrations significantly increased in apoplast fluids collected from cold-acclimated and frost hardened crowns (**Table 5.8**). After frost hardening, total sugar concentrations were significantly higher ($P < 0.05$) in the SAM compared to the VTZ. Frost hardened SAM in Puma had 1.6 times higher ($P < 0.05$) total sugar concentrations compared to Norstar.

Table 5.4 Effect of tissue washing on the mean ice nucleation temperatures of cold-acclimated Norstar and Puma leaf sheath, shoot apical meristem (SAM) and vascular transition zone (VTZ).

Samples were either washed with distilled water and blotted dry with an absorbent tissue or left unwashed prior to the determination of the ice nucleation temperature. Data was presented as a means of the total number of individuals (N = 30; 10 replicates and 3 replicates in time and space). Means followed by the same letter within each column (lowercase) or row (uppercase) are not significantly different based on Fisher's LSD test (Two-way ANOVA, $P < 0.05$).

Cultivar	Treatment	Ice nucleation temperature (°C)			
		Leaf Sheath	SAM	VTZ	$LSD_{0.05}$
Norstar	Washed	-6.2 b A	-7.6 a B	-6.5 b A	0.5
	Unwashed	-3.8 a A	-7.5 a C	-5.7 a B	0.6
Puma	Washed	-6.3 b A	-8.6 c B	-6.3 b A	0.4
	Unwashed	-4.0 a A	-8.0 b C	-5.3 a B	0.7
$LSD_{0.05}$		0.2	0.3	0.4	

Table 5.5 Mean ice nucleation temperatures of cold-acclimated Norstar and Puma leaf sheath washing fluid, homogenate or cell wall extractions.

Data was presented as a means of the total number of individuals (N = 30; 10 replicates and 3 replicates in time and space). Means followed by the same letter within each column are not significantly different based on Fisher's LSD test (Two-way ANOVA, $P < 0.05$). Means within a row were determined to be significantly different using the two-tailed t-test (NS $P > 0.05$, * $P < 0.05$, ** $P < 0.01$, *** $P < 0.001$).

		Ice nucleation temperature (°C)								
Cultivar	Treatment	Leaf Sheath			SAM			VTZ		
		INT	AC	P	INT	AC	P	INT	AC	P
Norstar	Washing fluid	-3.8 a	-9.7 c	***	-10.8 a	-13.1 c	**	-5.7 a	-6.9 b	**
	Homogenate	-8.2 c	-8.2 b	NS	-12.2 c	-12.0 a	NS	-8.4 b	-9.5 c	**
	Cell Wall	-6.8 b	-7.0 a	NS	-10.7 a	-12.3 a	**	-6.1 a	-6.2a	NS
Puma	Washing fluid	-4.2 a	-9.4 c	***	-11.6 b	-13.2 c	**	-5.8 a	-7.0 b	**
	Homogenate	-8.2 c	-8.3 b	NS	-12.7 c	-12.2 a	NS	-8.8 b	-9.6 c	**
	Cell Wall	-6.6 b	-6.9 a	NS	-10.5 a	-12.8 b	**	-6.0 a	-6.2 a	NS
	$LSD_{0.05}$	0.4	0.3		0.5	0.4		0.4	0.3	

Table 5.6 Ice nucleation temperatures of apoplast fluids collected from the SAM and VTZ of non-acclimated, cold-acclimated and frost hardened (cold-acclimated plants cooled to then held at -4°C for 72 h) winter wheat and rye crowns.

Data was presented as a means of the total number of individuals (N = 40; 10 replicates and 4 replicates in time and space). Means followed by the same lowercase letter within each column are not significantly different based on Fisher's LSD test (Two-way ANOVA, $P < 0.05$). Means followed by the same uppercase letter within each column are not significantly different based on Fisher's LSD test (One-way ANOVA, $P < 0.05$).

Cultivar	Tissue	Ice nucleation temperature (°C)			
		Non-acclimated	Cold-acclimated	Frost hardened	$LSD_{0.05}$
Norstar	SAM	-5.8 a A	-8.6 b B	-9.4 c C	0.6
	VTZ	-5.7 a A	-7.9 a B	-8.6 a C	0.8
Puma	SAM	-5.6 a A	-9.3 c B	-11.3 d C	0.6
	VTZ	-5.6 a A	-9.1 c B	-9.2 bc B	0.5
$LSD_{0.05}$		0.4	0.4	0.6	

Table 5.7 Effect of infiltration with frost hardened apoplast fluids in non-acclimated Norstar and Puma crowns on ice nucleation temperature and freezing survival.

Frost hardened (FH) apoplast fluids collected from the whole crown were diluted 10, 100 or 1000 times in phosphate buffered saline (PBS). The ice nucleation temperature data was presented as a means of the total number of individuals (N = 30; 10 replicates and 3 replicates in time and space). The LT_{50} data was presented as a means of three independent experiments (N =3; 20 crowns per temperature per treatment in each LT_{50} experiment and 3 replicates in time and space). Means followed by the same letter within each column are not significantly different based on Fisher's LSD test (One-way ANOVA, $P < 0.05$).

Treatment	Ice nucleation temperature (°C)			LT_{50} (°C)	
	Fluids only	Norstar	Puma	Norstar	Puma
Non-infiltrated	NA	-5.7 d	-6.1 d	-5.6 d	-5.7 d
0.1 M PBS	-5.1 e	-5.1 d	-5.4 e	-4.6 e	-5.0 e
10 PBS : 1 NorFH	-7.9 c	-9.4 a	-9.3 a	-9.4 a	-9.7 a
100 PBS : 1 NorFH	-7.7 c	-7.9 c	-8.3 b	-7.6 c	-8.5 b
1000 PBS : 1 NorFH	-7.1 d	-7.6 c	-7.5 c	-7.2 c	-7.4 c
10 PBS : 1 PumaFH	-9.0 a	-9.5 a	-9.6 a	-9.7 a	-9.7 a
100 PBS : 1 PumaFH	-8.5 b	-8.8 b	-8.1 b	-8.2 b	-8.5 b
1000 PBS : 1 PumaFH	-7.6 cd	-7.9 c	-7.6 c	-7.5 c	-7.4 c
$LSD_{0.05}$	0.5	0.5	0.5	0.4	0.5

Table 5.8 Sugar concentrations of apoplast fluids collected from Norstar and Puma non-acclimated, cold-acclimated and frost hardened (acclimated and then exposed to -4°C for 72 h) SAM and VTZ.

Total sugars were calculated as the sum of all measured carbohydrates. Data was presented as a means of the total number of replicates (N = 4; 4 biological replicates). Within each column, means were significantly different when followed by a different letter (Two-way ANOVA, $P < 0.05$, Fisher's LSD).

Cultivar	Treatment	Tissue	Fructose	Glucose	Raffinose	Stachyose	Total Sugars
			---- mg mL^{-1} ----				
Norstar	NA	SAM	Bdl	Bdl	Bdl	Bdl	Bdl
		VTZ	Bdl	Bdl	Bdl	Bdl	Bdl
	ACC	SAM	1.8 d	1.8 cd	Bdl	Bdl	3.6 d
		VTZ	2.8 c	3.4 ab	Bdl	Bdl	6.2 c
	FH	SAM	3.4 c	2.9 b	0.2 a	1.4 a	7.9 b
		VTZ	2.9 c	2.0 c	0.2 a	0.5 b	5.7 c
Puma	NA	SAM	0.2 e	0.1 e	Bdl	Bdl	0.3 e
		VTZ	0.2 e	0.1 e	Bdl	Bdl	0.3 e
	ACC	SAM	1.6 d	1.2 d	Bdl	Bdl	2.7 d
		VTZ	1.9 d	1.5 d	Bdl	Bdl	3.4 d
	FH	SAM	7.7 a	3.7 a	0.1 a	1.4 a	12.8 a
		VTZ	5.5 b	2.2 c	0.1 a	0.5 b	8.3 b
		$LSD_{0.05}$	0.8	0.6	0.02	0.2	1.6

Abbreviations include; shoot apical meristem (SAM), vascular transition zone (VTZ), non-acclimated (NA), cold-acclimated (ACC), frost hardened (FH), below detectable limits (Bdl).

5.4.4 Ice localization

After cooling and freezing Norstar and Puma crowns to -4°C, visual observations of SEM micrographs indicate the space between the outer and inner leaf sheaths expand (**Figure 5.1**). By -14°C, the Norstar leaf sheath was visually disrupted. Visual observations of cold-acclimated Norstar (**Figure 5.2**) and Puma (data not shown) main shoots cooled to -4°C indicates the presence of ice crystals between the leaf sheath and a darker green colouration below the SAM (**Figure 5.2B**). After cooling Norstar to -8°C, off-white discolouration was observed at the base of the crown near the nodal plate (**Figure 5.2C**). After cooling Norstar to -12°C the off-white discolouration was visually observed to expand towards the VTZ (**Figure 5.2D**). Larger ice crystals were visually observed in cold-acclimated Puma crowns frozen with intact tillers (**Figure 5.2F**) and Norstar (data not shown). At lower sub-zero temperatures near the LT_{50}, complete ice encasement was visually observed in tillers (**Figure 5.2G**) and the leaf layers surrounding the SAM (**Figure 5.2F, G, H**). In contrast, an absence of large ice crystals were observed in the tissue below the SAM (**Figure 5.2G**), and the SAM itself (**Figure 5.2G**). Ice can form in the SAM (**Figure 5.2H**) at low sub-zero temperatures.

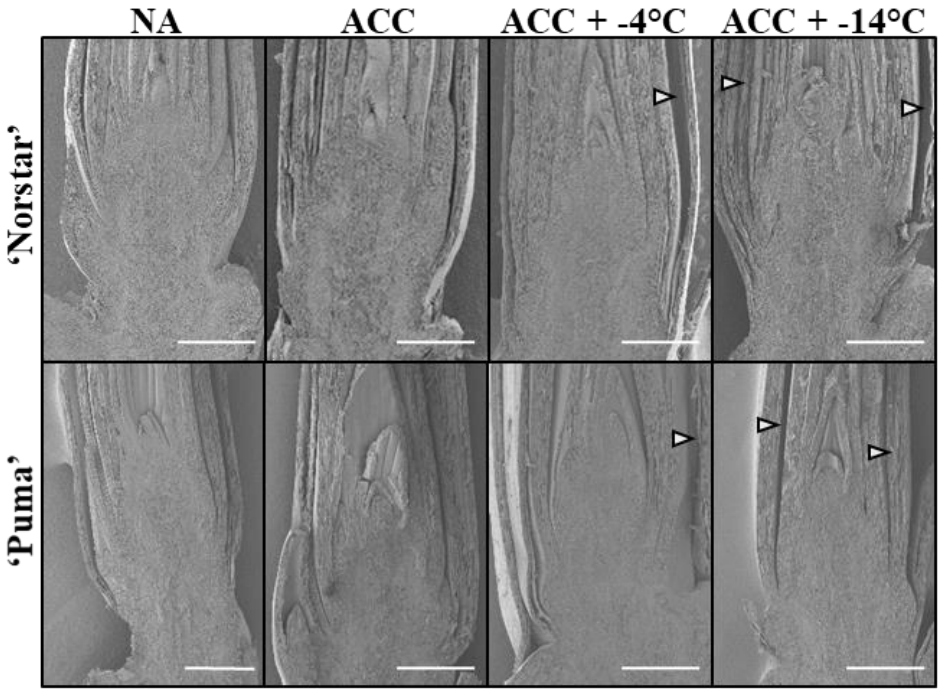

Figure 5.1 Scanning electron micrographs of Norstar and Puma rye crowns.

Crowns were either non-acclimated (NA), cold-acclimated (ACC), or cold-acclimated and cooled at 2°C h^{-1} using the low temperature bath test tube system to -4°C or -14°C. Arrows indicate expansion of the leaf sheath. Scale bar = 0.5 cm.

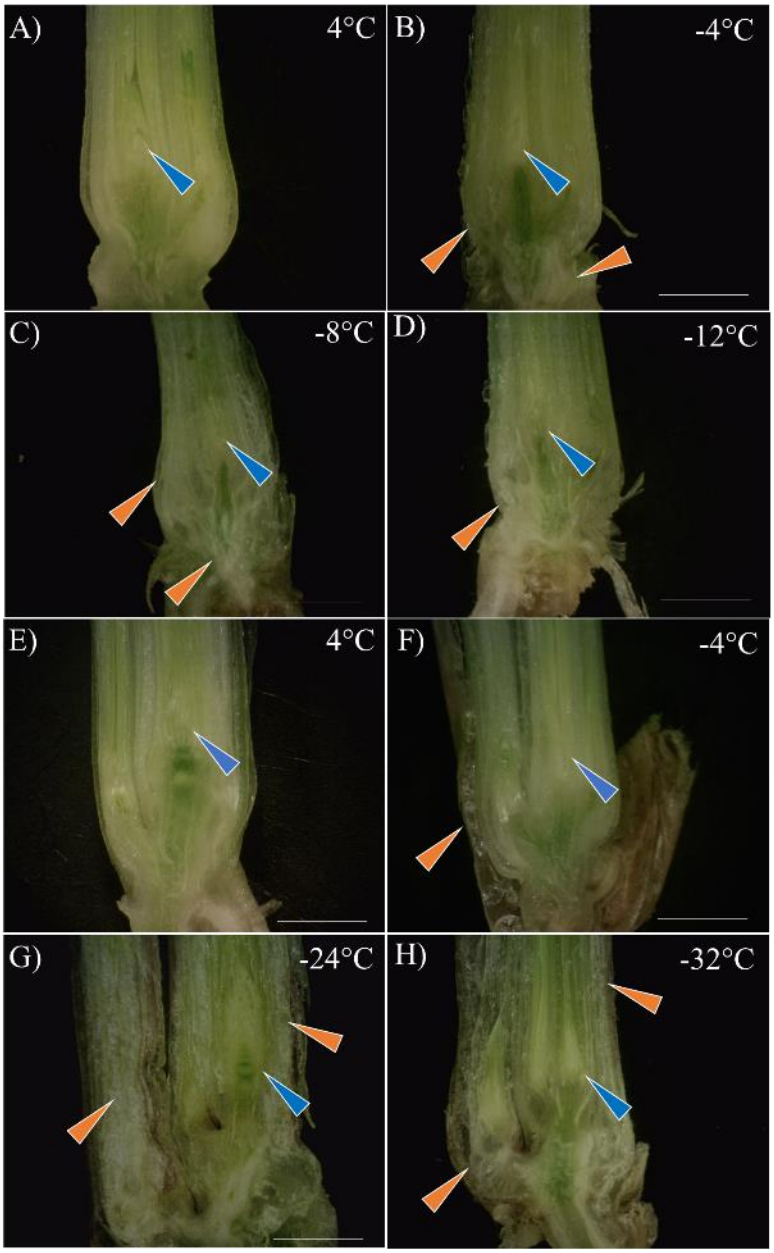

Figure 5.2 Ice localization in cold-acclimated Norstar crowns.

Cold-acclimated plants with (A-D) tillers removed and (E-H) left intact were cooled separately. Cold-acclimated plants were cooled to pre-determined temperatures, sectioned longitudinally in a cold room at (A, E) 4°C or (B-D, F-H) -4°C and imaged using a dissecting microscope. (A, E) Unfrozen plants were included as controls. (B, F) After the initial freezing event, ice crystals form between the leaf sheath and crown. (C) Injury begins at the base of the crown near the nodal plate (D) and progresses up the crown. (G) At lower sub-zero temperatures, tillers if present, can be encased in ice. (G) The absence of large ice crystals below and within the SAM. (H) Injury to the SAM. Orange arrows denote ice. Blue arrows denote the shoot apical meristem. Similar patterns of freezing were observed in Norstar wheat and Puma rye. Scale bar = 0.4 cm

5.4.5 Leaf sheath removal

To test the role of the leaf sheath in freezing injury, a series of crown manipulation experiments were conducted. Crowns frozen in the absence of tillers had a warmer LT_{50} than crowns frozen with tillers (**Table 5.1**; **Table 5.9**). The removal of the leaf sheath decreased the LT_{50} of the Norstar and Puma main shoots (**Table 5.9**). Interestingly the removal of the leaf sheath resulted in a differential injury pattern in cold-acclimated Norstar (**Figure 5.3**). There was an absence of TTC staining in the intact main shoot VTZ near -10°C in cold-acclimated Norstar and -12°C in Puma (**Figure 5.3**; **Table 5.9**). In intact main shoots, injury to the SAM in Norstar and Puma corresponded to the whole plant freezing survival. In Norstar main shoots with a removed leaf sheath, the injury occurred first in the SAM at -6°C and then later in the VTZ at -10°C. In cold-acclimated Puma, the removal of the leaf sheath did not affect the initial location of injury. The VTZ in cold-acclimated Puma had a TTC_{50} of -11°C whereas the SAM TTC_{50} was around –15°C (**Table 5.9**).

Thermocouples attached to the crowns recorded three exothermic events when the main shoot was cooled at 2°C h^{-1} (**Table 5.9**; **Figure 5.4**). The high temperature exotherm was observed around -4°C in all treatment groups. The mid temperature exotherm was observed at a significantly more negative temperature ($P < 0.05$) in main shoots with an intact leaf sheath than those with the leaf sheath removed. The low temperature exotherm was visible in crowns with an intact leaf sheath (**Figure 5.4A**) and corresponded with the calculated LT_{50} value (**Table 5.9**). Cold-acclimated plants with excised leaf sheaths did not have detectable low temperature exotherms (**Table 5.9**; **Figure 5.4B**).

Table 5.9 Freezing of cold-acclimated Norstar and Puma main shoots with intact or removed leaf sheaths using the tube-bath system.

Determination of the temperature at which 50 % of the population was unable to recover from freezing (LT_{50}) and the temperature at which 50 % of the Norstar crown shoot apical meristem (SAM) or vascular transition zone (VTZ) tissues stained positive for tetrazolium chloride vital staining (TTC_{50}). The LT_{50} data was presented as a means of three independent experiments (N = 3; 20 crowns per temperature per treatment in each LT_{50} experiment, 3 replicates in time and space). The TTC_{50} data was presented as a means of three independent experiments (N = 3; 20 crowns per temperature per treatment in each LT_{50} experiment). During each freezing test, seven plants were monitored for exothermic events using thermocouples. The exotherm data was presented as a means the total number of individuals (N = 21; 7 crowns per temperature per treatment and 3 replicates in time and space). Means followed by the same letter within each column are not significantly different based on Fisher's LSD test ($P < 0.05$). Means within a row (TTC_{50}) were determined to be significantly different using the two-tailed t-test (ns $P > 0.05$, * $P < 0.05$).

Cultivar	Leaf sheath	LT_{50}	TTC_{50}			Exotherm		
			SAM	VTZ	P	High	Mid	Low
					---- °C ----			
Norstar	Intact	-15 b	-14.4 b	-10.0 c	*	-3.7 a	-7.8 a	-16.5 b
	Removed	-9 c	-5.7 c	-10.0 c	*	-3.8 a	-6.2 b	Bdl
Puma	Intact	-25 a	-23.6 a	-12.1 a	*	-3.7 a	-8.2 a	-26.3 a
	Removed	-12 b	-14.7 b	-11.1 b	*	-3.7 a	-6.5 b	Bdl
$LSD_{0.05}$		1	0.5	0.3		0.1	0.8	2.5

Abbreviations include: below detectable limits (Bdl)

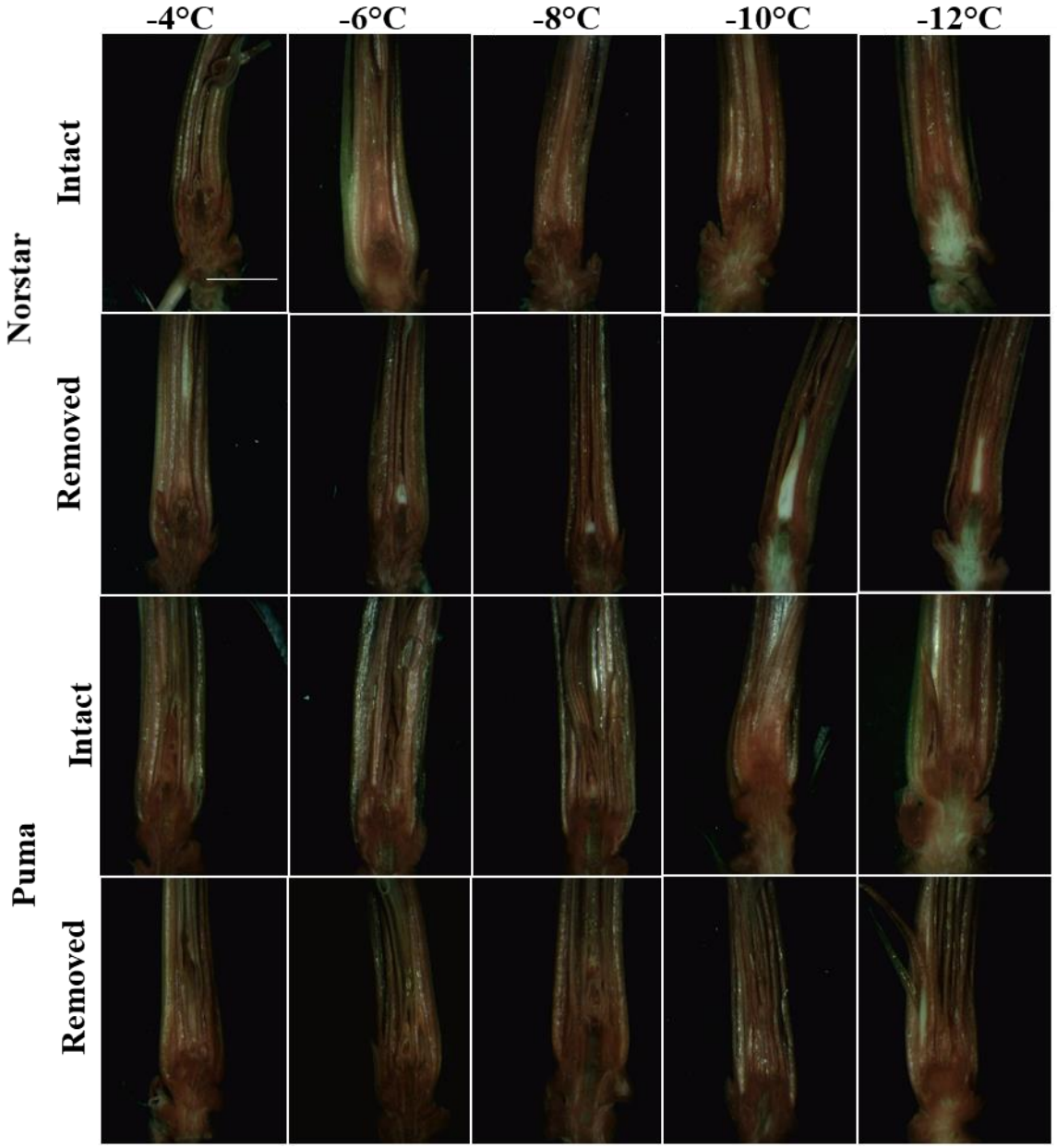

Figure 5.3 Tetrazolium chloride staining of cold-acclimated Norstar and Puma main shoots with either an intact or removed outer leaf sheath.

Crowns were cooled at a rate of 2°C h^{-1} to -12°C. Crowns were sampled every 2°C, allowed to recover for 3 d at 20°C, then rinsed with distilled water, sectioned longitudinally, and then stained with tetrazolium chloride. Scale bar = 0.8 cm.

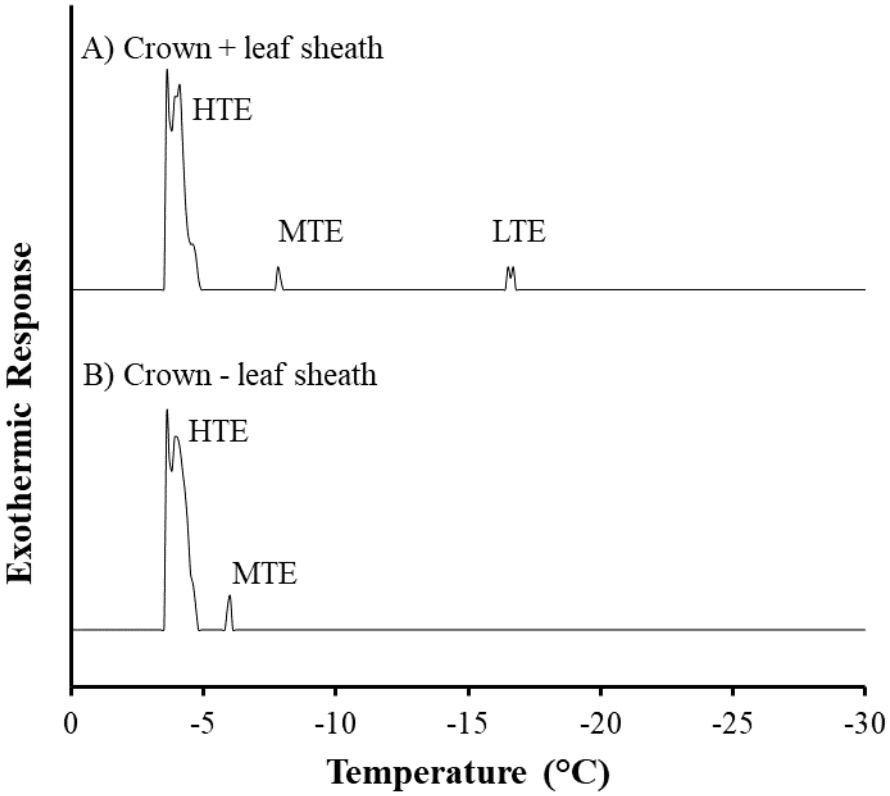

Figure 5.4 Differential thermal analysis (DTA) of cold-acclimated Norstar wheat main shoots.

Representative DTA profiles of A) main shoots with an intact leaf sheath were observed to have a high (HTE), mid (MTE) and low (LTE) temperature exotherm. B) Main shoots without a leaf sheath were observed to have a HTE and MTE. Thermocouples were placed near the VTZ at the base of the crown and held in place with parafilm. Plants were placed in a test tube with INA^{+} suspension. Similar DTA profiles were generated for cold-acclimated Puma rye (data not shown).

5.5 Discussion

5.5.1 Functional role of high ice nucleation temperatures and their origin

A large volume of water was required (2.3 x 10^{312} kg) for ice nucleation to occur at temperatures warmer than -10°C in a pure sample (Franks, 1985). Therefore, additional ice nucleators are required to initiate freezing in plant tissues. Using the test tube method outlined by Kishimoto et al. (2014a), Differences in ice nucleation temperatures were observed using small volumes and/or masses of tissue (**Table 5.2**; **Table 5.3**; **Table 5.4**; **Table 5.5**; **Table 5.6**). Decreased leaf sheath and washing fluids ice nucleation temperatures after autoclaving (**Table 5.3**; **Table 5.5**) imply the ice nucleators were either of bacterial origin or loosely bound to the plant tissue. Lindow (1978) reported INA^+ lost their capacity to initiate ice formation if exposed to high temperatures (> 40°C). Ishikawa et al. (2015) reported the ice nucleation temperature was unaffected by heating in overwintering bud scales. While the leaf sheath and bud scale may have similar roles in terms of the overall freezing behaviour of the crown and tree bud, the ice nucleators present may differ in origin.

In cold-acclimated winter wheat and rye, high ice nucleation temperatures were localized to the leaf sheath (**Table 5.3**) and corresponded with ice formation between the leaf sheath and crown tissues (**Figure 5.2**). In field-acclimated winter wheat, ice nucleation occurred in the crown at numerous positions within the outer leaves, resulting in the crown freezing in layers (Livingston et al., 2017). Whether this holds true in field-acclimated winter rye crowns will require additional experimentation to confirm using precise INA tests in conjunction with IRVT. Leaf sheath cell wall extracts had similar ice nucleation temperatures (**Table 5.5**) as those reported in Rhododendron tree bud scales (Ishikawa et al., 2015). The leaf sheath may acquire this additional nucleator through its relative location in the plant. Crowns in the field are located 4 to 8 cm below ground. Ice nucleation-active microorganisms are present in the Fall soil microbiome (Lindow et al., 1978a; Gross et al., 1984). The leaf sheath would be a potential colonization site due to its location within the soil. In contrast, overwintering tree buds are typically located > 1 m above the soil level. While precipitation and snow do contain active INA^+, the difference in micro-habitat (crown as opposed to tree bud) will affect which micro-organisms are capable of colonizing.

Ice nucleation temperatures associated with intact VTZ or the cell wall extracts of VTZ and leaf sheath were unaffected by autoclave pre-treatment (**Table 5.5**). This indicates the VTZ ice nucleation temperature and cell wall extracts were intrinsic, rather than bacterial in origin. The

ice nucleation temperatures reported in blueberry stems were resistant to various anti-microbial and heating treatments (Kishimoto et al., 2014a; Kishimoto et al., 2014b). In *Prunus* stems, ice nucleators were resistant to various disinfectants (Ashworth and Davis, 1984).

5.5.2 Accumulation of cryo-protectants in the apoplast fluids and their role in freezing survival

Infiltration of non-acclimated crowns with apoplast fluids lowered the ice nucleation temperature and depressed the supercooling point (**Table 5.7**). Crowns were killed at the moment of nucleation as indicated by a similar LT_{50} and ice nucleation temperature. By avoiding freezing injury, the infiltrated crowns were more prone to damage upon nucleation due to a greater build up of kinetic energy when supercooled (Olien and Livingston, 2006). Cold-acclimated plant apoplast fluids mitigate the formation of intracellular ice by controlling the formation and rate of ice propagation in plant tissues. If the fraction of unbound liquid water is lowered by evaporation or frost hardening, freezing can proceed as an equilibrium process. Along the cell wall, unfrozen water molecules orient in a 'short-range pattern' based on its dipole electromagnetic properties (Olien, 1961, 1965; Olien, 1973; Olien and Livingston, 2006). The degree of orientation is dependent on the water molecule's intermolecular bonding energy and can be influenced by increased concentrations of total sugars (**Table 5.8**) and arabinoxylans (Olien, 1965; Olien and Smith, 1977; Olien and Lester, 1985; Kindel et al., 1989). Accumulation of arabinoxylans, sucrose or fructans significantly depress the freezing point, bind free water to reduce the possibility of complete desiccation, and play a role in the cell wall and membrane gelation (Livingston and Henson, 1998; Gusta et al., 2004).

During slow freezing, small ice crystals in the VTZ mitigates lethal ice propagation into the SAM. When cold-acclimated cereals are slowly cooled ($\leq 2°C\ h^{-1}$; Chapter 4) and have a low crown water content (Olien, 1964), both the VTZ and SAM freeze in an equilibrium process. Increased concentrations of total sugars could account for the greater cold hardiness of the SAM of frost hardened Puma compared to Norstar when plants were exposed to faster cooling rates °C h^{-1}, 10°C h^{-1}) or after the removal of the leaf sheath (**Table 5.9**; **Figure 5.3**). Sugars depress the freezing point and promote supercooling (reviewed by Levitt, 1980). Equilibrium freezing in cold-acclimated VTZ could be influenced by increased concentrations of AFPs. Cold-acclimated VTZ of Norstar accumulated higher concentrations of AFPs than the SAM (Chapter 3). Active AFPs

bind to the face of the growing ice crystal lattice, to reduce the rate of ice propagation and mitigate its spread into the intracellular space (Jia and Davies, 2002; Griffith and Yaish, 2004).

5.5.3 The relevance of high ice nucleation temperatures in the leaf sheath

The localization of high ice nucleation temperatures to the leaf sheath and to a lesser extent the VTZ (**Table 5.3**) correspond with the localization of ice observed in frozen tissue sections (**Figure 5.2**) and IRVT (Chapter 4). As was the case in *Cornus florida* L. (Sakai, 1979; Ishikawa et al., 2016), *Cornus officinalis* L. (Ishikawa and Sakai, 1985) and Larch (*Larix kaempferi* Lamb.) Carr.) (Endoh et al., 2014) the smaller peaks in the low-temperature exotherm were associated with the freezing of supercooled florets, anthers or primordia. In contrast, cold-acclimated Norstar and Puma SAM had relatively low ice nucleation temperatures (**Table 5.3**). There was an average decrease in SAM ice nucleation temperatures due to cold-acclimation. There was either an absence of ice nucleators associated with the SAM or an increase in anti-ice nucleators. Livingston et al. (2005) reported a significant increase in frost hardened barley SAM compared to VTZ sucrose and total sugar concentrations.

The high temperature exotherm represented the non-lethal freezing of the scales and connecting tissues in tree buds (Ishikawa and Sakai, 1982; Ishikawa and Sakai, 1985; Endoh et al., 2014; Ishikawa et al., 2015). When Norstar winter wheat and Puma winter rye main shoots were cooled, a similar pattern of high, mid and low temperature exotherms were identified (**Figure 5.4**; Chapter 4). Removal of the leaf sheath resulted in the pre-mature freezing injury of the SAM (**Figure 5.3**). In the case of Norstar, removal of the leaf sheath resulted in injury to the SAM prior to injury in the VTZ. This was not the case in Puma rye. In Chapter 4 during slow cooling (2°C h^{-1}), cold-acclimated Norstar VTZ was injured before the SAM. This was corroborated by previous reports using the TTC staining assay (Tanino and McKersie, 1985; Livingston et al., 2013; Chapter 3), observations of root regrowth (Chen et al., 1983) and observations of tissue browning as a measure of necrosis (Chapter 4) (Olien, 1964; Olien and Marchetti, 1976). In Chapter 4, increased rates of cooling (5°C h^{-1} or 10°C h^{-1}) resulted in SAM injury at warmer sub-zero temperatures. The data support the theory the SAM supercools, and fast cooling rates (Chapter 3) or the loss of an ice sink resulted in injury to the SAM. Differences in the SAM freezing avoidance mechanism in winter wheat and rye are currently unknown in the literature. Similar avoidance mechanisms were reported in *Cornus* (Sakai, 1979; Ishikawa and Sakai, 1985; Ishikawa et al., 2016), larch

(Endoh et al., 2014), rhododendron (Graham and Mullin, 1976; Ishikawa and Sakai, 1981; Ishikawa et al., 2015), and *Prunus* (Quamme, 1978; Quamme et al., 1995) flower buds. This avoidance mechanism will be further addressed in Chapter 6.

Localization of high ice nucleation temperatures to the leaf sheath corresponds to the formation of ice between the leaf sheath layers and the high temperature exotherm (**Table 5.9**; **Figure 5.2**; **Figure 5.5**). The existence of high ice nucleation temperatures corroborates reports of IRVT of crowns spontaneously frozen in the absence of an endogenously applied extrinsic nucleator (Fuller et al., 2001; Livingston et al., 2018) and more general observations that cold-acclimated winter cereals initiated freezing at warm sub-zero temperatures both in the field (Livingston et al., 2018) and when grown under artificial conditions (Chapter 4). This also explains why cold-acclimated wheat and rye crowns froze spontaneously without artificial ice inoculation between -4°C to -5°C (Chapter 4). Extrinsic nuclei do not guarantee ice nucleation provided there was an intact cuticle or barrier (Fuller et al., 2003). Excessive supercooling of cold-acclimated tissues increases the rate of ice crystal growth (Pruppacher, 1967). Freezing at higher temperatures at the cellular level in conjunction with the formation of ice sinks at the tissue level minimize the risk of excessive water supercooling in the absence of extrinsic ice nuclei. The VTZ or leaf sheath would undergo extracellular freezing according to the chemical potential difference between the extracellular ice and intracellular sap. A similar mechanism for freezing was reported between the blueberry stem bark serving as an ice sink for pith tissues, while also having high cell wall ice nucleation temperatures to presumably induce extracellular freezing (Kishimoto et al., 2014b). The leaf sheath and VTZ could undergo a similar cellular and tissue level freezing mechanism to survive exposure to sub-zero temperatures.

5.5.4 Conclusions

In cold-acclimated wheat and rye, high leaf sheath ice nucleation temperatures increased crown cold hardiness by acting as an ice sink relative to the SAM and VTZ. Norstar winter wheat, Hazlet and Puma winter rye cold hardiness was dependent on the warm ice nucleation temperature of the leaf sheath and its ability to accumulate ice. Leaf sheath ice nucleators were identified as heat sensitive and loosely associated with the tissue surface, could be due to the presence of INA^+ or an unknown extrinsic substance of warm INA. Recently, Hill et al. (2014) developed a quantitative PCR test for the *ina*$^+$ gene to directly count ice nucleation active bacteria in

environmental samples. Alignment of *ina*$^{+}$ sequences could reveal the specific bacteria present within the leaf sheath. Additional fungicide and anti-microbial treatments prior to freezing could be used to identify the importance of live bacteria in ice nucleation temperatures. Identification of heat resistant ice nucleators in the cell wall extract will be more difficult to identify. This could require metabolome analysis of the cell wall extract. From that list, compounds of interest could be isolated and tested for their ice nucleating temperatures.

In Chapter 5, the ice nucleation temperatures associated with crown tissues and its cellular extracts were explored. The maximum cold hardiness was dependent in part on ice nucleation and ice formation in the leaf sheath. In the absence of a leaf sheath, cold-acclimated Norstar and Puma SAM were injured at a warmer sub-zero temperature. In the case of Norstar lacking a leaf sheath, the SAM was injured before the VTZ. In Chapter 3, different cold-acclimation patterns were reported in the SAM and VTZ. This supports observations in Chapter 4 that fast cooling rates resulted in injury at warmer temperatures to the SAM. This supports the theory of a tissue level structure-function freezing mechanism of survival in the winter wheat crown. The objective of the next chapter will be to further investigate whether the crown tissue-specific cold-acclimation and injury patterns are associated with the ice segregation mechanism of freezing survival.

Chapter 6

6 Ice segregation in the crown of winter cereals: evidence for extra-organ and extra-tissue freezing

6.1 Abstract

Meaningful improvements on winter cereal cold hardiness require a more complete model of freezing behaviour in the critical crown organ. Water content, NMR microimaging and diffusion weighted imaging were used to visualize and quantify tissue water behaviour in cold-acclimated winter wheat (*Triticum aestivum* L. Norstar) and rye (*Secale cereale* L. Hazlet). Cold-acclimation significantly decreased shoot apical meristem (SAM) water content but not water mobility. Cold-acclimation significantly decreased water mobility in the vascular transition zone (VTZ) and intermediate zone, located between the SAM and VTZ, to a greater degree in rye compared to wheat. The differential thermal analysis identified three exotherms. The high temperature exotherm (-3°C to -5°C) corresponded with ice formation and high ice nucleating activity in the leaf sheath, the tissue surrounding the crown. The mid temperature exotherm (-6°C and -8°C) corresponded with cavity formation in the VTZ and no observed ice in the SAM. The low temperature exotherm corresponded with SAM injury and the killing temperature in wheat (-21°C) and rye (-27°C). The SAM had lower ice nucleating activity and lower freezing survival rate than the VTZ when excised and frozen *in vitro*. Rye SAM had a higher freezing avoidance than wheat SAM. In crowns, the intermediate zone acts as an ice barrier from the leaf sheath or VTZ ice sinks to the SAM. This is the first reported evidence of an extra-organ freezing-like mechanism in cereal crowns and identifies the higher freezing tolerance of rye compared to wheat was due to improved physiological and biochemical ice barriers in the SAM.

6.2 Introduction

In overwintering plants, tissue water compartmentalization is crucial for tolerating extracellular freezing-induced desiccation while avoiding lethal intracellular freezing. Although an understanding of cellular freezing has been described in detail (reviewed by Levitt, 1980; Gusta et al., 2009), the mechanism behind freezing survival among tissues in complex organs are not completely understood. In cold-acclimated winter cereal crowns, the mechanism of freezing survival is associated with a heterogeneous pattern of tissue injury (Olien, 1964; Olien and Marchetti, 1976; Chen et al., 1983; Tanino and McKersie, 1985; Livingston et al., 2005b; Chapter 3). Initial crown injury in cold-acclimated winter wheat (*Triticum aestivum* L.) occurs at -10°C in the vascular transition zone (VTZ) located between the shoot apical meristem (SAM) and the nodal plate at the base of the crown (Chapter 3). The cold-acclimated winter wheat SAM is injured at or near the LT_{50}, or lethal temperature at which half the population is unable to recover from freezing (Chapter 3). These separate injury events in the SAM and VTZ occur less than 1 mm apart. One possible explanation for the difference in tissue-specific injury is cold-acclimated crowns survive through extra-organ freezing.

Water translocation from supercooled tissues or organs to ice sinks in adjacent tissues (extra-tissue freezing) or outside the freezing sensitive organ (extra-organ freezing) (Sakai and Larcher, 1987). To differentiate extra-organ and/or extra-tissue freezing from extracellular freeze dehydration, the following criteria must be met. Tissues have high an ice nucleating activity (INA) to accommodate ice within or associated with the plant organ (Junttila and Stushnoff, 1977; Ishikawa and Sakai, 1981; Ishikawa et al., 1997; Kishimoto et al., 2014a; Ishikawa et al., 2015; Ishikawa et al., 2016). These ice accommodating tissues are known as ice sinks. INA is defined as the capacity of a specific tissue to initiate heterogeneous ice nucleation *in vitro* and can be determined using a modified test tube-based assay (Kishimoto et al., 2014a; Kishimoto et al., 2014b).

Freezing at a slow natural rate (< 5°C h^{-1}) promotes water migration to the ice sink from the freezing-sensitive tissue, promoting supercooling and avoiding lethal non-equilibrium freezing (Junttila and Stushnoff, 1977; Sakai, 1979; Ishikawa and Sakai, 1981; Ishikawa and Sakai, 1985; Endoh et al., 2014). Ice propagation into the freezing-sensitive tissue from the ice sink is impeded by a barrier (Sakai, 1979; Ashworth, 1984; Ashworth et al., 1989; Quamme et al., 1995; Yooyongwech et al., 2008; Kuprian et al., 2014; Kuprian et al., 2016; Kuprian et al., 2017) and

freezing-sensitive tissue has a high tolerance for dehydration (Quamme, 1978; Sakai, 1979; Quamme et al., 1982; Sakai, 1982; Sakai, 1983; Ashworth, 1984; Quamme et al., 1995; Kuprian et al., 2014; Kuprian et al., 2016).

Ice nucleation at warm, sub-zero temperatures (~ -3°C) is crucial to the formation of an ice sink. A vapour difference between the ice sink (low) and freezing sensitive tissue (high) withdraws water from and increases the supercooling capacity of the freezing-sensitive tissue. If the cooling rate is higher than 5°C h^{-1}, enough water remains in the freezing-sensitive tissue to break supercooling at a higher temperature (Ishikawa and Sakai, 1981; Ishikawa et al., 2015). In trees, slow cooling and active nucleators initiates extra-organ ice nucleation in the bud scales, which act as an ice sink to withdraw water from the primordia in the tree bud (Wiegand, 1906b; Dorsey, 1934; Graham and Mullin, 1976; Dereuddre, 1978; Quamme, 1978; Sakai, 1979; Ishikawa and Sakai, 1981; Ishikawa and Sakai, 1982; Ashworth et al., 1989; Quamme et al., 1995; Ishikawa et al., 1997; Ishikawa et al., 2015; Ishikawa et al., 2016). Stem bark (Kishimoto et al., 2014a; Kishimoto et al., 2014b) and seed endosperm (Junttila and Stushnoff, 1977) can also act as ice sinks to promote the supercooling of freezing-sensitive tissues.

Ice sinks can also form in a plant organ which initiate an extra-tissue freezing strategy. Additional ice sinks form in the stem tissues subtending the overwintering buds of peach (*Prunus* spp) (Dorsey, 1934; Quamme, 1978; Ashworth, 1984; Ashworth et al., 1989) larch (*Larix kaempferi* Lamb.) (Endoh et al., 2014) and conifers (Sakai, 1979, 1982; Sakai, 1983; Kuprian et al., 2017). In frozen cold-acclimated winter cereal crowns, the VTZ is injured before the SAM (Olien, 1964; Olien and Marchetti, 1976; Chen et al., 1983; Tanino and McKersie, 1985; Livingston et al., 2005b; Livingston et al., 2013). The VTZ has a proportionally high volume of water relative to the remainder of the crown (Olien and Smith, 1977; Gusta et al., 1979). Chen et al. (1983) observed freezing injury impeded root morphogenesis in Norstar winter wheat whole crowns and suspension cultures. Therefore, the VTZ cannot act exclusively as an ice sink. Winter wheat has a visually analogous bud scale structure, known as the leaf sheath, encapsulating the SAM and upper one third of the VTZ (Tanino and McKersie, 1985; Willick et al., 2018a). Livingston and Tuong (2014) used a freeze-fixation histological technique to observe cavity formation between the leaf sheath of cold-acclimated winter oat (*Avena sativa* L.) cooled at 2°C h^{-1} to -12°C. Infrared video thermography of cold-acclimated barley (*Hordeum vulgare* L.) following an initial freezing event around -6°C, reported a temperature gradient between the

external and internal crown tissues (Pearce and Fuller, 2001). If ice segregation occurs in cold-acclimated winter cereal crowns, then supercooling of the SAM would correspond with a loss of water and a low INA relative to the leaf sheath or VTZ.

Supercooling of reproductive tissues to avoid freezing injury is a significant adaptation in plant freezing survival (Ishikawa and Sakai, 1982; Kuprian et al., 2014; Ishikawa et al., 2015; Kuprian et al., 2016; Kuprian et al., 2017). Ishikawa et al. (2015) suggested the flower bud supercooling mechanism was associated with water migration from the primordia to the scales. The primordia desiccate and increase solute concentration. Willick et al. (2018a) reported cold-acclimated Norstar SAM preferentially accumulated dehydrins. Multiple researchers have suggested during cold-acclimation, the vascular bud trace or crown plate desiccates, resulting in a barrier to ice propagation (George et al., 1974; Ishikawa and Sakai, 1981; Kuprian et al., 2014; Ishikawa et al., 2015; Kuprian et al., 2016). This decrease in water translocation is associated with decreased aquaporin activity (Yooyongwech et al., 2008), increased oligosaccharides and pectin concentration (Kuprian et al., 2017).

During cold-acclimation, the reorganization of the plasma membrane, cell wall and subsequent increase in intra- and extracellular solutes affect the binding properties and physical state of water, which in turn reduces the amount of water available for ice crystallization (Levitt, 1980; Olien and Livingston, 2006). Single and Olien (1967) postulated the re-distribution of water in cereals during cold-acclimation resulted in ‘dry barrier regions’ slowing ice propagation. Post-freezing of cold-acclimated oat was reported to have a suberized band of cells between the VTZ and SAM (Livingston et al., 2005b; Livingston et al., 2013; Livingston and Tuong, 2014). Three days after exposure to sub-lethal low temperatures, injury to the intermediate region was observed as the boundary of crown injury in recovering winter wheat (Tanino and McKersie, 1985; Willick et al., 2018a) and oat (Livingston et al., 2013; Livingston and Tuong, 2014). This region was denoted as the intermediate zone (Gusta et al., 2009), but its role in mitigating ice propagation into the SAM has not been elaborated in the literature. It is possible the crown survives freezing by using this intermediate region as a barrier to ice propagation, allowing the SAM to avoid ice propagation from the leaf sheath or VTZ in a similar fashion to the bud scale and vascular bud trace region in overwintering tree buds (George et al., 1974; Ishikawa and Sakai, 1981; Ishikawa and Sakai, 1985; Quamme et al., 1995; Ishikawa et al., 2015).

Several approaches have been proposed to further identify the freezing process and

subsequent injury in plants. Thermocouples are used in differential thermal analysis (DTA) to measure the release of exothermic latent heat during freezing (George et al., 1974; Ishikawa and Sakai, 1981; Endoh et al., 2009; Ishikawa et al., 2015). Advances in infrared video thermography have built upon this work to provide real-time images of the initial site of ice propagation, and the route and rate of initial ice growth throughout the plant (Wisniewski et al., 1997; Gusta et al., 2004; Griffith et al., 2005; Kuprian et al., 2014).

Unlike the measurement and visualization of individual exotherms, nuclear magnetic resonance (NMR) quantifies the amount of free unbound water within the crown during cold-acclimation and after exposure to sub-zero temperatures (Gusta et al., 1975; Gusta et al., 1979; Yoshida et al., 1997). Magnetic resonance micro-imaging (MRMI) localizes tissue-specific fluctuations in water content at high resolution (50 µm x 50 µm) in seeds during storage (Gruwel et al., 2007), tree buds during cold-induced dormancy induction (de Faÿ et al., 2000; Yooyongwech et al., 2008; Kalcsits et al., 2009) or on exposure to non-lethal sub-zero temperatures (Ishikawa et al., 1997; Ishikawa et al., 2016). The translational mobility of water among cells or tissues can be measured by producing diffusion weighted MRMI images to provide contrast within a voxel of plant tissue (Tanner, 1983). The ADC, a measure of the translational mobility of water, can be calculated from the diffusion weighted images (Tanner, 1983; Kalcsits et al., 2009).

6.2.1 Hypothesis

Cold-acclimated winter wheat and rye crowns survive freezing using the extra-organ freezing strategy and rye is better able to survive due to higher SAM freezing avoidance.

6.2.2 Objectives

To meet the requirements of extra-organ freezing as described by Ishikawa and colleagues (Sakai, 1979; Ishikawa and Sakai, 1982; Ishikawa et al., 2015) the following objectives were tested in cold-acclimated winter wheat and rye. (I) Identify if water mobility among crown tissues decreases during cold-acclimation. (II) Identify if the leaf sheath has a high INA and can accommodate ice. (III) Determine if the SAM has the capacity to supercool and can avoid freezing. To test these objectives, Norstar winter wheat (Grant, 1980) and the comparatively more freezing resistant Hazlet winter rye (McLeod and Gan, 2008) were used as model systems

6.3 Materials and methods

6.3.1 Plant material

Norstar winter wheat and Hazlet rye were germinated and grown hydroponically as described in section 3.3.1.

6.3.2 Freezing survival by whole plant recovery (LT_{50})

The experimental design was a 2 (genotype) x 13 (acclimation) factorial in a three-replicate randomized complete block design. Plants were evaluated over 14 acclimation periods (0, 7, 14, 21, 28, 35, 42, 49, 56, 63, 70, 77, 84, and 91 d) at 4°C for their freezing survival and crown water content. Plants were trimmed to 5 cm above the base of the crown and roots were trimmed to 1 cm below the base of the crown. For LT_{50} determination, crowns were covered in moist sand in aluminum weighing cans and placed in a programmable freezer (Cincinnati Sub-Zero, Cincinnati, OH, USA) ramped down from 0°C to -4°C at -2°C h^{-1}. Ice nucleation was initiated with ice shavings at -4°C. The temperature was held at -4°C for 12 h, and then cooled at 2°C h^{-1} down to -34°C. Fifteen crowns were removed from the freezer at five pre-determined test temperatures at two-degree intervals over a temperature range expected to bracket the LT_{50}. Samples were thawed overnight at 4°C and then transplanted into 12 cm pots containing Sunshine Mix #4 (TerraLink Horticulture Inc., Abbotsford, BC, Canada). Pots were placed in a growth chamber set at 20°C, under a 16 h photoperiod and 350 μmol m^{-2} s^{-1} PPFD. Plant recovery (alive or dead) was rated after 21 d and the LT_{50} was calculated for each sample as described in section 3.3.2.

At each cold-acclimation time point, five plants were sampled for crown water content. Crowns were collected as described above but the roots were removed flush with the crown tissue and immediately weighed. Tissue was dried to a constant weight at 60°C and then re-weighed to obtain the dry weight to calculate crown water content (g H_2O per g dry weight) as described by Gusta et al. (1975). The experiment was repeated three times.

6.3.3 Crown critical water content

Crowns acclimated at 4°C for 42 d were placed in test tubes with 200 μL of INA^+ suspended in phosphate buffered saline (137 mM NaCl, 2.7 mM KCl, 10 mM Na_2HPO_4, 1.8 mM KH_2PO_4, pH 6.5, ice nucleation at -3°C). The INA^+ was collected from fall acclimated field grasses as described in section 4.3.2. Test tubes were placed in a circulating low-temperature bath (Endocal

LT-50DD, Neslab, USA), held at 0°C for 1 h, then slowly cooled (2°C h^{-1}) to -32°C. A subsample of plants (20 crowns per temperature treatment) were used to calculate an LT_{50} using the freezing recovery method. In a parallel experiment, crowns were subsampled (30 crowns per temperature treatment) at six time points (-12°C, -16°C, -20°C, -24°C, -28°C, -32°C) to determine crown water content (Gusta et al., 1975). The critical crown water content at the LT_{50} was determined as described by Metcalf et al. (1970). Experiments were independently run three times.

6.3.4 Osmotic potential and rate of ice migration

Crown tissues were excised and 0.5 g of tissue (fresh weight) from five crowns was ground with an LN_2 chilled mortar and pestle in a 1:4 (w/v) with phosphate buffered saline. The sample was centrifuged (4°C at 7,000 rpm) for 15 min and the supernatant was collected and filtered through miracloth prior to analysis. Samples were collected from three independent experiments prior to analysis. Five replicates per treatment group were collected and the experiment was conducted three times.

A Wescor Psypro (Wescor Inc., Logan, UT, USA) data logger was used to measure cell sap osmotic pressure. All measurements with a C-52 psychrometer sample chamber (Wescor Inc., Logan, UT, USA) were taken in a 5°C cold room to reduce any temperature difference between the sample disc surface and the thermocouple within the C-52 chamber. The psychrometer was calibrated with filter paper discs (SS-033, Wescor Inc., Logan, UT, USA) soaked with NaCl standard solutions (0 to 1200 mmol kg). For each sample, the solute osmotic potential was obtained by soaking filter paper discs in collected cell sap. Phosphate buffered saline controls were prepared as a control.

The rate of ice migration of collected cell sap along a filter paper strip was determined according to Gusta et al. (2004) using an infrared camera (FLIR 65HS, California, USA). Strips of filter paper (1 cm x 8 cm) were soaked with 200 µL of cell sap and placed perpendicularly to a filter paper strip (10 cm x 2 cm) soaked with distilled water. Strips were placed in a rate-controlled chamber set to 0°C and allowed to equilibrate for 20 min. The chamber was cooled at 2.5°C h^{-1} from 0°C to -5°C, and ice nucleation on the fuse strip was initiated with an LN_2 chilled toothpick. Samples of phosphate buffered saline (average rate of ice migration = 1.2 cm s^{-1}) and MilliQ water (average rate of ice migration = 1.0 cm s^{-1}) were prepared as controls.

6.3.5 Individual tissue water content

To determine individual tissue water content after 0 and 42 d at 4°C, harvested crowns were rinsed with distilled water and dissected into individual tissues. Roots were prepared as 1 cm sections from the base of the crown. Crowns were sectioned approximately 4 cm from the nodal plate. A subsection of crowns was dissected into SAM, VTZ, and the leaf sheath surrounding the base of the crown. Fresh and dry weight measurements were collected to determine tissue water content as described by Gusta et al. (1975).

6.3.6 Magnetic resonance micro-imaging (MRMI)

Plant samples were imaged using a Bruker Avance 300 MHz (S040 configuration) with ParaVision (PV5.0) imaging software. Non- and cold-acclimated crowns were excised 4 cm above the base of the crown and roots were trimmed 1 mm below the base were placed in a 10 mm diameter birdcage radio frequency coil which was then placed within the NMR bore (7.05 T) for imaging. A matrix was designed to orient cross-sectional images and ensure uniformity across samples. For morphological images, a 1 cm radio frequency coil was used. For the generation of MRMI crown cross-section images (N = 4) the following parameters were used: field of view (8 mm x 8 mm), slice thickness (0.6 mm), echo time (14 ms), repetition time (1400 ms), in-plane resolution (31 µm x 31 µm). For longitudinal MRMI, the following parameters were used: field of view (8 mm x 24 mm), slice thickness (0.6 mm), echo time (14 ms), repetition time (1400 ms), in-plane resolution (31 µm x 49 µm).

6.3.7 Diffusion-weighted experiments

Diffusion measurements were performed using a 3 cm radio frequency coil. Diffusion-weighted images (N = 5) were acquired using spin-echo diffusion weighting factors of 25, 50, 75, 125, 250, 400, 600, and 1000 s mm^{-2}. Weighting factors (b) were plotted against the region of interest's mean intensity (I). The best-fit equation was extrapolated to determine I_0. To calculate ADC, two higher weighting factors (250 and 600 s mm^{-2}) were selected to create the greatest contrast between less mobile tissue-bound water (greater weighting factors) from mobile extracellular water (lower weighting factors). The following equation was used to calculate ADC:

$$ADC = [\ln (I_0 - I_{b2}) - \ln (I_0 - I_{b1})] / (b_2 - b_1)$$

where b_1 and b_2 are the two selected weighting factors (250 and 600 s mm^{-2}) while I_{b1} and I_{b2} are the corresponding regions of interest mean pixel intensities (Kalcsits et al., 2009). Pixel ADC values were averaged over each region of interest.

6.3.8 Ice localization and water content of frozen tissues

Ice crystal formation was observed in cross-sectioned crowns according to a modified protocol used to observe ice crystals in overwintering flower buds as described by Endoh et al. (2014) with the following modifications. Plants in test tubes were equilibrated at 0°C for 30 min, then cooled to -2°C in a circulating low-temperature bath (Endocal LT-50DD, Neslab, USA), held for 30 min, and then ice nucleated with INA^+. The bath was cooled at a rate of 2°C h^{-1}. Twenty plants were removed at -4°C and -10°C, immediately sectioned using a pre-chilled razor blade in a temperature-controlled room (set to -4°C or -10°C) and imaged with a dissecting microscope. Plants cooled to 0°C were used for non-frozen controls. A subsection of cold-acclimated crowns (30 per temperature treatment) were dissected to determine the water content of the SAM, VTZ and leaf sheath at 0°C, -4°C or -10°C.

6.3.9 Electrolyte leakage (EL_{50})

For electrolyte leakage analysis, crown tissues from three plants were placed into a test tube with 1 mL of deionized water. Tubes were placed in a low-temperature bath. Samples were held at -2°C for 12 h, cooled to -4°C then held at this temperature for 20 min to allow samples to reach equilibrium. Samples were nucleated with ice shavings, held at -4°C for 1 h and then cooled at 2°C h^{-1} to the desired test temperature. Determination of an LT_{50} using the electrolyte leakage method (EL_{50}) was calculated as described by Chen et al (1983). Five replicates of each cultivar were used for each test temperature and the experiment was conducted three times.

6.3.10 Test tube assay for ice nucleating activity (INA)

Crown tissues were dissected with sterilized razor blades and forceps. Each tissue was placed into 2 mL autoclaved phosphate buffered saline in 12 cm x 3 cm test tubes, placed in a rate-controlled low-temperature bath beneath a 5 cm thick transparent sheet of plexiglass. The plexiglass held the tubes in place while facilitating top down viewing of tubes. The controlled low-

temperature ethylene glycol bath (Haake 50, Thermofisher Scientific, New Hampshire, USA) was cooled stepwise from 0°C to -20°C at a rate of 0.5°C every 15 min. At the end of every 15 min period, the number of frozen tubes were counted. To determine the heat stability of the INA, tubes containing crown tissues were autoclaved for 20 min at 121°C. After cooling to room temperature, the autoclaved tubes were tested for their INA. To determine the effects of the leachate, crown tissues were rinsed in phosphate buffered saline water and then aseptically transferred to a new sterile tube containing sterilized phosphate buffered saline. In each experiment, 20 tubes per treatment group were tested and the experiment was independently repeated three times.

6.3.11 Differential thermal analysis

Differential thermal analysis was conducted as described in section 4.3.6 with the following modifications. Seven plants for each treatment (non-acclimated, cold-acclimated, killed in LN_2) were selected based upon their similar development stage. The LN_2 treated plants were tested to determine if the absence of a barrier (physical or biochemical) altered exothermic patterns in plant tissue freezing. To initiate freezing, 200 µL of INA^+ suspension was pipetted into each sterile 10 x 75 mm glass tubes. Roots were the only tissue in direct contact with INA^+ to initiate freezing. To initiate supercooling, plants were exposed to decreasing temperature in the absence of an ice nucleator. The experiment was repeated three times.

6.3.12 Statistical analysis

For the 2 x 13 factorial experiment, analyses of variance (ANOVA) determined the level of significance of differences due to genotype, acclimation period and their interactions. Where significant differences were identified, regression analyses of treatment means were used to plot curves that gave the best description of the shape and behaviour of the responses. The peak four parameter Weibull equation was used to describe the relationship between LT_{50} or crown dry weight and days of acclimation at 4°C.

$$y = a\left(\frac{c-1}{c}\right)^{\frac{1-c}{c}}\left[\frac{x-xo}{b}+\left(\frac{c-1}{c}\right)^{\frac{1}{c}}\right]^{c-1} e^{-\left[\frac{x-xo}{b}+\left(\frac{c-1}{c}\right)^{\frac{1}{c}}\right]^{c}} + \left(\frac{c-1}{c}\right)$$

The peak five parameter Weibull equation was used to describe the relationship between crown water content and days of acclimation or crown exposure to sub-zero temperatures.

$$y = yo + a\left(\frac{c-1}{c}\right)^{\frac{1-c}{c}}\left[\frac{x-xo}{b} + \left(\frac{c-1}{c}\right)^{\frac{1}{c}}\right]^{c-1} e^{-\left[\frac{x-xo}{b} + \left(\frac{c-1}{c}\right)^{\frac{1}{c}}\right]^{c}} + \left(\frac{c-1}{c}\right)$$

Non-linear regression procedures outlined in the SigmaPlot 12.5 (Systat Software Inc., California, USA) user guide provided least squares estimates of the regression coefficients for all equations. Calculated coefficients are provided in Tables S6.1, S6.2 and S6.3. In the remaining experiments, two-tailed t-tests, one- or two-way ANOVA and Fisher's Least Significant Difference test were performed using SigmaPlot 12.5 to detect treatment effects and determine differences ($P < 0.05$) among mean values. Normality and homogeneity of variance were confirmed prior to analysis. In instances where data was not normally distributed, analysis of variance was conducted with the Kruskal-Wallis H-test. Dunn's post hoc method was used to detect treatment effects and determine differences ($P < 0.05$) among mean values.

6.4 Results

6.4.1 Effect of cold-acclimation on crown dry weight, water content and LT_{50}

From 7 to 21 d of cold-acclimation, the rate of change in Norstar and Hazlet freezing survival (LT_{50}) markedly increased (**Figure 6.1**). After 21 d of cold-acclimation, the rate of change declined, producing a curvilinear relationship between LT_{50} and the stage of acclimation of all cultivars (**Figure 6.1A**). Norstar (LT_{50} = -21°C) and Hazlet (LT_{50} = -27°C) reached the maximum LT_{50} by 42 d at 4°C (**Table S6.1**). At 42 d of cold-acclimation, there was a significant ($P < 0.01$) difference in Norstar and Hazlet LT_{50}. The difference in Hazlet and Norstar LT_{50} corresponded with a significantly ($P < 0.05$; **Figure 6.1A**; **Table S6.1**) higher crown dry matter accumulation ($P < 0.05$; **Figure 6.1B**; **Table S6.1**) and crown water content (**Figure 6.1C**; **Table S6.2**) in Hazlet as compared to Norstar. The gradual loss of freezing survival after 42 d of exposure to 4°C corresponded with an increase in crown water content and not a decrease in crown dry weight. Based upon these findings, cold-acclimation in the following experiments was defined as exposure to 4°C for 42 d. Cold-acclimated crowns cooled at 2°C h^{-1} from 0°C to -12°C lost between 18 % (Norstar) and 25 % (Hazlet) of their crown water content (**Figure 6.2**; **Table S6.3**). Hazlet crowns had a higher crown water content than Norstar at all sub-zero temperatures. Cold-acclimated Hazlet crowns had a higher water content than Norstar throughout the entire sub-zero temperature

range. The critical crown water content at the LT_{50} was 1.8 ± 0.1 g H_2O per g dry weight for Norstar (LT_{50} = -21°C) and 1.8 ± 0.1 g H_2O per g dry weight for Hazlet (LT_{50} = -27°C).

6.4.2 Effect of cold-acclimation on free water visualized by MRMI

A combination of high resolution and magnification microimaging allowed for the non-destructive capture of 0.6 mm cross-sectional images and the identification of individual leaf sheath, tiller, root vessel, the SAM tissues plus a level of detail including vessel elements within the VTZ of the crown (**Figure 6.3**). The MRMI micrographs depict an intermediate zone between the SAM and VTZ (**Figure 6.3C**). For morphological comparison to whole crowns, longitudinal images confirmed a dense signal band between the SAM and VTZ (**Figure S6.3**). The intermediate zone was visually more prevalent in non-acclimated Hazlet (**Figure 6.4C**; **Figure S6.1**) than in Norstar (**Figure 6.4A**; **Figure S6.3**). In the cross-sectional images, intermediate zone signal intensity visually decreased as a result of cold-acclimation (**Figure 6.4**). Visual reductions in signal intensity between cold-acclimated and non-acclimated tissues were observed in the VTZ and the leaf sheath surrounding the SAM (**Figure 6.4**).

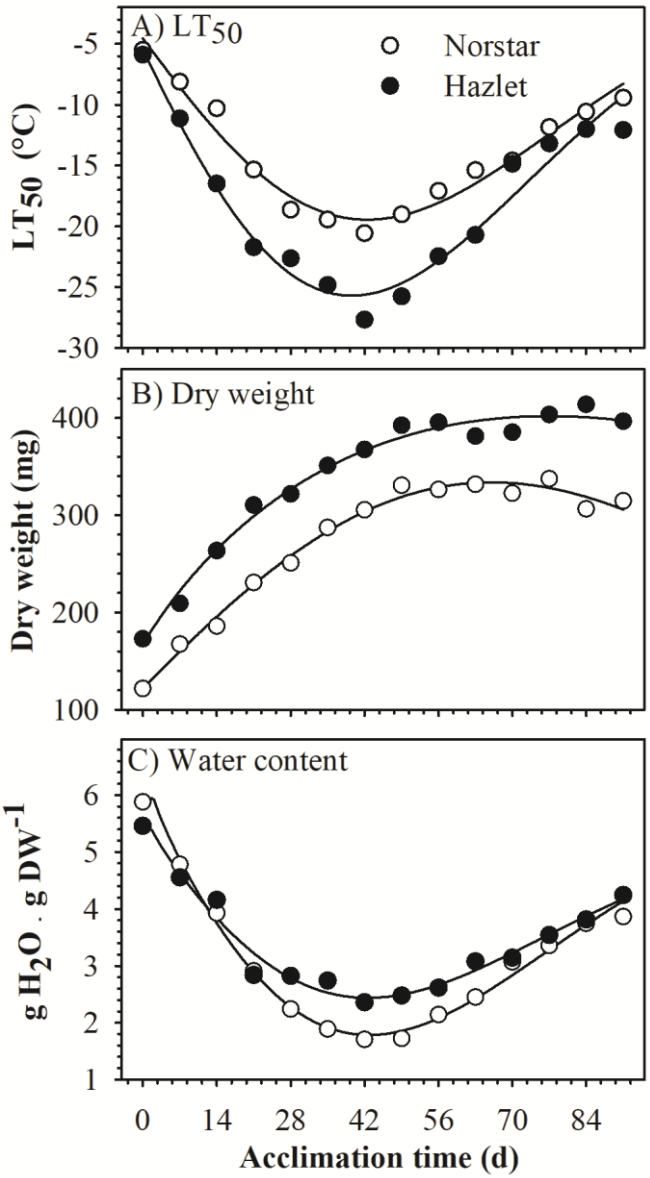

Figure 6.1 Norstar wheat and Hazlet rye crown LT_{50}, crown dry weight and water content when acclimated at 4°C from 0 to 91 d.

A, Crown LT_{50}, lethal temperature at which 50 % of the crowns recover (standard error of data points = 1.1). B, crown dry weight (standard error = 15.4). C, Crown water content (standard error = 0.2). Norstar winter wheat and Hazlet rye were cold-acclimated at 4°C for 0 to 91 d. For regression coefficients see **Table S6.1** (LT_{50} and crown dry weight) and **Table S6.2** (crown water content). The LT_{50} data was presented as a means of three independent experiments (N = 3; 20 crowns per temperature per treatment in each LT_{50} experiment, 3 replicates in time and space). Dry weight and moisture content is presented as a means of the total number of individuals (N = 45; 15 plants with 3 replicates in time and space).

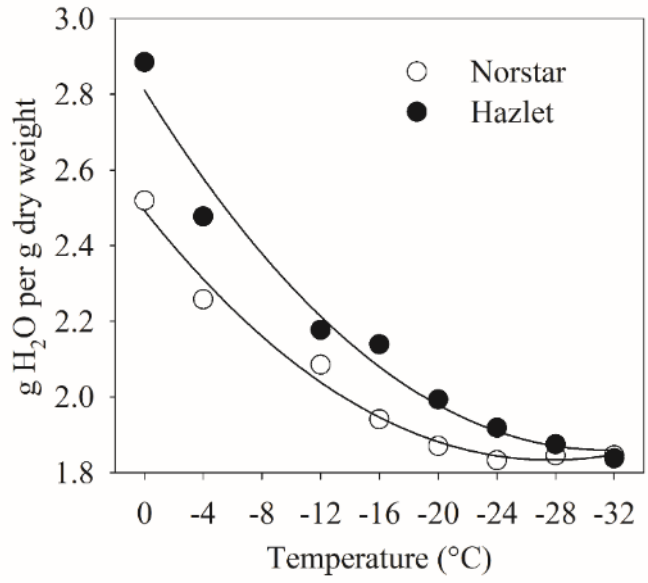

Figure 6.2 Crown water content of cold-acclimated Norstar and Hazlet crowns exposed to sub-zero temperatures (standard error = 0.2).

Crowns were cooled at a rate of 2°C h^{-1} from 0°C to -32°C in test tubes in a low-temperature bath. Plants were ice nucleated at -2°C. Crowns were removed at each specific temperature treatment and measured for fresh and dry weights. The crowns critical water content was determined at the LT_{50} for each respective cultivar. Data is presented as a means of the total number of individuals (N = 30; 10 plants with 3 replicates in time and space)

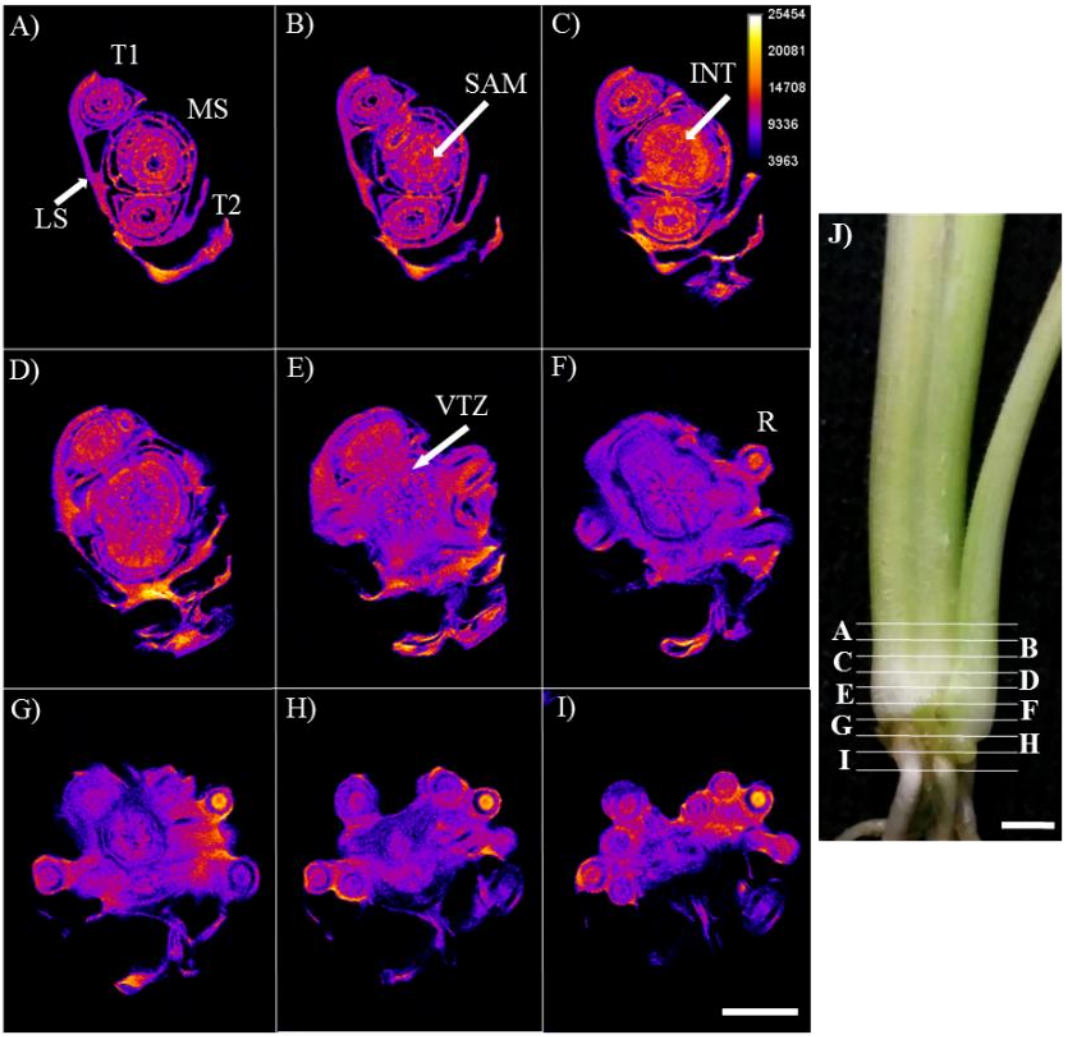

Figure 6.3 Magnetic resonance micro-imaging (MRMI) cross-sectional images of non-acclimated Norstar.

The numbered images correspond to the numbered level marks in panel J. Lighter colours represent higher water mobility while darker colours represent lower water mobility. Abbreviations include: tiller 1 (T1), tiller 2 (T2), main shoot (MS), shoot apical meristem (SAM), leaf sheath (LS), vascular transition zone (VTZ), intermediate zone (INT) and root (R). Images are representative of 5 biological replicates (N = 5). Scale bar = 0.4 cm.

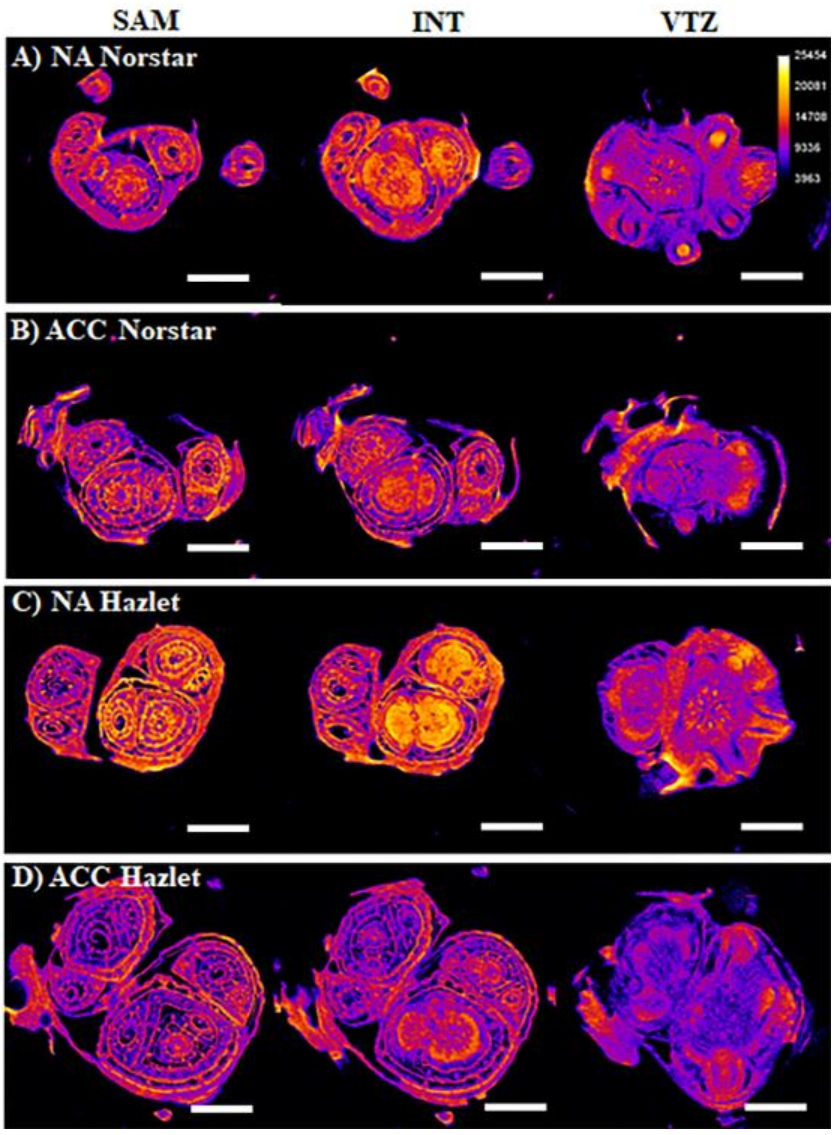

Figure 6.4 Magnetic resonance micro-imaging (MRMI) cross-sectional images of non- and cold-acclimated Norstar and Hazlet crowns.
MRMI cross-section images of non- (NA) and cold- (ACC) acclimated Norstar and Hazlet crown tissues. Abbreviations include: shoot apical meristem (SAM), vascular transition zone (VTZ) and intermediate zone (INT). Images are representative of 5 biological replicates (N = 5). Scale bar = 0.2 cm.

Water diffusion-weighted images were used (**Figure S6.2**) to calculate the translocational mobility of water (ADC). Bright regions (**Figure S6.2D**, **E** and **F**) in the heavier weighted images (400, 600, and 1000 s mm^{-2}) correspond to cells and tissue, with reduced water mobility compared to the low (**Figure S6.2A**) and intermediate (**Figure S6.2B** and **C**) weighted images. In cold-acclimated crowns, the ADC was highest in the leaf sheath, roots and SAM, then the intermediate zone and VTZ (**Table 6.1**). In cold-acclimated Hazlet, the ADC significantly decreased in the VTZ, leaf sheath, roots and intermediate zone (**Table 6.1**). Water mobility in the SAM was not affected by cold-acclimation nor did it vary between Norstar and Hazlet ($P > 0.05$). Cold-acclimated Hazlet had a significantly lower ADC ($P < 0.05$) in the intermediate zone and VTZ than Norstar. In response to cold-acclimation, the VTZ had the greatest ADC decrease (21 % in Norstar and 37 % in Hazlet) followed by the intermediate zone (6 % in Norstar and 26 % in Hazlet).

6.4.3 In vitro analysis of crown tissues

Cold-acclimated plants, irrespective of cultivar, accumulated higher dry weight and lower crown water content ($P < 0.05$) than crowns grown under non-acclimated conditions (**Table 6.2**). Cold-acclimated leaf sheaths and the VTZ accumulated significantly higher dry weight and less water content ($P < 0.05$) than non-acclimated crowns. Cold-acclimated Hazlet accumulated significantly more dry weight than cold-acclimated Norstar SAM. Cold-acclimated crown tissue cell sap, irrespective of cultivar, had significantly higher osmotic potential and reduced rates of ice migration ($P < 0.05$) than cell sap collected from non-acclimated plants (**Table 6.3, Table 6.4**). When considering only the cold-acclimated plants, cell sap collected from Hazlet SAM and the whole crown had significantly higher ($P < 0.05$) osmotic potential than the respective Norstar tissues. Cell sap collected from cold-acclimated Hazlet VTZ had significantly lower ($P < 0.05$) rates of ice migration than cell sap collected from the Norstar VTZ.

Whole crowns and individual tissues were tested for EL_{50} (**Table 6.5**). Differences between non-acclimated crown tissue survival of Norstar and Hazlet were not significant ($P > 0.05$). Cold-acclimation increased the survival of crown tissues and EL_{50} were VTZ > leaf sheath > SAM > roots. Only whole crowns and excised VTZ had a greater EL_{50} ($P < 0.01$) in cold-acclimated Hazlet compared to Norstar.

Table 6.1 Apparent diffusion coefficients of crown tissues in non- (NA) and cold-acclimated (ACC) Norstar winter wheat and Hazlet rye.

Values were calculated from diffusion-weighted series such as those shown in Figure S6.1. Data was presented as a means of the total number of individuals (N = 5 plants). Means followed by the same letter within each column (lowercase) and row (uppercase) were not different based on Fisher's Least Significant Difference test ($P < 0.05$).

Cultivar	Treatment	Leaf Sheath	SAM	INT	VTZ	Root	$LSD_{0.05}$
		----- *mm* s^{-1} *x* 10^{-4} -----					
Norstar	NA	20.5 b B	23.4 a A	23.3 a AB	23.0 b AB	25.1 a A	2.8
	ACC	22.1 b A	21.9 a A	21.8 a A	18.2 c B	22.0 b A	2.9
Hazlet	NA	29.7 a A	23.2 a BC	22.4 a C	25.4 a B	24.9 a C	2.7
	ACC	22.1 b A	22.8 a A	16.6 b B	15.9 d B	22.1 b A	2.3
$LSD_{0.05}$		1.8	4.9	1.9	1.8	1.6	

Table 6.2 Mean dry weight and water content of non-acclimated (NA) or cold-acclimated (ACC) Norstar and Hazlet crown tissues.

Means followed by the same lowercase letter within each column are not different based on Fisher's Least Significant Difference test ($P < 0.05$). Dry weight means followed by the same uppercase letter within the same row are not different based on Kruskal-Wallis H-test with Dunn's post hoc method ($P < 0.05$). Water content means followed by the same lowercase letter within the same row are not different based Fisher's Least Significant Difference test ($P < 0.05$). Data is presented as a means of the total number of individuals (N = 30; 10 plants with 3 replicates in time and space).

Treatment	Dry weight				Water content				
	Leaf Sheath	SAM	VTZ	Root	Leaf Sheath	SAM	VTZ	Root	$LSD_{0.05}$
	------ *mg* ------				------ *g H_2O per g dry weight* ------				
Norstar NA	76.9 b AB	14.7 a C	104.3 c A	57.9 a BC	4.5 b A	2.3 a C	3.9 b B	4.1 a B	0.4
Norstar ACC	86.5 a AB	14.9 a C	127.1 b A	61.7 a BC	3.5 c B	2.1 a D	2.6 c C	4.4 a A	0.3
Hazlet NA	75.7 b AB	13.4 a C	110.5 c A	57.5 a BC	5.2 a A	2.0 a C	4.5 a B	4.2 a B	0.5
Hazlet ACC	86.3 a AB	15.7 a C	134.7 a A	59.1 a BC	4.5 b A	2.2 a C	2.4 c C	4.0 a B	0.3
$LSD_{0.05}$	4.6	2.3	4.1	4.6	0.4	0.4	0.3	0.4	

Abbreviations include: shoot apical meristem (SAM), vascular transition zone (VTZ).

Table 6.3 Mean osmotic potential of crown cell sap.

Sap was collected from Norstar and Hazlet crown tissues that were non-acclimated (NA) or cold-acclimated (ACC) at 4°C for 42 d. Means followed by the same lowercase letter within each column are not different based on Fisher's Least Significant Difference test ($P < 0.05$). Means followed by the same uppercase letter within the same row are not different based on Kruskal-Wallis H-test with Dunn's post hoc method ($P < 0.05$). Data is presented as a means of the total number of individuals (N = 15; 5 plants with 3 replicates in time and space).

Cultivar	Osmotic Potential				
	Leaf Sheath	SAM	VTZ	Root	Crown
			------ *MPa* ------		
Norstar NA	-0.47 a B	-1.46 a A	-1.35 a B	-0.49 a A	-1.26 a A
Norstar ACC	-0.83 c B	-1.85 c A	-1.57 b B	-0.62 b A	-1.58 b A
Hazlet NA	-0.61 b B	-1.57 b A	-1.43 a B	-0.62 b A	-1.27 a A
Hazlet ACC	-0.89 c B	-1.96 d A	-1.67 b B	-0.79 c A	-1.81 c A
$LSD_{0.05}$	0.07	0.07	0.11	0.11	0.13

Abbreviations include: shoot apical meristem (SAM), vascular transition zone (VTZ).

Table 6.4 Mean rate of ice migration of cell sap along a filter paper strip.

Sap was collected from Norstar and Hazlet crown tissues that were non-acclimated (NA) or cold-acclimated (ACC) at 4°C for 42 d. Means followed by the same letter within each column are not different based on Fisher's Least Significant Difference test ($P < 0.05$). Means followed by the same uppercase letter within the same row are not different based on Kruskal-Wallis H-test with Dunn's post hoc method ($P < 0.05$). Data is presented as a means of the total number of individuals (N = 15; 5 plants with 3 replicates in time and space).

Cultivar	Rate of ice migration				
	Leaf Sheath	SAM	VTZ	Root	Crown
			------ *cm* s^{-1} ------		
Norstar NA	0.65 a AB	0.30 a C	0.71 b A	0.35 a C	0.42 a BC
Norstar ACC	0.43 b A	0.23 bc B	0.32 c A	0.32 a A	0.20 b B
Hazlet NA	0.63 a A	0.25 b B	0.82 a A	0.32 a B	0.39 a B
Hazlet ACC	0.35 b A	0.21 c B	0.20 d B	0.30 a A	0.20 b B
$LSD_{0.05}$	0.09	0.03	0.09	0.06	0.04

Abbreviations include: shoot apical meristem (SAM), vascular transition zone (VTZ).

Table 6.5 Electrolyte leakage analysis of frozen non- and cold-acclimated crown tissues.

The temperature in the freeze test (EL_{50}) where 50 % of the total electrolyte leakage occurred in crowns and individual tissues collected from Norstar winter wheat and Hazlet winter rye grown under non- (0 d at 4°C) and cold-acclimation (42 d at 4°C) conditions. Significant differences between Norstar and Hazlet within an acclimation regime were determined with a two-tailed t-test (^{ns} P > 0.05, * P < 0.05, ** P < 0.01). Data is presented as a means of the total number of individuals (N = 15; 5 plants with 3 replicates in time and space).

Tissue	Non-acclimated		Cold-acclimated	
	Norstar	Hazlet	Norstar	Hazlet
	----- *°C* -----		----- *°C* -----	
Root	-4.9	-5.2 ^{ns}	-7.8	-7.7 ^{ns}
Leaf sheath	-5.2	-5.1 ^{ns}	-14.6	-14.7 ^{ns}
SAM	-5.5	-5.3 ^{ns}	-13.3	-13.7 ^{ns}
VTZ	-5.3	-5.3 ^{ns}	-16.5	-17.6**
Crown	-5.6	-5.6 ^{ns}	-23.3	-26.5**

6.4.4 In vitro analysis of tissue ice nucleating activity (INA)

All non-acclimated crown tissues had an INA between -5 and -7°C (data not shown). Cold-acclimation did result in a difference in INA amongst intact excised tissues of the leaf sheath > VTZ > SAM (**Table 6.6**). In cold-acclimated SAM, there was significantly higher INA for intact compared to autoclaved treatments (two-way ANOVA, Fisher's LSD, $P < 0.05$). Norstar VTZ INA was significantly higher than Hazlet ($P < 0.05$) in the autoclave treatment. There was a significant decrease in INA in the autoclaved and autoclave/water treatments (Two-way ANOVA, Fisher's LSD, $P < 0.05$). The INA of tissues in the autoclave/water treatment group was comparable to the INA of non-acclimated excised crowns.

6.4.5 Observations during freezing, exotherm temperature and tissue water content

Microscopic observation (**Figure 6.5**), DTA (**Figure 6.6**; **Figure S6.3**; **Table 6.7**) and tissue water content determination (**Table 6.8**) of crowns cooled at -2°C h^{-1} to -10°C were conducted to determine if individual freezing events occurred in cold-acclimated Norstar and Hazlet crowns. In cold-acclimated Norstar (**Figure 6.5**) and Hazlet (data not shown) cooled to -4°C, ice filled the space between the leaf sheaths. The leaf sheath had on average 1 g H_2O per g dry weight more than the VTZ and on average a 2 g H_2O per g dry weight than the SAM at 4°C, -4 and -10°C (**Table 6.8**). The SAM had a lower water content when cooled to -4°C or -10°C (**Table 6.8**) than the critical water content of whole crowns (**Figure 6.2**). The significant decrease in SAM and VTZ water content after cooling to -4°C and -10°C was accompanied by a significant increase in tissue dry weight (**Table 6.8**). Cold-acclimated Hazlet SAM had a significantly lower water content ($P < 0.05$) than Norstar when cooled to -4°C or -10°C. Visual observations indicated that the VTZ section was partially frozen at -4°C (**Figure 6.5**). In a separate test, visual observation of ice nucleation in the -4°C VTZ section was initiated with a chilled toothpick (data not shown). Ice sectioning of crowns cooled to -10°C showed a complete freezing of the VTZ and the formation of cavities due to the absence of water or ice in the VTZ (**Figure 6.5**). In contrast, sectioning of crowns cooled to -10°C showed an absence of ice near the SAM and a darker green colouration compared to 4°C SAM sections (**Figure 6.5**).

Table 6.6 Ice nucleation temperatures of cold-acclimated leaf sheath, SAM and VTZ collected from Norstar and Hazlet crowns.

Tissues were placed in 2 mL of autoclaved and filtered phosphate buffered saline in a sterile test tube. Samples were left unwashed and intact (INT), autoclaved (AC) or autoclaved, rinsed and then placed in a new sterile tube (AC/WC). Samples were cooled at a rate of 2°C h^{-1}. Data is presented as a means of the total number of individuals (N = 60; 20 plants with 3 replicates in time and space). Means followed by the same letter within each column (lowercase) and row (uppercase) are not significantly different based on Fisher's LSD test (Two-way ANOVA, $P < 0.05$).

Cultivar	Treatment	INT	AC	AC/WC	$LSD_{0.05}$
			----- °C -----		
	SAM	-7.0 c A	-11.7 d C	-8.0 c B	0.6
Norstar	VTZ	-5.5 b A	-10.5 b C	-7.3 a B	0.4
	Leaf sheath	-3.6 a A	-9.3 a C	-7.7 b B	0.8
	SAM	-7.5 d A	-12.9 e B	-8.0 c A	0.6
Hazlet	VTZ	-5.5 b A	-11.2 c C	-7.4 a B	0.6
	Leaf sheath	-3.7 a A	-9.1 a C	-7.7 b B	0.7
$LSD_{0.05}$		0.2	0.3	0.2	

Table 6.7 Summary of exothermic events in live and LN_2 killed non- and cold-acclimated winter cereals with or without an ice nucleator.

Freezing was induced by a phosphate buffered solution with the presence (Nuc^+) or absence (Nuc^-) of INA^+ at the base of the test tube and monitored with a thermocouple placed at the base of the crown and held in place with parafilm. Plants were cooled at a rate of 2°C h^{-1}. Non-acclimated plants only produced an intense high-temperature exotherm. Cold-acclimated plants produced three separate exotherms. Instances, where exotherms were not shown, are indicated as below detectable limits (Bdl). Values are the means of three independent experiments. Data is presented as a means of the total number of individuals (N = 21; 7 plants with 3 replicates in time and space). Treatments sharing the same letter in each column were not significantly different according to Fisher's LSD (Two-way ANOVA for high-temperature exotherms and One-way ANOVA for mid- and low-temperature exotherms, $P < 0.05$).

		Non-acclimated		Cold-acclimated					
Cultivar	LN_2	High-temperature		High-temperature		Mid-temperature		Low-temperature	
		Nuc^+	Nuc^-	Nuc^+	Nuc^-	Nuc^+	Nuc^-	Nuc^+	Nuc^-
		----- °C -----							
Norstar	-	-3.7 a	-4.6 a	-3.8 b	-4.6 b	-6.4 a	-5.8 a	-16.9 a	-12.2 a
	+	-3.6 a	-4.5 a	-3.3 a	-4.2 a	Bdl	Bdl	Bdl	Bdl
Hazlet	-	-3.8 a	-4.7 a	-3.7 b	-4.6 b	-7.2 b	-6.1 a	-27.3 b	-23.5 b
	+	-3.5 a	-4.5 a	-3.2 a	-4.2 a	Bdl	Bdl	Bdl	Bdl
$LSD_{0.05}$		0.5	0.3	0.4	0.2	0.5	0.3	3.0	0.8

Table 6.8 Changes in crown tissue water content of cold-acclimated Norstar winter wheat and Hazlet winter rye cooled (2°C h^{-1}) to -4°C and -10°C.

Following exposure to sub-zero temperatures, the crown was sectioned in a cold room (at 4, -4 or -10°C) and immediately weighed. Data is presented as a means of the total number of individuals (N = 30; 10 plants with 3 replicates in time and space). Means followed by the same lowercase letter within each column are not different based on Fisher's LSD test ($P < 0.05$). Dry weight means followed by the same uppercase letter within the same row are not different based on Kruskal-Wallis H-test with Dunn's post hoc method ($P < 0.05$). Water content means followed by the same uppercase letter within the same row are not different based on Fisher's LSD test ($P < 0.05$.

Cultivar	Temperature	Dry weight			Water content			
		Leaf Sheath	SAM	VTZ	Leaf Sheath	SAM	VTZ	$LSD_{0.05}$
	---°C ---	*------ mg ------*			*--- g H_2O per g dry weight ---*			
Norstar	4	82.2 c B	15.3 d C	132.2 d A	3.4 c A	2.1 a C	2.8 a B	0.1
Hazlet	4	87.0 b B	16.5 c C	135.4 cd A	3.6 b A	2.2 a C	2.9 a B	0.1
Norstar	-4	87.1 b B	17.0 bc C	138.6 bc A	3.6 b A	1.9 b C	2.4 b B	0.1
Hazlet	-4	89.4 a B	17.6 b C	138.2 bc A	3.9 a A	1.5 c C	2.7 a B	0.1
Norstar	-10	86.0 b B	18.3 a C	142.4 ab A	3.2 d A	1.8 b C	2.2 b B	0.1
Hazlet	-10	90.7 a B	18.9 a C	146.8 a A	3.1 d A	1.4 c C	2.2 b B	0.1
	$LSD_{0.05}$	2.0	0.6	5.1	0.2	0.1	0.2	

Abbreviations include: shoot apical meristem (SAM), vascular transition zone (VTZ).

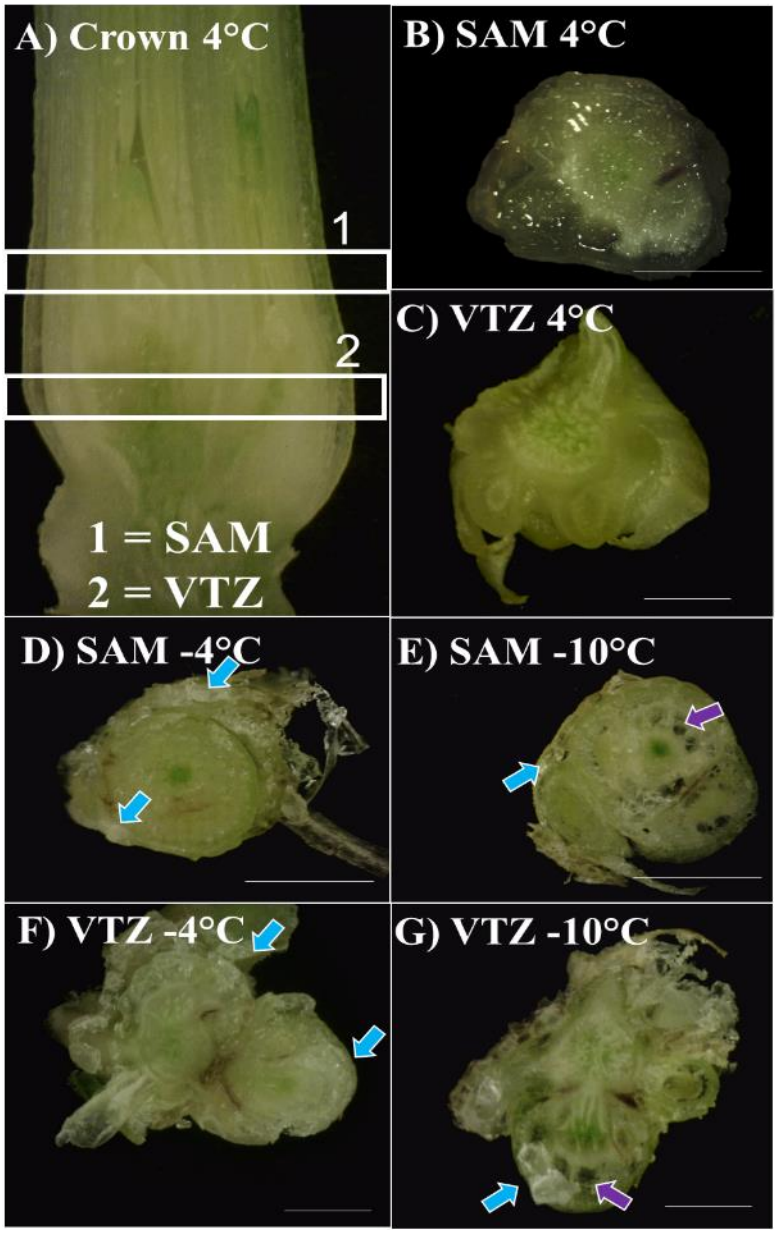

Figure 6.5 Macroscopic observation of ice crystals in cold-acclimated Norstar crown tissue.

A, Longitudinal section of an unfrozen, cold-acclimated Norstar crown. B,D and E, Cross-sections of cold-acclimated Norstar crowns, depicting slices for the SAM. C, F and G, Cross-sections of cold-acclimated Norstar crowns, depicting slices for the VTZ. Crowns placed in test tubes with wet kimwipes were cooled at a rate of 2°C h^{-1} from 0°C to -4°C or -10°C in a low-temperature bath. Plants were ice nucleated at -2°C. Representative images were selected from 30 plants per treatment group (N = 30). There were no differences in the localization of ice or patterns of injury between Norstar and Hazlet. Light blue arrows indicate the presence of ice crystals between the leaf sheaths. Purple arrows indicate cavities due to the absence of water/ice. Scale bar = 0.2 cm.

Norstar and Hazlet were monitored during freezing using thermocouples placed directly between the main shoot and first tiller. Three distinct high, intermediate and low-temperature exotherms in cold-acclimated plants were identified during freezing (**Figure 6.6**; **Figure 6.7**). Plants cooled at 2°C h^{-1} produced a high-temperature exotherm between -3.5°C to -6.1°C (**Table 6.7**). In the presence of an ice nucleator, the high-temperature exotherm occurred at a 1°C warmer temperature in non- and cold-acclimated Norstar and Hazlet. Non-acclimated DTAs display a single strong peak (**Figure 6.6A**; **Figure 6.7A**). Cold-acclimated Norstar and Hazlet freezing curves display a double ridged peak (**Figure 6.6B**, **C**; **Figure 6.7B**, **C**) corresponding to bulk water freezing (George et al., 1974). In cold-acclimated crowns, the inclusion of an ice nucleator resulted in a low intensity mid temperature exotherm (**Table 6.7**) between -5 and -8°C. In the absence of an ice nucleator, the mid temperature exotherm followed the high-temperature exotherm.

In cold-acclimated crowns, the low temperature exotherm (**Table 6.7**) occurred at a temperature comparable to the LT_{50} (**Figure 6.2**; **Table S6.1**) and crown EL_{50} (**Table 6.5**). The addition of an ice nucleator resulted in a significant increase ($P < 0.05$) in temperature in which the mid temperature exotherm was observed in cold-acclimated Norstar and Hazlet (**Table 6.6**). The addition of an extrinsic ice nucleator resulted in a significantly cooler Norstar and Hazlet low-temperature exotherm (**Figure 6.6C**; **Figure 6.7C**; **Table 6.7**). In the absence of an extracellular nucleator, Norstar had an LT_{50} of -14°C and Hazlet an LT_{50} of -20°C. The addition of an extracellular nucleator resulted in a 5°C decrease in Norstar LT_{50} and a 6°C decrease in Hazlet LT_{50}. Freeze-killing plants with liquid nitrogen and then thawing plants prior to DTA analysis resulted in a single exotherm peak (**Figure 6.6D**; **Figure 6.7D**).

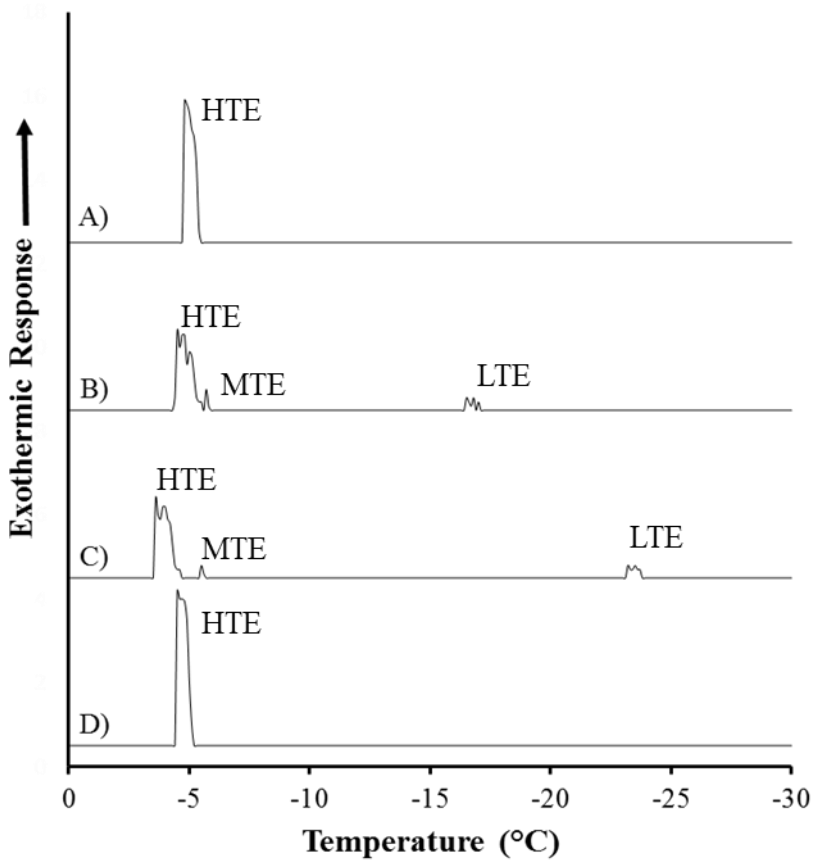

Figure 6.6 Representative differential thermal analysis (DTA) of Norstar plants.

A) Non-acclimated Norstar with no nucleator was observed to have a high temperature exotherm (THE). B) A typical DTA profile of cold-acclimated Norstar with no extrinsic nucleator was observed to have a HTE, a mid (MTE) and a low (LTE) temperature exotherm. C) the addition of a nucleator resulted in greater separation between the HTE and MTE as well as the MTE and LTE. D) A DTA profile of cold-acclimated Norstar freeze killed with liquid nitrogen and then thawed prior to cooling was observed to have a HTE. DTA of Norstar with 2 cm of roots and 4 cm of stem cooled at 2°C h^{-1}. Thermocouples were placed next to the base of the crown and held in place with parafilm. Crowns with a secure thermocouple were placed in test tubes with or without 200 µL of INA^{+}. Fluid at the bottom of the test tube only encountered the roots and not the crown tissue. Representative DTAs were selected from the total number of individuals (N = 21; 7 plants with 3 replicates in time and space). Mean values are presented in **Table 6.7**.

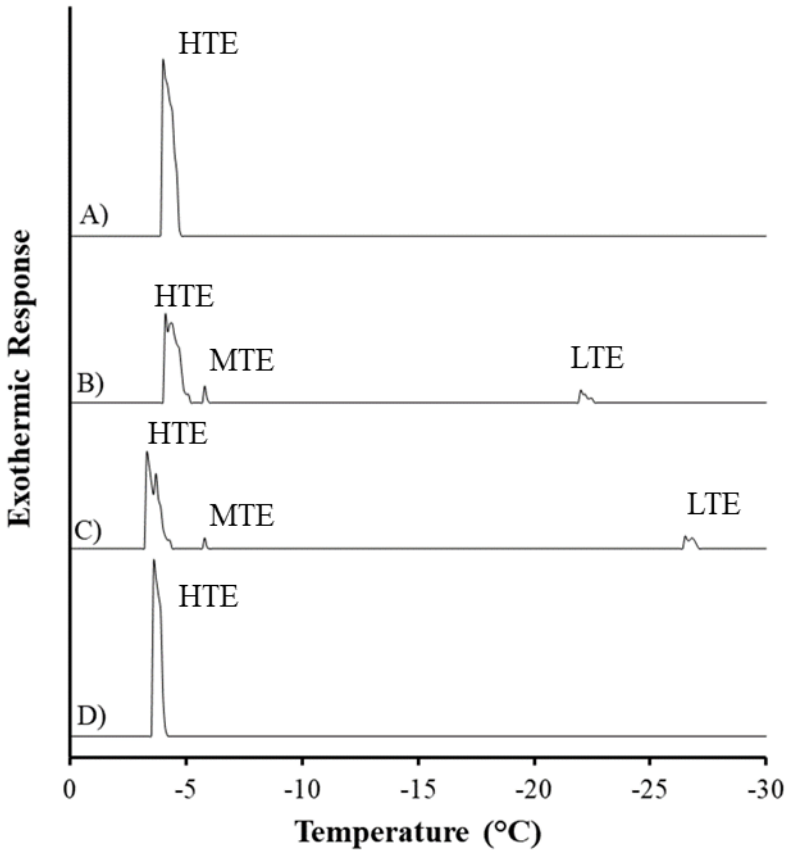

Figure 6.7 Differential thermal analysis (DTA) of Hazlet with 2 mm of roots and 4 mm of stem cooled at 2°C h^{-1}.

A) Non-acclimated Hazlet with no nucleator was observed to have a high temperature exotherm (THE). B) A typical DTA profile of cold-acclimated Hazlet with no extrinsic nucleator was observed to have a HTE, a mid (MTE) and a low (LTE) temperature exotherm. C) the addition of a nucleator resulted in greater separation between the HTE and MTE as well as the MTE and LTE. D) A DTA profile of cold-acclimated Hazlet freeze killed with liquid nitrogen and then thawed prior to cooling was observed to have a HTE. DTA of Hazlet with 2 cm of roots and 4 cm of stem cooled at 2°C h^{-1}. Thermocouples were placed next to the base of the crown and held in place with parafilm. Crowns with a secure thermocouple were placed in test tubes with or without 200 µL of INA^{+}. Fluid at the bottom of the test tube only encountered the roots and not the crown tissue. Representative DTAs were selected from the total number of individuals (N = 21; 7 plants with 3 replicates in time and space). Mean values are presented in **Table 6.7**.

6.5 Discussion

6.5.1 Effect of cold-acclimation on crown water partitioning

In this study, the acclimation time at 4°C required to attain maximum cold hardiness (**Figure 6.1**) was similar to earlier reports for Norstar winter wheat and comparable North American winter rye cultivars (Chen et al., 1983; Fowler et al., 1996; Limin and Fowler, 2002). Crown dry matter accumulated at a faster rate than the loss of water, resulting in the decrease in crown water content (Fowler and Carles, 1979; Yoshida et al., 1997). High crown water content in cold-acclimated Hazlet compared to Norstar supports previous research by Fowler and Carles (1979), that water content of rye crowns was equal to or higher than wheat during Fall acclimation but could survive exposure of lower temperatures. Differences in rye and wheat crown freezing survival cannot be explained by total crown water content and are more likely a result of tissue level responses. When slowly cooled, water can migrate to spaces or tissues that can accommodate ice crystal formation (Olien and Livingston, 2006). High tissue water content and the absence of internal crown ice barriers facilitate lethal ice propagation and intracellular freezing events (Olien, 1964). When slowly cooled, water can migrate to spaces or tissues which can accommodate ice crystal formation

The cold-acclimation induced loss of VTZ and intermediate zone mobile water is related to the establishment of a tissue-specific cold-acclimation strategy. Kalcsits et al. (2009) reported a cold-induced ADC decrease in the vascular bud trace. The formation of a cold-induced desiccative tissue barrier were observed in alpine shrub (Kuprian et al., 2014; Kuprian et al., 2016) and grape (*Vitis riparia L.)* (Fennell and Line, 2001) stems, the vascular bud trace in peach (*Prunus persica* L.) buds (Yooyongwech et al., 2008) and eight other *Prunus* species (Ashworth, 1984). Short day-induced bud dormancy was also associated with the development of a water-limiting barrier in the crown region of Norway spruce buds (Lee et al., 2017). Interestingly, cold-acclimated Hazlet had a lower VTZ and intermediate zone ADCs than Norstar. Chen et al. (1983) reported rye had a higher root meristem freezing survival than wheat. Additional research is needed to determine the specific cellular mechanism protecting root meristem cells from freezing injury in cold-acclimated wheat and rye crowns.

6.5.2 Role of tissue barriers in freezing survival

Quamme (1978) proposed barriers in *Prunus* tree buds were organized at the tissue, rather than the cellular level. Ishikawa and Sakai (1981) proposed that tissue barriers desiccate during cold-acclimation and sub-zero cooling to inhibit ice propagation into the primordia. Similarly, Ashworth (1984) hypothesized underdeveloped vascular tissue and increased segmentation within ice barriers restrict water movement into the primordia in cold-acclimated peach buds. Yooyongwech et al. (2008) reported cold-acclimation significantly decreased vascular bud trace ADC and aquaporin expression. Cold-acclimated SAM water content and ADC did not decrease in the winter cereals considered in this study. In contrast, the Hazlet intermediate zone and the Norstar and Hazlet VTZ ADC significantly decreased ($P < 0.05$; **Table 6.1**; **Figure 6.4**). Hazlet intermediate zone and VTZ ADC were significantly lower than Norstar. Together these observations support the theory that Hazlet SAM survives through a superior freezing avoidance mechanism. A desiccated region between the leaf sheath ice sink and SAM develops on exposure to cold-acclimating temperatures to a greater degree in Hazlet than Norstar.

Cold-acclimated winter oat 3 d after freezing accumulated suberin in the intermediate zone (Livingston et al., 2005b; Livingston et al., 2013). The suberized band of cells has been reported to act as a barrier to secondary pathogenic stress during recovery from freezing (Olien and Marchetti, 1976). Kuprian et al. (2014) observed an ice barrier in the pedicel of alpine shrubs inhibiting ice propagation from the vegetative stem into freezing-sensitive bud tissues. The pedicel ice barrier lacked pith and an intracellular space capable of containing ice (Kuprian et al., 2016). The cell walls contained higher lignin, suberin, cutin and smaller pit apertures. High concentrations of de-methylated pectin and callose have been reported in the cold-acclimated Norway spruce crown plate (Kuprian et al., 2017; Lee et al., 2017) which has high concentrations of pectin, di-, tri- and tetra-oligosaccharides relative to the rest of the bud (Kuprian et al., 2017). The intermediate zone in winter cereal crowns is comprised of small vacuolated cells (Gusta et al., 2009). *In vivo* VTZ freezing injury extended to a barrier region below the SAM in cold-acclimated winter wheat (Tanino and McKersie, 1985; Chapter 3). Additional research is required to determine the specific role and method of water and ice restriction associated with the intermediate zone in cold-acclimated cereal crowns.

6.5.3 INA and initial freezing in the leaf sheath

Low-intensity freezing initiated by the presence of an extrinsic nucleator induces equilibrium water transitions comparable to the INA observed in the field (Lindow et al., 1978a; Lindow et al., 1982). The addition of an ice nucleator increased cold-acclimated Norstar and Hazlet freezing survival by 5°C to 6°C (**Table 6.7**). When plant tissue supercools, the subsequent freezing intensity increases, resulting in detrimental changes in ice morphology, the pattern of injury and the LT_{50} (Olien, 1964; Olien and Livingston, 2006; Gusta et al., 2009). While DTA detected the addition of extrinsically added nucleators (**Table 6.7**; **Figure 6.6**; **Figure 6.7**), the initial site of freezing could not be determined. Cooling excised crown tissues using the test tube assay identified that the leaf sheath had a high INA relative to the VTZ and SAM (**Table 6.6**).

Freezing events in bud scales correspond with high-temperature exotherms (George et al., 1974; Ishikawa and Sakai, 1981; Endoh et al., 2014; Ishikawa et al., 2015). Similar test tube INA experiments have reported high tissue-specific INA corresponding with the establishment of ice sinks in rhododendron bud scales (Ishikawa et al., 2015) and blueberry stem bark (Kishimoto et al., 2014a; Kishimoto et al., 2014b). Low levels of INA in the SAM decreases the chance of ice nucleation in a freezing-sensitive tissue (as demonstrated in the electrolyte leakage tests) as well as freezing-sensitive florets (Endoh et al., 2014; Ishikawa et al., 2015). In my study, a high-temperature exotherm between -3°C to -5°C (**Table 6.7**) corresponded to a similar INA temperature in the intact leaf sheath (**Table 5.5**) and ice formation between the leaf sheaths (**Figure 6.5**). Differences in ice nucleation amongst crown tissues support the hypothesis of extra-organ freezing by initiating sites of freezing in non-reproductive tissues.

Decreased INA in autoclaved tissues can be explained by the release of tissue leachate containing anti-ice nucleators, such as sucrose (Gusta et al., 2004), tannins (Wang et al., 2012), flavanol glycosides (Kasuga et al., 2008; Kasuga et al., 2010) and arabinoxylans (Olien, 1965; Kindel et al., 1989). The loss of INA after tissue washing indicates the INA promoter is weakly associated with the tissue surface. Washing and heating to 35°C of fall field acclimated Norstar wheat and Puma rye aerial leaves and leaf sheaths resulted in a similar decrease in INA (Willick unpublished results). Ishikawa et al. (2015) reported bacteria cultured from excised scales. This could be a result of INA bacteria (INA^+) such as *Pseudomonas syringae* (Lindow et al., 1978a; Lindow et al., 1982) or organic intrinsic nucleators (Brush et al., 1994).

6.5.4 Freezing injury in the VTZ

In cold-acclimated crowns, there was a mid-temperature exotherm between -6 and -8°C (**Table 6.7**) and cooling to -10°C resulted in the formation of cavities in the VTZ (**Figure 6.5**). This could be a result of freezing-induced desiccation or intracellular freezing injury (Levitt, 1980). We previously reported injury in cold-acclimated Norstar crowns at -10°C in the VTZ and -21°C to the SAM when plants were cooled at 2°C h^{-1} (Chapter 3). Tanino and McKersie (1985) observed the VTZ was injured in half of all cold-acclimated Frederick winter wheat crowns between -10 and -12°C. Ice has the capacity to re-crystallize into larger masses at -10°C in plants (Knight et al., 1995; Griffith et al., 2005). The VTZ has a high concentration of water relative to the rest of the crown (Gusta et al., 1975; Gusta et al., 1979; Yoshida et al., 1997). A cold-induced decrease in VTZ free mobile water could act as a preventative measure to reduce freezing injury and protect root meristem cells (Chen et al., 1983).

Anti-freeze activity and apoplast protein content in winter rye leaves were correlated with durational freezing tolerance (Chun et al., 1998). Less than 10 μg of AFP from cold-acclimated perennial ryegrass (*Lollium perenne* L.) leaves was 300 times more effective at inhibiting ice re-crystallization than sucrose or other antifreeze substances (Sidebottom et al., 2000). In cold-acclimated crowns, ice formation can cause severe disruption of tissue structure as ice crystals in the VTZ (Olien, 1964; Olien and Marchetti, 1976; Tanino and McKersie, 1985; Livingston et al., 2005b). The VTZ accumulates a higher abundance of AFPs within cold-acclimated Norstar VTZ apoplast fluids as opposed to the SAM (Chapter 3). Most plant AFPs were initially identified as pathogenesis-related proteins (Hon et al., 1995; Griffith and Yaish, 2004). Cold-acclimation significantly increases AFP concentration in winter rye and confers anti-fungal resistance to early spring and overwintering snow molds (Hiilovaara-Teijo et al., 1999) that accumulate in cavities left by melted ice crystals (Olien and Marchetti, 1976; Livingston et al., 2005b).

Reduced water mobility decreases the rate of ice crystal growth and overall crystal size. One explanation for differences in VTZ and SAM water mobility could be explained by separate cold-acclimation strategies. In Chapter 3 using shotgun proteomic analysis, cold-acclimated Norstar accumulated higher concentrations of antifreeze and sugar hydrolyzing enzymes in the VTZ and anti-desiccation proteins in the SAM. As cell water migrates from the SAM either to the VTZ or the leaf sheath, it results in a significant increase in SAM cell sap concentration. The increase in cell sap concentration depressed the freezing point and enhanced the survival of the

SAM. Livingston et al. (2006) reported a 10 % higher accumulation of fructans within the SAM and surrounding tissues than in the VTZ and basal crown tissues after cold-acclimation of winter oat (*Avena sativa* L.) and rye. Following exposure to non-lethal freezing temperatures, both winter oat and rye SAM tissues preferentially accumulated sucrose at the expense of fructans (Livingston et al., 2006). Taken together, these results indicate the SAM and VTZ have separate acclimation strategies to cope with freezing.

6.5.5 Freezing avoidance in the SAM

In the present study, it is hypothesized that freezing avoidance is in part due to the supercooling of cold-acclimated Norstar and Hazlet SAM. Chapter 3 provided supporting evidence using the TTC viability stain of cold-acclimated Norstar SAM freezing injury corresponded with the LT_{50}. In the present study, the low-temperature exotherm occurred around the LT_{50} (**Table 6.7**; **Figure 6.1**). Similar relationships between freezing injury to the SAM and the LT_{50} were observed using the TTC staining method in cold-acclimated Puma rye (Chapter 4; Chapter 5). In overwintering tree buds, the low-temperature exotherm corresponds with the freezing of individual florets (Ishikawa and Sakai, 1981; Endoh et al., 2014; Ishikawa et al., 2015). In winter buds collected from various tree species, Ishikawa and Sakai observed primordia remain supercooled and survive temperatures as low as -60°C if frozen in the tree bud (Sakai, 1979; Ishikawa and Sakai, 1981; Ishikawa and Sakai, 1982).

In vitro freezing led to the VTZ having a higher EL_{50} than the SAM (**Table 6.5**), which was the opposite to observations from *in vivo* whole-crown freezing studies (Olien, 1964; Tanino and McKersie, 1985; Livingston et al., 2005b; Livingston et al., 2013; Chapter 3). Water withdrawal is an important component of *in vivo* SAM freezing. Dorsey (1934) hypothesized overwintering bud scales accommodate water from the primordia to promote supercooling. In the *in vitro* freeze test, the SAM was not able to re-distribute water to the leaf sheath or accumulate dry matter from other crown tissues and was forced to tolerate freezing. This lends credence to the SAM avoiding freezing within the crown. A similar decrease in freezing survival was noted after the *in vitro* freezing of larch (*Larix kaempferi*) primordia (Endoh et al., 2014) rhododendron (Ishikawa and Sakai, 1981; Ishikawa et al., 2015) and *Cornus floridia* (Ishikawa et al., 2016) florets.

A decrease in cold-acclimated SAM water content after cooling to -4°C and -10°C and cold-acclimated Hazlet SAM cooled to -4°C or -10°C had a significantly lower water content than Norstar (**Table 6.8**). Graham and Mullin (1976) demonstrated azalea primordia freezing resistance was correlated with decreased water content. Livingston and colleagues reported the older leaves surrounding the winter wheat crown after cold-acclimation had a significantly higher percentage of tissue water than younger leaves encapsulating the SAM (Livingston et al., 2017).

The decrease in total crown water content on exposure to cold-acclimating (**Table 6.2**) and sub-zero temperatures (**Table 6.8**) resulted from the accumulation of dry matter (Gusta et al., 1975; Gusta et al., 1979; Brule-Babel and Fowler, 1989; Yoshida et al., 1997; Gusta et al., 2004). Olien and colleagues hypothesized this increase in dry weight as associated with increased sucrose, fructan and oligosaccharide accumulation (Olien, 1965; Olien and Lester, 1985; Livingston et al., 2005b). This supports my findings of significantly increased osmotic potential from cold-acclimated Hazlet and Norstar SAM cell sap and dry matter in the SAM cooled to -4°C and -10°C. Livingston and colleagues reported a significant increase in crown winter oat and rye sucrose concentrations after sub-zero acclimation and significantly higher sucrose concentrations in the SAM as opposed to the VTZ (Livingston et al., 2005a; Livingston et al., 2006).

In artificial pore systems, reduced pore size mimicking reduced extracellular space in combination with increased sucrose, glucose or glycine concentrations significantly depressed the supercooling temperature (Ashworth and Abeles, 1984). Increased concentrations of carbohydrates and/or osmolytes decreased the amount of free water available to freeze. Gusta et al. (2009) hypothesized the decreased SAM cell size and extracellular space could increase the SAM freezing survival.

6.5.6 Conclusions

Cold-acclimated winter wheat and rye crowns survive sub-zero temperature stress by extra-organ freezing. During cold-acclimation, free water decreases in the VTZ, which results in an overall reduction in crown water content. The SAM decreases in water content after cooling to -4°C or -10°C. Water content and INA within the leaf sheath remains high relative to the rest of the cold-acclimated crown. The leaf sheath accommodates ice, facilitating the decrease in SAM and VTZ water. The intermediate zone acts as a barrier, be it desiccative, physical or chemical, to ice propagation from the ice sink and VTZ into the SAM. Hazlet rye SAM had a higher freezing

survival than Norstar due to increased SAM freezing avoidance, initiated by low intermediate zone and VTZ water mobility. Additional research is required to determine whether the intermediate zone in the more cold hardy winter rye undergoes greater physiological or biochemical modifications to reduce wall porosity and increase rigidity than winter wheat during cold- and sub-zero acclimation.

Supplementary information

Table S6.1 Regression coefficients (peak four parameter Weibull equation) for LT_{50} and crown dry weight of Norstar winter wheat and Hazlet fall rye acclimated at 4°C for 0 ± 91 d.

Parameter	Cultivar	a*	b	C	x_oǂ	R^2
LT_{50}	Norstar	-19.46	69.58	2.08	42.52	0.961
	Hazlet	-25.69	64.26	2.00	39.55	0.954
Dry weight	Norstar	333.79	120.71	2.13	66.00	0.987
	Hazlet	401.78	166.17	1.57	76.95	0.984

* Estimate of lowest LT_{50} or highest crown dry weight

ǂ Estimate of days to reach lowest LT_{50} or highest crown dry weight

Table S6.2 Regression coefficients (peak five parameter Weibull equation) for the crown water content of Norstar winter wheat and Hazlet fall rye acclimated at 4°C for 0 ± 91 d.

Cultivar	a*	b	C	x_oǂ	y_o‡	R^2	a + y_oΨ
Norstar	-4.15	61.78	1.86	42.86	5.94	0.990	1.78
Hazlet	-2.96	61.17	1.88	42.60	5.40	0.967	2.44

* Estimate of the difference between the lowest and highest crown water content

ǂ Estimate of days to reach the lowest crown water content

‡ Estimate of highest crown water content

Ψ Estimate of lowest crown water content

Table S6.3 Regression coefficients (peak five parameter Weibull equation) for crown water content and dry weight of cold-acclimated Norstar winter wheat and Hazlet fall rye cooled at 2°C h^{-1} from 0°C to -32°C.

Cultivar	a*	b	C	x_oǂ	y_o‡	R^2	a + y_oΨ
Norstar	-14.61	128200.05	1340.67	-27.67	16.44	0.967	1.83
Hazlet	-17.99	1860590.51	18546.44	-31.33	19.85	0.944	1.86

* Estimate of the difference between the lowest and highest crown water content

ǂ Estimate of days to reach the lowest crown water content

‡ Estimate of highest crown water content

Ψ Estimate of lowest crown water content

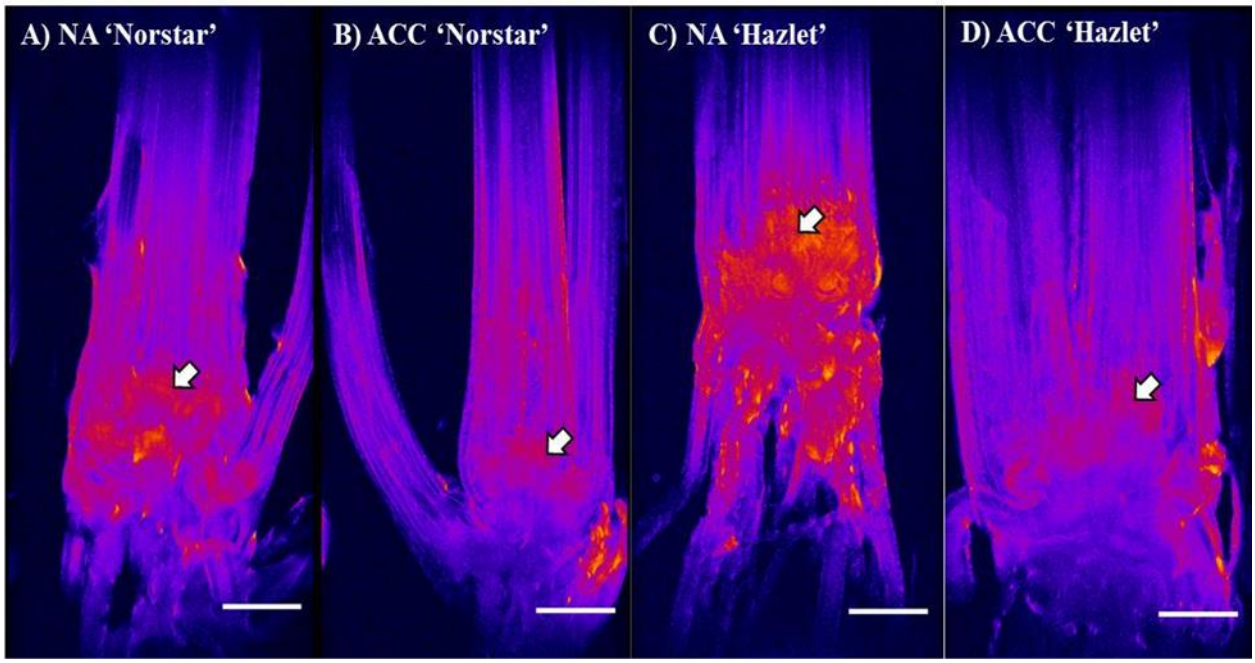

Figure S6.1 Longitudinal MRMI of non- (NA) and cold- (ACC) acclimated Norstar and Hazlet crowns.

White arrows indicate a water mobile region. Images are representative of 4 biological replicates (N = 4). Scale bar = 0.5 cm.

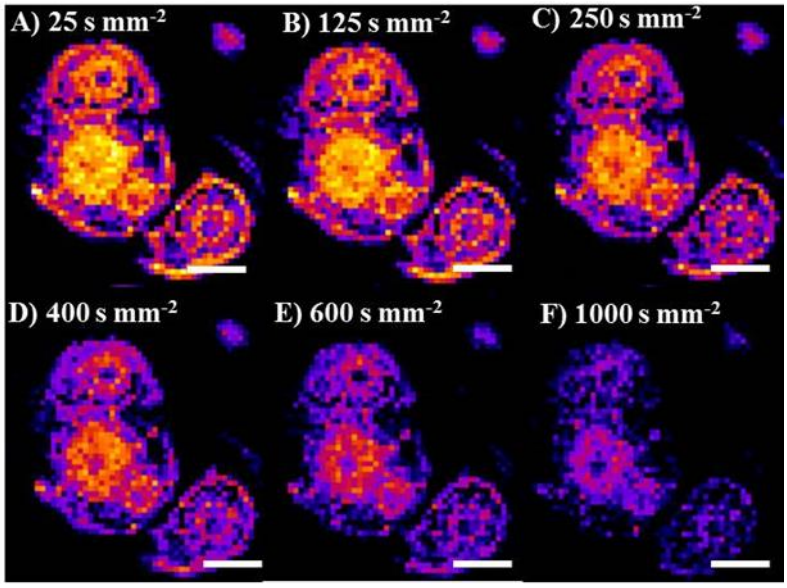

Figure S6.2 Diffusion-weighted images of non-acclimated Norstar used for ADC analysis.

Image series illustrates the differential tissue contrast provided by diffusion weighting. Areas containing highly mobile water lose signal as the weighting factor is increased. Diffusion restricted water is less affected by the increased weighting. Images are representative of 4 biological replicates (N = 4). Scale bar = 0.5 cm

Chapter 7

7 General discussion

Cold hardiness of winter cereals is controlled by the up or down regulation of genes in response to environmental cues. Responses to these cues (acclimation) are converted into transposable signals such as the accumulation of AFPs, low molecular weight sugars, and growth regulators such as ABA. On a cellular and tissue level, cold-acclimation induces physiological and biochemical modifications to the plasma membrane and cell wall. The possibility of physiologically regulating the plant cold hardiness is an intriguing concept, as minor modifications to the plant phenotype could make a considerable difference in plant performance. In winter wheat, mitigating crown injury during mid-winter thaws or extending durational freezing survival in late winter to levels comparable to winter rye would provide Western Canadian farmers additional options to diversify their crop rotations.

A clear understanding of crown freezing tolerance and avoidance mechanisms was needed to help identify physiological or biochemical markers of cold hardiness. Previous research established how individual crown tissues recover from freezing (Pauli, 1960; Beard and Olien, 1963; Olien, 1964; Olien and Marchetti, 1976; Chen et al., 1983; Tanino and McKersie, 1985; Livingston et al., 2005b; Livingston et al., 2013; Livingston and Tuong, 2014). There is less available information on how individual crown tissues cold-acclimate (Livingston et al., 2005a). The purpose of this thesis was to observe how individual crown tissues contribute to cold hardiness and draw parallels between differences in winter wheat and winter rye freezing survival.

7.1 Cold-induced modifications to the cell wall and the apoplast proteome

The findings from this research have provided a deeper understanding of the effects of cold-acclimation on the tissue-specific development of crowns, which advances the current knowledge of winter wheat cold hardiness (**Table 7.1**). Similar trends were noted in the SAM and VTZ apoplast proteomes (Chapter 3). The SAM of Norstar accumulated higher concentrations of dehydrins, vernalization responsive proteins, cold-shock and anti-desiccative proteins compared to the VTZ. Accumulation of anti-desiccation proteins in the SAM minimize injury from extracellular freeze dehydration on a cellular level or dehydration associated with the SAM avoiding freezing.

The VTZ accumulated higher abundances of CWMPs, oxidative response proteins, AFPs, pathogenesis-related proteins and sugar hydrolyzing proteins compared to the SAM. After 42 d of cold-acclimation, VTZ cell wall FTIR signal intensities associated with methyl-esterification (carbonyl ester, 1740 cm^{-1}) and carbohydrates (glycosidic bond, 1050 cm^{-1}) significantly increased compared to the SAM. In *Poaceae,* peroxidase and Germin B proteins mediate diferulic crosslinking of glucuronoarabinoxylans. Cross-linking of glucuronoarabinoxylans increases cell wall and tissue rigidity. In Chapter 5 cold-acclimated crowns were observed to have increased resistance to mechanical shearing. Cold-induced increases in cell wall thickness and rigidity corresponds with improved cold hardiness by preventing ice propagation into cells, protection against cellular collapse, cytorrhysis or cellular deformation (Siminovitch and Scarth, 1938; Scarth, 1941; Fujikawa et al., 1999; Yamada et al., 2002; Solecka et al., 2008).

Greater accumulation of VTZ AFPs (Chapter 3) mitigate rates of ice propagation and re-crystallization. The cold-acclimated VTZ has a high water content relative to other crown tissues (Chapter 6). In cold-acclimated crowns, high concentrations of AFPs reduce the formation of large ice crystals that disrupt the VTZ (Livingston et al., 2005b; Livingston and Tuong, 2014) and the probability of non-equilibrium freezing (Olien, 1964). The VTZ is further stressed by the pathogenic attack in cavities left by melted ice crystals (Olien and Marchetti, 1976). Most plant AFPs have anti-fungal properties (Griffith and Yaish, 2004) accounts for cold-acclimated winter cereal systemic but non-specific defense against pathogenic stress (Hiilovaara-Teijo et al., 1999; Griffith and Yaish, 2004).

Table 7.1 Summary of the physiological, biochemical and biophysical responses in the winter wheat crown to cold.

Treatment	Non-acclimation (20°C) ➡	Cold-acclimation (4°C) ➡	Frost hardening (< -4°C)
Physiological	Vegetative growth	Growth slows >> stops	No growth
Biochemical	No major trends in protein accumulation between the **SAM** and **VTZ**	**SAM**: ↑ dehydrins, vernalization proteins; ↑ total sugars **VTZ**: ↑ CWMPs, AFPs, PRs, sugar hydrolases; ↑ glucuronoarabinoxylans, lignin, methyl-esterification, total sugars	↑ **SAM** total sugars compared to **VTZ**
Biophysical	**Crown**: high water content	**Crown**: ↓ water content, ↑ shearing strength **SAM**: development of a dehydrated barrier (intermediate zone) **VTZ**: ↓ water content and mobility	**SAM**: ↓ water content if slowly cooled and the leaf sheath is intact **Leaf Sheath**: 1° ice sink **VTZ**: ↓ water content, 2° ice sink
Freezing response	**Crown**: non-equilibrium freezing Supercools to avoid freezing	**SAM**: avoids freezing due to the presence of a barrier ($2°C\ h^{-1}$). **VTZ**: non-equilibrium freezing	**Crown:** ↑ dehydration tolerance **SAM**: avoids freezing due to the presence of a barrier **VTZ**: reduction in water prior to freezing can induce an equilibrium freezing response – crown can survive VTZ injury
	Death at the high temperature exotherm	***Death at the low temperature exotherm***	***Death at the low temperature exotherm***

7.2 Cooling rates reveal separate freezing responses in the SAM and VTZ

In slowly cooled (2°C h^{-1}) plants tested for lethal temperatures (LT_{50}) and lethal duration (LD_{50}), the VTZ was injured prior to the SAM. Frost hardened crowns had a lower freezing injury to the nodal plate and VTZ compared to cold-acclimated crowns. Slow cooling rates (< 5°C) facilitate the re-distribution of water amongst plant tissues (Chapters 4 and 6) and increase the probability of equilibrium freezing (Olien, 1967). Faster cooling rates (5°C h^{-1} and 10°C h^{-1}) were used as a tool to observe structure-function mechanisms of freezing survival in the SAM and VTZ. Faster cooling rates induced non-equilibrium freezing in the SAM at ≥ 5°C h^{-1} in Norstar and 10°C h^{-1} in Puma. The SAM in cold-acclimated Puma had a greater resistance to fast cooling rates (5°C h^{-1} or 10°C h^{-1}) compared to Norstar. Cooling plants at greater than 5°C h^{-1} mitigates the re-distribution of water amongst plant tissue and facilitate non-equilibrium freezing (Olien, 1964). Hydrated lettuce (*Lactuca sativa* L.) seeds exposed to cooling rates below 1.3°C h^{-1} resulted in an undetectable low temperature exotherm and an LT_{50} below -50°C (Ishikawa and Sakai, 1982). Cooling rates greater than 5°C h^{-1} resulted in a warmer low temperature exotherm and LT_{50} around -15°C. Similar results were obtained with hydrated canola seeds (*Brassica napus* L. cv Quest) (Gusta et al., 2006) and *Cornus officinalis* overwintering buds (Ishikawa and Sakai, 1985). Fast cooling of cold-acclimated Norstar and Puma crowns, overwintering tree buds, partially hydrated lettuce and canola seeds disrupts the establishment of an ice sink that can accommodate large ice crystals.

7.3 Localization of initial ice nucleation to the leaf sheath and development of ice sinks

Infrared video thermography was used to observe intrinsic ice nucleation at the base of cold-acclimated crowns (Chapter 4). The location and source of this nucleator could not be determined with MRMI or IRVT. This thesis work is the first to hypothesize that the leaf sheath acts as an ice sink for the crown and is required for crowns to attain maximum cold hardiness. Winter wheat and rye cold hardiness were dependent on the initial nucleation and accumulation of ice in the crown leaf sheath (Chapter 5). Ice was visually observed to accumulate between the leaf sheathes and confirmed to initiate from the leaf sheath with a heterogeneous ice nucleation test. Ishikawa and Sakai (1982) reported the extra-organ ice accumulation between the integument and the endosperm in lettuce and between the endosperm and testa of Oriental bittersweet (*Celastrus*

orbicalatus Thunb) seeds. The leaf sheath ice nucleators had a similar ice nucleation temperature, heat sensitivity and physical association with tissue as was previously reported in INA^+ bacteria (Lindow et al., 1982; Lindow, 1983; Hill et al., 2014). Removal of the leaf sheath decreased cold hardiness of Norstar and Puma crowns and resulted in injury to the SAM of Norstar before the VTZ. In partially hydrated seeds the endosperm envelope acts as a barrier to ice propagation. Disruption of the seed coat by radicle emergence or by mechanical disruption with a needle resulted in the loss of the low temperature exotherm (Junttila and Stushnoff, 1977; Ishikawa and Sakai, 1982).

In cold-acclimated crowns, the low temperature exotherm coincided with the LT_{50} and injury to the SAM. In partially hydrated lettuce, the low temperature exotherm corresponded with an inability to germinate (Junttila and Stushnoff, 1977). In winterfat (*Eurotia lanata* (Pursh) Moq.) seeds the low temperature exotherm corresponded to freezing injury which manifested in decreased seedling vigour and germination rates (Bai et al., 1998). Excised lettuce embryos imbibed for 2 or 12 h produced only one exotherm which coincided with the killing temperature (Junttila and Stushnoff, 1977). A similar pattern was noted in cold-acclimated crowns after the removal of the leaf sheath. In both cold-acclimated crowns and hydrated seeds, the space between the crown and leaf sheath or seed coat and endosperm acted as an ice sink. The disruption of the ice sink resulted in a break in SAM or embryo supercooling.

7.4 Mechanism of ice segregation: extra-organ and extra-tissue freezing

The terms freezing tolerance and avoidance are not sufficient to describe the mixed freezing events in complex plant organs, such as overwintering tree buds, dormant seeds and cold-acclimated cereal crowns. Sakai (1979) and Derreudre (1978) suggested the term extra-organ freezing as its own separate classification to describe the segregation of ice from a supercooled tissue in an ice sink under slow freezing rates. Ishikawa and Sakai (1982) further divided extra-organ freezing into three sub-classes. In Type I extra-organ freezing, the supercooling tissue is fully dehydrated and has a high tolerance to desiccation. The low temperature exotherm is difficult to detect due to the lack of freezable water. Dormant lettuce seeds (Junttila and Stushnoff, 1977), *Larix* and *Picea* buds (Sakai, 1979; Ishikawa and Sakai, 1982; Sakai, 1982; Endoh et al., 2014) are classified as Type I. In Type II extra-organ freezing, the supercooled tissue is injured by extreme desiccation, as was the case in peach buds (Quamme et al., 1982; Ashworth, 1984). Type

III extra-organ freezing is differentiated from Types I and II in that the supercooling tissue undergoes partial dehydration and is injured by a break in supercooling, as in the case in *Cornus officinalis*, azalea and rhododendron flower buds (George et al., 1974; Graham and Mullin, 1976; Ishikawa and Sakai, 1981; Ishikawa and Sakai, 1985; Ishikawa et al., 2015; Ishikawa et al., 2016).

The novel type of freezing behaviour found in Norstar winter wheat and Hazlet rye crowns meets the general requirements of extra-organ and extra-tissue freezing (**Figure 7.1**). During frost hardening ice accumulates in the leaf sheath (extra-organ). Water content in the VTZ and the SAM decreases relative to the leaf sheath ice sink. The decreased water content in the VTZ facilitates equilibrium freezing. The SAM avoids freezing by accumulating higher total sugars compared to the VTZ and was protected by a dehydrated intermediate zone (extra-tissue). The intermediate zone inhibits ice propagation from the VTZ into the SAM. Extra-tissue freezing is commonly associated with the formation of large ice crystals in xylem tissue. Similar extra-tissue freezing mechanisms were observed in the vascular bundle in frozen roots of table beets (*Beta vulgaris* subsp. *Vulgaris*) (Terumoto, 1960), in the lacuna (tissue in contact with vascular tissue) of *Buxus smpervirens* Pojark. leaves (Hacker and Neuner, 2008) and in bark of blueberry stems (Kishimoto et al., 2014a,b). Similar to the VTZ in the crown, non-equilibrium freezing in the vascular tissue of the beet root or *Buxus* leaf results in lethal injury to the organ. Whether this is a general response in organs that employ an extra-tissue freezing response is currently an active area of research

The presence of an observed low temperature exotherm, partial dehydration and the reduced freezing survival when the SAM is frozen *in vitro* would preclude cold-acclimated Norstar wheat and Hazlet rye crowns from surviving exclusively through desiccation tolerance. Cold-acclimated SAM lack the freezing survival traits exhibited by Type I primordia and Type II florets and can be killed at a warmer sub-zero temperature by a break in supercooling (*in vitro* freezing). Freezing survival of excised cold-acclimated Norstar and Hazlet SAM was comparable with lethal temperatures observed in excised primordial shoots from *Abies homolepis* (L.) and *Abies balsamea* (L.) (Sakai, 1979). Variation exists between winter wheat and rye SAM freezing responses. Hazlet rye SAM had a significantly higher freezing survival and a higher freezing avoidance compared to Norstar wheat. In Chapter 3, cold-acclimation at 4°C induced the preferential accumulation of dehydrins and anti-desiccation proteins within the SAM as opposed to the VTZ. This indicates the potential for phenotypic differences in desiccation tolerance among winter cereals. However, the primary survival mechanism for cold-acclimated SAM appears to be freezing avoidance. This

research highlights the importance of continued analysis of tissue specific mechanisms of crown survival amongst a wide range of cereals with varying levels of cold hardiness.

A second possibility regarding the similarity in freezing survival among cold-acclimated cereal crowns and Type III tree buds is the composition of the tissue beneath the SAM or primordia. While no definitive study has been conducted to compare the composition of this barrier region, recent publications by Lee et al. (2017) and Kuprian et al. (2017) on Norway spruce proposed higher crown plate pectin and oligosaccharide concentrations increase primordia freezing avoidance. Grasses and cereals leaves have low pectin concentrations in their cell walls compared to other angiosperms (Hatfield et al., 2016). In cold-acclimated oat (*Avena sativa* L.), high concentrations of oligosaccharides and fructans have been reported in bulk analysis of the crown core tissues below the SAM (Livingston et al., 2005a). While the present study does not analyze the chemical composition of the intermediate zone, lower ADC was observed in cold-acclimated Hazlet compared to Norstar. A larger study is required to compare differences in intermediate zone composition among North American winter cereals and determine if increases in oligosaccharides are correlated with increased freezing survival.

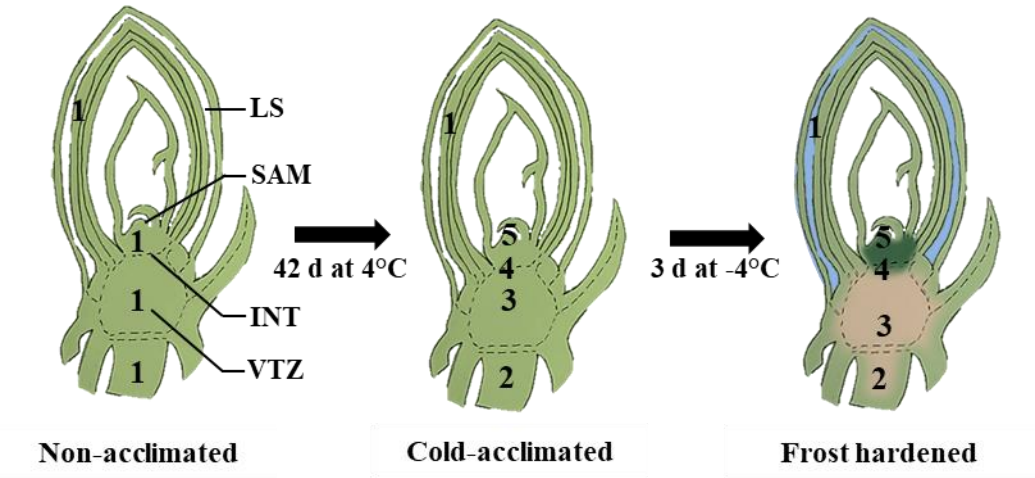

Figure 7.1 The order of tissue freezing of non-acclimated, cold-acclimated, and frost hardened crowns.

Numbers indicate the order of ice nucleation amongst tissues. In non-acclimated crowns, high water content and an absence of tissue level barriers indicate a non-equilibrium freezing throughout the crown. Cold-acclimation establishes the leaf sheath (LS) as the initial site of ice nucleation. The leaf sheath acts as an ice sink for the crown. Nucleation then occurs in the roots and the vascular transition zone (VTZ). Freezing injury to the shoot apical meristem (SAM) corresponds with an inability for the whole plant to recover. After the initial freeze event, water content in the VTZ and SAM decreases relative to the LS. This facilitates equilibrium freezing in the VTZ. In frost hardened crowns, the SAM avoids freezing by accumulating higher total sugars (dark green) compared to the VTZ and is protected by a dehydrated intermediate zone (INT). During frost hardening, the VTZ desiccates (light brown) relative to the rest of the crown. The INT inhibits ice propagation from the VTZ into the SAM. Broken lines indicate vascular tissues.

7.5 Future perspectives

Although this thesis provides new insights into the freezing behaviours of cold-acclimated winter wheat and rye crowns, several questions still need to be addressed.

I) Do the SAM of other winter cereals avoid freezing and is SAM freezing injury correlated with crown survival? Does the difference in SAM survival explain the differences in cold hardiness between winter wheat, winter oat and winter barley? To test this theory, multiple winter wheat and rye cultivars with a large range in cold hardiness could be screened to determine if there was a correlation between the LT_{50} and the low temperature exotherm and SAM injury (absence of TTC stain).

II) What is the chemical composition of the intermediate zone? The intermediate zone should be isolated to determine if a higher concentration of methyl esterified cross-linked glucuronoarabinoxylan reduces ice propagation into the SAM?

III) Cell walls from the SAM and VTZ should be isolated and analyzed with GC/MS and linkage analysis to determine how hemicellulose, hydroxycinnamic acids and lignin concentrations increase or decrease in response to cold-acclimation.

IV) Ice nucleators isolated from the leaf sheath (washing fluids and cell wall extracts) should be tested to confirm whether nucleation was induced by bacteria or if it was associated with a currently unknown plant intrinsic nucleator. The identification of novel, non-toxic, ice nucleators would be of interest to the food and transportation industry. The application of non-toxic ice nucleators to foods during cold storage at warmer sub-zero temperatures would reduce the propagation of large ice crystals to improve the flavour and textural properties of frozen foods.

V) Do similar trends observed among apoplast proteins collected from chamber acclimated crowns correlate to the proteomes of field grown crowns? A proteomic study is needed to determine if similar trends were observed in the SAM and VTZ of Norstar and Puma grown in fall conditions in Saskatchewan.

7.6 Overall assessment

Exposure to 4°C induces a tissue-specific cold-acclimation response. Cold-acclimated crowns survive freezing using an ice segregation survival mechanism. The leaf sheath acts as an ice sink relative to the crown. The SAM avoids freezing by I) accumulating high concentrations of total sugars II) dehydrins, and anti-desiccation proteins. III) Ice propagation is inhibited into the SAM by a dehydrated intermediate zone between the SAM and VTZ. The VTZ cold-acclimates by accumulating pathogenesis-related AFPs and CWMPs. Methyl-esterification of the VTZ cell wall increases rigidity. Frost hardening desiccates the VTZ. A combination of increased tissue rigidity, reduced water mobility and content allows the VTZ to undergo non-lethal equilibrium freezing and act as an ice sink for the SAM. The crown can recover if injury is limited to the VTZ of the main shoot. The major difference in cold hardiness between winter wheat and rye was associated with increased SAM freezing survival. These results provide a better understanding of crown freezing behaviours and avenues for future research on physiological and biochemical markers targeted to tissue specific freezing survival.

References

Albersheim P, Darvill A, Roberts K, Sederoff R, Staehelin A (2011) Plant cell walls. New York, New York: Garland Science, Taylor and Francis Group. 1-430.

Aloni R, Griffith M (1991) Functional xylem anatomy in root-shoot junctions of six cereal species. Planta 184: 123-129

Andrews C, Pomeroy M (1975) Survival and cold hardiness of winter wheats during partial and total ice immersion. Crop Sci 15: 561-566

Andrews C, Pomeroy M (1981) The effect of flooding pretreatment on cold hardiness and survival of winter cereals in ice encasement. Can J Plant Sci 61: 507-513

Andrews CJ, Pomeroy MK (1979) Toxicity of anaerobic metabolites accumulating in winter wheat seedlings during ice encasement. Plant Physiol 64: 120-125

Antikainen M, Griffith M (1997) Antifreeze protein accumulation in freezing-tolerant cereals. Physiol Plant 99: 423-432

Antikainen M, Griffith M, Zhang J, Hon W-C, Yang DS, Pihakaski-Maunsbach K (1996) Immunolocalization of antifreeze proteins in winter rye leaves, crowns, and roots by tissue printing. Plant Physiol 110: 845-857

Aoki K, Asahina E, Terumoto I (1953) Analysis of the freezing process of living organisms. IX. The relation between the shape of the freezing curve and the frost hardiness. Low Temp Sei 10: 69-80

Aryal B, Neuner G (2010) Leaf wettability decreases along an extreme altitudinal gradient. Oecol 162: 1-9

Asahina E (1956) The freezing process of plant cell. Contributions from the Institute of Low Temperature Science 10: 83-126

Ashworth E, Davis G (1984) Ice nucleation within peach trees. J Am Soc Hortic Sci 109: 198-201

Ashworth E, Davis G, Wisniewski M (1989) The formation and distribution of ice within dormant and deacclimated peach flower buds. Plant, Cell Environ 12: 521-528

Ashworth EN (1984) Xylem development in Prunus flower buds and the relationship to deep supercooling. Plant Physiol 74: 862-865

Ashworth EN, Abeles FB (1984) Freezing behavior of water in small pores and the possible role in the freezing of plant tissues. Plant Physiol 76: 201-204

Ashworth EN, Davis GA, Anderson JA (1985) Factors affecting ice nucleation in plant tissues. Plant Physiol 79: 1033-1037

Avery Jr GS (1930) Comparative anatomy and morphology of embryos and seedlings of maize, oats, and wheat. Bot Gaz 89: 1-39

Bai Y, Booth DT, Romo JT (1998) Winterfat (*Eurotia lanata*(Pursh) Moq.) Seedbed ecology: low temperature exotherms and cold hardiness in hydrated seeds as influenced by imbibition temperature. Ann Bot 81: 595-602

Baldwin L, Domon J-M, Klimek JF, Fournet F, Sellier H, Gillet F, Pelloux J, Lejeune-Hénaut I, Carpita NC, Rayon C (2014) Structural alteration of cell wall pectins accompanies pea development in response to cold. Phytochemistry 104: 37-47

Ball MC, Wolfe J, Canny M, Hofmann M, Nicotra AB, Hughes D (2002) Space and time dependence of temperature and freezing in evergreen leaves. Funct Plant Biol 29: 1259-1272

Bauerfeind MA, Winkelmann T, Franken P, Druege U (2015) Transcriptome, carbohydrate, and phytohormone analysis of *Petunia hybrida* reveals a complex disturbance of plant functional integrity under mild chilling stress. Front Plant Sci 6: 583

Bäurle I, Dean C (2006) The timing of developmental transitions in plants. Cell 125: 655-664

Beard JB, Olien CR (1963) Low temperature injury in the lower portion of *Poa annua* L. crowns. Crop Sci 3: 362-363

Bonner J, Devirian PS (1939) Growth factor requirements of four species of isolated roots. Am J Bot 26: 661-665

Bouché F, Woods DP, Amasino RM (2017) Winter memory throughout the plant kingdom: different paths to flowering. Plant Physiol 173: 27-35

Boudart G, Jamet E, Rossignol M, Lafitte C, Borderies G, Jauneau A, Esquerré-Tugayé MT, Pont-Lezica R (2005) Cell wall proteins in apoplastic fluids of *Arabidopsis thaliana* rosettes: identification by mass spectrometry and bioinformatics. Proteomics 5: 212-221

Boyd L, Avery Jr GS (1936) Grass seedling anatomy: the first internode of *Avena* and *Triticum*. Bot Gaz 97: 765-779

Boyer JS (2001) Growth-induced water potentials originate from wall yielding during growth. J Exp Bot 52: 1483-1488

Boyer JS, Silk WK (2004) Hydraulics of plant growth. Funct Plant Biol 31: 761-773

Bredow M, Tomalty HE, Smith L, Walker VK (2017) Ice and anti-nucleating activities of an ice-binding protein from the annual grass, *Brachypodium distachyon*. Plant Cell Environ doi: 10.1111/pce.12889

Bret-Harte MS, Baskin TI, Green PB (1991) Auxin stimulates both deposition and breakdown of material in the pea outer epidermal cell wall, as measured interferometrically. Planta 185: 462-471

Brown WV, Heimsch C, Emery W (1957) The organization of the grass shoot apex and systematics. Am J Bot 44: 590-595

Brule-Babel A, Fowler D (1989) Use of controlled environments for winter cereal cold hardiness evaluation: controlled freeze tests and tissue water content as prediction tests. Can J Plant Sci 69: 355-366

Brush RA, Griffith M, Mlynarz A (1994) Characterization and quantification of intrinsic ice nucleators in winter rye (*Secale cereale*) leaves. Plant Physiol 104: 725-735

Burke M, Gusta L, Quamme H, Weiser C, Li P (1976) Freezing and injury in plants. Annu Rev Plant Physiol 27: 507-528

Bushuk W (2001) Rye production and uses worldwide. Cereal Food World 46: 70-73

Carpita NC (1983) Hemicellulosic polymers of cell walls of *Zea* coleoptiles. Plant Physiol 72: 515-521

Carpita NC (1984) Cell wall development in maize coleoptiles. Plant Physiol 76: 205-212

Carpita NC, Defernez M, Findlay K, Wells B, Shoue DA, Catchpole G, Wilson RH, McCann MC (2001) Cell wall architecture of the elongating maize coleoptile. Plant Physiol 127: 551-565

Carpita NC, Gibeaut DM (1993) Structural models of primary cell walls in flowering plants: consistency of molecular structure with the physical properties of the walls during growth. Plant J 3: 1-30

Carvajal F, Palma F, Jamilena M, Garrido D (2015) Cell wall metabolism and chilling injury during postharvest cold storage in zucchini fruit. Postharvest Biol Technol 108: 68-77

Charrier G, Charra-Vaskou K, Kasuga J, Cochard H, Mayr S, Améglio T (2014) Freeze-thaw stress: effects of temperature on hydraulic conductivity and ultrasonic activity in ten woody angiosperms. Plant Physiol 164: 992-998

Chateigner-Boutin A-L, Bouchet B, Alvarado C, Bakan B, Guillon F (2014) The wheat grain contains pectic domains exhibiting specific spatial and development-associated distribution. PLOS ONE 9: e89620

Chen K, Renaut J, Sergeant K, Wei H, Arora R (2013) Proteomic changes associated with freeze-thaw injury and post-thaw recovery in onion (*Allium cepa* L.) scales. Plant Cell Environ 36: 892-905

Chen TH-H, Gusta LV, Fowler DB (1983) Freezing injury and root development in winter cereals. Plant Physiol 73: 773-777

Chun J, Yu X, Griffith M (1998) Genetic studies of antifreeze proteins and their correlation with winter survival in wheat. Euphytica 102: 219-226

Cosgrove DJ (2000) Loosening of plant cell walls by expansins. Nature 407: 321-326

Crevillen P, Dean C (2011) Regulation of the floral repressor gene FLC: the complexity of transcription in a chromatin context. Curr Opin Plant Biol 14: 38-44

Crowe LM, Mouradian R, Crowe JH, Jackson SA, Womersley C (1984) Effects of carbohydrates on membrane stability at low water activities. Biochim Biophys Acta Biomembr 769: 141-150

Danyluk J, Carpentier E, Sarhan F (1996) Identification and characterization of a low temperature regulated gene encoding an actin-binding protein from wheat. FEBS Lett 389: 324-327

Danyluk J, Perron A, Houde M, Limin A, Fowler B, Benhamou N, Sarhan F (1998) Accumulation of an acidic dehydrin in the vicinity of the plasma membrane during cold acclimation of wheat. Plant Cell 10: 623-638

de Faÿ E, Vacher V, Humbert F (2000) Water-related phenomena in winter buds and twigs of *Picea abies* L. (Karst.) until bud-burst: a biological, histological and NMR study. Ann Bot 86: 1097-1107

Dereuddre J (1978) Effets de divers types de refroidissements sur la teneur en eau et sur la resistance au gel des bourgeons de rameaux d'Epicea en vie ralentie. Physiol Veg 16: 469-489 (English translation)

Davies PL (2014) Ice-binding proteins: a remarkable diversity of structures for stopping and starting ice growth. Trends Biochem Sci 39: 548-555

DeVries AL (1971) Glycoproteins as biological antifreeze agents in antarctic fishes. Science 172:1152–1155

DeVries AL, Wohlschlag DE (1969) Freezing resistance in some Antarctic fishes. Science 163: 1073-1075

Domon J-M, Baldwin L, Acket S, Caudeville E, Arnoult S, Zub H, Gillet F, Lejeune-Hénaut I, Brancourt-Hulmel M, Pelloux J (2013) Cell wall compositional modifications of *Miscanthus* ecotypes in response to cold acclimation. Phytochemistry 85: 51-61

Dorsey M (1934) Ice formation in the fruit bud of the peach. Proc Am Soc Hort Sci 31: 22-27

Dorsey MJ, Strausbaugh PD (1923) Plum investigations. I. winter injury to plum during dormancy. Bot Gaz 76: 113-143

Doxey AC, Yaish MW, Griffith M, McConkey BJ (2006) Ordered surface carbons distinguish antifreeze proteins and their ice-binding regions. Nature Biotech 24: 852-855

Dreischmeier K, Budke C, Wiehemeier L, Kottke T, Koop T (2017) Boreal pollen contain ice-nucleating as well as ice-binding 'antifreeze' polysaccharides. Sci Rep 7: 41890

Duman JG (1994) Purification and characterization of a thermal hysteresis protein from a plant, the bittersweet nightshade *Solanum dulcamara*. Biochim Biophys Acta Protein Struct Mol Enzymol 1206: 129-135

Duman JG, Wisniewski MJ (2014) The use of antifreeze proteins for frost protection in sensitive crop plants. Environ Exp Bot 106: 60-69

Dvorak J, Deal KR, Luo M-C, You FM, von Borstel K, Dehghani H (2012) The origin of spelt and free-threshing hexaploid wheat. J Hered 103: 426-441

Eagles C, Williams J, Louis D (1993) Recovery after freezing in *Avena sativa* L., *Lolium perenne* L. and *L. multiflorum* Lam. New Phytol 123: 477-483

Edstam MM, Blomqvist K, Eklöf A, Wennergren U, Edqvist J (2013) Coexpression patterns indicate that GPI-anchored non-specific lipid transfer proteins are involved in accumulation of cuticular wax, suberin and sporopollenin. Plant Mol Biol 83: 625-649

Endoh K, Kasuga J, Arakawa K, Ito T, Fujikawa S (2009) Cryo-scanning electron microscopic study on freezing behaviors of tissue cells in dormant buds of larch (*Larix kaempferi*). Cryobiology 59: 214-222

Endoh K, Kuwabara C, Arakawa K, Fujikawa S (2014) Consideration of the reasons why dormant buds of trees have evolved extraorgan freezing as an adaptation for winter survival. Environ Exp Bot 106: 52-59

Evans AT, Janssen G (1922) Winter wheat in South Dakota. Agricultural Experiment Station, South Dakota State College of Agriculture and Mechanic Arts. Bulletin No. 200. 485-516

Evert RF (2006) Esau's plant anatomy: meristems, cells, and tissues of the plant body: their structure, function, and development. 3rd Edition. Hoboken, New Jersey: John Wiley & Sons 1-624

Fennell A, Line MJ (2001) Identifying differential tissue response in grape (*Vitis riparia*) during induction of endodormancy using nuclear magnetic resonance imaging. J Am Soc Hort Sci 126: 681-688

Fleischer A, O'Neill MA, Ehwald R (1999) The pore size of non-graminaceous plant cell walls is rapidly decreased by borate ester cross-linking of the pectic polysaccharide rhamnogalacturonan II. Plant Physiol 121: 829-838

Fowler D (1979) Selection for winterhardiness in wheat. II. Variation within field trials. Crop Sci 19: 773-775

Fowler D, Byrns B, Greer K (2014) Overwinter low-temperature responses of cereals: analyses and simulation. Crop Sci 54: 2395-2405

Fowler DB, Carles RJ (1979) Growth, development, and cold tolerance of fall-acclimated cereal grains. Crop Sci 19: 915-922

Fowler D, Chauvin L, Limin A, Sarhan F (1996) The regulatory role of vernalization in the expression of low-temperature-induced genes in wheat and rye. Theor Appl Genet 93: 554-559

Fowler D, Dvorak J, Gusta L (1977) Comparative cold hardiness of several *Triticum* species and *Secale cereale* L. Crop Sci 17: 941-943

Fowler D, Gusta L (1982) Fall growth and cold acclimation of winter wheat and rye differentially fertilized with phosphorus. Agron J 74: 539-540

Fowler D, Gusta L, Bowren K, Crowle W, Mallough E, McBean D, McIver R (1976) Potential for winter wheat production in Saskatchewan. Can J Plant Sci 56: 45-50

Fowler D, Gusta L, Tyler N (1981) Selection for winterhardiness in wheat. III. Screening methods. Crop Sci 21: 896-901

Fowler D, Limin A (2004) Interactions among factors regulating phenological development and acclimation rate determine low-temperature tolerance in wheat. Ann Bot 94: 717-724

Fowler DB (2008) Cold acclimation threshold induction temperatures in cereals. Crop Sci 48: 1147-1154

Fowler DB (2010) CDC Buteo hard red winter wheat. Can J Plant Sci 90: 707-710

Fowler DB (2012b) Moats hard red winter wheat. Can J Plant Sci 92: 191-193

Fowler DB (2012a) Wheat production in the high winter stress climate of the Great Plains of North America—an experiment in crop adaptation. Crop Sci 52: 11-20

Franks F (1985) Complex aqueous systems at subzero temperatures. In Smatos D, Multon Eds. Properties of water in foods. NATO ASI Series (Series E: Applied Sciences) Vol 90. Dordrecht, Netherlands: Springer. 497-509

Freyman S (1978) Influence of duration of growth, seed size, and seeding depth on cold hardiness of two hardy winter wheat cultivars. Can J Plant Sci 58: 917-921

Fry SC (1986) Cross-linking of matrix polymers in the growing cell walls of angiosperms. Annu Rev Plant Physiol 37: 165-186

Fujikawa S, Jitsuyama Y, Kuroda K (1999) Determination of the role of cold acclimation-induced diverse changes in plant cells from the viewpoint of avoidance of freezing injury. J Plant Res 112: 237-244

Fujikawa S, Kuroda K, Fukazawa K (1994) Ultrastructural study of deep supercooling of xylem ray parenchyma cells from *Styrax obassia*. Micron 25: 241-252

Fujikawa S, Kuroda K, Ohtani J (1997) Seasonal changes in dehydration tolerance of xylem ray parenchyma cells of *Stylax obassia* twigs that survive freezing temperatures by deep supercooling. Protoplasma 197: 34-44

Fukuta N (1963) Ice nucleation by metaldehyde. Nature 199: 475-476

Fuller M, Eagles C (1980) The effect of temperature on cold hardening of *Lolium perenne* seedlings. J Agric Sci 95: 77-81

Fuller M, Hamed F, Wisniewski M, Glenn D (2003) Protection of plants from frost using hydrophobic particle film and acrylic polymer. Ann Appl Biol 143: 93-98

Fuller MP, Fuller AM, Kaniouras S, Christophers J, Fredericks T (2007) The freezing characteristics of wheat at ear emergence. Eur J Agron 26: 435-441

Galiba G, Vágújfalvi A, Li C, Soltész A, Dubcovsky J (2009) Regulatory genes involved in the determination of frost tolerance in temperate cereals. Plant Sci 176: 12-19

Gavish M, Popovitz-Biro R, Lahav M, Leiserowitz L (1990) Ice nucleation by alcohols arranged in monolayers at the surface of water drops. Science 250: 973-975

George MF, Burke MJ, Weiser CJ (1974) Supercooling in overwintering azalea flower buds. Plant Physiol 54: 29-35

Gott M (1957) Vernalization of green plants of a winter wheat. Nature 180: 714-715

Grabber JH, Hatfield RD, Ralph J, Zoń J, Amrhein N (1995) Ferulate cross-linking in cell walls isolated from maize cell suspensions. Phytochemistry 40: 1077-1082

Grabber JH, Ralph J, Hatfield RD (1998) Ferulate cross-links limit the enzymatic degradation of synthetically lignified primary walls of maize. J Agric Food Chem 46: 2609-2614

Grabber JH, Ralph J, Hatfield RD (2000) Cross-linking of maize walls by ferulate dimerization and incorporation into lignin. J Agric Food Chem 48: 6106-6113

Graf RJ, Beres BL, Laroche A, Gaudet DA, Eudes F, Pandeya RS, Badea A, Randhawa HS (2013) Emerson hard red winter wheat. Can J Plant Sci 93: 741-748

Graham P, Mullin R (1976) A study of flower bud hardiness in azalea [Rhododendron]. J Am Soc Hort Sci 101: 3-7

Grant M (1980) Registration of Norstar wheat (Reg. No. 626). Crop Sci 20: 552

Gray GR, Chauvin L-P, Sarhan F, Hüner NP (1997) Cold acclimation and freezing tolerance (a complex interaction of light and temperature). Plant Physiol 114: 467-474

Gray GR, Savitch LV, Ivanov AG, Hüner NP (1996) Photosystem II excitation pressure and development of resistance to photoinhibition (II. Adjustment of photosynthetic capacity in winter wheat and winter rye). Plant Physiol 110: 61-71

Gregory AL, Hurley BA, Tran HT, Valentine AJ, She Y-M, Knowles VL, Plaxton WC (2009) In vivo regulatory phosphorylation of the phosphoenolpyruvate carboxylase AtPPC1 in phosphate-starved *Arabidopsis thaliana*. Biochem J 420: 57-65

Griffith M, Ala P, Yang DS, Hon W-C, Moffatt BA (1992) Antifreeze protein produced endogenously in winter rye leaves. Plant Physiol 100: 593-596

Griffith M, Antikainen M (1996) Extracellular ice formation in freezing-tolerant plants. Adv Low-Temp Biol 3: 107-139

Griffith M, Brown GN (1982) Cell wall deposits in winter rye *Secale cereale* L. 'Puma' during cold acclimation. Bot Gaz 143: 486-490

Griffith M, Hüner N, Espelie K, Kolattukudy P (1985) Lipid polymers accumulate in the epidermis and mestome sheath cell walls during low temperature development of winter rye leaves. Protoplasma 125: 53-64

Griffith M, Lumb C, Wiseman SB, Wisniewski M, Johnson RW, Marangoni AG (2005) Antifreeze proteins modify the freezing process in planta. Plant Physiol 138: 330-340

Griffith M, Yaish MW (2004) Antifreeze proteins in overwintering plants: a tale of two activities. Trends Plant Sci 9: 399-405

Gross D, Cody Y, Proebsting Jr E, Radamaker G, Spotts R (1984) Ecotypes and pathogenicity of ice-nucleation-active *Pseudomonas syringae* isolates from deciduous fruit tree orchards. Phytopathology 74: 241-248

Gruwel ML, Ghosh PK, Latta P, Jayas DS (2007) On the diffusion constant of water in wheat. J Agric Food Chem 56: 59-62

Guo L, Yang H, Zhang X, Yang S (2013) Lipid transfer protein 3 as a target of MYB96 mediates freezing and drought stress in *Arabidopsis*. J Exp Bot 64: 1755-1767

Gupta R, Deswal R (2014) Refolding of β-stranded class I chitinases of *Hippophae rhamnoides* enhances the antifreeze activity during cold acclimation. PloS one 9: e91723

Gusta L, Fowler D (1977) Factors affecting the cold survival of winter cereals. Can J Plant Sci 57: 213-219

Gusta L, Fowler D, Tyler N (1982) Factors influencing hardening and survival in winter wheat. Plant cold hardiness and freezing stress: mechanism and crop implications 2: 23-40

Gusta L, O'Connor B, MacHutcheon M (1997) The selection of superior winter-hardy genotypes using a prolonged freeze test. Can J Plant Sci 77: 15-21

Gusta L, Wisniewski M, Nesbitt N, Gusta M (2004) The effect of water, sugars, and proteins on the pattern of ice nucleation and propagation in acclimated and nonacclimated canola leaves. Plant Physiol 135: 1642-1653

Gusta L, Wisniewski M, Trischuk R (2009) Patterns of freezing in plants: the influence of species, environment and experiential procedures. Plant cold hardiness: from the laboratory to the field: 214-225

Gusta LV, Burke MJ, Kapoor AC (1975) Determination of unfrozen water in winter cereals at subfreezing temperatures. Plant Physiol 56: 707-709

Gusta LV, Fowler DB, Chen P, Russell DB, Stout DG (1979) A nuclear magnetic resonance study of water in cold-acclimating cereals. Plant Physiol 63: 627-634

Gusta LV, Gao YP, Benning NT (2006) Freezing and desiccation tolerance of imbibed canola seed. Physiol Plant 127: 237-246

Gusta LV, Tyler NJ, Chen TH-H (1983) Deep undercooling in woody taxa growing north of the −40°C isotherm. Plant Physiol 72: 122-128

Gusta LV, Wisniewski M (2013) Understanding plant cold hardiness: an opinion. Physiol Plant 147: 4-14

Hacker J, Ladinig U, Wagner J, Neuner G (2011) Inflorescences of alpine cushion plants freeze autonomously and may survive subzero temperatures by supercooling. Plant Sci 180: 149-156

Hacker J, Neuner G (2007) Ice propagation in plants visualized at the tissue level by infrared differential thermal analysis (IDTA). Tree Physiol 27: 1661-1670

Hacker J, Neuner G (2008) Ice propagation in dehardened alpine plant species studied by infrared differential thermal analysis (IDTA). Arct Antarct Alp Res 40: 660-670

Hatfield R, Rancour DM, Marita MM (2016) Grass cell walls: a story of cross-linking. Front Plant Sci 7: 2056

Hayes H, Aamodt O (1927) Inheritance of winter hardiness and growth habit in crosses of marquis with *minhardi* and *minturki* wheats. No. REP-9725. CIMMYT.

Heber U, Santarius KA (1964) Loss of adenosine triphosphate synthesis caused by freezing and its relationship to frost hardiness problems. Plant Physiol 39: 712-719

Herman EM, Rotter K, Premakumar R, Elwinger G, Bae R, Ehler-King L, Chen S, Livingston DP (2006) Additional freeze hardiness in wheat acquired by exposure to −3°C is associated with extensive physiological, morphological, and molecular changes. J Exp Bot 57: 3601-3618

Hiilovaara-Teijo M, Hannukkala A, Griffith M, Yu X-M, Pihakaski-Maunsbach K (1999) Snow-mold-induced apoplastic proteins in winter rye leaves lack antifreeze activity. Plant Physiol 121: 665-674

Hill TC, Moffett BF, DeMott PJ, Georgakopoulos DG, Stump WL, Franc GD (2014) Measurement of ice nucleation-active bacteria on plants and in precipitation by quantitative PCR. Appl Environ Microbiol 80: 1256-1267

Hirsh AG (1987) Vitrification in plants as a natural form of cryoprotection. Cryobiology 24: 214-228

Hon W-C, Griffith M, Chong P, Yang DS (1994) Extraction and isolation of antifreeze proteins from winter rye (*Secale cereale* L.) leaves. Plant Physiol 104: 971-980

Hon W-C, Griffith M, Mlynarz A, Kwok YC, Yang DS (1995) Antifreeze proteins in winter rye are similar to pathogenesis-related proteins. Plant Physiol 109: 879-889

Hsiao C, Chatterton N, Asay K, Jensen K (1995) Phylogenetic relationships of the monogenomic species of the wheat tribe, *Triticeae* (*Poaceae*), inferred from nuclear rDNA (internal transcribed spacer) sequences. Genome 38: 211-223

Huang T, Duman JG (2002) Cloning and characterization of a thermal hysteresis (antifreeze) protein with DNA-binding activity from winter bittersweet nightshade, *Solanum dulcamara*. Plant Mol Biol 48: 339-350

Hüner N, Palta J, Li P, Carter J (1981) Anatomical changes in leaves of Puma rye in response to growth at cold-hardening temperatures. Bot Gaz 142: 55-62

Hüner NPA, Dahal K, Bode R, Kurepin LV, Ivanov AG (2016) Photosynthetic acclimation, vernalization, crop productivity and 'the grand design of photosynthesis'. J Plant Physiol 203: 29-43

Hurry VM, Hüner NP (1991) Low growth temperature effects a differential inhibition of photosynthesis in spring and winter wheat. Plant Physiol 96: 491-497

Hurry VM, Strand A, Tobiaeson M, Gardestrom P, Öquist G (1995) Cold hardening of spring and winter wheat and rape results in differential effects on growth, carbon metabolism, and carbohydrate content. Plant Physiol 109: 697-706

Ishikawa M, Ide H, Yamazaki H, Murakawa H, Kuchitsu K, Price WS, Arata Y (2016) Freezing behaviours in wintering *Cornus florida* flower bud tissues revisited using MRI. Plant Cell Environ 39: 2663-2675

Ishikawa M, Ishikawa M, Toyomasu T, Aoki T, Price WS (2015) Ice nucleation activity in various tissues of Rhododendron flower buds: their relevance to extraorgan freezing. Front Plant Sci 6: 149

Ishikawa M, Price WS, Ide H, Arata Y (1997) Visualization of freezing behaviors in leaf and flower buds of full-moon maple by nuclear magnetic resonance microscopy. Plant Physiol 115: 1515-1524

Ishikawa M, Sakai A (1981) Freezing avoidance mechanisms by supercooling in some Rhododendron flower buds with reference to water relations. Plant Cell Physiol 22: 953-967

Ishikawa M, Sakai A (1982) Characteristics of freezing avoidance in comparison with freezing tolerance: a demonstration of extraorgan freezing. In Li PH, Sakai A Eds. Plant cold hardiness and freezing stress Vol II: mechanisms and crop implications. New York, New York: Academic Press. 325-340

Ishikawa M, Sakai A (1985) Extraorgan freezing in wintering flower buds of *Cornus officinalis* Sieb. et Zucc. Plant Cell Environ 8: 333-338

Janssen G (1929) Effect of date of seeding of winter wheat upon some physiological changes of the plant during the winter season. Jour Amer Soc Agron 21: 169-200

Jarvis MC (1984) Structure and properties of pectin gels in plant cell walls. Plan Cell Environ 7: 153-164

Jia Z, Davies PL (2002) Antifreeze proteins: an unusual receptor–ligand interaction. Trends Biochem Sci 27: 101-106

John UP, Polotnianka RM, Sivakumaran KA, Chew O, MacKin L, Kuiper MJ, Talbot JP, Nugent GD, Mautord J, Schrauf GE (2009) Ice recrystallization inhibition proteins (IRIPs) and freeze tolerance in the cryophilic Antarctic hair grass *Deschampsia antarctica* E. Desv. Plan Cell Environ 32: 336-348

Junttila O, Stushnoff C (1977) Freezing avoidance by deep supercooling in hydrated lettuce seeds. Nature 269: 325-327

Kalapos B, Novák A, Dobrev P, Vítámvás P, Marincs F, Galiba G, Vanková R (2017) Effect of the winter wheat Cheyenne 5A substituted chromosome on dynamics of abscisic acid and cytokinins in freezing-sensitive Chinese Spring genetic background. Front Plant Sci 8: 2033

Kalcsits L, Kendall E, Silim S, Tanino K (2009) Magnetic resonance microimaging indicates water diffusion correlates with dormancy induction in cultured hybrid poplar (*Populus* spp.) buds. Tree Physiol: tpp062

Kasuga J, Arakawa K, Fujikawa S (2007) High accumulation of soluble sugars in deep supercooling Japanese white birch xylem parenchyma cells. New Phytologist 174: 569-579

Kasuga J, Charrier G, Uemura M, Améglio T (2015) Characteristics of ultrasonic acoustic emissions from walnut branches during freeze–thaw-induced embolism formation. J Exp Bot 66: 1965-1975

Kasuga J, Endoh K, Yoshiba M, Taido I, Arakawa K, Uemura M, Fujikawa S (2013) Roles of cell walls and intracellular contents in supercooling capability of xylem parenchyma cells of boreal trees. Physiol Plant 148: 25-35

Kasuga J, Fukushi Y, Kuwabara C, Wang D, Nishioka A, Fujikawa E, Arakawa K, Fujikawa S (2010) Analysis of supercooling-facilitating (anti-ice nucleation) activity of flavonol glycosides. Cryobiology 60: 240-243

Kasuga J, Hashidoko Y, Nishioka A, Yoshiba M, Arakawa K, Fujikawa S (2008) Deep supercooling xylem parenchyma cells of katsura tree (*Cercidiphyllum japonicum*) contain flavonol glycosides exhibiting high anti-ice nucleation activity. Plan Cell Environ 31: 1335-1348

Kasuga J, Mizuno K, Miyaji N, Arakawa K, Fujikawa S (2006) Role of intracellular contents to facilitate supercooling capability in beech (*Fagus crenata*) xylem parenchyma cells. CryoLett 27: 305-310

Kato K, Sonokawa R, Miura H, Sawada S (2003) Dwarfing effect associated with the threshability gene Q on wheat chromosome 5A. Plant Breeding 122: 489-492

Kawamura Y, Uemura M (2003) Mass spectrometric approach for identifying putative plasma membrane proteins of Arabidopsis leaves associated with cold acclimation. Plant J 36: 141-154

Kim H, Orser C, Lindow S, Sands D (1987) *Xanthomonas campestris* pv. *translucens* strains active in ice nucleation. Plant Dis 71: 994-997

Kindel PK, Liao S-Y, Liske MR, Olien CR (1989) Arabinoxylans from rye and wheat seed that interact with ice. Carbohydr Res 187: 173-185

King GJ (2015) Crop epigenetics and the molecular hardware of genotype× environment interactions. Front Plant Sci 6: 968

Kishimoto T, Sekozawa Y, Yamazaki H, Murakawa H, Kuchitsu K, Ishikawa M (2014a) Seasonal changes in ice nucleation activity in blueberry stems and effects of cold treatments in vitro. Environ Exp Bot 106: 13-23

Kishimoto T, Yamazaki H, Saruwatari A, Murakawa H, Sekozawa Y, Kuchitsu K, Price WS, Ishikawa M (2014b) High ice nucleation activity located in blueberry stem bark is linked to primary freeze initiation and adaptive freezing behaviour of the bark. AoB Plants 6: plu044

Klinck H, Grant M (1964) Registration of Kharkov 22 MC wheat (Reg. No. 428). Crop Sci 4: 235-236

Knight CA, Wen D, Laursen RA (1995) Nonequilibrium antifreeze peptides and the recrystallization of ice. Cryobiology 32: 23-34

Kobayashi M, Nakagawa H, Asaka T, Matoh T (1999) Borate-rhamnogalacturonan II bonding reinforced by Ca^{2+} retains pectic polysaccharides in higher-plant cell walls. Plant Physiol 119: 199-204

Kosová K, Prášil IT, Vítámvás P, Dobrev P, Motyka V, Floková K, Novák O, Turečková V, Rolčik J, Pešek B (2012) Complex phytohormone responses during the cold acclimation of two wheat cultivars differing in cold tolerance, winter Samanta and spring Sandra. J Plant Physiol 169: 567-576

Krog JO, Zachariassen KE, Larsen B, Smidsrød O (1979) Thermal buffering in Afro-alpine plants due to nucleating agent-induced water freezing. Nature 282: 300-301

Kubacka-Zębalska M, Kacperska A (1999) Low temperature-induced modifications of cell wall content and polysaccharide composition in leaves of winter oilseed rape (*Brassica napus* L. var. *oleifera* L.). Plant Sci 148: 59-67

Kuprian E, Briceño VF, Wagner J, Neuner G (2014) Ice barriers promote supercooling and prevent frost injury in reproductive buds, flowers and fruits of alpine dwarf shrubs throughout the summer. Environ Exp Bot 106: 4-12

Kuprian E, Munkler C, Resnyak A, Zimmermann S, Tuong TD, Gierlinger N, Müller T, Livingston DP, Neuner G (2017) Complex bud architecture and cell-specific chemical patterns enable supercooling of *Picea abies* bud primordia. Plan Cell Environ 40:3101-3112

Kuprian E, Tuong TD, Pfaller K, Wagner J, Livingston III DP, Neuner G (2016) Persistent supercooling of reproductive shoots is enabled by structural ice barriers being active despite an intact xylem connection. PLoS One 11: e0163160

Kuroda K, Kasuga J, Arakawa K, Fujikawa S (2003) Xylem ray parenchyma cells in boreal hardwood species respond to subfreezing temperatures by deep supercooling that is accompanied by incomplete desiccation. Plant Physiol 131: 736-744

Lahlali R, Jiang Y, Kumar S, Karunakaran C, Liu X, Borondics F, Hallin E, Bueckert R (2014) ATR–FTIR spectroscopy reveals involvement of lipids and proteins of intact pea pollen grains to heat stress tolerance. Front Plant Sci 5: 747

Lahlali R, Karunakaran C, Wang L, Willick I, Schmidt M, Liu X, Borondics F, Forseille L, Fobert PR, Tanino K (2015) Synchrotron based phase contrast X-ray imaging combined with FTIR spectroscopy reveals structural and biomolecular differences in spikelets play a significant role in resistance to Fusarium in wheat. BMC Plant Biol 15: 24

Lahlali R, Kumar S, Wang L, Forseille L, Sylvain N, Korbas M, Muir D, Swerhone G, Lawrence JR, Fobert PR (2016) Cell wall biomolecular composition plays a potential role in the host type II resistance to Fusarium head blight in wheat. Front Microbiol 7: 910

Lee B-H, Henderson DA, Zhu J-K (2005) The *Arabidopsis* cold-responsive transcriptome and its regulation by ICE1. Plant Cell 17: 3155-3175

Lee Y, Karunakaran C, Lahlali R, Liu X, Tanino K, Olsen JE (2017) Photoperiodic regulation of growth-dormancy cycling through induction of multiple bud-shoot barriers preventing water transport into the winter buds of Norway spruce. Front Plant Sci 8: 2109

Legge W, Fowler D, Gusta L (1983) Cold hardiness of winter wheat tillers acclimated under field conditions. Can J Plant Sci 63: 879-888

Levitt J (1980) Responses of plants to environmental stress, volume 1: chilling, freezing, and high temperature stresses. New York, New York: Academic Press. 1-497

Li Q, Byrns B, Badawi MY, Diallo AB, Danyluk J, Sarhan F, Laudencia-Chingcuanco D, Zou J, Fowler DB (2017) Transcriptomic insights into phenological development and cold tolerance of wheat grown in the field. Plant Physiol 176: 1-19

Limin A, Fowler D (2002) Developmental traits affecting low-temperature tolerance response in near-isogenic lines for the vernalization locus Vrn-A1 in wheat (*Triticum aestivum* L. em *Thell*). Ann Bot 89: 579-585

Lindow S (1983) The role of bacterial ice nucleation in frost injury to plants. Annu Rev Phytopathology 21: 363-384

Lindow S, Arny D, Upper C (1978a) Distribution of ice nucleation-active bacteria on plants in nature. Appl Environ Microbiol 36: 831-838

Lindow S, Arny D, Upper C (1978b) *Erwinia herbicola*: a bacterial ice nucleus active in increasing frost injury to corn. Phytopathology 68: 523-527

Lindow SE, Arny DC, Upper CD (1982) Bacterial ice nucleation: a factor in frost injury to plants. Plant Physiol 70: 1084-1089

Liu F, Marquardt S, Lister C, Swiezewski S, Dean C (2010) Targeted 3′ processing of antisense transcripts triggers *Arabidopsis* FLC chromatin silencing. Science 327: 94-97

Livingston D, Premakumar R, Tallury SP (2005a) Carbohydrate concentrations in crown fractions from winter oat during hardening at sub-zero temperatures. Ann Bot 96: 331-335

Livingston DP, Henson CA (1998) Apoplastic sugars, fructans, fructan exohydrolase, and invertase in winter oat: responses to second-phase cold hardening. Plant Physiol 116: 403-408

Livingston DP, Henson CA, Tuong TD, Wise ML, Tallury SP, Duke SH (2013) Histological analysis and 3D reconstruction of winter cereal crowns recovering from freezing: a unique response in oat (*Avena sativa* L.). PloS One 8: e53468

Livingston DP, Premakumar R, Tallury SP (2006) Carbohydrate partitioning between upper and lower regions of the crown in oat and rye during cold acclimation and freezing. Cryobiology 52: 200-208

Livingston DP, Tallury SP, Premkumar R, Owens SA, Olien CR (2005b) Changes in the histology of cold-hardened oat crowns during recovery from freezing. Crop Sci 45: 1545-1558

Livingston DP, Tuong TD (2014) Understanding the response of winter cereals to freezing stress through freeze-fixation and 3D reconstruction of ice formation in crowns. Environ Exp Bot 106: 24-33

Livingston DP, Tuong TD, Isleib TG, Murphy JP (2016) Differences between wheat genotypes in damage from freezing temperatures during reproductive growth. Eur J Agron 74: 164-172

Livingston DP, Tuong TD, Murphy JP, Gusta LV, Willick I, Wisniewski ME (2017) High-definition infrared thermography of ice nucleation and propagation in wheat under natural frost conditions and controlled freezing. Planta: 1-16

Luyet BJ, Gehenio P (1937) The double freezing point of living tissues. Biodynamica 30: 1-23

Luyet BJ, Hodapp EL (1938) Revival of frog's spermatozoa vitrified in liquid air. Proc Soc Exp Biol Med 39: 433-434

MacDonald JE, Owens JN (1993) Bud development in coastal Douglas-fir seedlings under controlled-environment conditions. Can J Forest Res 23: 1203-1212

Maki LR, Galyan EL, Chang-Chien M-M, Caldwell DR (1974) Ice nucleation induced by *Pseudomonas syringae*. Appl Microbiol 28: 456-459

Martin J, Parker J (1926) Comparative hardiness of winter-wheat varieties. US Dept. Agr. Circ 378: 205-217

Martínez-Caballero S, Cano-Sánchez P, Mares-Mejía I, Díaz-Sánchez AG, Macías-Rubalcava ML, Hermoso JA, Rodríguez-Romero A (2014) Comparative study of two GH19 chitinase-like proteins from *Hevea brasiliensis,* one exhibiting a novel carbohydrate-binding domain. FEBS J 281: 4535-4554

Matoh T, Kobayashi M (1998) Boron and calcium, essential inorganic constituents of pectic polysaccharides in higher plant cell walls. J Plant Res 111: 179-190

Mazur P (1966) Theoretical and experimental effects of cooling and warming velocity on the survival of frozen and thawed cells. Cryobiology 2: 181-192

Mazur P (1969) Freezing injury in plants. Annu Rev Plant Physiol 20: 419-448

McCallum BD, DePauw RM (2008) A review of wheat cultivars grown in the Canadian prairies. Can J Plant Sci 88: 649-677

McCann M, Chen L, Roberts K, Kemsley E, Sene C, Carpita N, Stacey N, Wilson R (1997) Infrared microspectroscopy: sampling heterogeneity in plant cell wall composition and architecture. Physiol Plant 100: 729-738

McCann MC, Hammouri M, Wilson R, Belton P, Roberts K (1992) Fourier transform infrared microspectroscopy is a new way to look at plant cell walls. Plant Physiol 100: 1940-1947

McLeod J, Gan Y (2008) Hazlet winter rye. Can J Plant Sci 88: 527-529

Metcalf E, Cress C, Olein C, Everson E (1970) Relationship between crown moisture content and killing temperature for three wheat and three barley cultivars. Crop Sci 10: 362-365

Meyer K, Keil M, Naldrett MJ (1999) A leucine-rich repeat protein of carrot that exhibits antifreeze activity. FEBS Lett 447: 171-178

Middleton AJ, Brown AM, Davies PL, Walker VK (2009) Identification of the ice-binding face of a plant antifreeze protein. FEBS Lett 583: 815-819

Millard M, Veisz O, Krizek D, Line M (1995) Magnetic resonance imaging (MRI) of water during cold acclimation and freezing in winter wheat. Plan Cell Environ 18: 535-544

Min K, Chen K, Arora R (2014) Effect of short-term versus prolonged freezing on freeze–thaw injury and post-thaw recovery in spinach: Importance in laboratory freeze–thaw protocols. Environ Exp Bot 106: 124-131

Minami A, Fujiwara M, Furuto A, Fukao Y, Yamashita T, Kamo M, Kawamura Y, Uemura M (2008) Alterations in detergent-resistant plasma membrane microdomains in *Arabidopsis thaliana* during cold acclimation. Plant Cell Physiol 50: 341-359

Nakamura T, Ishikawa M, Nakatani H, Oda A (2008) Characterization of cold-responsive extracellular chitinase in bromegrass cell cultures and its relationship to antifreeze activity. Plant Physiol 147: 391-401

Neuner G (2014) Frost resistance in alpine woody plants. Front Plant Sci 5: 654

Neuner G, Hacker J (2012) Ice formation and propagation in alpine plants. In Lütz C Ed. Plants in Alpine Regions. Vienna: Springer. 163-174

Newton SS, Duman JG (2000) An osmotin-like cryoprotective protein from the bittersweet nightshade *Solanum dulcamara*. Plant Mol Biol 44: 581-589

O'Neill MA, Warrenfeltz D, Kates K, Pellerin P, Doco T, Darvill AG, Albersheim P (1996) Rhamnogalacturonan-II, a pectic polysaccharide in the walls of growing plant cell, forms a dimer that is covalently cross-linked by a borate ester in vitro conditions for the formation and hydrolysis of the dimer. J Biol Chem 271: 22923-22930

Olien C (1973) Thermodynamic components of freezing stress. J Theor Biol 39: 201-210

Olien C, Lester G (1985) Freeze-induced changes in soluble carbohydrates of rye. Crop Sci 25: 288-290

Olien C, Marchetti B (1976) Recovery of hardened barley from winter injuries. Crop Sci 16: 201-204

Olien C, Smith MN (1977) Ice adhesions in relation to freeze stress. Plant Physiol 60: 499-503

Olien CR (1961) A method of studying stresses occurring in plant tissue during freezing. Crop Sci 1: 26-28

Olien CR (1964) Freezing processes in the crown of ‘Hudson’ barley, *Hordeum vulgare* (L., emend. Lam.). Crop Sci 4: 91-95

Olien CR (1965) Interference of cereal polymers and related compounds with freezing. Cryobiology 2: 47-54

Olien CR (1967) Freezing stresses and survival. Annu Rev Plant Physiol 18: 387-408

Olien CR (2012) The equilibrated state of freezing as a basis for distinguishing lethal stresses of freezing in plants. Thermochim Acta 534:17-20

Olien CR, Livingston DP (2006) Understanding freeze stress in biological tissues: Thermodynamics of interfacial water. Thermochim Acta 451: 52-56

Oliver SN, Finnegan EJ, Dennis ES, Peacock WJ, Trevaskis B (2009) Vernalization-induced flowering in cereals is associated with changes in histone methylation at the VERNALIZATION1 gene. Proc Natl Acad Sci USA 106: 8386-8391

Öquist G, Hüner NP (2003) Photosynthesis of overwintering evergreen plants. Annu Rev Plant Biol 54: 329-355

Owens JH, Molder M (1976) Bud development in Sitka spruce. I. Annual growth cycle of vegetative buds and shoots. Can J Bot 54: 313-325

Palmer R, Cornuault V, Marcus SE, Knox JP, Shewry PR, Tosi P (2015) Comparative in situ analyses of cell wall matrix polysaccharide dynamics in developing rice and wheat grain. Planta 241: 669-685

Passardi F, Penel C, Dunand C (2004) Performing the paradoxical: how plant peroxidases modify the cell wall. Trends Plant Sci 9: 534-540

Passarelli Jr RE, Chessin H, Vonnegut B (1974) Ice nucleation in a supercooled cloud by CuI-3AgI and AgI aerosols. J Appl Meteorl 13: 946-948

Pauli A (1960) Relation of crown tissue to winter survival in hard red winter wheat. Agron J 52: 265-266

Pearce RS (2001) Plant freezing and damage. Ann Bot 87: 417-424

Pearce RS, Fuller MP (2001) Freezing of barley studied by infrared video thermography. Plant Physiol 125: 227-240

Pielot R, Kohl S, Manz B, Rutten T, Weier D, Tarkowská D, Rolčík J, Strnad M, Volke F, Weber H (2015) Hormone-mediated growth dynamics of the barley pericarp as revealed by magnetic resonance imaging and transcript profiling. J Exp Bot 66: 6927-6943

Pihakaski-Maunsbach K, Griffith M, Antikainen M, Maunsbach AB (1996) Immunogold localization of glucanase-like antifreeze protein in cold acclimated winter rye. Protoplasma 191: 115-125

Pihakaski-Maunsbach K, Tamminen I, Pietiäinen M, Griffith M (2003) Antifreeze proteins are secreted by winter rye cells in suspension culture. Physiol Plant 118: 390-398

Pomeroy M, Andrews C (1983) Flooding and ice encasement damage to winter wheat. In Fowler DB, Gusta LV, Slinkard AE, Hobin BA Eds. New frontiers in winter wheat production. Saskatoon, Saskatchewan: The University of Saskatchewan Printing Services. 39-56

Pomeroy M, Andrews C, Fedak G (1975) Cold hardening and dehardening responses in winter wheat and winter barley. Can J Plant Sci 55: 529-535

Pruppacher H (1967) Interpretation of experimentally determined growth rates of ice crystals in supercooled water. J Chem Phys 47: 1807-1813

Pukacki P, McKersie B (1990) Supercooling and ice nucleation events in the crown of winter wheat seedlings. Can J Plant Sci 70: 1179-1182

Purvis O, Gregory F (1937) Studies in vernalisation of cereals: I. A comparative study of vernalisation of winter rye by low temperature and by short days. Ann Bot 1: 569-591

Quamme H (1978) Mechanism of supercooling in overwintering peach flower buds. J Amer Soc Hort Sci 103: 57-61

Quamme H, Layne R, Ronald W (1982) Relationship of supercooling to cold hardiness and the northern distribution of several cultivated and native *Prunus* species and hybrids. Can J Plant Sci 62: 137-148

Quamme H, Stushnoff C, Weiser C (1972) The relationship of exotherms to cold injury in apple stem tissues. J Amer Soc Hort Sci 97: 608-613

Quamme H, Su WA, Veto L (1995) Anatomical features facilitating supercooling of the flower within the dormant peach flower bud. J Amer Soc Hort Sci 120: 814-822

Rajashekar C (1989) Supercooling characteristics of isolated peach flower bud primordia. Plant Physiol 89: 1031-1034

Rajashekar C, Burke MJ (1996) Freezing characteristics of rigid plant tissues (development of cell tension during extracellular freezing). Plant Physiol 111: 597-603

Rajashekar C, Lafta A (1996) Cell-wall changes and cell tension in response to cold acclimation and exogenous abscisic acid in leaves and cell cultures. Plant Physiol 111: 605-612

Reaney MJT, Gusta LV, Abrams SR, Robertson AJ (1989) The effects of abscisic acid, kinetin and gibberellin on freezing tolerance in smooth bromegrass (*Bromus inermis*) cell suspension. Can J Bot 67: 3640-3646.

Rinalducci S, Egidi MG, Mahfoozi S, Godehkahriz SJ, Zolla L (2011) The influence of temperature on plant development in a vernalization-requiring winter wheat: a 2-DE based proteomic investigation. J Proteom 74: 643-659

Rizza F, Pagani D, Stanca A, Cattivelli L (2001) Use of chlorophyll fluorescence to evaluate the cold acclimation and freezing tolerance of winter and spring oats. Plant Breeding 120: 389-396

Sakai A (1979) Freezing avoidance mechanism of primordial shoots of conifer buds. Plant Cell Physiol 20: 1381-1390

Sakai A (1982) Freezing tolerance of shoot and flower primordia of coniferous buds by extraorgan freezing. Plant Cell Physiol 23: 1219-1227

Sakai A (1983) Comparative study on freezing resistance of conifers with special reference to cold adaptation and its evolutive aspects. Can J Bot 61: 2323-2332

Sakai A, Larcher W (1987) Frost survival of plants. Responses and adaptation to freezing stress. Billings WD, Golley F, Lange OL, Olson JS, Remmert H Eds. Ecological Studies Vol. 62. Springer-Verlag, Berlin, Germany. 1-200

Sakai A, Yoshida S (1968) The role of sugar and related compounds in variations of freezing resistance. Cryobiology 5: 160-174

Sakurai J, Ishikawa F, Yamaguchi T, Uemura M, Maeshima M (2005) Identification of 33 rice aquaporin genes and analysis of their expression and function. Plant Cell Physiol 46: 1568-1577

Sasaki K, Kim MH, Imai R (2013) Arabidopsis COLD SHOCK DOMAIN PROTEIN 2 is a negative regulator of cold acclimation. New Phytol 198: 95-102

Scalbert A, Monties B, Lallemand J-Y, Guittet E, Rolando C (1985) Ether linkage between phenolic acids and lignin fractions from wheat straw. Phytochemistry 24: 1359-1362

Scarth G (1941) Dehydration injury and resistance. Plant Physiol 16: 171

Scarth G, Levitt J (1937) The frost-hardening mechanism of plant cells. Plant Physiol 12: 51

Sharman B, Hitch P (1967) Initiation of procambial strands in leaf primordia of bread wheat, *Triticum aestivum* L. Ann Bot 31: 229-243

Shebeski LH, McGinnis RC, Evans LE, Zuzens D (1973) Puma, a new cultivar of winter rye. Can J Plant Sci 53: 67-67

Shiferaw B, Smale M, Braun H-J, Duveiller E, Reynolds M, Muricho G (2013) Crops that feed the world 10. Past successes and future challenges to the role played by wheat in global food security. Food Secur 5: 291-317

Sidebottom C, Buckley S, Pudney P, Twigg S, Jarman C, Holt C, Telford J, McArthur A, Worrall D, Hubbard R (2000) Phytochemistry: heat-stable antifreeze protein from grass. Nature 406: 256-256

Siminovitch D, Briggs D (1953) Studies on the chemistry of the living bark of the black locust in relation to its frost hardiness. III. The validity of plasmolysis and desiccation tests for determining the frost hardiness of bark tissue. Plant Physiol 28: 15

Siminovitch D, Levitt J (1941) The relation between frost resistance and the physical state of the protoplasm: II. The protoplasmic surface. Can J Res 19: 9-20

Siminovitch D, Rheaume B, Pomeroy K, Lepage M (1968) Phospholipid, protein, and nucleic acid increases in protoplasm and membrane structures associated with development of extreme freezing resistance in black locust tree cells. Cryobiology 5: 202-225

Siminovitch D, Scarth G (1938) A study of the mechanism of frost injury to plants. Can J Res 16: 467-481

Singh CB, Jayas DS, Borondics F, White ND (2011) Synchrotron based infrared imaging study of compositional changes in stored wheat due to infection with *Aspergillus glaucus*. J Stored Prod Res 47: 372-377

Single W (1964) Studies on frost injury to wheat. II. Ice formation within the plant. Aust J Agric Res 15: 869-875

Single W, Olien C (1967) Freezing processes in wheat stems. Aust J Biol Sci 20: 1025-1028

Skinner DZ, Bellinger BS (2016) Freezing tolerance of winter wheat as influenced by extended growth at low temperatures and exposure to freeze–thaw cycles. Can J Plant Sci 97: 250-256

Solecka D, Boudet A-M, Kacperska A (1999) Phenylpropanoid and anthocyanin changes in low-temperature treated winter oilseed rape leaves. Plant Physiol Biochem 37: 491-496

Solecka D, Żebrowski J, Kacperska A (2008) Are pectins involved in cold acclimation and de-acclimation of winter oil-seed rape plants? Ann Bot 101: 521-530

Stefanowska M, Kuras M, Kacperska A (2002) Low temperature-induced modifications in cell ultrastructure and localization of phenolics in winter oilseed rape (*Brassica napus* L. var. *oleifera* L.) leaves. Ann Bot 90: 637-645

Steponkus PL (1984) Role of the plasma membrane in freezing injury and cold acclimation. Annu Rev Plant Physiol 35: 543-584

Steponkus PL, Dowgert MF, Gordon-Kamm WJ (1983) Destabilization of the plasma membrane of isolated plant protoplasts during a freeze-thaw cycle: the influence of cold acclimation. Cryobiology 20: 448-465

Stitt M, Hurry V (2002) A plant for all seasons: alterations in photosynthetic carbon metabolism during cold acclimation in *Arabidopsis*. Curr Opin Plant Biol 5: 199-206

Strand Å, Hurry V, Henkes S, Hüner N, Gustafsson P, Gardeström P, Stitt M (1999) Acclimation of *Arabidopsis* leaves developing at low temperatures. Increasing cytoplasmic volume accompanies increased activities of enzymes in the Calvin cycle and in the sucrose-biosynthesis pathway. Plant Physiol 119: 1387-1398

Stressmann M, Kitao S, Griffith M, Moresoli C, Bravo LA, Marangoni AG (2004) Calcium interacts with antifreeze proteins and chitinase from cold-acclimated winter rye. Plant Physiol 135: 364-376

Sun Y, Fu L, Chen L, Wang X, Song Y, Li Z (2017) Characterization of two winter wheat varieties' responses to freezing in a frigid region of the People's Republic of China. Can J Plant Sci 97: 808-815

Takahashi D, Kawamura Y, Uemura M (2013a) Changes of detergent-resistant plasma membrane proteins in oat and rye during cold acclimation: association with differential freezing tolerance. J Proteome Res 12: 4998-5011

Takahashi D, Kawamura Y, Uemura M (2016) Cold acclimation is accompanied by complex responses of glycosylphosphatidylinositol (GPI)-anchored proteins in *Arabidopsis*. J Exp Bot 67: 5203-5215

Takahashi D, Li B, Nakayama T, Kawamura Y, Uemura M (2013b) Plant plasma membrane proteomics for improving cold tolerance. Front Plant Sci 4: 90

Takahashi D, Nakayama T, Miki Y, Kawamura Y, Uemura M (2014) Proteomic approaches to identify cold-regulated plasma membrane proteins. Plant Cold Acclimation: Methods and Protocols: 159-170

Takata N, Kasuga J, Takezawa D, Arakawa K, Fujikawa S (2007) Gene expression associated with increased supercooling capability in xylem parenchyma cells of larch (*Larix kaempferi*). J Exp Bot 58: 3731-3742

Tanino KK, Chen THH, Fuchigami LH, Weiser CJ (1990) Metabolic alterations associated with abscisic acid-induced frost hardiness in bromegrass suspension culture cells. Plant Cell Physiol 31: 505-511

Tanino KK, Chen THH, Fuchigami LH, Weiser CJ (1991) abscisic acid-induced cellular alterations during the induction of freezing tolerance in bromegrass cells. J Plant Physiol 137: 619-624

Tanino KK, Kobayashi S, Hyett C, Hamilton K, Liu J, Li B, Borondics F, Pedersen T, Tse J, Ellis T (2013) *Allium fistulosum* as a novel system to investigate mechanisms of freezing resistance. Physiol Plant 147: 101-111

Tanino KK, McKersie BD (1985) Injury within the crown of winter wheat seedlings after freezing and icing stress. Can J Bot 63: 432-436

Tanner J (1983) Intracellular diffusion of water. Arch Biochem Biophys 224: 416-428

Taschler D, Beikircher B, Neuner G (2004) Frost resistance and ice nucleation in leaves of five woody timberline species measured in situ during shoot expansion. Tree Physiol 24: 331-337

Tenhaken R (2015) Cell wall remodeling under abiotic stress. Front Plant Sci 5: 771

Terumoto I (1960) Ice masses in the root tissue of table beet. Low Temp Sci Ser B 18: 39-42

Thomas JB, Conner RL, Graf RJ (2012) Radiant hard red winter wheat. Can J Plant Sci 92: 169-175

Thomashow MF (1999) Plant cold acclimation: freezing tolerance genes and regulatory mechanisms. Ann Rev Plant Biol 50: 571-599

Towill LE, Mazur P (1976) Osmotic shrinkage as a factor in freezing injury in plant tissue cultures. Plant Physiol 57: 290-296

Tremblay K, Ouellet F, Fournier J, Danyluk J, Sarhan F (2005) Molecular characterization and origin of novel bipartite cold-regulated ice recrystallization inhibition proteins from cereals. Plant Cell Physiol 46: 884-891

Trischuk RG, Schilling BS, Low NH, Gray GR, Gusta LV (2014) Cold acclimation, de-acclimation and re-acclimation of spring canola, winter canola and winter wheat: The role of carbohydrates, cold-induced stress proteins and vernalization. Environ Exp Bot 106: 156-163

Tumanov I, Krasasvtsev O (1959) Hardening of northern woody plants in temperatures below zero. Sov Plant Physiol 6: 654-657

Tyler N, Gusta L, Fowler D (1981) The influence of nitrogen, phosphorus and potassium on the cold acclimation of winter wheat (*Triticum aestivum* L.). Can J Plant Sci 61: 879-885

Uemura M, Joseph RA, Steponkus PL (1995) Cold acclimation of *Arabidopsis thaliana* (effect on plasma membrane lipid composition and freeze-induced lesions). Plant Physiol 109: 15-30

Uemura M, Steponkus PL (1997a) Effect of cold acclimation on membrane lipid composition and freeze-induced membrane destablization. In Li PH, Chen THH Eds. Plant cold hardiness. Boston, Massachusetts: Springer. 171-179

Uemura M, Steponkus PL (1997b) Effect of cold acclimation on the lipid composition of the inner and outer membrane of the chloroplast envelope isolated from rye leaves. Plant Physiol 114: 1493-1500

Uemura M, Tominaga Y, Nakagawara C, Shigematsu S, Minami A, Kawamura Y (2006) Responses of the plasma membrane to low temperatures. Physiol Plant 126: 81-89

Urrutia ME, Duman JG, Knight CA (1992) Plant thermal hysteresis proteins. Biochim Biophys Acta Protein Struct Mol Enzymol 1121: 199-206

Vali G (1995) Principles of ice nucleation. In Lee RE, Warren GJ, Gusta LV Eds. Biological ice nucleation and its applications. St. Paul, Minnesota: APS Press. 1-28

Vasilyev I (1961) Wintering of plants [translated from the 1956 Russian original by J Levitt]. Washington, District of Columbia: American Institute of Biological Sciences. 1-300

Verslues PE, Agarwal M, Katiyar-Agarwal S, Zhu J, Zhu JK (2006) Methods and concepts in quantifying resistance to drought, salt and freezing, abiotic stresses that affect plant water status. Plant J 45: 523-539

Vijayan P, Willick IR, Lahlali R, Karunakaran C, Tanino KK (2015) Synchrotron radiation sheds fresh light on plant research: The use of powerful techniques to probe structure and composition of plants. Plant Cell Physiol 56: 1252-1263

Vítámvás P, Prášil IT, Kosova K, Planchon S, Renaut J (2012) Analysis of proteome and frost tolerance in chromosome 5A and 5B reciprocal substitution lines between two winter wheats during long-term cold acclimation. Proteomics 12: 68-85

Vizcaíno JA, Csordas A, Del-Toro N, Dianes JA, Griss J, Lavidas I, Mayer G, Perez-Riverol Y, Reisinger F, Ternent T (2015) 2016 update of the PRIDE database and its related tools. Nucleic Acids Res 44: D447-D456

Vonnegut B (1947) The nucleation of ice formation by silver iodide. J Appl Phys 18: 593-595

Waalen WM, Tanino KK, Olsen JE, Eltun R, Rognli OA, Gusta LV (2011) Freezing tolerance of winter canola cultivars is best revealed by a prolonged freeze test. Crop Sci 51: 1988-1996

Wagner W, Keller F, Wiemken A (1983) Fructan metabolism in cereals: induction in leaves and compartmentation in protoplasts and vacuoles. Z Pflanzenphysiol 112: 359-372

Wakabayashi K, Soga K, Hoson T (2011) Cell wall oxalate oxidase modifies the ferulate metabolism in cell walls of wheat shoots. J Plant Physiol 168: 1997-2000

Wang D, Kasuga J, Kuwabara C, Endoh K, Fukushi Y, Fujikawa S, Arakawa K (2012) Presence of supercooling-facilitating (anti-ice nucleation) hydrolyzable tannins in deep supercooling xylem parenchyma cells in *Cercidiphyllum japonicum*. Planta 235: 747-759

Weiser C (1970) Cold resistance and injury in woody plants. Science 169: 1269-1278

Weiser RL, Wallner SJ, Waddell JW (1990) Cell wall and extensin mRNA changes during cold acclimation of pea seedlings. Plant Physiol 93: 1021-1026

Westermark U (1985) The occurrence of p-hydroxyphenylpropane units in the middle-lamella lignin of spruce (*Picea abies*). Wood Sci Technol 19: 223-232

Wiegand K (1906a) The occurrence of ice in plant tissue. The Plant World 9: 25-39

Wiegand KM (1906b) Some studies regarding the biology of buds and twigs in winter. Bot Gaz 41: 373-424

Williams R, Sharman B, Langer RHM (1975) Growth and development of the wheat tiller. I. Growth and form of the tiller bud. Aust J Bot 23: 715-743

Willick IR, Lahlali R, Vijayan P, Muir D, Karunakaran C, Tanino KK (2018b) Wheat flag leaf epicuticular wax morphology and composition in response to moderate drought stress are revealed by SEM, FTIR-ATR and synchrotron X-ray spectroscopy. Physiol Plant 162: 316-332

Willick IR, Takahashi D, Fowler B, Uemura M, Tanino KK (2018a) Tissue-specific changes in apoplastic proteins and cell wall structure during cold acclimation of winter wheat crowns. J Exp Bot 69: 1221-1234

Wisniewski M, Davis G, Arora R (1991a) Effect of macerase, oxalic acid, and EGTA on deep supercooling and pit membrane structure of xylem parenchyma of peach. Plant Physiol 96: 1354-1359

Wisniewski M, Davis G, Schafter K (1991b) Mediation of deep supercooling of peach and dogwood by enzymatic modifications in cell-wall structure. Planta 184: 254-260

Wisniewski M, Fuller M (1999) Ice nucleation and deep supercooling in plants: new insights using infrared thermography. In Margesin R, Schinner F Eds. Cold-adapted organisms. Berlin, Heidelberg: Springer. 105-118

Wisniewski M, Glenn DM, Gusta L, Fuller MP (2008) Using infrared thermography to study freezing in plants. HortScience 43: 1648-1651

Wisniewski M, Lindow SE, Ashworth EN (1997) Observations of ice nucleation and propagation in plants using infrared video thermography. Plant Physiol 113: 327-334

Wolber PK, Deininger CA, Southworth MW, Vandekerckhove J, van Montagu M, Warren GJ (1986) Identification and purification of a bacterial ice-nucleation protein. Proc Natl Acad Sci USA 83: 7256-7260

Workmaster BAA, Palta JP, Wisniewski M (1999) Ice nucleation and propagation in cranberry uprights and fruit using infrared video thermography. J Am Soc Hort Sci 124: 619-625

Worrall D, Elias L, Ashford D, Smallwood M, Sidebottom C, Lillford P, Telford J, Holt C, Bowles D (1998) A carrot leucine-rich-repeat protein that inhibits ice recrystallization. Science 282: 115-117

Wright S (1890) The relation of low temperature to the growth of wheat. Agric Sci 4: 338-345

Yan L, Loukoianov A, Blechl A, Tranquilli G, Ramakrishna W, SanMiguel P, Bennetzen JL, Echenique V, Dubcovsky J (2004) The wheat VRN2 gene is a flowering repressor down-regulated by vernalization. Science 303: 1640-1644

Yan L, Loukoianov A, Tranquilli G, Helguera M, Fahima T, Dubcovsky J (2003) Positional cloning of the wheat vernalization gene VRN1. Proc Natl Acad Sci USA 100: 6263-6268

Xin H, Zhang X, Yu P (2013) Using synchrotron radiation-based infrared microspectroscopy to reveal microchemical structure characterization: frost damaged wheat vs. normal wheat. Int J Mol Sci 14: 16706-16718

Yamada T, Kuroda K, Jitsuyama Y, Takezawa D, Arakawa K, Fujikawa S (2002) Roles of the plasma membrane and the cell wall in the responses of plant cells to freezing. Planta 215: 770-778

Yeh S, Moffatt BA, Griffith M, Xiong F, Yang DSC, Wiseman SB, Sarhan F, Danyluk J, Xue YQ, Hew CL, Doherty-Kirby A, Lajoie G (2000) Chitinase genes responsive to cold encode antifreeze proteins in winter cereals. Plant Physiol 124: 1251-1264

Yooyongwech S, Horigane AK, Yoshida M, Yamaguchi M, Sekozawa Y, Sugaya S, Gemma H (2008) Changes in aquaporin gene expression and magnetic resonance imaging of water status in peach tree flower buds during dormancy. Physiol Plant 134: 522-533

Yoshida M, Abe J, Moriyama M, Shimokawa S, Nakamura Y (1997) Seasonal changes in the physical state of crown water associated with freezing tolerance in winter wheat. Physiol Plant 99: 363-370

Yoshida T, Nishida H, Zhu J, Nitcher R, Distelfeld A, Akashi Y, Kato K, Dubcovsky J (2010) Vrn-D4 is a vernalization gene located on the centromeric region of chromosome 5D in hexaploid wheat. Theor Appl Genet 120: 543-552

Yu XM, Griffith M (1999) Antifreeze proteins in winter rye leaves form oligomeric complexes. Plant Physiol 119: 1361-1370

Yu XM, Griffith M, Wiseman SB (2001) Ethylene induces antifreeze activity in winter rye leaves. Plant Physiol 126: 1232-1240

Yu XM, Griffith M (2001) Winter rye antifreeze activity increases in response to cold and drought, but not abscisic acid. Physiol Plant 112: 78-86

Zabotin AI, Barisheva TS, Zabotina OA, Larskaya IA, Lozovaya VV, Beldman G, Voragen AG (1998) Alterations in cell walls of winter wheat roots during low temperature acclimation. J Plant Physiol 152: 473-479

Zamani A, Sturrock R, Ekramoddoullah A, Wiseman S, Griffith M (2003) Endochitinase activity in the apoplastic fluid of *Phellinus weirii*-infected Douglas-fir and its association with over wintering and antifreeze activity. For Pathol 33: 299-316

Zámećník J, Bieblová J, Grospietsch M (1994) Safety zone as a barrier to root-shoot ice propagation. Plant Soil 167: 149-155

Zwieniecki M, Holbrook N (1998) Diurnal variation in xylem hydraulic conductivity in white ash (*Fraxinus americana* L.), red maple (*Acer rubrum* L.) and red spruce (*Picea rubens* Sarg.). Plant Cell Environ 21: 1173-1180

Zwieniecki MA, Holbrook NM (2000) Bordered pit structure and vessel wall surface properties. Implications for embolism repair. Plant Physiol 123: 1015-1020

Zwieniecki MA, Melcher PJ, Holbrook NM (2001) Hydrogel control of xylem hydraulic resistance in plants. Science 291: 1059-1062